Methanol quality and its effects on the fuel-cell reformer off-gas composition

BA Solms

orcid.org/0000-0002-3945-8153

Dissertation submitted in fulfilment of the requirements for the degree *Master of Engineering in Mechanical Engineering* at the North-West University

Supervisor: Mr J Markgraaff

Graduation: October 2019

Student Number: 24292753

PREFACE

I am a mechanical engineer undertaking this study for my masters in mechanical engineering. The objective of this dissertation is to inform mechanical and chemical engineers of the effect that fuel quality would have on the methanol steam reformer's off-gases in an attempt to decrease the operating costs of hydrogen production by using a cheaper, lower quality methanol as a fuel.

Acknowledgements

I would firstly like to thank our heavenly Father for His love, guidance, and grace to help me finish this undertaking. I would like to thank my parents for their constant love and support. My study leader Johan Markgraaff has given me so much guidance and, without it I would not have gotten as far as I have. Thank you to everyone at the NWU Mechanical department: Mr. Sarel Naude, Mr. Willem van Tonder, Mr. Thabo Diobe, Mr. Bartlo, and Mr. Andre. Their tireless effort and assistance helped shape the design and final fuel qualifying experimental facility. To Andre and Drikus, and everyone at FlowjetWest, thank you for all of your assistance and advice regarding this study.

Brian Solms, Potchefstroom Northwest University,2019.

ABSTRACT

Previous research articles that deal with methanol-steam reforming with $Cu/ZnO/Al_2O_3$ catalyst do not take into account the quality of methanol used and the effect that it would have on catalyst performance and the off-gas composition as a result.

This study focuses on three methanol qualities, and qualifies and quantifies the change in the off-gas composition over a period of 30 hours of operation using each methanol quality. In order to achieve this aim, the problem statement is as follows: The full impact of various methanol fuel qualities on the operation of the reformer and subsequently the composition of the off-gases which is not commonly known nor addressed in literature. The addressing of the problem statement was approached by three experiments on a methanol steam reformer filled with catalyst similar to commercial $Cu/ZnO/Al_2O_3$. Each experiment analysed the off-gas condensate, as well as the analysis of gas samples and catalyst in 10 hour intervals. A fuel qualifying experimental facility was designed and built which delivered the respective methanol-water mixture qualities into an evaporator after which it was reformed into hydrogen, carbon dioxide, and carbon monoxide while condensing the unreformed methanol and water. The experimental facility was evaluated according to the design outcomes and requirements stipulated by the design criteria. The catalyst was manufactured using methods described by various articles. Condensate samples confirmed that lower methanol quality decreased the maximum methanol conversion and lifespan of the catalyst when compared to that of the higher methanol quality. An increase in acidity of the condensate was observed due to chloride compounds which were presented faster when reforming lower quality methanol. The gas samples indicated that the methanol quality did not significantly affect the stoichiometric concentrations of hydrogen and carbon dioxide. The carbon monoxide concentration was highest during the first 10 hours while reforming all methanol qualities and converged to about 0.3mol% for all methanol qualities. No hydrogen sulphide was detected in the reformer outlet stream. The analysed catalyst samples revealed signs of sintering while reforming by a change in pore size, roughing and coarser catalytic surface texture, and indications of cleavage and brittle fracture when compared to fresh catalyst. Sintering was independent of methanol quality and the lower methanol qualities did not drastically alter the catalyst topology. The catalyst exposed to lower quality methanol presented an increased amount of chloride impurities chemisorbed to the catalyst compared to the catalyst exposed to higher quality methanol as well as an increased penetration depth into the catalyst pellet. There was no carbon deposition detected from any of the methanol qualities.

Keywords: Methanol quality. Analytical Reagent. Chemically Pure. Industrial grade. Methanol steam reformer. Catalyst. Off-gases. Condensate. Methanol Conversion.

TABLE OF CONTENTS

LIST OF TABLES

LIST OF FIGURES

LIST OF ACRONYMS

AR	-	Analytical Reagent
BET	-	Brunauer–Emmett–Teller
CP	-	Chemically Pure
DMFC	-	Direct Methanol Fuel Cell
E1	-	Element 1
EBSD	-	Electron Backscatter Diffraction
EDS	-	Energy Dispersive X-ray Spectroscopy
GC	-	Gas Chromatography
IMPCA	-	International Methanol Producers and Consumers Association
MCFC	-	Molten Carbonate Fuel Cell
PEM	-	Polymer Electrolyte Membrane
PET	-	Polyethylene Terephthalate
ppb	-	Parts Per Billion
ppm	-	Parts Per Million
SEM	-	Scanning Electron Microscope
SOFC	-	Solid Oxide Fuel Cell
TEM	-	Transmission Electron Microscopy
XRD	-	X-Ray Diffraction

LIST OF SYMBOLS AND SUBSCRIPTS

Al	-	Aluminium	
CO_2	-	Carbon Dioxide	
CO	-	Carbon Monoxide	
Cu	-	Copper	
D_i	-	Inner Diameter	[m]
H_2	-	Hydrogen	
HCl	-	Hydrochloric Acid	
H_2S	-	Hydrogen Sulphide	
L	-	Length	[m]
m	-	Mass	[kg]
$\dot{m}$	-	Mass Flow Rate	[kgs^{-1}]
Mol	-	Mole	[mol]
MethConv	-	Methanol Conversion	[%]
Na	-	Sodium	
P	-	Pressure	[Pa]
ρ	-	Density	[kgm^{-3}]
T_i	-	Initial Temperature	[°C]
T_o	-	Outlet Temperature	[°C]
Vol	-	Volume	[m^3]
WHSV	-	Weight Hourly Speed Velocity	[h^{-1}]
wt%	-	Weight Percentage	[%]
Zn	-	Zinc	

CHAPTER 1 - INTRODUCTION

1.1 Background

In South Africa it is often difficult or unfeasible for Eskom to deliver power to remote locations. This is often the case for the initial phases of construction projects, mining and farming operations, or wireless telecom stations. In these cases, petrol and diesel generators are often used to supply the necessary electricity to the equipment and infrastructure. Generators, however, create air and noise pollution; as well as having high operating costs. These include fuel, maintenance, and the replacement and repairing of components.

In other parts of the world fuel cells are becoming an alternative source of electricity for remote locations. Their lack of moving parts, which effectively lowers maintenance requirements, and far fewer emissions have made fuel cells a possible viable alternative. For example, in October 2008 the Canadian company, Ballard, entered into an agreement with ACME Telepower and IdaTech. Together, from 2009 to 2010, they produced and deployed 10 000 Ballard Electragen ME fuel cell systems to provide power to wireless telecom bay-stations in India.

These fuel cell systems comprise of several linearly interdependent sub-systems, where one sub-system feeds into the next. Each sub-system is responsible for conforming to a sub-system interface requirement to allow the delivery of processing outcomes that again conform to the next subsequent sub-system requirements. Consequently, the mentioned fuel cell systems consist of three processing sub-systems, namely fuel processing system, power generation system, energy storage/supply system.

For power generation, fuel cells use a process whereby chemical energy is directly converted into electrical energy. This electrical energy can be made directly available to energise small electrical networks, or can be stored in batteries until required by end users. Figure 1 is a simple flow diagram displaying how a fuel cell system would operate using hydrogen as fuel. Figure 2 focuses on the power generation in the fuel cell stack, showing how the electricity is produced from hydrogen.

Fuel cells use a reduction-oxidation reaction to produce electricity. The oxidation reaction happens at the anode terminal, which is considered the catalyst material. The hydrogen's electrons are stripped and flow toward the cathode. The now positive hydrogen ions are allowed to pass through the electrolyte to the cathode terminal, where the reduction reaction takes place. The hydrogen and oxygen react with the electron, closing the circuit and allowing for the flow of electricity, with water forming as a product. This process constitutes one fuel cell, a large number of these cells are compressed together to form a fuel cell stack.

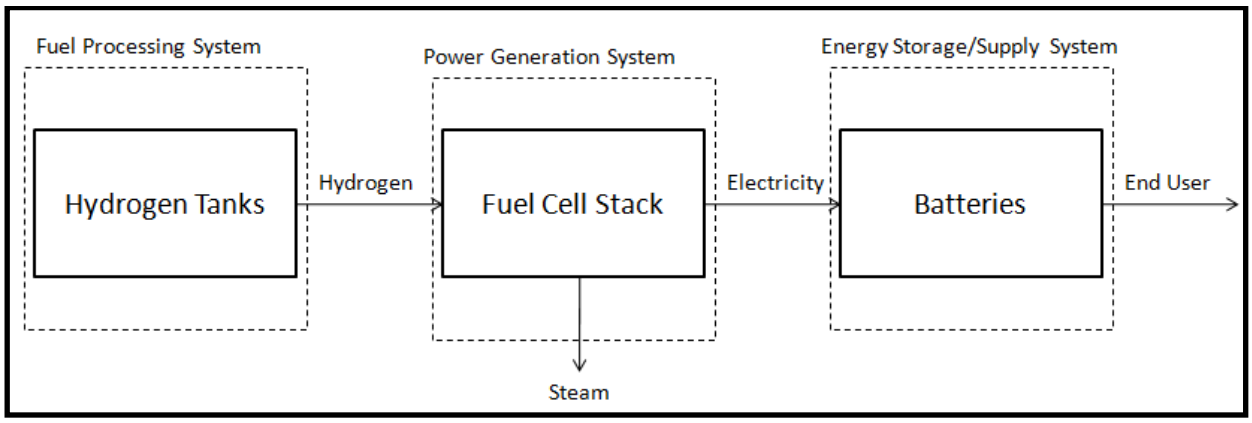

Figure 1 - Simplified Flow Diagram for a Common Fuel Cell System

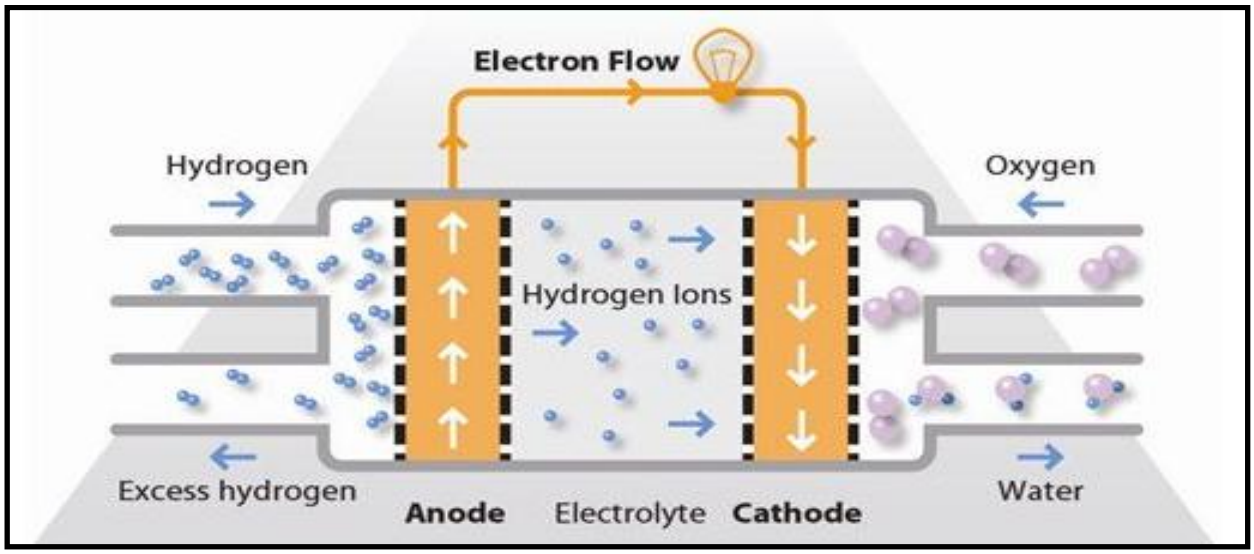

Figure 2 - Single Fuel Cell (Matthey, 2017)

There are a number of different types of fuel cells each based on the fuel used as well as the catalyst material, the electrolyte, and operating temperatures. The most common fuel cell is the PEM (Polymer Electrolyte Membrane) fuel cell. This is represented in Figure 2 above. It is compact, easy to use in a number of applications, and operates at a low temperature allowing it fast start up times and little heat energy required. This is all possible due to it using pure hydrogen to generate electricity.

Hydrogen is used due to its natural abundance; however, it is not abundant in its elemental form. It is found in many gaseous or liquid compounds such as water, methane, as well as in various hydrocarbons. Once hydrogen has been produced it must be stored and transported to the remote locations where the fuel cell systems will be operating. Due to its low density, it must be compressed for any practical applications, making it difficult and potentially dangerous to store and

transport. Hydrogen combusts very violently and leaks are near-impossible to detect without proper equipment or sensors.

These problems lead to the use of other fuels that are easier and safer to transport and store. However, using fuels other than hydrogen would require alternative types of fuel cells. SOFC (Solid Oxide Fuel Cell) and MCFC (Molten Carbonate Fuel Cell) systems can overcome the challenges of using hydrogen as a fuel. They can internally reform most hydrocarbons to produce hydrogen, allowing for the fuel processing system and power generation system to become a single sub-system. Processing a hydrocarbon, however, produces carbon dioxide, but not as much as a generator would. This allows for the use of methane (CH_4), ethanol (C_2H_6O), and propane (C_3H_8), among others, which are easier to transport and store. However, SOFC and MCFC have high operating temperatures requiring a large amount of heat energy and long start-up times.

Figure 3 displays a simplified diagram of the SOFC system.

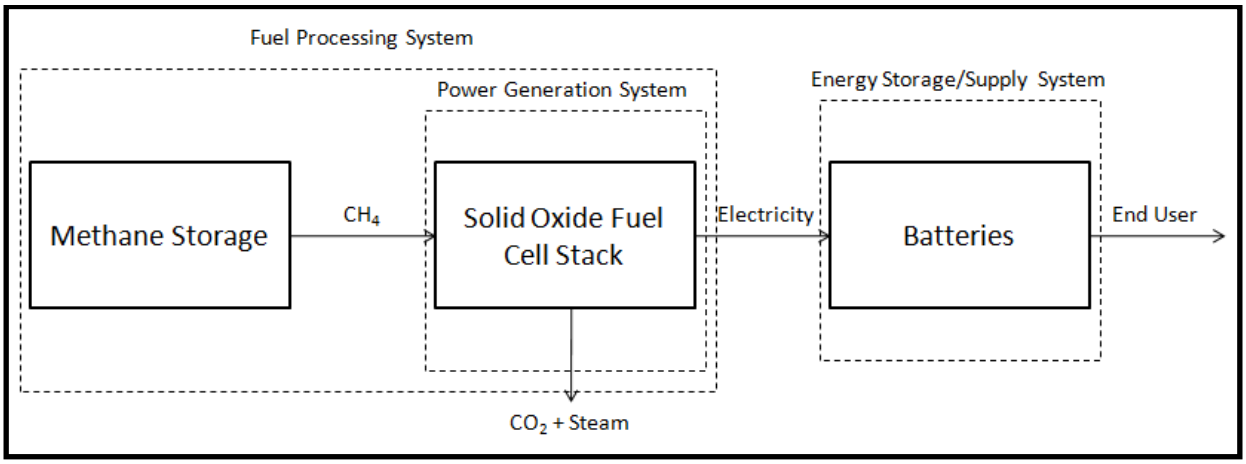

Figure 3 - Flow Diagram for a SOFC System

The MCFC is very similar in function to the SOFC except for the fact that it uses carbon dioxide with the fuel instead of the oxygen in the air.

A drawback to these hydrocarbon fuels is that they are gases, and although they are not as violently reactive as hydrogen, transportation and storage can be problematic.

Another alternative fuel is methanol, which is a liquid at room temperature and has a low boiling temperature. It can be transported and stored easily and safely, while requiring low amounts of heat energy to be processed as a gas within the fuel processing system.

This process will require extra processing steps in the fuel processing system, namely evaporation, reforming, and hydrogen separation. This can be observed in Figure 4 and is discussed below.

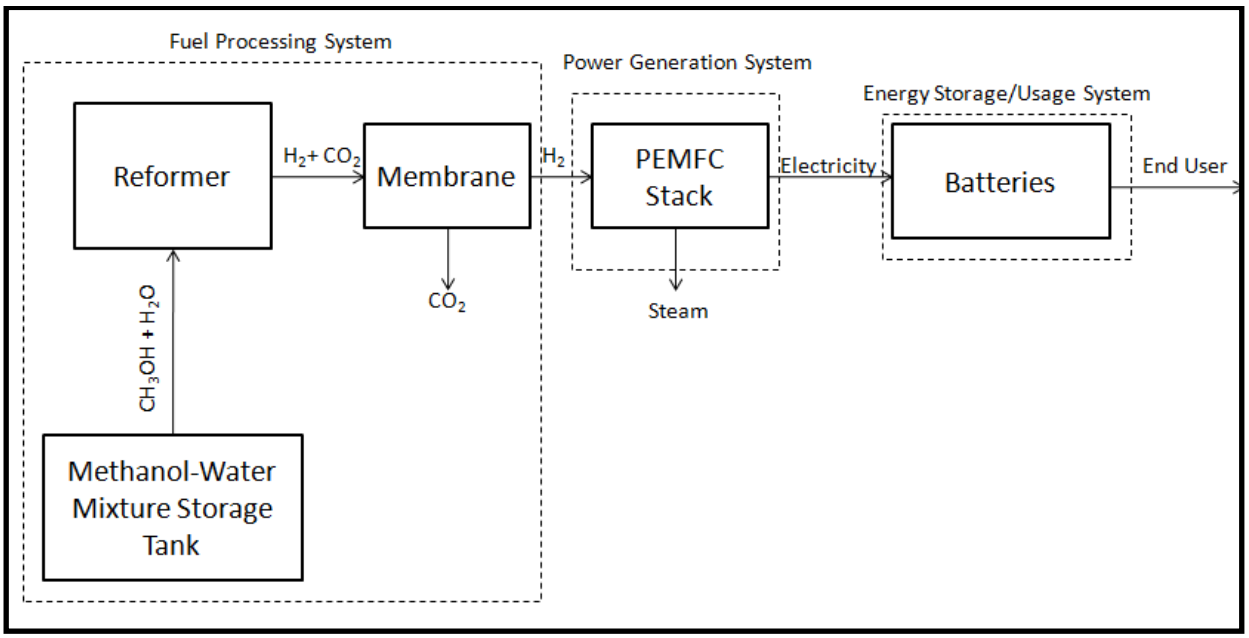

Figure 4 - Flow Diagram for a Methanol Fuel Cell System

A common fuel processing method to produce hydrogen from methanol for a PEMFC is via a methanol steam reformer with a copper-based catalyst. Gas-separation membrane technology is implemented for the removal of carbon dioxide from the off-gas providing a hydrogen stream. The catalyst and membrane are the main fuel processing system components that determine the effectiveness of hydrogen production in the fuel processing system.

Attempts to use this technology in South Africa have not been as successful as in other parts of the world. The Electragen ME fuel cell system was used for a community project and it was found that it was not able to compete with a generator delivering the same amount of electricity. The operational costs of components that were depleted and needed replacing, and the price of the specific fuel used to power the fuel cell system, were very high.

The specific fuel, as required by the specification of the Ballard fuel cell system, is a methanol-water mixture, called HydroPlus. It is classified as E1 (Element 1) which is hydrogen generator reformer fuel. The composition of E1 fuel is methanol mixed with water in a molar ratio of 1:1.1 methanol to water. E1 specifies methanol adhering to IMPCA (International Methanol Producers and Consumers Association) standards. IMPCA dictates a maximum of 0.5ppm of sulphur as well as a possibility of trace amounts of chlorine and other impurities. While adhering to IMPCA

standards there are a number of different qualities of methanol based on their purity, which are produced depending on the application, specifically AR (Analytical Reagent), CP (Chemically Pure), and Industrial grade.

Taking this into account, the prices of the different qualities of methanol can be compared. The cost to create a certain volume of methanol-water mixture is displayed by Table 1.

Table 1 - Various Methanol Fuel Qualities R/L costs compared to Petrol and Diesel

Fuel Type	Cost [RL^{-1}]
AR Methanol	15.16
CP Methanol	13.53
Industrial grade Methanol	12.48
93 Unleaded Petrol	15.96
50 ppm Diesel	14.94

By comparing methanol fuel quality prices to the current price of 93 Unleaded petrol and 50ppm diesel, both inland, it can be observed that by using a lower quality methanol could in fact make a fuel cell reformer system a viable replacement for a generator, taking into account less maintenance and component replacement required by the fuel cell system as compared to the generator. Despite this, the use of lower quality methanol could negatively impact functioning of the system, increasing operating costs and decreasing the viability of the system.

It is not known what quality of methanol is used in the HydroPlus fuel. Likewise, it is also unknown whether the quality of the fuel would have a significant impact on the composition of the methanol steam reformer off-gas. If the off-gas contains high concentrations of poisons known to degrade fuel cell systems, it would negatively affect the degradation rate and lifespan of the system's critical components.

In order to make this technology more viable than generators in South Africa, it would have to be better understood. This can be done by an investigation into whether the operational conditions of the methanol steam-reformer and exhaust gas composition would significantly be impacted by the use of various fuel qualities.

1.2 Problem Statement

The full impact of various methanol fuel qualities on the operation of the reformer and subsequently the composition of the off-gases is neither commonly known nor addressed in literature.

1.3 Aim

This study aims to determine the impact of different quality methanol fuels in a fuel cell system on reformer operation and off-gas composition. This would include investigating the performance of the reformer by determining the methanol and water fuel percentage converted to hydrogen. Furthermore, the off-gases will be sampled and analysed to determine the composition, including the presence and approximate concentration of poisons.

The capacity of this study will extend to the following tasks with the intent of achieving the previously mentioned aim.

1.4 Objectives

- Research on fuel cell systems, reformer, and catalyst technologies.
- Design and manufacture system to operate at typical reformer conditions.
- Setup of a functional fuel qualifying experimental facility using a catalyst commonly used in fuel cell system reformers.
- Setup of a number of experiments using different qualities of methanol fuel and implement data recording methods.
- Measure and record operating condition data from the system.
- Verify the fuel qualifying experimental facility and experiments by comparing design outcomes and requirements with the experimental observations during system operation to ensure the fuel qualifying experimental facility operates as expected and will be able to produce reliable results.
- Analysis and validation of the fuel qualifying experimental observations and results according to similar experiments done in this field and the posed problem statement to determine if the problem statement has been addressed.

- Conclusions and recommendations will follow.

1.5 Document Overview

In the previous sections, the background of the fuel cell, as well as the fuel cell system's various subsystems, including the methanol steam reformer, has been discussed. It has been found that the implementation of the fuel cell systems in South Africa has not been successful and that there is a lack of knowledge in terms of the E1 fuel used to generate hydrogen and the effect a lower quality methanol fuel would have on the reformer and subsequent exhaust gas composition. It has been decided that an investigation will be done into the operation of a methanol steam reformer with the intent of quantifying the effect that methanol quality would have on the operation of a methanol steam reformer and its off-gas composition.

Chapter 2 includes various studies done in this field and their results and conclusions which lead to the design of a fuel qualifying experimental facility.

Chapter 3 discusses and addresses the design outcomes and requirements for the fuel qualifying experimental facility that will be used to address the problem statement.

Chapter 4 evaluates and verifies the proposed method of addressing the problem statement according to the design outcomes and requirements stipulated by Chapter 3.

Chapter 5 presents the findings gathered from the fuel qualifying experimental facility and will be discussed and validated according to the published research results discussed in Chapter 2 as well as whether it has answered the problem statement fully.

Chapter 6 concludes the study and presents recommendations and future work to be undertaken. Appendixes will follow.

CHAPTER 2 - LITERATURE REVIEW

In this chapter, the most important aspects of a methanol steam reformer will be investigated. The focus will be on methanol fuel and its properties, reformer operation conditions, catalyst used along with its composition and physical properties, and its reforming abilities as well as variables affecting catalyst reactivity as described by literature. Furthermore, the subsequent subsystems downstream of the reformer that would be affected by the reformer off-gases will be considered, as well as the reformer off-gas composition from typical reformers from the perspective of other published studies.

2.1 Hydrocarbon Fuel

A hydrocarbon is a hydrogen containing molecule with carbon bonds. There are a number of these types of molecules, for example, methane (CH_4), methanol (CH_3OH), and ethanol (C_2H_5OH). There is a lot more focus on methanol as an alternative energy source due to its transportability and low toxicity to the environment.

Methanol, also known as methyl-alcohol, is a colourless, poisonous, highly flammable liquid that is most often used in anti-freeze and as an additive in gasoline.

Methanol quality is dictated by the IMPCA standards, which indicates the following impurities as shown by Table 2.

Table 2 - Methanol Quality Parameters Adapted from (IMPCA, 2015)

Impurity	Maximum Amount [ppm]
Acetone	30.0
Ethanol	50.0
Chlorine	0.5
Sulphur	0.5
Iron	0.1

Inside these parameters, three different methanol qualities exist, namely Analytical Reagent (AR), Chemically Pure (CP), and Industrial grade.

The most prominent method of producing methanol today is through a method developed in 1920, whereby hydrogen and carbon dioxide react together to form methanol and water. Similarly, hydrogen and carbon monoxide can be used to make pure methanol. By reversing these reactions, methanol and water can disassociate to produce hydrogen and carbon dioxide (Marine Methanol, 2018).

In order to generate hydrogen from methanol, the carbon bonds must be broken, and a common method to achieve this would be to use a reforming process.

2.2 Reforming

Reforming is a chemical process whereby chemicals undergo decomposition, otherwise known as cracking, specifically to produce hydrogen and carbon dioxide from a hydrocarbon fuel.

There are three main types of reformers; Steam reformers, Auto-thermal reformers, and Partial Oxidation reformers. Steam reforming uses steam along with a hydrocarbon to produce the highest hydrogen concentration compared to the other two reforming types. Steam reforming is a highly endothermic reaction, requiring large amounts of heat energy, however, steam reforming is the most common reforming method.

Steam reforming uses high temperature steam to react with the hydrocarbon fuel. This type of reforming is more common in fuel cell technology as it can turn most hydrocarbons like methane (CH_4), ethanol (C_2H_6O), propane (C_3H_8), and even gasoline, into hydrogen, carbon monoxide, and carbon dioxide. Carbon dioxide and carbon monoxide, which are the by-products of a reformer, are often called the reformate (US Department of Energy, 2012).

$C_xH_x + H_2O + Heat \rightarrow H_2 + CO + CO_2$

This initial reaction is an endothermic reaction and will require heat energy to react and produces carbon dioxide, carbon monoxide, and hydrogen.

A water-gas shift reaction is initiated by the steam that has not reacted with the fuel, allowing the carbon monoxide and steam to react causing more hydrogen and carbon dioxide to be produced. This process increases the efficiency of the system.

$CO + H_2O \rightarrow H_2 + CO_2$

In a final step called the pressure swing absorption, the carbon dioxide and impurities are removed from the hydrogen gas stream. This process, however, can be expensive and complex (US Department of Energy, 2012). Instead, in a typical fuel cell system, a membrane filter is used.

Each steam reformer is classified by the fuel being reformed, and this will, in turn, determine the operating temperatures, pressures, and type of catalyst to be used to reform the specific fuel. The advantage of using methanol for hydrogen production is that it is a liquid at ambient conditions making it much easier to transport, as well as a low evaporation temperature allowing for less heat energy to be required. It is also the simplest alcohol molecule creating a more predictable decomposition reaction.

Methanol reforming operates at conditions between 200˚C and 300˚C, at 200kPa (Makertihartha & Gunawan, 2009). These are significantly lower temperatures compared to the reforming of other hydrocarbons, like methane, which operates between 700˚C and 1000˚C (US Department of Energy, 2012). This will decrease the energy required to initiate the reforming reaction which increases the efficiency of the system.

In order for the reformer to crack the hydrocarbon and steam into its elemental components, it requires a catalyst. Methanol steam reforming most often uses a $Cu/ZnO/Al_2O_3$ catalyst due to its availability and affordability (Lee *et al.,* 2004). Before discussing the details of the $Cu/ZnO/Al_2O_3$ catalyst, the principle and characteristics of catalysts must be understood.

2.3 Catalyst

A catalyst is defined as a substance that can initiate a reaction, or increase or decrease the rate of a reaction. Its main characteristic is that it does not physically react within the reaction that it initiates and it is collectable once the reaction has been completed.

Catalysts can be homogenous, the same phase as the reacting chemicals, or heterogeneous, a different phase to the reacting chemicals (Rojas, 2013). Steam reforming catalyst is classified as heterogeneous catalyst.

Catalysts have two main properties namely reactivity and selectivity.

Reactivity is an indication of the strength of bonds that the catalyst reacts with the target molecule. Low reactivity will only react with weaker bonds. Selectivity is an indication of the areas that the catalyst reacts with other than the target. More selective catalysts will only react with the target material.

Generally, the reactivity and selectivity are inversely correlated. The more reactive a catalyst is the less selective it becomes and vice versa. This is especially true for difficult transformations like hydrogen-carbon bonds (Fogler, 2005).

2.3.1 Catalyst Reaction

Fogler (2005) describes the catalytic reaction happening in several steps, namely:

1. Mass transfer towards the catalyst surface,
2. Diffusion into catalyst pores,
3. Adsorption of reactant A,
4. Reaction on the surface of the catalyst,
5. Desorption of product B,
6. Diffusion out from the catalyst pores,
7. Mass transfer away from the catalyst.

These reaction steps can be visualised as shown in Figure 5:

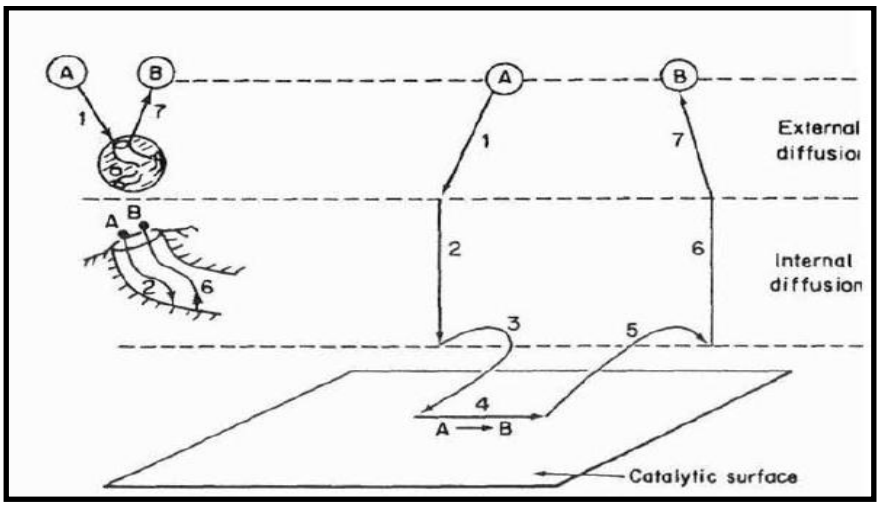

Figure 5 - Steps in a Catalytic Reaction (Fogler, 2005)

The overall rate of reaction is equal to the slowest step. Steps 1, 2, 6, 7 are very fast compared to the others. Therefore, the focus lies on the slower steps 3, 4, and 5 and are considered as the characteristic reactions.

- Adsorption

There are two types of adsorption:

  - Physical Adsorption: Molecules form on the active sites of the catalyst with weak VanderWaals forces between the gas molecules and solid surface allowing for adsorption and then desorption to take place once the reaction is completed.

  - Chemisorption: Stronger valence forces held by chemical bonds which occur when a gas molecule or impurity poisons an active site on the catalyst surface by not allowing desorption to take place.

- Surface reaction: This step happens between adsorption and desorption. The reaction takes place on the active site on the surface of the catalyst.

- Desorption: The molecules are then released from the active site.

The adsorption and desorption rates are different for each catalyst material. This will determine how active a catalyst is depending on its active site material.

2.3.2 Catalyst Materials

For general purposes, nickel-based catalysts are the most common. They offer sufficient activity, low cost, and high availability. Precious metal catalysts like Rhodium and Ruthenium have high activity, but high cost and low availability.

Copper-based catalysts are the most commonly used in methanol steam reforming due to copper's selectivity towards hydrogen and are considered the active site. $Cu/ZnO/Al_2O_3$ is the most popular methanol reforming catalyst due to its reasonable price and availability. There are various studies focused on weight variations of the Cu, ZnO, and Al_2O_3, as well as using different oxides along with the copper active site or changing the active site material entirely. Palladium is currently being studied for a catalyst as $Pd/ZnO/Al_2O_3$ and has shown more stability than $Cu/ZnO/Al_2O_3$ when used in a methanol steam reformer. (Iulianelli *et al.,* 2013). However, to make this study relevant to the current methanol steam reforming industry, the focus will be on $Cu/ZnO/Al_2O_3$ catalyst.

2.3.3 Manufacturing Method

There are many variables concerning the manufacturing of a catalyst. The combination of chemicals can change the activity and the stability of the catalyst. For example, Sa' *et al.* (2010) described that the addition of Al_2O_3 inhibits sintering. Similarly Kurr *et al.* (2008) discusses how ZnO reduces the sintering of copper as well as removes sulphide poisons.

The way in which the different elements are added can also have an effect. Co-precipitation is most often used and considered as a "traditional method" (Luan *et al,.* 2012). It creates a double layered hydrotalcite and gives the chemicals a very intimate bond (Kurr *et al.*, 2008). This allows for lower calcination temperatures and faster catalyst manufacture. A study done by Hammoud *et al.* (2014) used other methods including impregnation and wet precipitate mixing. Reaction times and pH levels can also affect the activity and stability of the catalyst (Rojas, 2013).

For the methanol steam reforming catalyst, high values of copper dispersion and metal surface area, along with small particle sizes, are beneficial toward good methanol conversion. This can be achieved by slow reaction times as well as a reaction pH of 10. (Rojas, 2013)

The methods described by Hammoud *et al.* (2014), Kim *et al.* (2016), Kurr *et al.* (2008), and Prasetyaningsih *et al.* (2016) all follow the same general procedure of mixing aqueous nitrates of copper, zinc, and aluminium, and precipitating with sodium carbonate at a pH value between 7 and 10 to produce copper-zinc-aluminium carbonates which can then be filtered, washed, and dried. In order to oxidise the catalyst and remove the carbonates, it is calcined in an oven at 400 °C for 4 hours and activated by passing hydrogen gas, mixed with an inert gas like argon or nitrogen to reduce hydrogen flammability, over it for 3 hours to remove the oxygen atoms from the copper.

2.3.4 Catalyst Composition and Physical Properties

The physical properties of a catalyst play a large role in performance. Therefore, a catalyst is characterised by its composition, surface area, pore size and volume, as well as its crystallinity and how all of these factors affect its reactivity and reforming ability.

A high surface area gives the reactants a large area to react with; large pore radii and volumes allows for penetration into the catalyst also increasing the reaction area and ease with which reactant molecules can enter and access active sites.

Kurr *et al.* (2008) used XRD analysis to investigate the effect that crystallinity has on the surface area, pore volumes, and reforming abilities of the catalyst. This will, however, not be discussed in this study as it is outside of the scope and is not largely focused on in most literature. The various

studies using commercial catalysts or catalysts with compositions similar to commercial catalysts have been included in Table 3 to display their compositions as well as their surface areas and pore volumes. These values are what should be expected from the catalyst used in this study.

Table 3 - $CuO/ZnO/Al_2O_3$ Catalyst Composition and Physical Properties Adapted from (Lee *et al.,* 2004), (Kurr *et al.,* 2008), (Sá *et al.*, 2010), (Sa´ *et al.*, 2011), (Prasetyaningsih *et al.*, 2016), and (Kim *et al.*, 2016)

	Study				
Physical Property	**(Lee *et al.*, 2004)**	**(Kurr *et al.*, 2008)**	**(Sa´ *et al.*, 2011)**	**(Prasetyaningsih *et al.*, 2016)**	**(Kim *et al.*, 2016)**
	Commercial Synetix 33-5	Commercial	Commercial	Co-Precipitation	Co-Precipitation
CuO [wt%]	64.0	61.7	66.0	60.0	55.0
ZnO [wt%]	24.0	29.7	23.0	30.0	20.0
Al_2O [wt%]	10.0	8.6	11.0	10.0	25.0
BET Surface Area [m^2g^{-1}]	66.00	-	70.00	77.02	64.00
Average Pore Radius [nm]	8.000	-	-	15.015	13.500
Pore Volume [cm^3g^{-1}]	-	-	-	0.578	-

It can be observed that the various studies done have very similar catalyst compositions which will make their data readily comparable to one another. This will also allow for the results of this study to be validated more easily with literature, as well as being relevant to the field.

The compositions and the surface area of the commercial catalysts are very similar but have slight variations between suppliers. These are, however, commercially made catalysts and these values could change if produced by non-commercial means. The studies presented by Prasetyaningsih *et al*. (2016) and Kim *et al*. (2016) used catalysts that are not commercially made but have similar compositions and surface areas to commercial catalysts.

The study presented by Kim *et al*. (2016) used variations in catalyst compositions to see the effect that such variations would have on the physical properties of the catalyst. It was concluded that the catalyst with the composition most similar to commercial catalyst had the best overall properties which are displayed in Table 3. Similarly, the study presented by Prasetyaningsih *et al*. (2016), prepared a number of catalysts with compositional variation to observe the effect on physical properties and also concluded that the catalyst with the highest surface area and pore sizes was the catalyst most similar to the commercial catalyst with its properties displayed in Table 3. However, the application of the catalyst produced by Prasetyaningsih *et al*. (2016) is for methanol synthesis by the reaction of carbon monoxide and hydrogen and therefore only its catalyst properties and topology are discussed.

The $Cu/ZnO/Al_2O_3$ catalyst can be considered a ceramic due to the various metal oxides in its composition.

2.3.5 Methanol Reforming Temperatures, Flow Rates, and Fuel Mixtures

For steam reforming of methanol, the factors with the largest impact on reforming ability and its ability to convert methanol to hydrogen, are the operating temperatures of the reformer, the methanol-water molar ratio, as well as the flow rate to the reformer.

Using 0.3 g of catalyst with an average particle size of 0.5-1 nm diameter and a constant fuel flow Weight Hourly Space Velocity (WHSV) rate of 8.69 h^{-1} (2.61 gh^{-1}) with a methanol:water molar ratio of 1:1.4, Gu *et al.* (2003) produces the following results on methanol conversion displayed in Table 4.

Table 4 - Methanol Conversion for Various Temperatures with Catalysts from Various Suppliers adapted from (Gu *et al.*, 2003)

Temperature[°C]	Methanol Conversion [%]			
	KATALCO 83-3	C18-7-01	C18 HA	C18 HALM
180	39.66	40.35	32.52	34.27
210	68.40	72.84	77.79	55.34
230	93.61	98.14	97.34	95.91
275	100.00	100.00	100.00	100.00

Table 4 displays the findings of at 180 °C the methanol conversion is between 40.35 % and 34.27 %. While the reformer is at 275 °C, the methanol conversion reaches 100 % for all catalysts used. The methanol conversions at the various temperatures are very similar for all the various catalyst suppliers indicating that the supplier and possible differences in catalyst composition do not affect the overall effectivity of the catalyst.

The study presented by Makertihartha and Gunawan (2009) did similar experiments by varying the operating temperature as well as varying the mass flow rate through the reformer. 1 g of catalyst was used with a reformer size of 8 mm in diameter and methanol:water molar ratio of 1:1.2. It was concluded that a lower flow rate increases methanol conversion and provides an increased hydrogen yield. This would be due to longer contact times of the methanol and steam on the catalyst allowing for more time for adsorption to take place, increasing the number of methanol particles able to react with the catalyst. The ideal flow rate was a WHSV of $1h^{-1}$. This can be converted to 1 gh^{-1} per g of catalyst.

These results are displayed in Figure 6.

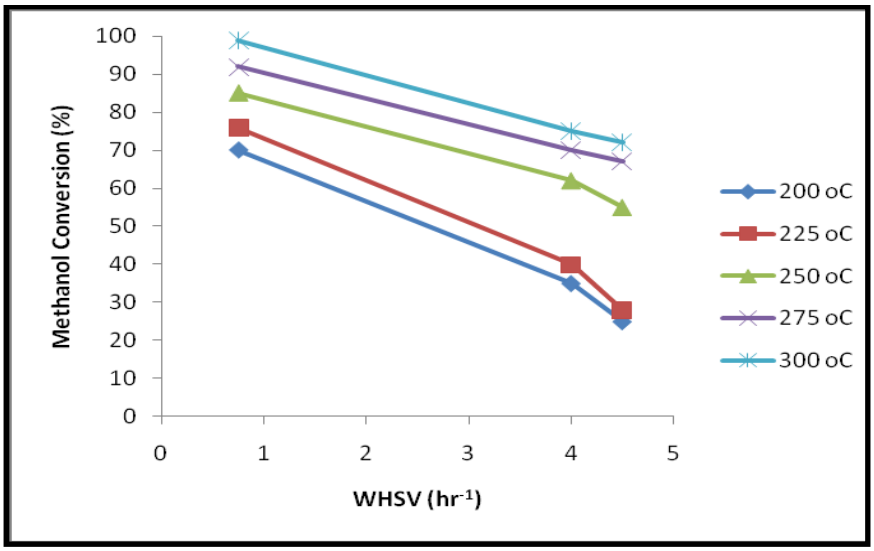

Figure 6 - Mass flow vs. Conversion (Makertihartha & Gunawan, 2009)

The study presented by Lee *et al.* (2004) considers the effect that the methanol/water fuel ratio would have on the reformer methanol conversion. Utilising 1 g of catalyst inside a 6.35 mm diameter reformer with a constant flow rate of 200 $mlmin^{-1}$ and 1:1, 1:1.5, 1:2 methanol:water molar ratios, the results were similar to that described by Gu *et al.* (2003), where an increased temperature increases the methanol conversion from nearly 0 % at 140 °C to 100 % at 260 °C. It

was also concluded that by varying the methanol to water ratio did not affect the methanol conversion. These results are illustrated in Figure 7.

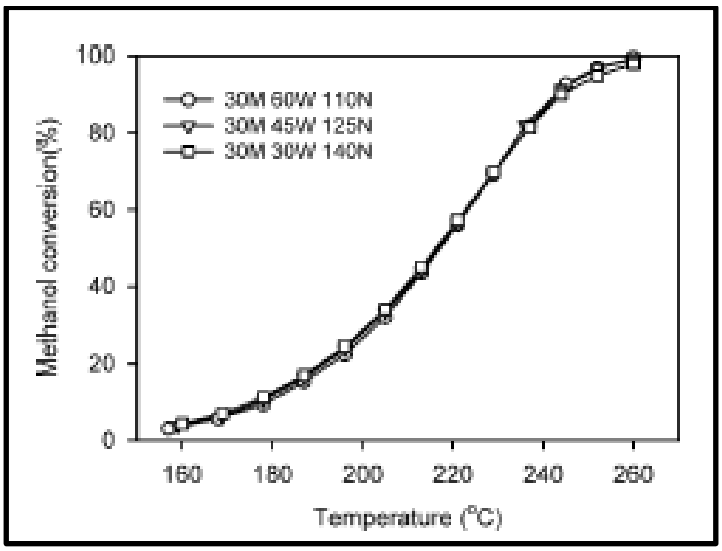

Figure 7 - Effect of Methanol/Water Partial Pressure on Methanol conversion vs Temperature (Lee *et al.*, 2004)

It was concluded that the molar ratios of methanol, water, and nitrogen have little to negligible effect on the methanol conversion and at 260 °C the methanol conversion converges to 100 %.

The catalyst discussed by Sá *et al.* (2010) produced a 79 % methanol conversion at 260 °C. However, the details regarding flow rates, reformer size, and methanol-water molar ratios are unavailable. Further research by Sá *et al.* (2011) utilised a 7.75 mm diameter reformer inserting 0.2 g of catalyst and applying a 1:1.5 methanol:water ratio as fuel. The flow rate was of 3 $\frac{W}{F^0_{methanol}}$ to 15 $\frac{W}{F^0_{methanol}}$ which translates to a mass flow rate of 2.83 gh^{-1} to 14.17 gh^{-1}. By varying the flow rates and temperatures the results are as displayed by Figure 8.

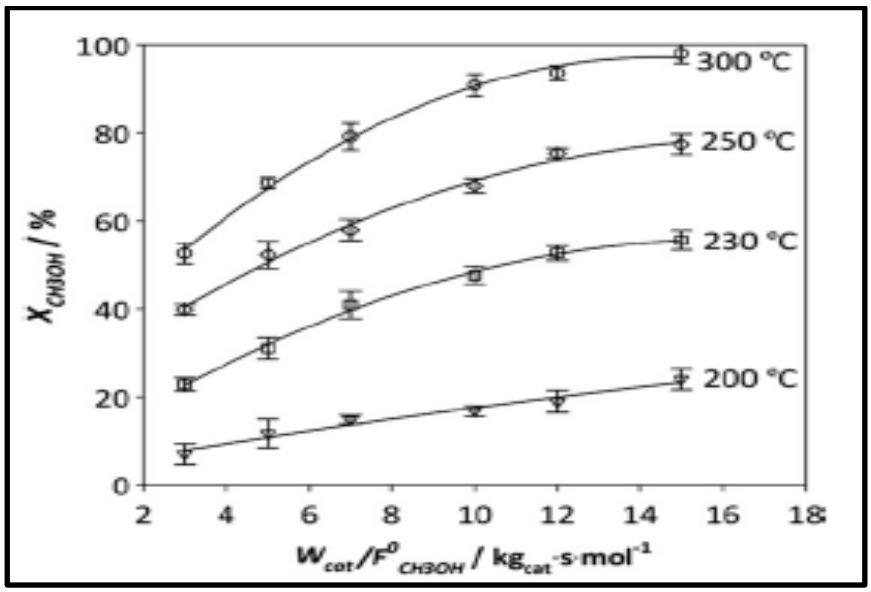

Figure 8 - Methanol Conversion at Various Temperatures vs Flow Rate (Sa´ *et al.*, 2011)

Figure 8 indicates how the methanol conversion is the highest at 300 °C at the lowest flow rate on the far right. This is similar to the results displayed by Makertihartha and Gunawan (2009) concluding a decreased flow rate would increase reforming ability due to the increased reaction times.

A study conducted by Kim *et al.* (2016) varied the catalyst elemental composition while varying the temperature. It was concluded that for a methanol:water molar ratio of 1:1.1, and mass flow rate of 12 gh^{-1}, the commercial catalyst showed the best activity at 300 °C providing 79 % methanol conversion. Figure 9 displays the results of the study.

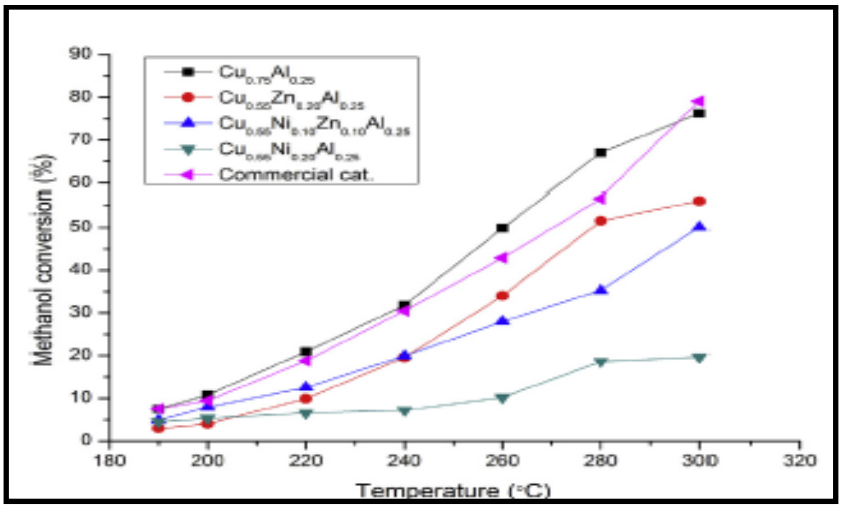

Figure 9 - Methanol Conversion vs Temperature (Kim *et al.*, 2016)

A study produced by Kurr *et al.* (2008) compared catalyst manufacturing methods while using commercial catalyst as the standard. It was stated that with 0.05 g of the commercial catalyst reforming 5136.5 gh^{-1} fuel of 1:1 methanol:water molar ratio at 248 °C, the methanol conversion was concluded to be 84.4 %.

Similar to Sá *et al.* (2011) and Makertihartha and Gunawan (2009), the study presented by Purnama (2003) displays a variation in temperature and flow rates. While reforming 0.2 g of catalyst with volume flow rates between 0.05 $mlmin^{-1}$ and 0.5 $mlmin^{-1}$ and varying the temperatures between 230 °C and 300 °C, Figure 10 displays the resulting methanol conversion from 10 % to near 100 %.

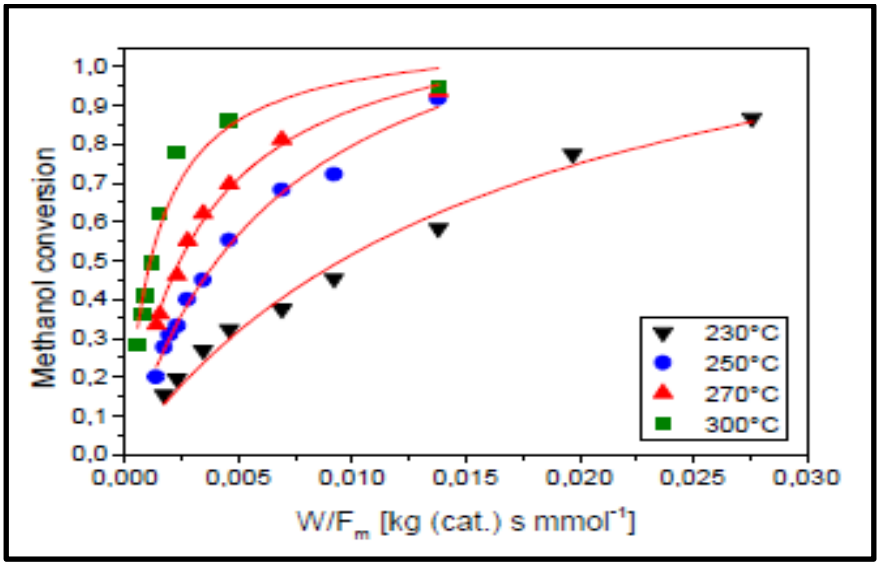

Figure 10 - Methanol Conversion from Temperature Variation vs Flow Rate (Purnama, 2003)

Unfortunately, in practice, catalysts cannot maintain constant methanol conversions indefinitely. Deactivation is a process that catalysts will undergo as operation times increase due to sintering or poisoning, especially if there are impurities in the methanol.

2.3.6 Deactivation

Although the catalyst is not consumed during the reaction, certain processes can inhibit or destroy the catalyst. Deactivation can happen due to a number of different processes namely sintering, carbon deposition, and poisoning.

2.3.6.1 Sintering

Sintering would be the loss of catalytic activity due to the loss of surface area of the catalyst caused by prolonged exposure to high gas-phase temperatures.

Sá *et al.* (2010) describes a dramatic drop in methanol conversion when operating a methanol steam reformer at 350 ˚C. This was described as being due to the sintering of the catalyst as the internal structure of the catalyst was damaged by high temperatures.

Something to consider is that reported operating temperatures could refer to reformer inlet and outlet temperatures and not the temperatures inside various points in the reformer bed. The observations of Shekhawat *et al.* (2011) by reforming diesel emphasises the need to measure temperatures throughout the catalyst bed. The study describes how the temperature can vary at different points inside the catalyst bed which can also change over time. Simply because the temperature of the inlet and outlet gases are not above the sintering temperatures does not mean that the centre of the reformer and the catalyst itself is at a safe temperature.

Figure 11 and Figure 12 displays the hydrogen yield increasing as the temperature increases deeper into the reformer. If the temperature was uniform over the entire reformer the hydrogen yield would be more constant and provide a more predictable hydrogen yield throughout the reformer bed. Therefore, it is important to have temperature sensors throughout the catalyst bed.

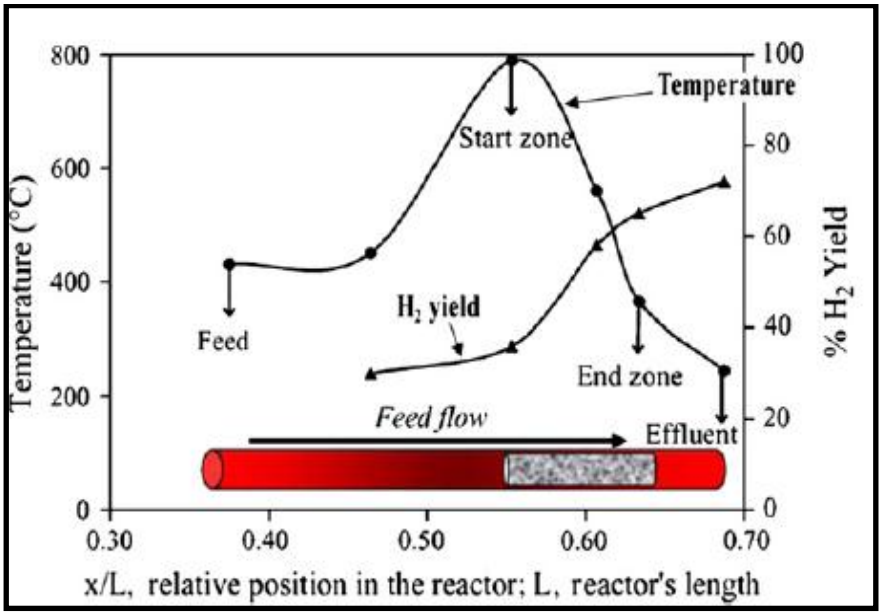

Figure 11 - Pt Based Catalyst in Diesel reformer Temperature Dispersion and Hydrogen Yield (Shekhawat *et al.*, 2011)

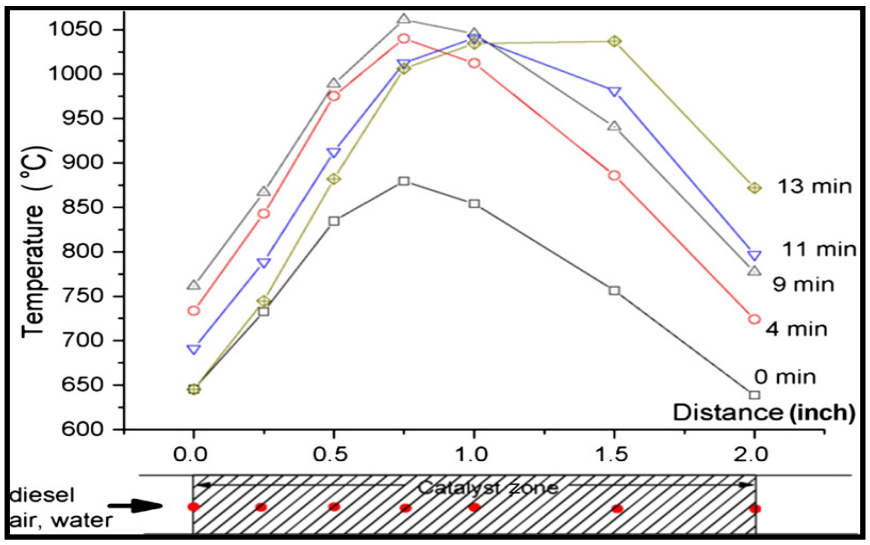

Figure 12 - Diesel Reformer Temperature Dispersion Over Time (Shekhawat *et al.*, 2011)

A visible indicator of sintering is cleavage of the catalyst. During sintering, the ceramic material would become brittle and a fracture would propagate along its grain boundaries, producing cleavage planes along with small sintered fractured particles. This mechanism is displayed in Figure 13.

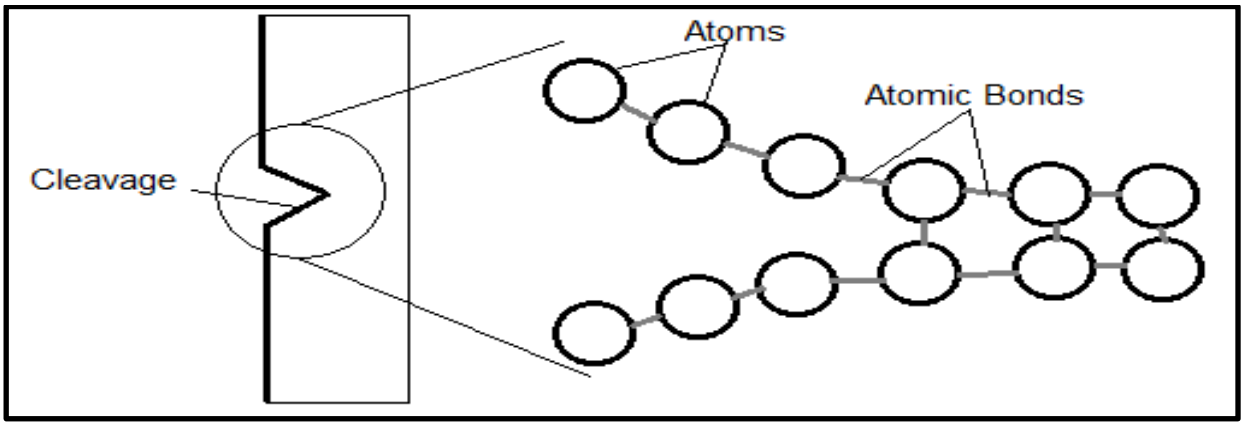

Figure 13 - Cleavage Mechanism Diagram Adapted from (UNSW Sydney School of Materials Science and Engineering, 2013)

Under a SEM a brittle fracture would appear reasonably smooth on a large specimen as displayed in Figure 14. It can also appear as smaller particles having broken off from the body of larger particle or cracks that have not yet produced a fully developed cleavage plane.

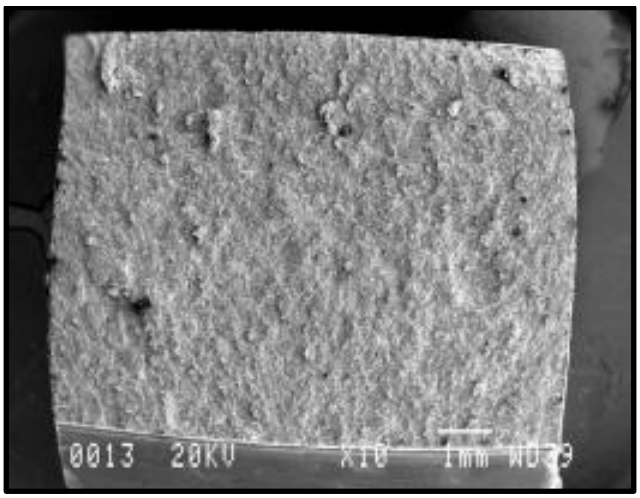

Figure 14 - Cleavage Plane SEM Micrograph (UNSW Sydney School of Materials Science and Engineering, 2013)

2.3.6.2 Carbon Deposition

Also known as coking or fouling, carbon deposition is common in processes using hydrocarbons. This mechanism happens due to carbonaceous material being deposited on the surface of the catalyst, essentially decreasing the active surface area. This mechanism can be seen in Figure 15.

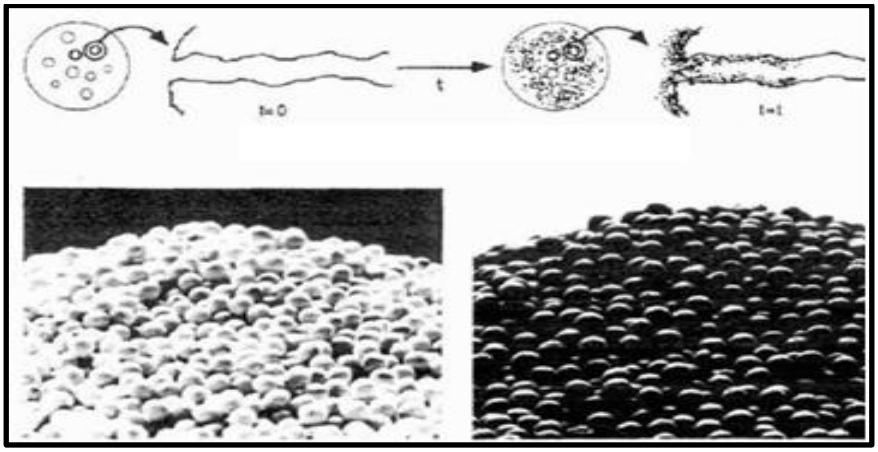

Figure 15 - Carbon Deposition on Surface and Inside Caverns (Fogler, 2005)

Carbon deposition is strongly affected by the presence of sulphur and aromatic compounds. Aromatics increases carbon deposition far more than expected from their concentration in the fuel. Aromatics are cyclic, planar molecules with a ring of resonance bonds. They are far more stable and less reactive than other geometric or connective arrangements with the same set of atoms. Due to their low reactive properties, they serve as nucleation sites for the formation of polynuclear

coke compounds. Therefore, high temperatures are required to break the aromatic bonds (Fogler, 2005).

2.3.6.3 Poisoning

Poisoning occurs when the poisoning molecules are permanently chemisorbed to active sites on the catalyst, reducing the number of active sites for the main reactions. These poisoning molecules can either be a reactant, a product, or an impurity in the stream (Fogler, 2005). This mechanism is displayed in Figure 16.

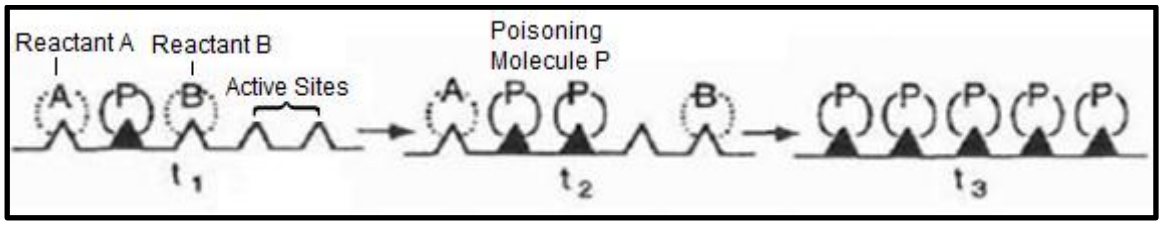

Figure 16 - Catalyst Poisoning Mechanism. Adapted from (Fogler, 2005)

Sulphur and its various compositions are dangerous to metallic compounds. They easily chemisorb themselves to active sites and can corrode metals. The main problem with sulphur poisoning is that its effects are cumulative. Even low levels of sulphur can deactivate a reforming catalyst over time (Forzatti & Lietti, 1999).

Research articles focusing on methanol steam reforming do not discuss the quality of methanol used and the effect that the impurities can have. Methane reforming often has sulphur based impurities and would be the best way in which to describe the effects of sulphur poisoning on a catalyst. A study presented by Forzatti and Lietti (1999) discussed the progression of sulphur poisoning over time on the catalyst. Between 0.5 hours and 3.5 hours, the concentrations of hydrogen yield and carbon monoxide decrease significantly along the reformer length as displayed by Figure 17. Even sulphur concentrations as small as 20 ppb can significantly decrease catalytic activity over a wide variety of catalyst materials. This effect is displayed in Figure 18.

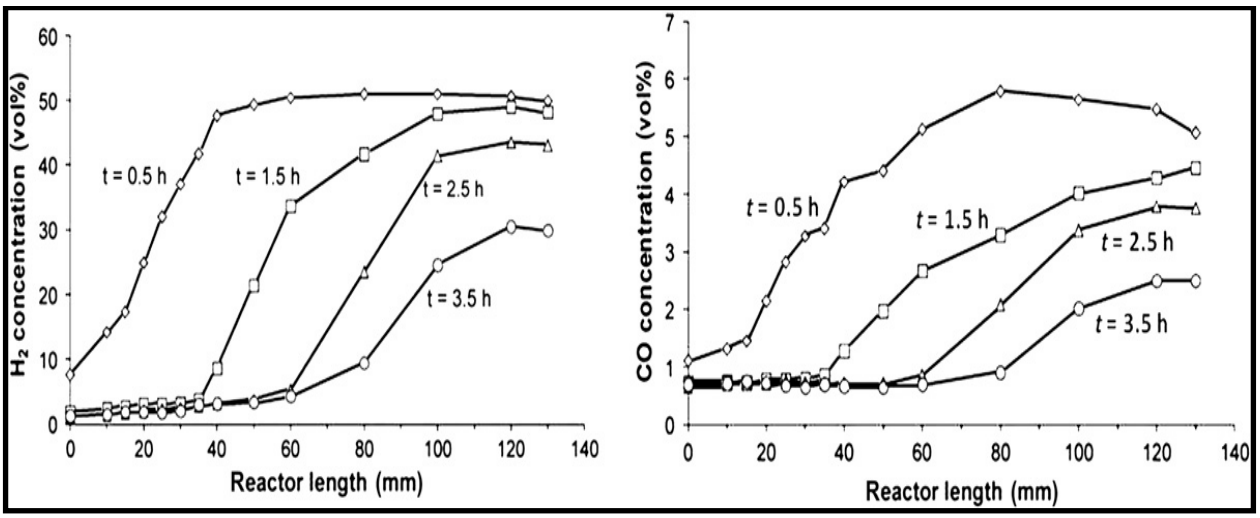

Figure 17 - Poisoning of Methane Reformer (Forzatti & Lietti, 1999)

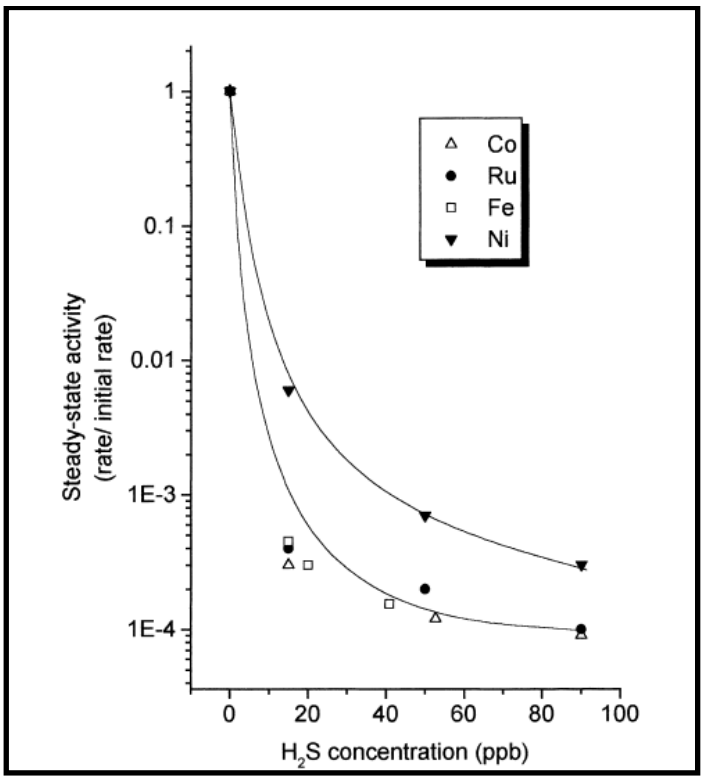

Figure 18 - H_2S Poisoning of various catalysts (Forzatti & Lietti, 1999)

Similar experiments are done with 1000ppm to poison different material based catalysts faster. This indicates that research is currently focused on reducing the effects of sulphur and quantifying its effects instead of comparing its effects to the quality of fuel used.

Sulphur is not the only poisonous impurity that can be found in hydrocarbon fuels used in reforming. As discussed in Section 2.1, chlorine is also a corrosive impurity found in methanol.

For the steam reforming of methanol, copper-based catalysts are used due to high H_2 generation, however, are very prone to chlorine and sulphur poisoning. Similarly, components further downstream in the fuel cell system are also susceptible to chlorine, sulphur, and carbon monoxide poisoning.

2.4 Membranes

Membranes are a semi-permeable material that allows the passage of certain molecules, either by the restriction of pore size to the physical size of the molecule or by charging the membrane to allow the flow of certain ions.

This is useful for the filtering and purifying of liquids and gases. In the case of a fuel cell system, a membrane would separate the hydrogen product from the reformate as the mixture exits the reformer.

Palladium membranes are the most viable option for hydrogen production due to their high selectivity of hydrogen. Palladium membranes are also the most often used in the industry when it comes to hydrogen recovery and purification (NCHT, 2010). However, palladium is extremely sensitive to CO and HCl and is rapidly poisoned with only a few parts per billion of H_2S (NCHT, 2010). All of those poisons can form part of the exhaust gases produced by a methanol steam reformer due to carbon monoxide being a by-product of the reforming process, and the trace amounts of sulphur and chlorine that be found in methanol as discussed in 2.1.

After the hydrogen has been purified by the membrane, it passes to a fuel cell that will utilise it to produce electrical energy.

2.5 Fuel Cells

There are a number of different fuel cell types each with different operating conditions, catalyst materials, and electrolytes, depending on the fuel being used to generate electricity. The most common is the Polymer Electrolyte Membrane (PEM) which is discussed below.

The PEMFC uses a membrane as an electrolyte, and operates at low temperatures, under 80˚C, allowing for quick start-up. This is beneficial for the automotive industry that would require a non-continuous power supply. However, the low temperature only allows it to use pure hydrogen as a

fuel and cannot perform internal reforming, as well as only being able to use platinum as a catalyst. Figure 19 displays the process of the PEMFC.

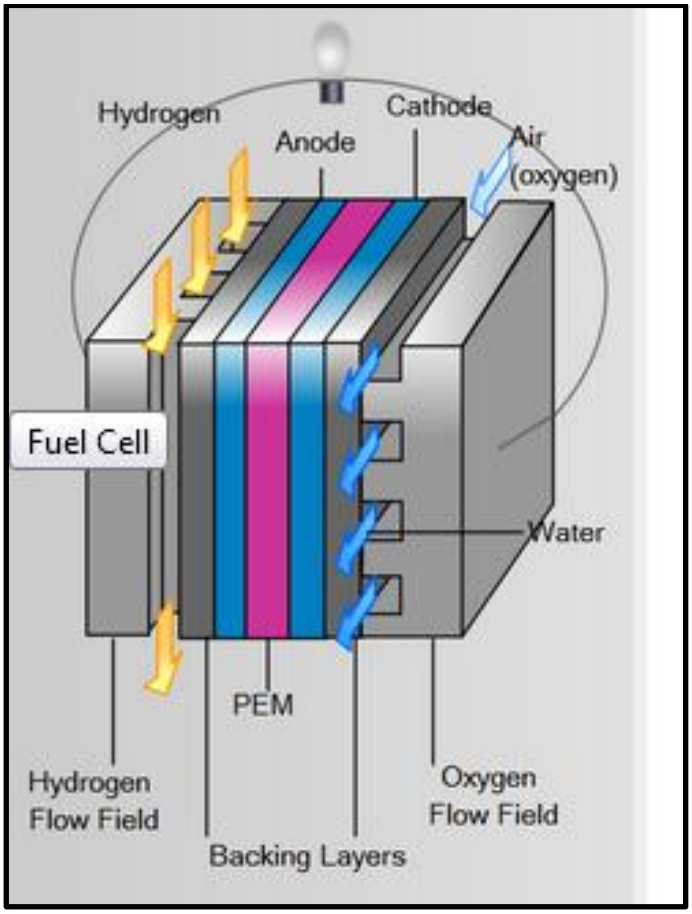

Figure 19 - PEMFC Flow Diagram (Hydrogenics, 2019)

The anode catalyst is where the oxidation reaction occurs where the hydrogen gives off an electron which flows toward the cathode. The now positively charged hydrogen ions pass through the electrolyte toward the cathode catalyst where the reduction process takes place. The hydrogen and the oxygen react with the electron, closing the circuit, and forming water as a product (Hydrogenics, 2019).

The reactions are:

Oxidation: $2H_2 \rightarrow 4H^+ + 4e^-$

Reduction: $4H^+ + O_2 + 4e^- \rightarrow 2H_2O$

Similar to the palladium membrane, the platinum catalyst used by a PEM fuel cell is very sensitive to carbon monoxide. It can only tolerate 10 to 100 ppm of carbon monoxide before showing signs of deactivation and will also be susceptible to H_2S and HCl poisoning (Matthey, 2017).

2.6 Exhaust Gases

Due to membranes and fuel cell catalysts being sensitive to poisoning and deactivation, the off-gases from the reformer must be well monitored, especially if an attempt is made to use lower quality methanol as a fuel source.

The study presented by Purnama (2003) investigates the various off-gases of a methanol steam reformer and concentrations of each gas. It was found that as reforming time increases the concentrations of methanol and water decrease while the concentrations of H_2, CO_2, and CO increase. The expected partial pressure for H_2, CO_2, and CO is 0.7 kPa, 0.23 kPa, and 0.02 kPa respectively. This can be converted to a mole percentage of 73.68 % of H_2, 24.22 % of CO_2, and 2.1 % of CO. This is displayed by Figure 20.

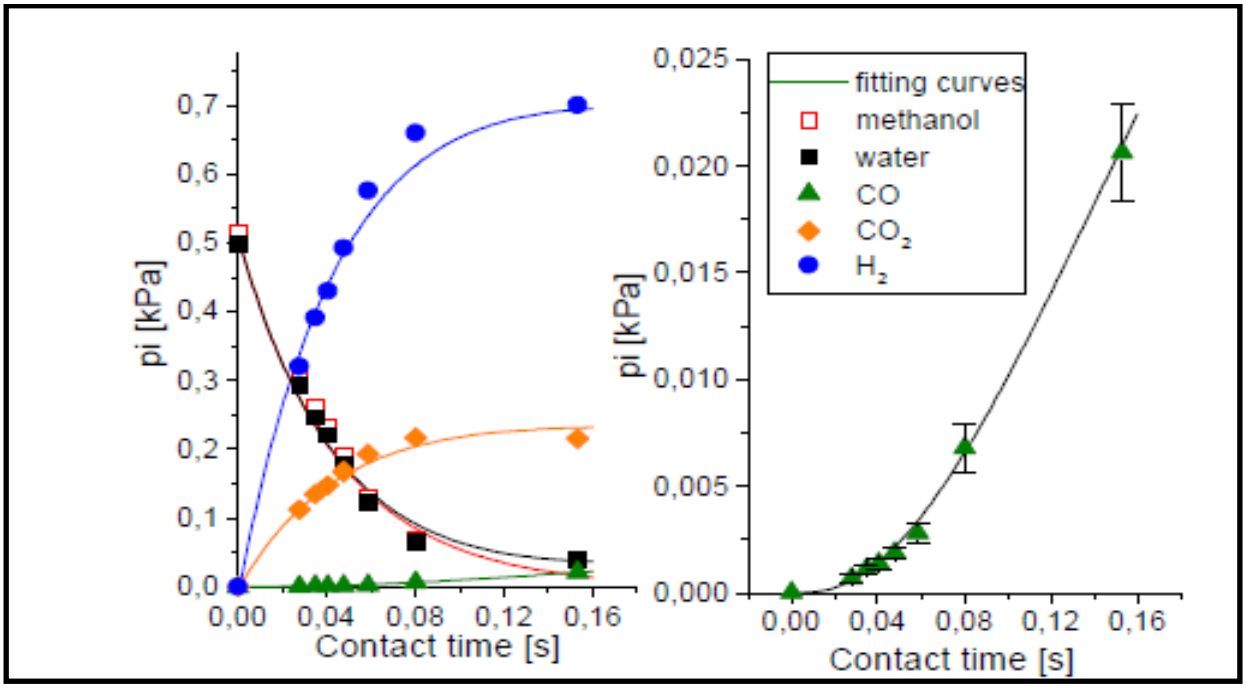

Figure 20 - Hydrogen, CO2, CO production (Purnama, 2003)

The study presented by Lee *et al.* (2004) discussed the off-gases in terms of the amount of carbon monoxide produced dependent on the water concentration in the fuel. The CO mol% is at its lowest at 0.3 mol% for 30 mol% of water as displayed in Figure 21.

Experiments done by Kurr *et al.* (2008) display similar gas compositions to Purnama (2003) with Kurr *et al.* (2008) presenting the off-gases for their reformer while using commercial catalyst, CZA-1, as H_2 of 75.23 mol%, CO_2 of 24.67 mol%, and CO of 0.11 mol%.

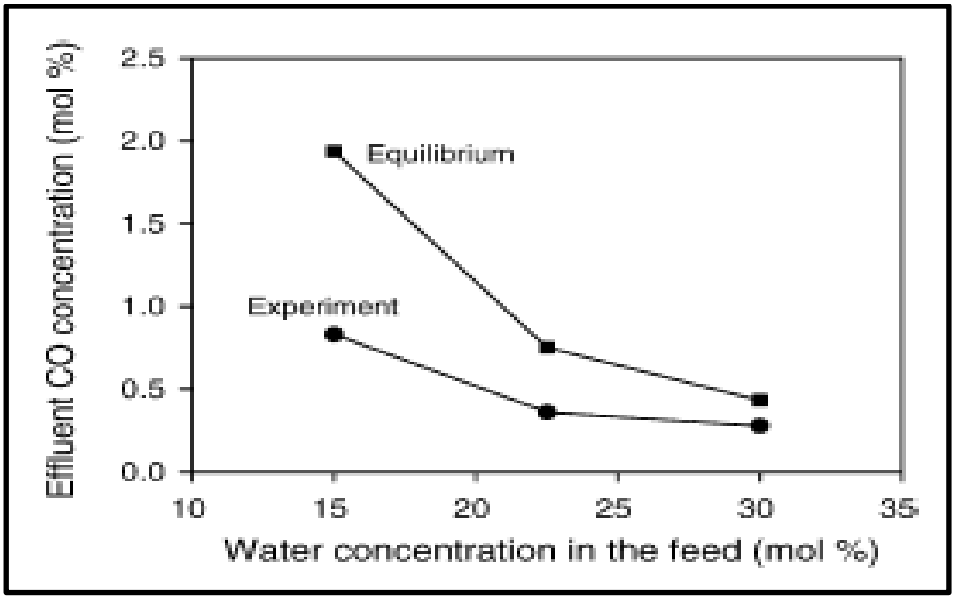

Figure 21 - Carbon Monoxide Production as a Function of Water Concentration (Lee *et al.*, 2004)

As discussed in 2.3.5, as the reacting temperature increases, the amount of methanol conversion increases, however, the water-gas shift reaction is an exothermic reaction and the higher the temperature the more difficult it is for this reaction to take place and could slightly reverse it, allowing for molecules of carbon monoxide to not take part in the water-gas shift reaction.

This phenomenon is discussed by the research presented by Sá *et al.* (2011). As the temperature increased from 200 °C to 300 °C, the concentration of carbon monoxide increased from 0 mol% to nearly 2.6 mol% as displayed by Figure 22.

A similar effect was displayed by Kim *et al.* (2016) where the carbon monoxide production increased from 0 % at 190 °C to a maximum of 1.7 % at 300 °C. This is displayed in Figure 23.

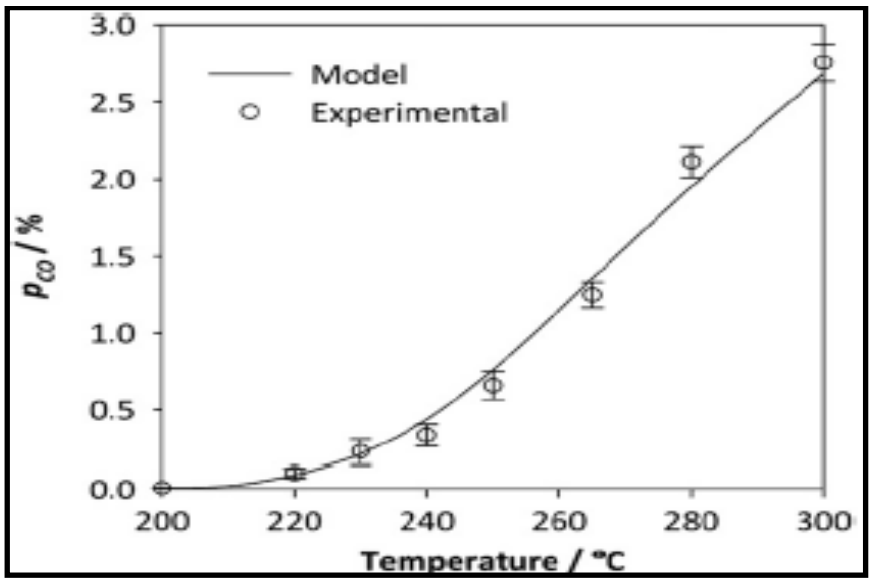

Figure 22 - Temperature vs CO Concentration mol% (Sá *et al.*, 2011)

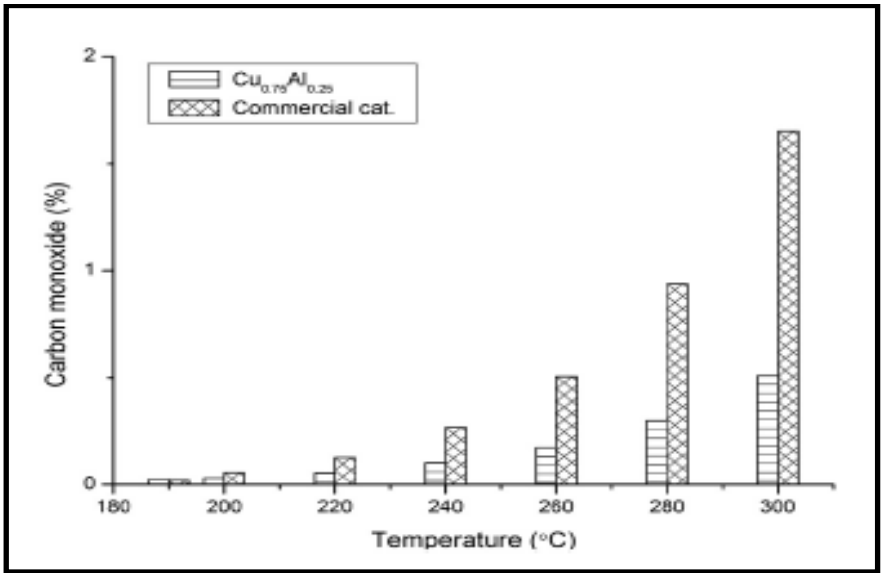

Figure 23 - CO vs Temperature (Kim *et al.*, 2016)

It is important to note that over the range of different catalysts and studies, the methanol conversion differs, however, the product composition remains reasonably constant. Both Purnama (2003) and Kurr *et al.* (2008) have similar gas composition results due to the reactions adhering to stoichiometry.

As briefly discussed in Section 2.2, the stoichiometric reaction equations, along with their mole balances, are as follows:

$$2CH_3OH + H_2O \leftrightarrows 5H_2 + CO_2 + CO \quad (2.1)$$

$$2(32.04) + 18.02 \leftrightarrows 5(2) + 44.01 + 28.01$$

$$CO + H_2O \leftrightarrows H_2 + CO_2 \quad (2.2)$$

$$28.01 + 18.02 \leftrightarrows 2 + 44.01$$

This dictates a mol percentage of 75 % H_2, 25 % CO_2 without any CO. However, due to variations in fuel water content and higher temperatures affecting the water-gas shift reaction, CO will appear in the off-gas.

Hydrogen, carbon dioxide, and carbon monoxide are readily analysed by a Gas Chromatograph (GC), as long as it is calibrated for those specific gases. However, hydrogen sulphide is not as easily detected and measured. The expected concentrations of H_2S and HCl are too small for a GC to quantify and could damage the GC in higher concentrations, therefore different methods of detection must be attempted.

2.6.1 Measurement of Hydrogen Sulphide

Despite the known poisons to catalyst, membrane, and fuel cell materials, none of the above sources mention the possible presence of poisons that could be found inside the methanol or the water. Due to the sensitivity of membranes and metal compounds to hydrogen sulphide, the presence of H_2S must be considered. The detection and measurement of H_2S concentrations can be done by various methods.

The company, *Liquid Gas Analysers* is a common name in the gas industry. Their gas sensors can measure in the single digit ppb to 500 ppm range (Anon, 2017). This equipment is, however, very expensive. Draeger tubes are prevalent in a chemistry laboratory. A disposable small glass vial is filled with reagents that change colour as the concentration of hydrogen sulphide increases.

The doctor test is also often used in a chemistry laboratory. Passing gas across filter paper wetted with aqueous lead oxide, lead acetate, or lead nitrate solution and observing a colour change. Lead oxide has a lower detection limit for concentrations from 0.5 ppm to 8 ppm turning the paper dark brown or black according to the concentration of H_2S (Moore & Spitler, 2003). However, this reaction takes time, whereas a lead acetate indicator has much faster reaction times and has a lower detection limit of 50-60 ppb making it much more sensitive (Bethea, 2012).

2.6.2 Measurement of Hydrochloric Acid

Another poison which metal membranes and fuel cell catalysts are very sensitive to is hydrochloric acid. This is something that could be formed due to chloride ions in the methanol or even water if the water is not pure. Chloride products would not be readily found as a gas phase and when in contact with moisture will rapidly form hydrochloric acid which is a liquid at room temperature. Therefore, it will be required to test the liquid components of the reformer off-gases.

A possible detection and measurement method could be titration. Titration will use known concentrations of a titrant and an indicator to observe a change in the colour of the indicator as the titrant is slowly added to it. By reading the volume of titrant left over, the concentration of the titrand can be determined from the volume used during the titraion. This is a very accurate method, however, it is also a very time consuming process.

It is well known that any form of chloride products are acidic, therefore, a pH strip test can be done to determine if there is enough HCl to create a change in the pH value. Although not very accurate, it is a quick and easy procedure to implement and read.

2.7 Summary

In Chapter 2, the details of hydrocarbon fuels were discussed as well as the fact that methanol is favoured above other hydrocarbons for the production of hydrogen due to its availability, transportability, low toxicity, low evaporation temperatures, and low reforming temperatures. Reformers were discussed in general and it was concluded that steam reformers, although requiring reasonable heat energy, provide the best hydrogen production. The catalyst reaction process was discussed and it was decided that the commercial $Cu/ZnO/Al_2O_3$ catalyst for methanol steam reforming will be focused on during this study due to it being commonly used in the industry and the majority of studies. The precise composition and physical properties of commercial catalyst, and catalyst used by other studies, was investigated and found to be near 60 %Cu, 30 %ZnO, and 10 $\%Al_2O_3$; with BET surface areas between 64 m^2g^{-1} and 90.8 m^2g^{-1}, average pore radii between 8 nm and 15.015 nm, and pore volume of 0.578 cm^3g^{-1}.

Furthermore, the methanol conversion of the catalyst was discussed and it was concluded that the higher the temperature of the reformer, the higher the methanol conversion will be to a maximum of 300 °C due to potential sintering to the catalyst for temperatures above 300 °C. It was also evident that as the flow rate decreases there is more time for adsorption to take place, increasing methanol conversion, and concluded that a WHSV between $0.75h^{-1}$ and $2h^{-1}$ is optimal.

Deactivation of catalyst and the damage of metallic membrane filters along with PEM fuel cell catalysts due to H_2S and HCl poisoning was discussed along with methods to detect and measure the concentrations that may be found in the off-gases. Lead acetate indicator paper will be used for the detection and measurement of H_2S and pH strips will be implemented to measure the acidity of the off-gas condensate for the detection of HCl.

The quantities of hydrogen, carbon dioxide, and carbon monoxide provided by literature were similar to stoichiometry of H_2 75 mol%, CO_2 25 mol%; and CO being anywhere between 0.3mol% to 2.6 mol% depending on reacting temperatures and methanol-water molar ratio. These products can readily be measured by a gas chromatograph. However, it was noticed that the studies did not indicate the requirement of measuring H_2S or HCl which may be present in the reforming product from the impurities in the methanol. Furthermore, the catalyst used in literature was not analysed after the experimentation was concluded and no information is available in terms of the change in catalyst topology, possible poisoning, and carbon deposition.

For the purposes of this study, suspecting the presence of sulphur and chlorine ions in the methanol-water mixture, the catalyst will be analysed for the presence of chemisorbed poisons to supplement the results from the above mentioned methods for off-gas analysis of H_2S and HCl. Furthermore, the influence of the sulphur and chlorine poisons, related to the methanol fuel quality will be considered.

CHAPTER 3 - DESIGN AND IMPLEMENTATION

Chapter 3 will discuss the design of the fuel qualifying experimental facility used to address the problem statement of this study. The experimental process will be a batch process, each batch operating with a different methanol quality. The methanol and water will be mixed in a molar ratio of 1:1.1, as prescribed by Hydro-Plus, and supplied to an evaporator to evaporate the methanol-water mixture into the reformer. The reformer off-gases are to be cooled and condensate separated from the product gases. Both the condensate and product gases are to be collected and sampled, along with catalyst samples.

3.1 Design Outcomes and Requirements

From the information gathered in Chapter 2, the design outcomes for the fuel qualifying experimental facility and subsequent design requirements to obtain the design outcomes for the addressing of the problem statement are as follows:

1. The controlled delivery of methanol-water mixture to the methanol steam reformer.
    1.1. The delivery of a methanol-water mixture at a controlled and constant flowrate.
    1.2. The maintaining of constant methanol:water molar ratio of 1:1.1. The evaporator was required to evaporate a flow rate of 193 gh^{-1} of fuel while maintaining a temperature of 200 °C.
2. The controlled reaction kinetics of the methanol steam reformer.
    2.1. The reformer contained 140 g of catalyst where the catalyst and reformer was required to be brought up to a temperature of 300 °C and uniformly maintained at this temperature during experimentation.
    2.2. The produced catalyst was required to conform to the composition and physical properties of the commercial catalyst described in literature.
3. The automated setting and control of the temperatures of the fuel delivery method and the reformer.
    3.1. Monitoring of thermal distribution of the fuel qualifying experimental setup.
    3.2. The manner in which the experimental setup controls the temperatures was required to be automated and temperature data continuously logged and saved in an accessible format.
4. The complete separation of the off-gas condensate from the gas products and sampling of both reformer off-gas components.

4.1. Ambient temperatures of 25 °C would be sufficient to fully condense methanol and water to a liquid phase.

4.2. The collection of condensate in such a manner as to be able to sample and analyse without interrupting experimentation.

5. Sampling of catalyst after experimentation.

5.1. Ease of access to the catalyst.

For each design outcome, the long experimentation durations dictated materials that can withstand, as well as resist the corrosive properties of a methanol and water mixture. Consideration also had to be made for the production of hydrogen at high temperatures creating a flammable environment and the presence of asphyxiation gases such as carbon dioxide and carbon monoxide products as well as a purging gas. The Hazard Identification and Risk Assessment for the fuel qualifying experimental facility can be found in Appendix B.

It was a design requirement to perform methanol reforming with 140 g of catalyst as it will be substantially more than the amount of catalyst used in literature. This decision was made to allow for higher methanol mass flows and provide a larger sample size for poisons to be identified more easily, either in the off-gas of the reformer or poisons on the catalyst. The mass flow of methanol-water mixture was fixed at 193 gh^{-1}.

3.2 System Layout Overview

The fuel qualifying experimental facility includes the following subsystems:

- Fuel Delivery and Processing subsystem
- Reformer subsystem
- Off-gas Processing and Sampling subsystem

A simple flow diagram can be used displaying the Fuel Delivery and Processing subsystem, the Reformer subsystem, and the Off-gas Processing and Sampling subsystem. It also displays the components requiring heat energy applied and removed as dictated by the design requirements.

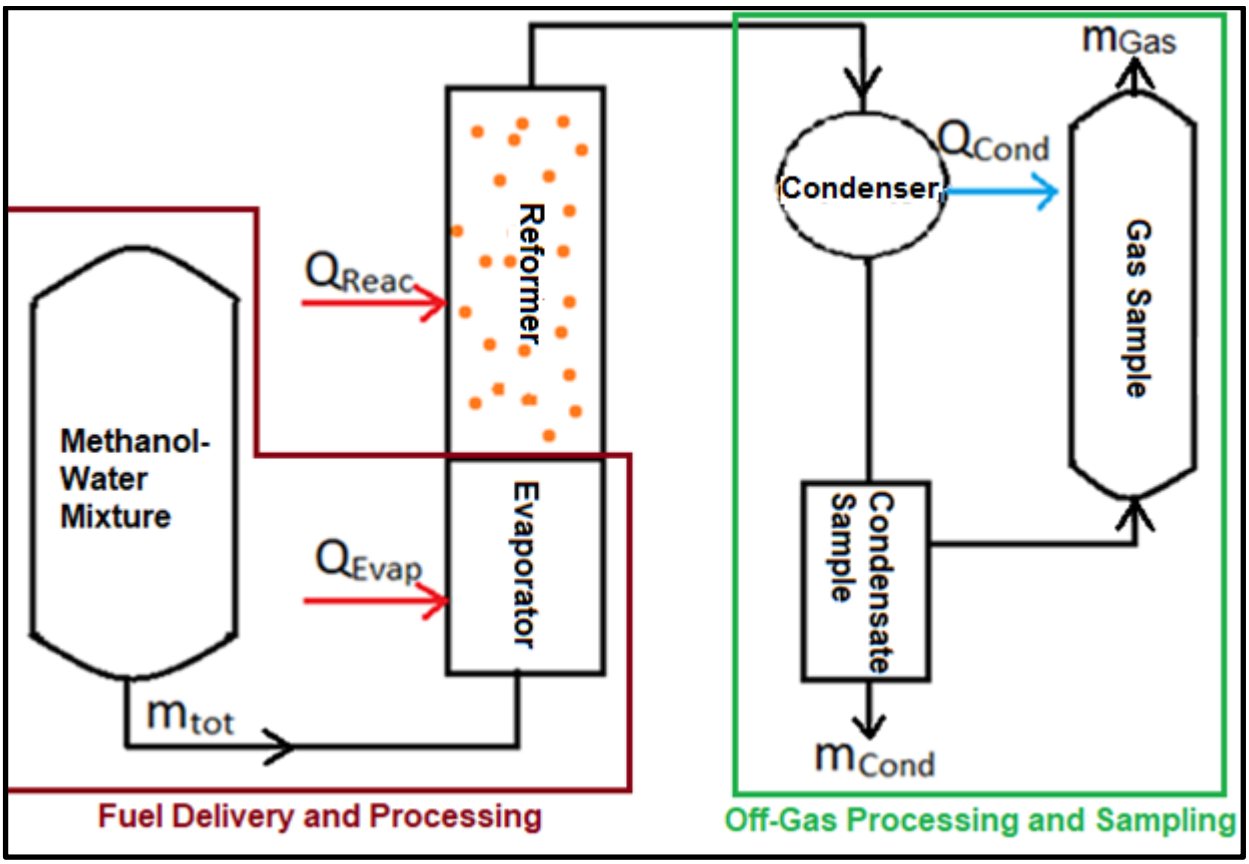

Figure 24 - Fuel Qualifying Experimental Facility Layout

In order to reduce the chance of separation of the methanol from the water vapour and ensure minimal fluid heat loss, the reformer was positioned directly above the evaporator. For better catalyst bed packing and gas flow, the reformer was positioned vertically. The condenser coil was also positioned vertically to avoid condensate build-up. The condensate sampler bleed-off was positioned directly below it to collect as much condensate as possible for result accuracy. The gas flow from the condensate sampler to the gas sampler was located high above the condensate to avoid fluids in the gas stream.

3.2.1 Piping and Instrumentation Diagram

Figure 25 displays the piping and instrumentation diagram (P&ID) of the system, a more detailed version of Figure 24. It includes the inlet and required outlet operating temperatures and pressures, as well as the interfacing components required namely valves (V1, V4, V5, V6, V7, and V8), pressure controllers (V2 and V3), and relief valves (V9 and V10). Sampling points have been indicated.

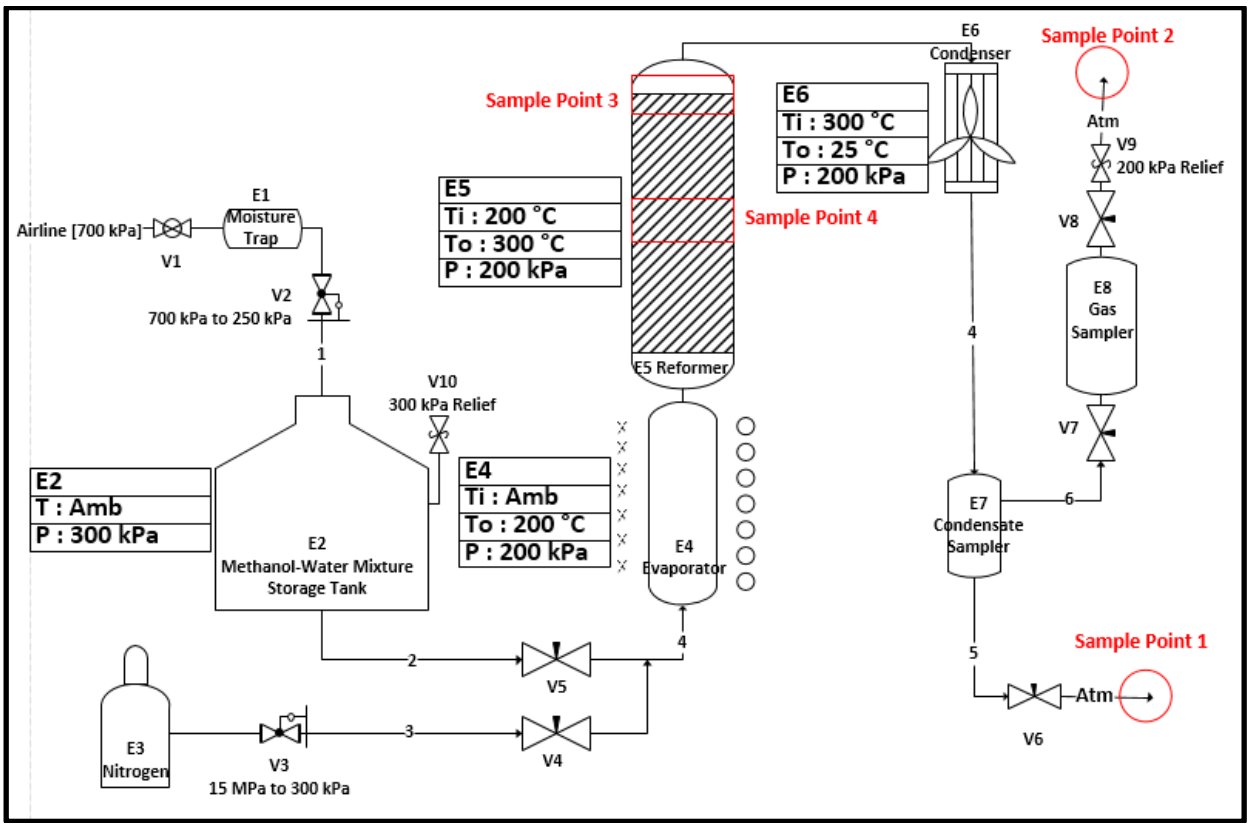

Figure 25 - P&ID of Fuel Qualifying Experimental Facility Layout

The pressurised air-line received a connection point and a shutoff valve, V1, along with a moisture trap, E1, to remove moisture from the air. The air compressor supplied air at a maximum of 700 kPa which was reduced to the required 250 kPa by reducer valve V2. V10 relief valve was installed onto the tank and set to 300 kPa for safety.

The system was purged with nitrogen from Nitrogen Tank, E3. The nitrogen bottle was supplied pressurised to 15 MPa and required the pressure controller, V3, to reduce the pressure to 300kPa. Both the methanol-water tank, E2, and the nitrogen tank, E3, had valves, V5 and V6 respectively to start and stop the supply of their respective contents.

Once the fuel supply valve V5 had been opened, the evaporator E4 was required to heat and vapourise the methanol-water mixture from ambient temperature to vapourisation temperature and was required to maintain a temperature of 200 °C to supply the reformer, E5, with superheated vapourised methanol and steam in the correct molar ratio of 1:1.1.

The reformer, E5, was required to maintain a catalytic temperature of 300 °C allowing for good reaction kinetics as discussed in Section 2.3.5. The top of the reformer was the third sampling point where catalyst was removed after a certain time interval. At the end of each experiment life

cycle, a catalyst sample could be removed from the centre of the reformer and used as Sample Point 4.

The condenser, E6, was required to cool the outlet gases from an estimated outlet temperature of 300 °C to ambient temperature and separate the unreformed methanol and water from the product gases. The condensate was collected in the condensate sampler, E7, and analysed as it was considered part of the reformer off-gas. The outlet of the condensate sampler through valve V6 along line number 5 was Sample Point 1.

With the condensate having been separated from the gas product stream, the gases followed line number 6 and were captured in the gas sampler E8. The pressure relief valve V9 at the outlet of the system kept the system at 200 kPa allowing for the continuous flow from the fuel storage tank E2 along line number 4 into the evaporator E4. The outlet of the pressure relief valve V9 was Sample Point 2 to analyse the outlet product gases.

3.3 Detailed Design

The detailed design of each subsystem and its components are discussed below. This includes the Fuel Delivery and Processing, Reformer, Temperature Control and Recording, and Off-gas Processing and Sampling.

Ambient conditions are assumed to be 25 °C and 100 kPa.

3.3.1 Fuel Delivery and Processing Subsystem

The fuel delivery and processing consisted of the mass flow controlling of the methanol and water mixture to the evaporator and the evaporation method to vapourise the methanol and water mixture.

The stainless steel methanol-water storage tank required a connection to the air supply line number 1 as well as a fitting to fill up the tank and a fitting to supply fluids to the evaporator along line number 2. Quick fittings and nylon pipes were used to connect all of the components because they are resistant to methanol corrosion as well as being readily available and easy to use for high pressure applications.

As can be seen in Figure 25, a needle valve V5 was implemented between the tank and the evaporator to control the mass flow rate of the fluid accurately. The air pressure and the position of

the needle valve were adjusted simultaneously until the necessary flow rate for the methanol water mixture was reached.

By controlling the safety relief valve seen in Figure 25 as V9 at the outlet of the gas sampler, the pressure difference between the fluid pressure and pressure of the system was kept constant to keep the mass flow constant.

A selection process was undertaken to determine the best method of evaporating a methanol-water mixture. This process can be found in Appendix F. The evaporation method that was selected is discussed below.

As displayed in Figure 26, an induction heater coil was implemented around a pipe to heat the external wall by induction. The heat generated conducts towards the inner wall and conducts further to a cone.

In order to spread out the flow, the pipe in the centre has four 1mm diameter holes through which the methanol-water mixture flows and exits onto the heated large surface area and flash evaporates. The outer pipe diameter was selected through an experimental process described in Appendix G. It was concluded that thin walled stainless steel dairy tubing with a diameter of 44mm and wall thickness of 1.5mm was ideal for the induction heater.

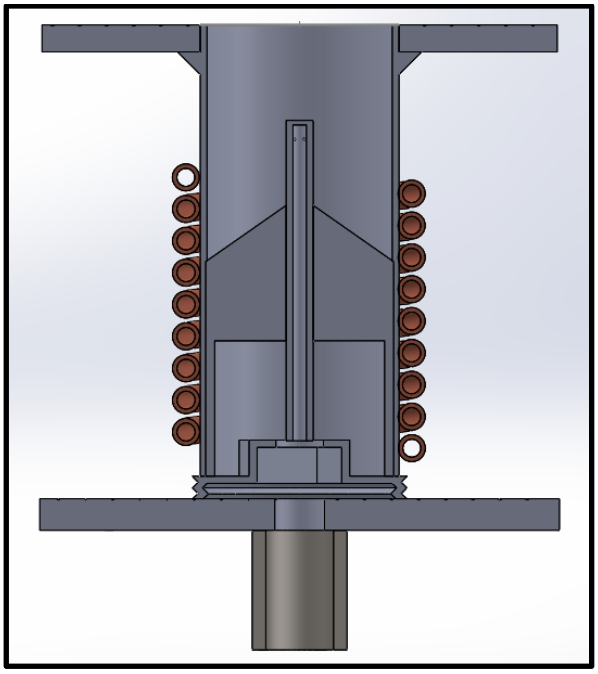

Figure 26 - Evaporator Design Cross-section

Due to methanol and water's corrosive properties, stainless steel was selected. Stainless steel 316L was selected due to its weldability and high resistance to electrical conductance which will cause a rapid heat increase in an induction heater.

3.3.2 Reformer Subsystem

The reformer subsystem description includes the reformer dimensions and heat transfer model, along with the heating method used. The catalyst manufacturing method is described thereafter.

The reformer diameter was selected to that which is the most similar to the diameter of the evaporator. An outer diameter of 33.4 mm was selected with wall thickness of Schedule 10, 2.77 mm, for easier welding.

According to the specifications of catalyst by Sá *et al.* (2011), the $Cu/ZnO/Al_2O_3$ catalyst has the following properties:

$\rho_{catalyst}$ = 2400 kgm^{-3}

$void$ =1.63

Catalyst of 140 g therefore, had a volume of:

$$m_{catalyst} = Vol_{catalyst} \times \rho_{catalyst} \tag{3.2}$$

$$Vol_{catalyst} = \left(\frac{m_{catalyst}}{\rho_{catalyst}}\right) \times (1 + void)$$

$$Vol_{catalyst} = \left(\frac{0.14}{2400}\right) \times (1 + 1.63)$$

$$Vol_{catalyst} = 0.00015342\ m^3$$

A NB32 Sc10 pipe (outer diameter of 33.4 mm and 2.77 mm thickness) was used.

$$L = \frac{Vol_{catalyst}}{\pi \times \left(\frac{Di}{2}\right)^2} \tag{3.3}$$

$$L = \frac{0.00015312}{\pi \times \left(\frac{0.02786}{2}\right)^2}$$

$$L = 0.25\ m$$

Therefore, the reformer was to be at least 250 mm long.

316L stainless steel flanges were used for ease of assembly between the evaporator and reformer as well as the top of the reformer for removal of catalyst. Flange interfaces were sealed with a high temperature rubber, formed and vulcanised to be resistant up to and above 400 °C and is very resistant to chemical corrosion. The sealing of threads was with HPTFE plumbers tape. It has an operating temperature of 260 °C. At temperature areas higher than the operating temperatures, more layers of HPTFE tape were applied so that small amounts of it burned away and that which was left ensured the seal. For complete reformer catalytic bed temperature monitoring, nine temperature sensors were installed. Three in the centre top, middle, and bottom; and the other six are staggered around the inner surface of the reformer. Figure 27 displays the cross-sectional representation of the reformer with the temperature sensors inside the thermo-wells.

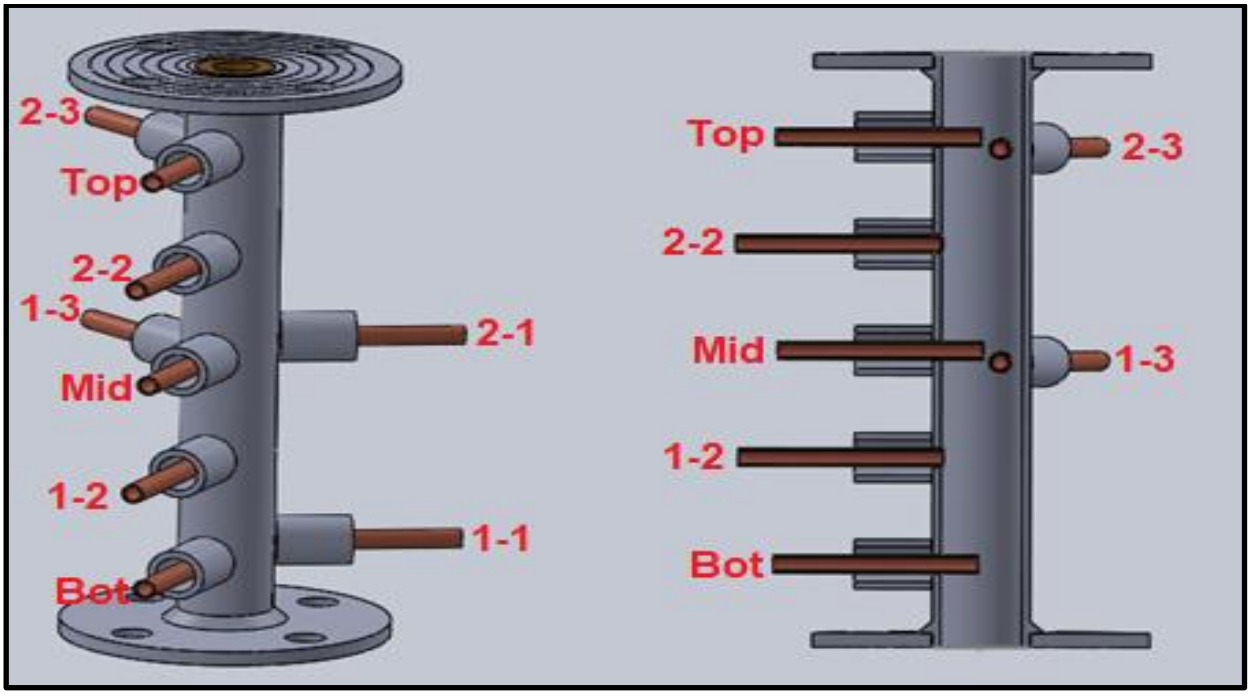

Figure 27 - Reformer Layout and Cross-section

For continuity, the same material was selected for the reformer as for the evaporator. Stainless steel 316L is corrosion and chemical resistant with excellent welding properties and negates the effects of hydrogen weld embrittlement. It would, therefore, not interfere with the catalyst reactions. Copper was used for the thermo-wells due to its high thermal conductivity allowing for higher heat transfer between the gas and the thermocouple.

3.3.2.1 Catalyst Manufacture

As discussed in 2.3.3, the focus of this study was on the commercial $Cu/ZnO/Al_2O_3$ catalyst which dictated the following composition:

- CuO = 60%
- ZnO = 30%
- Al_2O_3 = 10%

The manufacturing method used, was an amalgamation of the methods described by Hammoud *et al.* (2014), Kim *et al.* (2016), Kurr *et al.* (2008), and Prasetyaningsih *et al.* (2016).

A precipitation method of the various nitrates was used to obtain the required carbonates. A co-precipitation method was used to give the precipitates an intimate bond and laminar structure. In order to ensure all the products were precipitated so that the weight ratios were correct, as well as to create an active catalyst the pH was adjusted to 10 by the addition of NaOH. The product carbonates were then crushed and calcined at 400 °C to produce the required oxides. Copper oxide was reduced in a hydrogen flow rate of 10.95 $lmin^{-1}$ to convert CuO to Cu. The catalyst manufacturing process and activation oven is described in more detail in Appendix C and Appendix D respectively.

The reactions were as follows:

$2Cu(NO_3)_2 + 2Na_2CO_3 + H_2O \rightleftarrows Cu_2CO_3(OH)_{2(s)}\downarrow + 2Na_2(NO_3)_2 + CO_2$

$Cu_2CO_3(OH)_2 + Heat \longrightarrow 2CuO + CO_2 + H_2O$

$Zn(NO_3)_2 + Na_2CO_3 \rightleftarrows ZnCO_{3(s)}\downarrow + 2(NaNO_3)$

$ZnCO_3 + Heat \longrightarrow ZnO + CO_2$

$2Al(NO_3)_3 + 3Na_2CO_3 + 3H_2O \rightleftarrows 2Al(OH_3)_{(s)}\downarrow + 6NaNO_3 + 3CO_2$

$2Al(OH)_3 + Heat \longrightarrow Al_2O_3 + 3H_2O$

$CuO + H_2 + Heat \longrightarrow Cu + H_2O$

Gloves, lab coat, and safety glasses were worn at all times to avoid chemical contact with the skin. Find the MSDS of the various chemicals used in Appendix C.

3.3.3 Temperature Control and Recording of Evaporator and Reformer

The electrical control of the reformer and evaporator was implemented using an Arduino Mega programmable microcontroller and was coded to control the temperature of the evaporator by opening a relay when it reached, or was above, 200 °C and to close the relay once it had fallen below 195 °C. The relay to the resistance wire around the reformer opened every time any one of the thermocouples displayed a value of 300 °C or above, and the relay closed once all the thermocouples temperature values had fallen below 297 °C. The temperatures were read and recorded directly into an Excel spread sheet for the verification of the system as well as to provide temperature data during the validation process of the methanol conversion and gas analysis, if required.

The coding of the Arduino can be found in Appendix I. The electrical P&ID diagram is displayed in Figure 28.

The same method was used to record the condenser outlet temperatures.

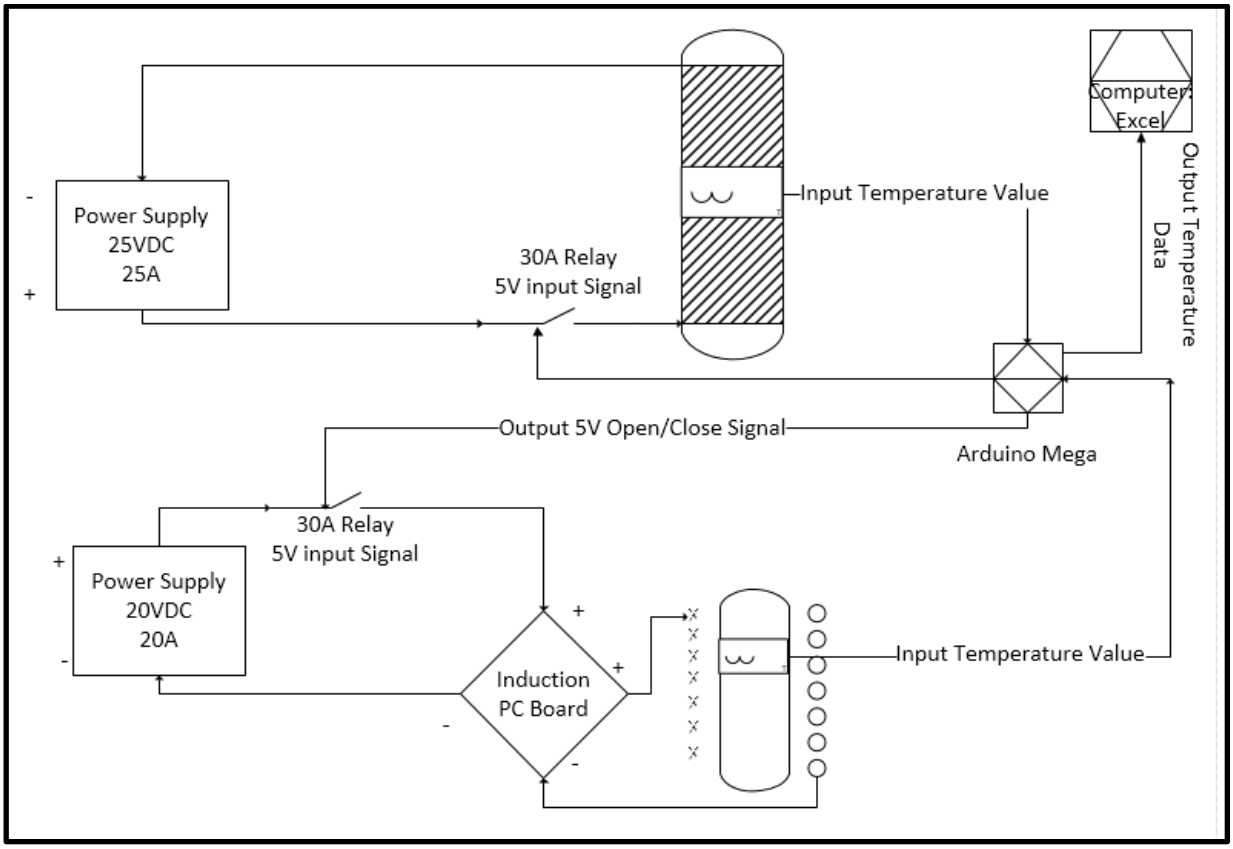

Figure 28 - P&ID Electrical Layout for Controlling and Recording of Reformer and Evaporator Heating Elements

3.3.4 Off-gas Processing and Sampling Subsystem

The off-gas processing and sampling subsystem description includes the condenser design and the off-gas sampling methods used.

The condenser was implemented as a vertical coil with convection cooling by a small fan and water used in a pipe-in-pipe heat exchanger. Stainless steel instrument tubing was used with an outer diameter of 6mm and an inner diameter of 2mm. This condenser was built and tested in Chapter 4.

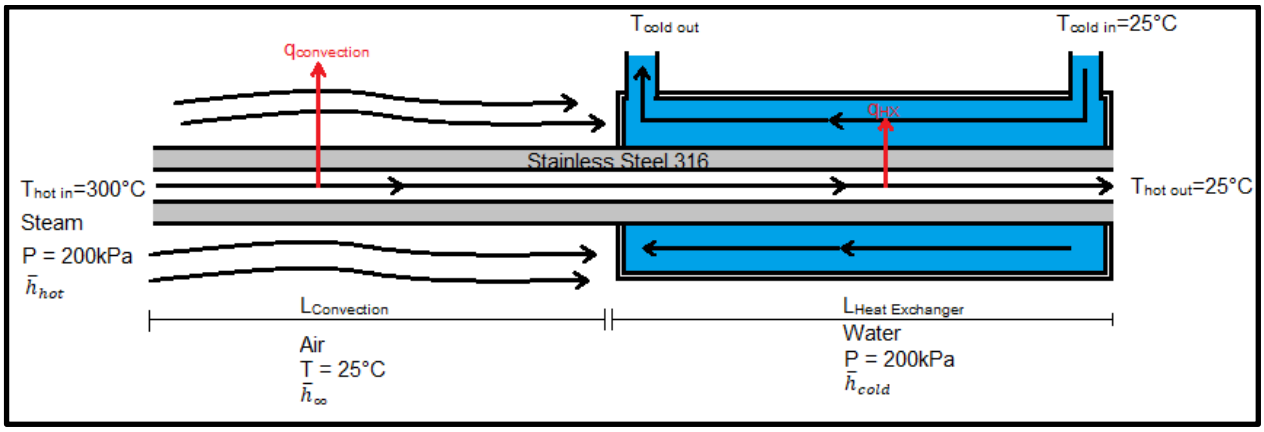

Figure 29 - Condenser Heat Transfer Model Diagram

A 500 ml polyethylene terephthalate (PET) cylinder was implemented to collect the methanol and water condensate with a valve at the outlet to bleed off condensate samples. PET is resistant to the effects of methanol and is able to maintain a pressure of 900 kPa. The condensate was sampled with a 20 ml pipette and weighed which provided the density of the sample which was used to determine the quantity of methanol in the sample. This quantity was compared to the ratio of methanol supplied to the evaporator and subsequently the methanol conversion that had taken place. Furthermore, the acidity of the condensate was measured every hour with the use of pH strips providing an indication for the presence of HCl.

Stainless steel pipe with domes and fittings welded on each end was used as a gas sampler. The domes prevent the possibility of gas particle build-up in corners as well as reducing stress concentrations. The volume of the gas sampler was taken from similar devices used in the industry and with an inner diameter of 36.66 mm and a length of 125 mm provides a volume of 131 ml providing more than sufficient volumes due to the gas chromatograph requiring very small volumes to analyse a gas sample. Valves were installed on each end into the fittings to remove the gas sampler for analysis.

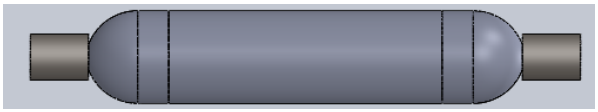

Figure 30 - Gas Sampler Representation

The fuel qualifying experimental facility was placed under an extraction hood for ventilation of the purging and product gases. The prescribed area in which the experimental facility would fit was taken into account in this layout

Figure 31 displays the physical layout of each component in the fuel qualifying experimental setup as well as the position of the valves, pressure gauges, and Sampling Points in association with the P&ID in Figure 25. The four sampling points are displayed as SP1, SP2, SP3, and SP4.

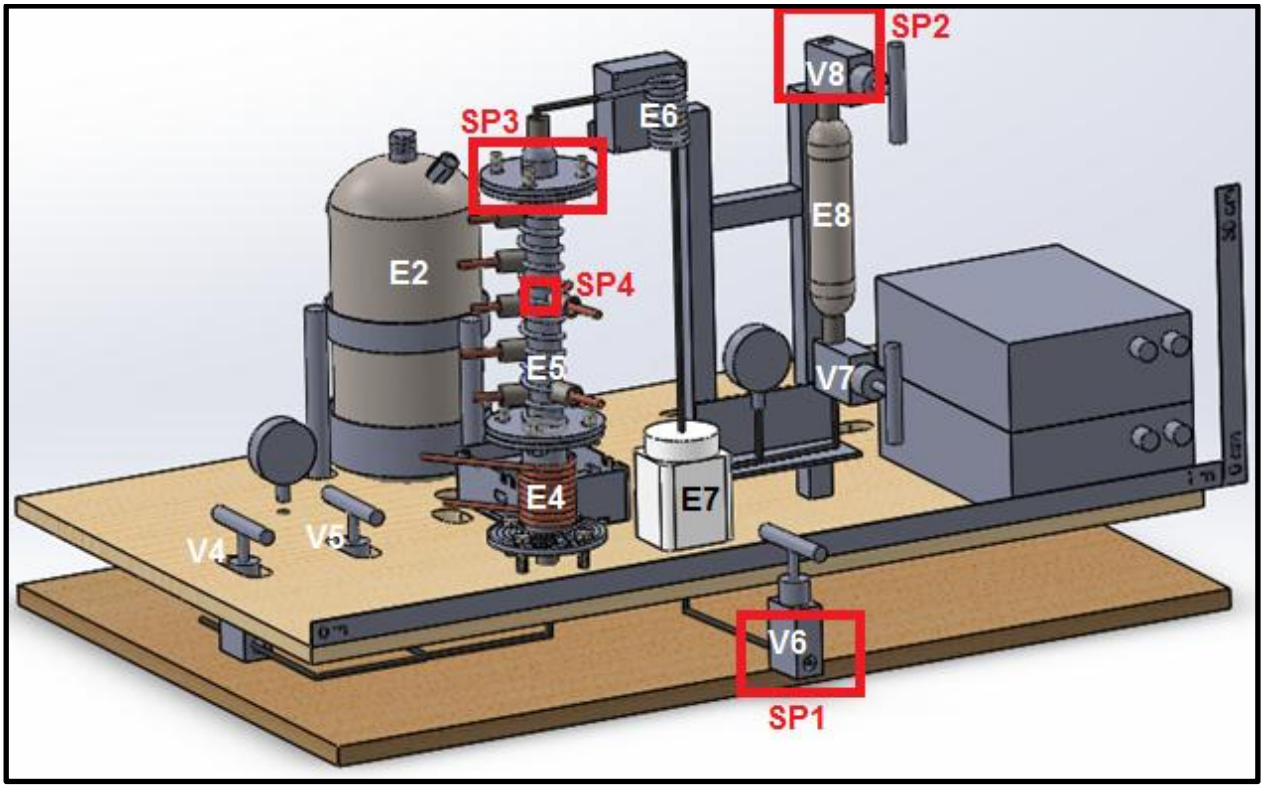

Figure 31 - Solidworks Representation of Fuel Qualifying Experimental Facility

3.4 Summary

In Chapter 3 the design outcomes and requirements of the method for addressing the problem statement were stipulated. The system overview was provided along with a detailed design of the fuel delivery and processing subsystem, the reformer subsystem, temperature control and recording, and off-gas processing and sampling subsystem and sampling methods. Material selection was discussed for each component. Using Solidworks CAD software, 3D assemblies were drawn and the component setup and layout was determined in the area prescribed by the extraction hood.

CHAPTER 4 - EVALUTION OF FUEL QUALIFYING EXPERIMENTAL FACILITY

In Chapter 4 the fuel qualifying experimental facility which was discussed and designed in Chapter 3 will be implemented and its effectiveness evaluated based on the design requirements stipulated. Data from the completed fuel qualifying experimental facility will be analysed and verified to determine if it operated as expected and if it is capable of providing reliable data required to address the problem statement as stated in Section 1.2. The various design requirements and evaluation methods of the fuel qualification experimental facility will be described. Each design requirement explains the reason for the requirement, along with the overview of the evaluation method. The results of the implementation and evaluation will be presented and discussed in the sections below. Verification will be done by comparing each design requirement determined in Chapter 3 to the experimental values gathered in Chapter 4. The design outcomes are achieved by the verification and acceptance of the design requirements. Any discrepancies will be reviewed in terms of its effects on the fuel qualification experimental facility's ability to provide reliable empirical data.

4.1 Evaluation Overview

The evaluation of the proposed design was done by the implementation of empirical procedures described below in Table 5. This determined each component's viability during the fuel qualification experimental facility experimentation process done in Chapter 5.

Table 5 - Design Evaluation Overview

Design Outcome	Design Requirement	Evaluation Method	Acceptance Criteria
Controlled Delivery of Methanol-water mixture to reformer	Flow rate consistency	10 minute flow measurement	3.75 $mlmin^{-1}$ $\pm$ 0.2 $mlmin^{-1}$
	Superheated Evaporator Temperature	Cold commissioning	200 °C$\pm$ 60 °C
	Evaporation method provides consistent Methanol:Water molar ratio	Cold Commissioning	1:1.1
Controlled Reaction Kinetics	Consistent reformer temperature & Uniform reformer temperature distribution	Hot commissioning	300 °C & Consistent Sector Temperatures
	Catalyst composition	EDS	CuO:60 %
			ZnO:30 %
			Al_2O_3:10 %
	Catalyst BET Surface Area and Pore Properties	BET N_2 adsorption	Compared to Literature
	Catalyst Topology	SEM Micrographs	Clay/Ceramic texture with laminar structure
	Catalyst Activity	Hot commissioning with $CaCO_3$	Turns lime water milky white
Off-gas liquid and gas separation	Condenser outlet temperature	Cold and Hot commissioning	25°C $\pm$ 10 °C
Sampling Ability	Sample condensate without interruption	Cold commissioning	No system pressure drop
	Catalyst sampling	Hot commissioning	Experimental method allows for catalyst sampling and replacement
Automated Control	Monitor-able and Accessible	Cold commissioning	Display all temperature data. Store in Microsoft accessible format
	Automated turning on/off of evaporator and reformer heating elements at set points	Cold commissioning	Relays successfully open and close continuously

4.2 Flow Rate Consistency

The flow rate of the methanol-water mixture is important due to the effect it has on the methanol conversion percentage as shown previously in literature. It is important to maintain a constant mass flow rate throughout the experimentation procedure for the controlled fuel delivery to the reformer.

The flow rate method described in Chapter 3 was evaluated by filling the storage tank displayed as E2 in the P&ID Figure 25 with the required methanol:water molar ratio of 1:1.1 and ensuring the air pressure to the tank was 50 kPa, which is the pre-set pressure difference between the fuel delivery subsystem, and the evaporator E4. The needle valve V5 was opened to the predetermined position with its outlet flowing into a small 50 ml measuring beaker with 0.2 ml accuracy for 10 minutes. The volumes measured after each minute interval are displayed below.

Table 6 - Flow Rate Consistency Measurement

Time [minutes]	Volume Measurement [ml]	Volumetric Flow Rate for Time Interval [$mlmin^{-1}$]
0	0.0	-
1	3.6	3.6
2	7.4	3.8
3	11.2	3.8
4	14.8	3.6
5	18.6	3.8
6	22.4	3.8
7	26.2	3.8
8	29.8	3.6
9	33.6	3.8
10	37.4	3.8

Once the 10 minutes had passed, the total measured contents were 37.4ml with a reasonably consistent volumetric flow rate of 3.8 $mlmin^{-1}$ of methanol-water mixture.

This is near the design requirement flow rate of 3.75 $mlmin^{-1}$ within the error of 0.2 $mlmin^{-1}$ and due to the consistency of the flow rate it can be stated that the flow rate control method conforms to the design requirements.

4.3 Cold Commissioning

Cold Commissioning is the evaluation of the completed and assembled fuel qualifying experimental facility while operating with methanol-water mixture without the presence of catalyst to ensure the correct operation of all components without harming the catalyst.

Figure 32 - Fuel Qualifying Experimental Facility for Cold and Hot Commissioning

4.3.1 Superheated Evaporator Temperature

Once the evaporator had reached 200 °C, it was required to maintain this temperature indefinitely while it was evaporating the methanol-water mixture. It is important to maintain this temperature to provide a consistent methanol-water vapour temperature to the reformer above it. Figure 33 displays the temperatures of the evaporator for 47 minutes of the full hour duration of the cold commissioning.

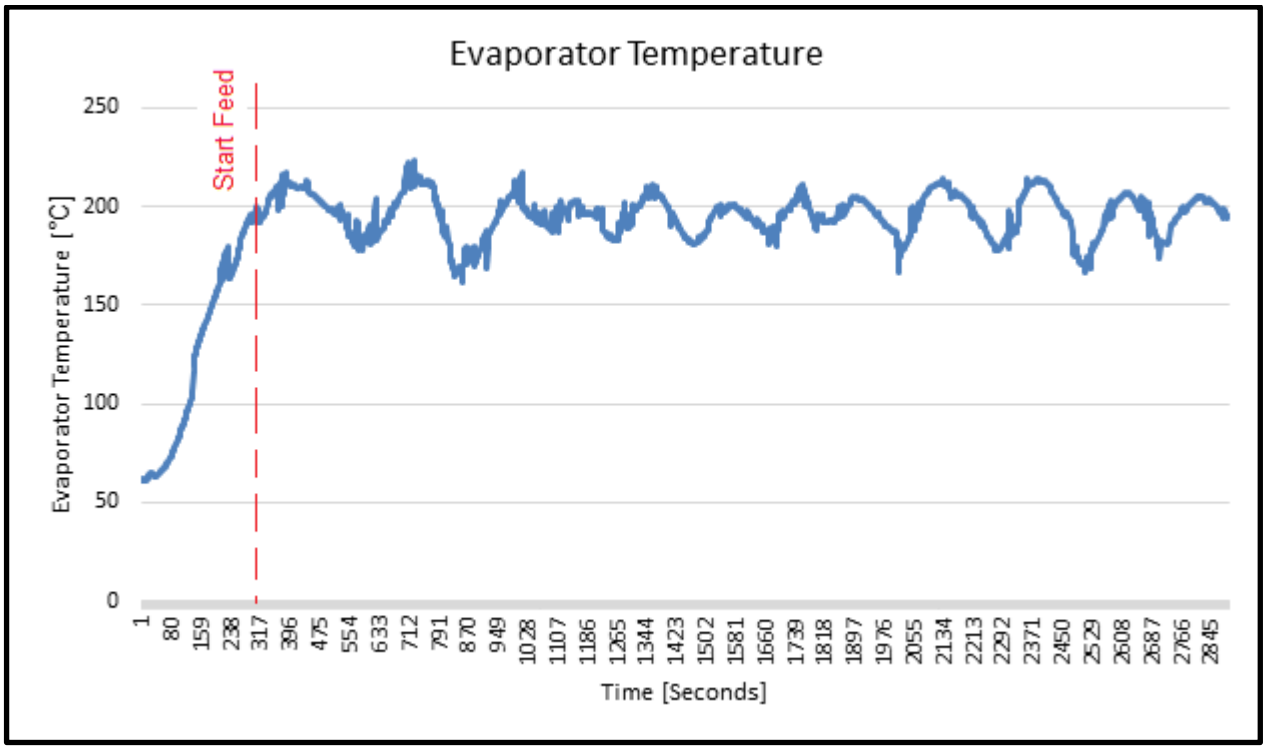

Figure 33 - Line Graph Displaying Evaporator Temperature during Cold Commissioning Evaporation of Methanol-Water Mixture

Figure 33 displays how the evaporator was able reach 200 °C, and once the flow had started, maintained a temperature near 200 °C. During the cold commissioning procedure, the evaporator temperatures varied between 163 °C and 212 °C. This concluded that the evaporator was sufficient to evaporate and superheat the prescribed methanol-water flow rate providing superheated methanol-water mixture to the reformer.

The evaporator heating element does not, however, provide a perfectly consistent temperature of 200 °C due to the evaporator's power being regulated by relay switching.

4.3.2 Reformer Heat Transfer

The reformer was required to be able to reach the prescribed temperature of 300 °C to achieve optimal reaction kinetics for reforming.

Computer Time	Timer	Temp Evap	Temp Reac_ Bot	Temp Reac_ 1-1	Temp Reac_ 1-2	Temp Reac_ 1-3	Temp Reac_ Mid	Temp Reac_ 2-1	Temp Reac_ 2-2	Temp Reac_ 2-3	Temp Reac_ Top	Temp_ Ave	Temp_ Cond
13:42:28	0.00	30	30	27	25	24.5	25.75	28.5	25.75	25.75	28	26.694	25
13:42:29	2.00	29.75	31	27.75	24.5	23.5	25	28.5	25.25	26	28.75	26.694	25
13:42:31	3.00	29.75	31	27.25	25.5	22.5	25.5	28.75	25	26	28	26.611	25
13:42:32	4.00	29.5	31	27	25	23.5	25.25	29	24.75	25.75	28.5	26.639	25
13:42:34	6.00	29.75	30.75	27	25.25	23.75	25.25	28.5	25	26	28.75	26.694	25
13:42:35	7.00	30	31.5	27	25	23.25	25.25	28.5	25.25	26	28.5	26.694	25
13:42:36	8.00	29.5	31	27.5	25	23.5	24.75	29	24.75	25.75	28.25	26.611	25
13:42:38	10.00	29.25	31	27.25	24.5	23.25	25.25	29	24.75	25.75	28.75	26.611	25
.	.	.	.	.	.	.	.	.	.	.	.	.	.
.	.	.	.	.	.	.	.	.	.	.	.	.	.
.	.	.	.	.	.	.	.	.	.	.	.	.	.
.	.	.	.	.	.	.	.	.	.	.	.	.	.
14:05:05	1347.00	101.3	289.25	253	297.75	269.5	299	294	272	245	252.75	274.69	28.25
14:05:06	1348.00	101	289.75	253.8	297.75	270.25	299.5	294.25	272.8	245	252.25	275.03	28
14:05:07	1349.00	101.5	289	253.5	297.75	269.5	299.8	294.5	272.8	245.3	253	275	28
14:05:09	1351.00	101.8	289	254	297.75	270.25	299.8	294.5	272.5	245.3	253.25	275.14	28.25
14:05:10	1352.00	101.5	289.75	254	297.75	270.75	299.8	295.25	272.8	245.5	253.25	275.42	28.5
14:05:11	1353.00	101.8	289.75	254.3	298.75	270	300	295	273	245.5	253.75	275.56	29
14:05:13	1355.00	101.5	290	255	298.5	269	300	295	273.5	245	253.75	275.53	28
14:05:14	1356.00	101.5	290	254.8	299	269	300.5	295	273.3	245.8	254.25	275.72	28.25
14:05:15	1357.00	101.8	290.5	255.3	299.25	269.25	300.5	295	273.8	245.8	254.25	275.94	28
14:05:17	1359.00	102	290.25	254.8	299.25	269.5	300.3	295.25	273.5	246.3	254.5	275.94	28.25
14:05:18	1360.00	102.3	290.25	255.3	300	269	300.8	295.5	273.8	245.8	254.5	276.08	28.75

Figure 34 - Fuel Qualifying Experimental Facility Start-up Temperature Distribution during Cold Commissioning

As displayed in Figure 34, the centre most probe in the reformer reached a temperature of 300 °C. However, presently, the reformer does not contain catalyst. Before a final conclusion was made about the reformer temperature distribution, hot commissioning with catalyst inside the reformer had to occur.

4.3.3 Condenser Outlet Temperature

For the design outcome of off-gas condensate and gas separation, it was required of the condenser to cool the off-gas to a temperature below the condensate temperature of water and methanol at 200 kPa. An ambient temperature was required to ensure complete condensation and separation between the liquid phase off-gas and the gaseous products for separate condensate and gas analysis. If there was not complete separation, condensate would be found in the pipeline

number 6 leading to the gas sampler E8 and the measuring of the condensate volume in the condensate sampler E7 would be inaccurate.

Computer Time	Timer	Temp Evap	Temp Reac_ Bot	Temp Reac_ 1-1	Temp Reac_ 1-2	Temp Reac_ 1-3	Temp Reac_ Mid	Temp Reac_ 2-1	Temp Reac_ 2-2	Temp Reac_ 2-3	Temp Reac_ Top	Temp_ Ave	Temp_ Cond
08:26:08	5257	191.5	250.3	272.75	205.3	266.8	299.8	243.5	248	238.8	252.3	253.03	32.25
08:26:09	5259	191.3	251	272.5	205	267	300	244	248	239.3	252	253.19	32
08:26:11	5260	185.8	251	272.75	212.3	267.3	300.3	243.75	248	240.3	249.8	253.92	32
08:26:12	5262	185	251	273.25	213	267.5	299.5	244	247.8	240.8	249.5	254.03	32
08:26:13	5263	185	251	273	212.8	267.3	300.3	244	248	240.5	249.8	254.06	31.75
08:26:15	5265	184.3	250.8	273.25	213.3	268	300.5	244.5	248.5	240.8	250	254.39	31.75
08:26:16	5266	185	250.8	273.5	213.5	268	300.5	244	248.8	241	250	254.44	31.75
08:26:18	5267	184.3	251.5	273.25	213.5	268	301	244.75	248.5	241	249.8	254.58	32
08:26:19	5269	184.3	251.5	273.5	213.5	268	300.8	244.5	248.5	241.3	250.5	254.67	32.25
08:26:21	5270	183	251.5	273.75	213.8	268.3	300.8	245	249	240.8	250	254.75	32.25
08:26:22	5272	182.3	251.5	273.75	213.8	268.3	301	245	249	241.3	250.5	254.89	32
08:26:23	5273	181.5	251.8	273.75	214	268.5	301.5	245.25	249.3	240.8	250.8	255.06	32
08:26:25	5274	181	251.3	274.5	214	268.3	300.3	244.75	249.8	241.5	250.8	255	32.75
08:26:26	5276	180.3	252.3	274.25	213.8	268.5	301.3	245	249.5	241.5	250.8	255.19	32.25
08:26:28	5277	180.8	252.3	274.5	214.3	268.5	302	245.25	249.5	241.5	251	255.42	32
08:26:29	5279	181	252.3	274.5	213.3	268.8	301.8	245.75	250	241.5	250.3	255.33	32
08:26:30	5280	180.3	252.5	274	214	268.5	302.5	245.25	250	242	250.8	255.5	31.75
08:26:32	5281	180.8	252.8	274.75	213.5	269	302.5	245.25	250	242	251	255.64	32.5
08:26:33	5283	180.5	252.5	275	213.8	269.3	302.3	246	250	242	251.3	255.78	32.5
08:26:35	5284	180	252.5	275.25	213.8	269.3	302.3	246.25	250.3	242.3	251	255.86	32.25

Figure 35 - Fuel Qualifying Experimental Facility Temperature Distribution during Cold Commissioning

As displayed in Figure 35, the temperature recorded by the thermocouple in the outlet of the condenser displayed as E6 in Figure 25 was a constant temperature of 32 °C during the last minutes of the cold commissioning. Although this was 7 °C higher than the design requirement, it was within the allowable error of ±10 °C well below the condensation temperature of methanol and water at 200 kPa and was most likely due to the heat from the reformer increasing the ambient temperatures. This concluded that the condenser was sufficient to remove all condensate constituents from the gas stream.

4.3.4 Ability to Sample Condensate without Interruption of Experimental Process

Due to the long experiment durations, it is crucial to be able to sample and analyse the condensate to determine the methanol conversion of the reformer and catalyst without disrupting the experimental procedure.

During the cold commissioning experimentation, the condensate was sampled at Sample Point 1 without interrupting the experiment and did not significantly reduce the pressure inside the system.

Therefore, it can be concluded that there is conformance of this design requirement for the fuel qualifying experimental facility.

4.3.5 Evaluation of Evaporation Method for Methanol-Water Mixture

For the design outcome of controlled fuel delivery to the reformer, it is important for the methanol:water molar ratio to remain constant during experimentation to ensure constant conditions within the reformer and ensure the validity of the results obtained during the fuel qualification experimentation.

Methanol and water was mixed to the prescribed molar ratio, evaporated at the prescribed flow rate, heated by the reformer and finally condensed by the condenser where the methanol-water mixture was sampled at Sample Point 1 every 15 minutes for a total of 1 hour. 20 ml of the sample was measured by a pipette and weighed by a scale accurate to 4 decimal places which provided the density required to determine the weight percentage methanol which could be translated to the molar ratio. The results of the cold commissioning evaluation are presented in Table 7.

Table 7 - Analysis of Cold Commissioning Condensate of Evaporated Methanol-Water Mixture

Time Interval [minutes]	Volume [ml]	Mass of 20 ml Sample [g]	Density [gml^{-1}]	Methanol [%]	Methanol:Water Mass Ratio	Methanol:Water Molar Ratio
Feed		17.170	0.8585	61.500	1:0.626	1:1.100
15	56.0	17.172	0.8586	61.534	1:0.625	1:1.113
30	55.5	17.157	0.8579	61.560	1:0.624	1:1.111
45	57.0	17.166	0.8583	61.531	1:0.625	1:1.113
60	56.5	17.170	0.8585	61.526	1:0.625	1:1.113
Average	56.25	17.166	0.8583	61.537	1:0.625	1:1.113

During the cold commissioning evaluation, it was found that the condensed methanol-water fuel mixture had remained in its prescribed 1:1.1 molar ratio with a 1.17% relative error.

From the results displayed in Table 7, it was concluded that the evaporator was evaporating the methanol-water mixture and delivering it to the reformer and catalyst at the required flow rate and in its correct methanol:water molar ratio of 1:1.1.

4.3.6 Automated Control

Due to the long operating times and the emphasis placed on the reaction kinetics of the reformer and catalyst, the temperature was required to be monitored throughout the fuel qualification experimentation as well as be recorded in an accessible format that can easily be displayed and adapted such as an Excel spread sheet.

Figure 34 and Figure 35 above, are sections of the real-time temperature data stored and displayed in an Excel spread sheet in an accessible and understandable format.

Due to the evaporator and reformer heating elements providing a thermal power above the design requirements, the temperatures were required to be regulated and controlled. An Arduino Mega with thermocouples and relays was implemented and programmed for the automatic control. By observing the behaviour of the relays and the temperature data provided by the thermocouples, the ability to control the fuel qualifying experimental facility temperatures was determined.

As can be observed by Figure 34 and Figure 35, the Arduino Mega correctly recorded the operating temperatures of the evaporator and all the temperatures of the reformer and automatically closed and opened the relays at the correct set-points of 195°C and 200°C, and 297°C and 300°C to maintain the required temperatures of the evaporator and reformer respectively. Therefore, it can be concluded that the control code written is correct and there is conformance of automated control of the evaporator and reformer at set points for the fuel qualifying experimental facility.

4.4 Evaluation of Catalyst

For the design outcome of controlled reaction kinetics, the catalyst composition and BET surface area was required for the characterisation of the catalyst used during the fuel qualifying experimentation. The general composition of fresh catalyst is required for comparison to the samples taken from Sample Point 3 and Sample Point 4 displayed in Figure 24 and Figure 31 during the fuel qualifying experimentation and for verification by comparing to the expected composition and BET surface area of catalyst used in literature.

4.4.1 Catalyst Composition

The catalyst composition was approached by performing an EDS (energy dispersive X-ray spectroscopy) on a FEI Quanta 250 FEG SEM electron microscope in a high vacuum and 15kV.

The SEM emits a focused beam of electrons or x-rays onto a sample exciting the electrons of the sample which ejects electrons as energy in the form of an x-ray. The number and energy of the x-rays is measured by an energy dispersive x-ray detector which can then determine an approximation of the elemental composition of the sample as a semi-qualitative analysis. (Materials Evaluation and Engineering, inc., 2019) . Generally EDS has a detection limit between 0.1% and 2% depending on the element and combined errors limit precision to $\pm$2%. However, lighter elements are difficult to measure with any precision (MyScope, 2014).

The sample was treated with a carbon coating to ensure proper conduction through the sample, and therefore carbon was eliminated from the spectrum.

An overall EDS analysis was done on an un-activated and activated catalyst sample to determine the overall catalyst composition. The results were observed as having a sodium content of 22.27% which was not expected in the sample. The remaining sodium ions from the sodium carbonate that caused the precipitating reaction had become part of the catalyst during the precipitation reaction and were not rinsed out completely. The results from this analysis are displayed in Table 8.

Table 8 - Un-activated and Activated Catalyst Composition

Sample	Cu [wt%]	Zn [wt%]	Al [wt%]	O [wt%]	Na [wt%]	Total [wt%]
Un-Activated	21.88	16.44	3.08	36.32	22.27	100.00
Activated	16.18	15.60	3.76	35.46	29.01	100.00

In order to verify the composition of the manufactured catalyst, the Cu, Zn, Al weight percentages in Table 8 were used to provide a general indication of the amounts of CuO, ZnO, and Al_2O_3.

$$Cu \rightarrow CuO$$

$$63.55\ gmol^{-1} \rightarrow 79.55\ gmol^{-1}$$

$$mass_{CuO} = 21.88g * \frac{79.55}{63.55} = 27.40\ g$$

$$Zn \rightarrow ZnO$$

$$65.38\ gmol^{-1} \rightarrow 81.38\ gmol^{-1}$$

$$mass_{ZnO} = 16.44g * \frac{81.38}{65.38} = 20.46\ g$$

$$Al \rightarrow Al_2O_3$$

$$26.98\ gmol^{-1} \rightarrow 101.96\ gmol^{-1}$$

$$mass_{Al_2O_3} = 3.08g * \frac{101.96}{26.98} = 11.64\ g$$

$$\therefore mass\% = \frac{x}{27.40 + 20.46 + 11.64} * 100$$

The sodium weight percentage was not considered and the EDS results normalised for CuO, ZnO, and Al_2O_3 and presented in relation to one another as displayed in Table 9. This was done so that the catalyst composition can be verified by comparing it to the design requirement weight percentage expected.

Table 9 - Selective Composition of Un-activated Catalyst

Component	Design Requirement [Mass%]	Practical [Mass%]	Relative Error [%]
CuO	60.00	46.05	-23.25
ZnO	30.00	34.39	14.63
Al_2O_3	10.00	19.56	95.60

The results of the EDS analysis of the unactivated catalyst represented by Table 9, indicates that the intended CuO, ZnO, and Al_2O_3 mass ratios were not achieved. The elemental distribution of the catalyst may have been affected by the unexpected sodium content and an EDS is an approximate analysis for the determination of the catalyst composition with an error between 5 % and 20 %, therefore, a small sample being analysed does not necessarily present the composition of the catalyst as a whole. The specific copper dispersion values were not taken into consideration in this study.

From the data thus presented, it can be concluded that the catalyst composition is not as prescribed by the design criteria, however, due to the fact that the same catalyst is used for all experiments it can be considered sufficient for the purpose of comparison to the mentioned

literature. Furthermore, since the scope of this study is limited to the determination of the impact of various methanol fuel qualities and its effects on the off-gas composition, the continuous use of the prepared and characterized catalyst can be considered acceptable.

The catalyst composition varying from that used in literature was taken into account during the validation of methanol conversion and off-gas composition.

The BET surface area, as well as pore size and volume of the catalyst were required for the characterisation of the catalyst used during the fuel qualifying experimentation for the design outcome of controlled reaction kinetics.

4.4.2 Catalyst BET Surface Area and Pore Properties

A sample of un-activated catalyst, activated catalyst, and a catalyst pellet, which was present in the reformer during the fuel qualifying experimentation, were each subjected to Brunauer–Emmett–Teller (BET) analysis to determine the physical adsorption of gas molecules on a solid surface by revealing pore morphology within the catalyst. Intrusion gases are used that do not chemically react with the material surfaces to quantify surface area. Nitrogen and carbon dioxide is most commonly used as intrusion gases to determine the BET characteristics of catalyst. This includes surface area, pore volumes, as well as the average pore sizes by carbon dioxide and nitrogen adsorption. This gives an indication of the reaction area available for methanol steam reforming.

The entire BET analysis report produced was summarised and the most relevant data displayed in Table 10.

Table 10 - BET Analysis of Catalyst via N_2 adsorption

Sample	BET Surface Area [m^2g^{-1}]	Pore Volume [cm^3g^{-1}]	Pore Size [nm]
Un-Activated	6.926	0.00188	1.08569
Activated	8.792	0.00138	0.62867
Pellet	15.848	0.00120	0.30158

From Table 10, it can be observed that during activation the BET surface area increases from 6.926 m^2g^{-1} to 8.792 m^2g^{-1} due to the removal of the oxygen atom. However, when increasing the surface area, the pore volume and pore sizes decrease by 26.48 % and 42.09 % respectively. This

would make it more difficult for methanol and steam molecules to enter into the pores of the catalyst and reduces its activity. Furthermore, if poisoning or carbon deposition were to occur, it would prohibit absorption into the pellet and thereby facilitate deactivation of the catalyst at an increased rate.

Table 10 indicates a further increase in BET surface area for the pellets that were used in the reformer during the fuel qualifying experimentation to 15.848 m^2g^{-1} and decreases in pore volume and pore size by a further 13.53 % and 52.03 % respectively due to the pelletization process.

The catalyst analysed in the study by Kim *et al.* (2016) has the lowest BET surface area of 66 m^2g^{-1}, which is 4.038 times greater than the pelletized catalyst. The pore size and pore volumes of the pelletized catalyst are also smaller than the catalysts used by literature.

The smaller surface areas and reduced pore volumes and pore sizes can be attributed to the unexpected sodium oxides that have formed part of the catalyst composition and the remaining carbonates as discussed in Section 4.4.

It was concluded that the catalyst physical properties are not as prescribed by the design requirements. However, due to the fact that the same catalyst is used for all experiments it can be considered a constant error and not random. The scope of this study, being the variation of fuel quality and its effect on the off-gas composition, can still be achieved. The catalyst physical properties varying from that used in literature was mentioned during the validation of methanol conversion percentages with those displayed by Lee *et al.* (2004), Gu *et al.* (2003), and Sá *et al.* (2010) in Section 5.1.4; and in Section 5.2.4 when validating the off-gas composition with those displayed by Kim *et al.* (2016), Kurr *et al.* (2008), Purnama (2008), and Sá *et al.* (2011).

4.4.3 Catalyst Topology

The catalyst surface topology was required for the characterisation of the catalyst used during the fuel qualifying experimentation and for comparison to the samples taken from Sample Point 3 and Sample Point 4 displayed in Figure 25 and Figure 31 during the fuel qualifying experimentation.

The surfaces of catalyst particles were photographed by a FEG SEM, FEI Quanta 250 electron microscope. The micrographs are displayed by Figure 36 and discussed below.

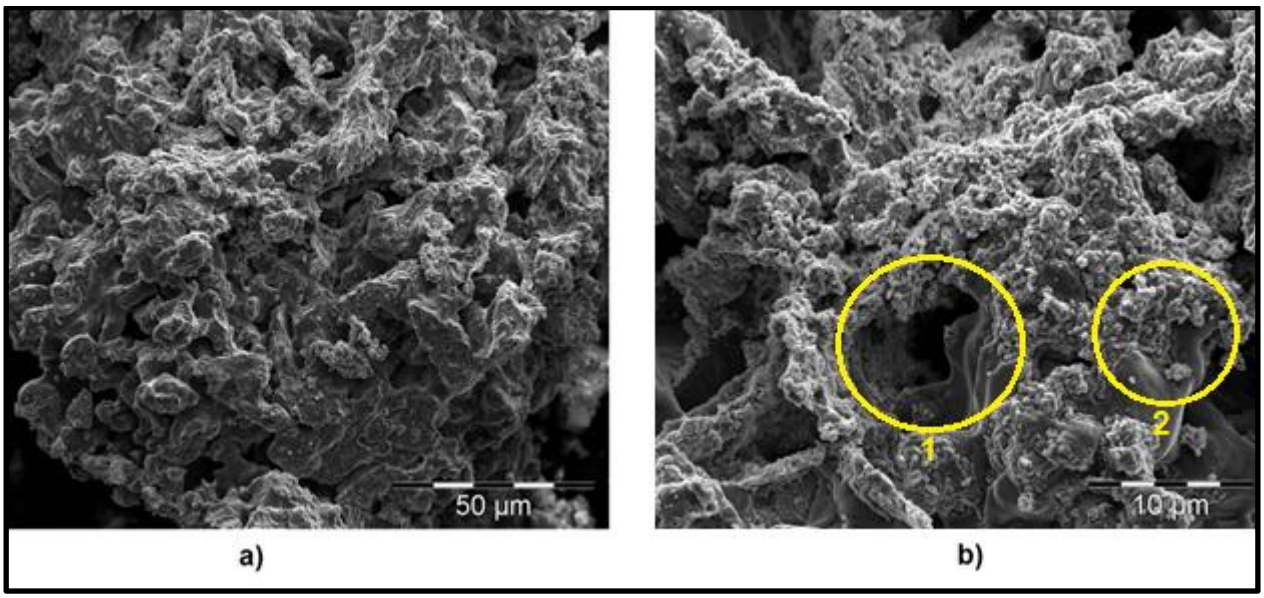

Figure 36 - Activated Catalyst Topology Micrograph by SEM a) 50 micrometres b) 10 micrometres

The micrographs of the activated catalyst show ceramic or clay-like particles that are porous and have intimate bonding between the different catalyst materials as displayed by Figure 36b) Area 2. There are pores inside the catalyst particles that increase the active surface area for better reforming ability. The caverns displayed in in Figure 36b) Area 1 were produced by the loss of the carbonates during the calcination process leaving behind gaps where they were present.

Figure 36b) displays a magnification on the particle and at Area 2 it can be seen how the catalyst forms layers as the co-precipitation reaction took place creating an intimately bonded laminar structure of copper, zinc oxide, and aluminium oxide, with the copper particles having formed on the surface serving as the active sites for the catalyst.

The observations made from Figure 36 are similar to those of the design requirements from Section 2.3.4, making the structure of the manufactured catalyst as anticipated in Chapter 2. Therefore, the structure and general topology of the catalyst can be considered conforming to the design requirements.

4.5 Hot Commissioning

Hot Commissioning is the evaluation of the completed and assembled fuel qualifying experimental facility while operating with methanol-water mixture in the presence of catalyst to ensure the correct operation of all components as well as the activity catalyst. Methanol and water was mixed in the prescribed molar ratio, evaporated at the prescribed flow rate, heated by the reformer and

finally condensed by the condenser where the outlet was placed through a solution of $CaCO_3$ for an hour. In the presence of CO_2, the $CaCO_3$ solution will turn milky white as a precipitate forms. During hot commissioning the thermal transfer rate of the reformer element, reformer temperature, and reformer temperature distribution will be discussed, along with the condenser outlet temperature, activity of the catalyst, and ease of catalyst pellet sampling.

4.5.1 Consistent Reformer Temperature and Uniform Temperature Distribution

Once the flow had commenced, the reformer temperatures were required to remain constant over the duration of the hot commissioning experiment. The temperature distribution was also important due to the effect temperature has on the reforming ability of the catalyst.

For the one-hour duration of the hot commissioning, the average temperatures in 10 minute intervals are displayed in Figure 37.

Time [min]	Temp Reac_ Bot	Temp Reac_ 1-1	Temp Reac_ 1-2	Temp Reac_ 1-3	Temp Reac_ Mid	Temp Reac_ 2-1	Temp Reac_ 2-2	Temp Reac _ 2-3	Temp Reac_ Top	Temp_ Ave	Temp_ Cond		Reac Min	Reac Max
10	253.5	276.1	221.13	269.45	290.07	234.6	235.82	226.14	228.16	248.33	33.7436		221.1	290.1
20	244.3	261.4	193.45	245.92	283.72	222	241.75	216.97	235.66	238.34	30.7769		193.5	283.7
30	257.6	275.8	207.92	251.37	294.08	233.8	257.53	228.7	249.75	250.73	36.0363		207.9	294.1
40	251.17	269.98	203.75	243.12	290.47	230.24	252.42	224.96	228.32	243.83	31.76		203.8	290.5
50	251.3	272.3	223.72	252.58	294.58	239.8	247.73	233.09	242.76	250.88	32.6177		223.7	294.6
60	250.7	271.5	215.09	264.6	293.1	242.3	247.68	238.08	246.78	252.16	33.4467		215.1	293.1
Min	244.3	261.4	193.45	243.12	283.72	222	235.82	216.97	228.16	238.34	30.7769			
Max	257.6	276.1	223.72	269.45	294.58	242.3	257.53	238.08	249.75	252.16	36.0363			

Figure 37 - Reformer Temperature Distribution during Hot Commissioning

Figure 37 displays how the reformer was able to maintain the required 300°C at the centre of the reformer during the provided flow rate from the evaporator, however, the temperature distribution varies with a range from 193.45 °C in Sector 1-2 to 294.58 °C in the Mid Sector.

However, it can also be seen that the individual sector temperatures remain reasonably constant with temperature differences between 10.86 °C and 30.27 °C. The average temperature value of 269.45 °C in Sector 1-3 is due to an outlying temperature value due to a thermocouple malfunction providing temperatures higher than reality.

These variations in temperature distribution are due to the uneven wrapping of the kanthal wire around the reformer pipe. The sockets used for the thermo-wells posed as obstacles for consistent kanthal wire wrapping causing uneven heat distribution. The heat lost due to insufficient insulation around the reformer and the top and bottom flanges also affected the heat distribution.

From Section 2.3.5, it was observed that temperature has an impact on methanol reforming, therefore, at certain sectors in the reformer there will be a lower percentage of methanol reformed than at other sectors of higher temperatures. Therefore, it can be speculated that by taking an average of all of the temperature values, an overall reformer operating temperature can be determined and referred to during the fuel qualifying experimentation in Chapter 5.

Although the observed temperature distribution is uneven, the individual sector temperatures remain reasonably constant and will not affect the validity of the results during fuel qualifying experimentation when implementing an overall average temperature for the reformer. Therefore, the reformer conforms to the design criteria of consistent sector temperatures for the design outcome of controlled reaction kinetics.

4.5.2 Catalyst Activity

For the continuation of the study, the catalyst was required to react with the methanol and steam mixture to produce hydrogen. As discussed in Section 2.6 the off-gases include carbon dioxide.

A simple test for carbon dioxide is with aqueous calcium carbonate, also known as lime water which will turn milky white when exposed to carbon dioxide. If reforming takes place, carbon dioxide will form part of the off-gases flowing through the calcium carbonate.

The outlet of the reformer was placed to flow through a beaker of aqueous $CaCO_3$. As displayed by Figure 38, the lime water turned milky white, indicating presence of CO_2 in the reformer outlet.

Figure 38 - Aqueous $CaCO_3$ After and Before Effect of Reformer Off-gases

This concludes that the catalyst is active and produces carbon dioxide, and subsequently hydrogen, from the methanol and steam mixture.

4.5.3 Catalyst Sampling

At 10 hour intervals during the fuel qualifying experimentation, catalyst samples were required to be taken and analysed.

Due to the flange interfaces included in the design in Chapter 3, the catalyst at the top of the reformer at Sample Point 3 is easily sampled by removing a pellet and replacing it with another to ensure constant catalyst weight inside the reformer. The catalyst in the centre of the reformer was sampled at Sample Point 4 at the end of the experiment. Therefore, the design requirement has been met and the required result of this experiment is achieved.

4.6 Fuel Qualifying Experimental Methodology

For the fuel qualifying experimental procedure producing the results in Chapter 5, the system was purged with nitrogen and the reformer was heated until one of the thermo-couples reached 300 °C, the evaporator was then heated to 200 °C. Once the flow of methanol-water mixture had commenced, at hourly intervals the volume of the reformer off-gas condensate was measured at Sample Point 1 and a 20 ml sample of the condensate was taken by a pipette and weighed by a scale accurate to 4 decimal places to determine the density which would allow the amount of methanol in the sample to be calculated. A pH test paper was also inserted into every condensate sample to measure the acidity. After 10 hours had passed, the flow was ceased and the gas

sampler isolated. The gas sampler served as Sample Point 2 and was analysed using a gas chromatograph calibrated for measuring hydrogen, carbon dioxide, carbon monoxide, and nitrogen. The wetted lead acetate strips for H_2S detection were photographed and labelled. Two catalyst pellets were removed from the top of the reformer at Sample Point 3 and replaced. They were analysed for poisons, sintering, and carbon deposition. After having repeated this process 3 times or until the methanol conversion indicated a value below 13 %, the experiment was concluded and a catalyst pellet was removed from the centre of the reformer at Sample Point 4 and its cross-section analysed by EDS.

4.7 Summary

In Chapter 4 the proposed method of addressing the problem statement was evaluated according to the design outcomes and subsequent design requirements stipulated and designed for in Chapter 3.

It was concluded that the controlled delivery of methanol-water mixture to the reformer was achieved by the continuous flow rate, the constant evaporator temperature, and the sufficient thermal energy provided by the evaporator to evaporate and superheat the methanol-water mixture while maintaining the required methanol-water molar ratio.

Controlled reaction kinetics was achieved by the reformer, due to its ability to reach and maintain the required temperature during the flow of methanol-water vapours. Although the temperature distribution was not ideal, the individual reformer sector temperatures remained constant and would not affect the reaction kinetics of the reformer. Temperature averages were taken into account and an overall reformer temperature was used.

The catalyst topology was found to be similar to that described in literature, however the composition differed from the design requirements and the BET surface areas and pore sizes were smaller than anticipated. Despite this, by performing the experiments with the same catalyst throughout the fuel qualification, the design outcome of controlled reaction kinetics was deemed achievable.

It was concluded that the condenser was able to condense and separate the liquids out of the gas stream at the ambient temperature, however, the ambient temperatures were not constant during experimentation and increased the condensate temperatures. These temperatures were still well below the vapourisation temperatures of methanol and water at 200 kPa, therefore, the design outcome of off-gas liquid and gas separation was achieved.

The design outcome of sampling ability was achieved by allowing in-situ condensate sampling without interruption of the experiment. Ease of catalyst sampling from the top of the reformer further satisfied this outcome.

The design outcome of automated control was achieved by utilising an Arduino mega programmable microcontroller and coding it to receive temperature data and generate a real-time Excel spread sheet which is a Microsoft accessible format. The temperature data was used to control relays which switched the reformer and evaporator's heating elements on and off at certain set-points to control the temperatures.

CHAPTER 5 - METHANOL FUEL ANALYSIS, AND FUEL QUALIFYING EXPERIMENTATION RESULTS AND DISCUSSION

From the problem statement and scope of work in Chapter 1 the focus of this study is the methanol quality and its effects on the reformer off-gas composition. The three methanol qualities considered by this study are Analytical Reagent (AR) Chemically Pure (CP) and Industrial grade. The data sheets of each quality are presented in Appendix E.

The majority of the studies discussed in Chapter 2 measured and presented the unreformed methanol as an indication of reformer effectiveness and is considered part of the reformer off-gases. The experimental condensate will be measured, and discussed and validated according to literature. It was noted that the concentration of HCl in the off-gases was not considered in literature, therefore, for this study, the acidity of the condensate will be analysed.

The molar percentages of the product gases, hydrogen, carbon dioxide, and carbon monoxide, presented by literature in Chapter 2 will be used to validate the experimental gas product compositions measured using a gas chromatograph every 10 hours and when the experiment ends. However, literature does not consider the content of H_2S in the reformer off-gas and in this study it has been addressed by the use of lead acetate indicator strips.

The catalyst composition will be analysed at 10 hour intervals for the presence of chlorine and sulphur ions to supplement the results from the pH and lead acetate indicator strips. The catalyst will also be analysed for carbon deposition.

5.1 Analysis of Reformer Off-gas Condensate

At a constant time interval of 1 hour, the volume of the reformer off-gas condensate was measured from Sample Point 1 and a 20 ml sample was weighed. Table 12, Table 13, and Table 14 display the various volumes of off-gas condensate along with the sample masses. This information was used to determine the densities and subsequent methanol conversions.

Table 11 displays the structure and equations used to produce Table 12, Table 13, and Table 14:

Density of Condensate - $$\rho_{condensate} = \frac{m_{condensate}}{20ml} \quad (5.1)$$

$m_{condensate}$ is the mass of the 20ml sample of the condensate for that hour interval in grams.

Methanol Mass % - $$m_{methanol}\% = \frac{\frac{\rho_{methanol}}{\rho_{condensate}} - \rho_{methanol}}{1 - \rho_{methanol}} * 100 \quad (5.2)$$

Methanol Mass [g] - $m_{methanol} = Vol * \rho_{condensate} * \frac{m_{methanol}\%}{100}$ (5.3)

Methanol Conversion[%]- MethConv= $\left(1 - \frac{m_{methanol}}{(m_{condensate\ expected} * \frac{m_{methanol\ expected}\%}{100})}\right) * 100$ (5.4)

$m_{condensate\ expected} = 193$ g due to the flow rate.

$m_{methanol\ expected}\% = 61.5\ \%$ due to the required mixing ratio.

Table 11 - Methanol Conversion Tables Layout

Time [hours]	Condensate Volume [ml]	Mass of 20ml Sample [g]	Density [gml^{-1}]	Methanol [%]	Methanol [g]	[1]Methanol Conversion [%]
1	Vol	m_{cond}	(5.1)	(5.2)	(5.3)	(5.4)

Figure 40, Figure 43, and Figure 46 are produced by determining the percentage change between each hourly methanol conversion value.

Percentage Change - Change%= $\frac{x_i - x_{i-1}}{x_{i-1}} * 100$ (5.5)

x_i is the current interval methanol conversion value ($i > 1$)

x_{i-1} is the methanol conversion value one hour interval behind the current methanol conversion value.

[1] Only one iteration of experiments was produced for each methanol quality. Time and cost constraints limited this study to the production of enough catalyst for one iteration of experiments for each methanol quality. Large amounts of time are required to produce such large quantities of catalyst. As discussed in Chapter 3, in comparison to literature, this study's reformer diameter is far larger with 140 times more catalyst to introduce higher fuel flow rates to increase the amount of poisons being exposed to the catalyst to make detection easier. The entire process can be viewed in Appendix C and as can be seen in the results, experimental times reach from 16 to 30 hours. The scope of this study, as presented by the title, is the methanol fuel quality and its effects on the fuel cell reformer off-gas composition which has been presented and addressed by the varying of methanol quality for each experiment and observing the effect the methanol quality has on the change in methanol conversion and catalyst lifespan as well as the gas product composition.

5.1.1 Results from Reformer Off-gas Condensate Analysis while Reforming AR Methanol

By the method described above with fresh catalyst and reforming AR methanol, Table 12 can be produced.

Table 12 - Reformer Off-gas Condensate Analysis while Reforming AR Methanol

Time [hours]	Condensate Volume [ml]	Mass of 20ml Sample [g]	Density [gml^{-1}]	Methanol [%]	Methanol [g]	Methanol Conversion [%]
1	33.0	18.4485	0.9224	31.34	9.54	91.96
2	46.0	18.0374	0.9019	40.55	16.82	85.82
3	50.0	17.9340	0.8967	42.93	19.25	83.78
4	53.0	17.8995	0.8950	43.73	20.74	82.52
5	52.0	17.8511	0.8926	44.86	20.82	82.45
6	61.0	17.8063	0.8903	45.91	24.94	78.98
7	75.0	17.7751	0.8888	46.65	31.09	73.79
8	107.6	17.7277	0.8864	47.77	45.56	61.60
9	90.0	17.4490	0.8725	54.48	42.78	63.94
10	95.0	17.7358	0.8868	47.58	40.08	66.22
11	98.0	17.9099	0.8955	43.49	38.17	67.83
12	100.0	17.7482	0.8874	47.28	41.96	64.63
13	93.0	17.6986	0.8849	48.46	39.88	66.39
14	81.0	17.7406	0.8870	47.46	34.10	71.26
15	93.5	18.0600	0.9030	40.03	33.80	71.51
16	72.5	17.6993	0.8850	48.44	31.08	73.80
17	84.0	17.6937	0.8847	48.58	36.10	69.57
18	70.5	17.6680	0.8834	49.19	30.64	74.18
19	93.0	17.7000	0.8850	48.43	39.86	66.41
20	120.0	17.6799	0.8840	48.91	51.88	56.27
21	132.0	17.7990	0.8900	46.08	54.14	54.37
22	141.0	17.7440	0.8872	47.38	59.27	50.04
23	141.0	17.6966	0.8848	48.51	60.52	48.99
24	150.0	17.6708	0.8835	49.12	65.10	45.13
25	153.0	17.6825	0.8841	48.84	66.07	44.31
26	165.0	17.6793	0.88400	48.92	71.35	39.86
27	173.0	17.6448	0.8822	49.74	75.92	36.01
28	188.5	17.6457	0.8823	49.72	82.69	30.30
29	210.0	17.6443	0.8822	49.76	92.18	22.30
30	225.0	17.6352	0.8818	49.97	99.15	16.43

From the last column of Table 12 above, Figure 39 can be drawn to display the methanol conversion over the 30 hours of the experiment.

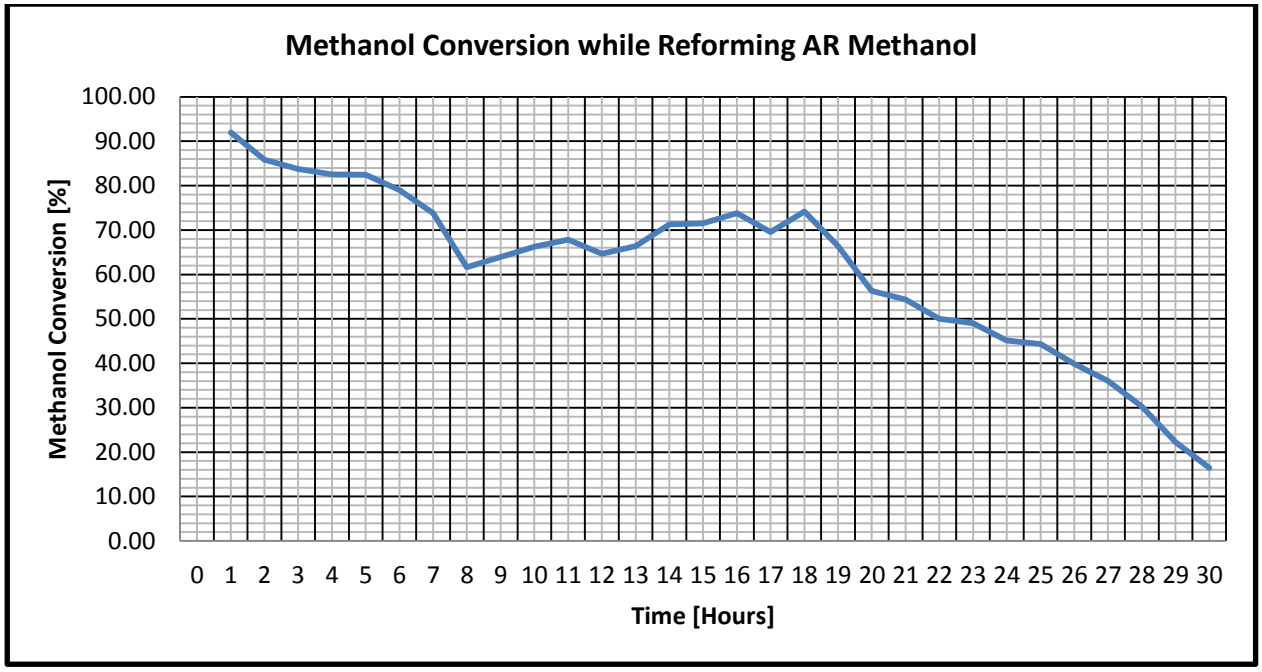

Figure 39 - Line Graph of Methanol Conversion over Time while Reforming AR Methanol

Using the information from Table 12 and Figure 39, it can be seen that in the first hour the reforming catalyst has a conversion of about 91.96 % which decreases over the first 8 hours to 61.60 %.

Between 8 hours and 11 hours there is an increase to 67.83 % and from 14 hours to 18 hours the conversion remains between 71.26 % and 74.18 %. However, soon after 18 hours the methanol conversion undergoes a linear decreasing trend from 74.18 % to 16.43 % which ends the experiment at 30 hours.

From the above information in Table 12 and Figure 39, a change in hourly methanol conversion can be determined to display the overall change in conversion as described earlier by Equation 5.5 by comparing the current methanol conversion value to the value one hour interval prior which produces Figure 40. This provides a better portrayal of the percentage change fluctuations and general trend.

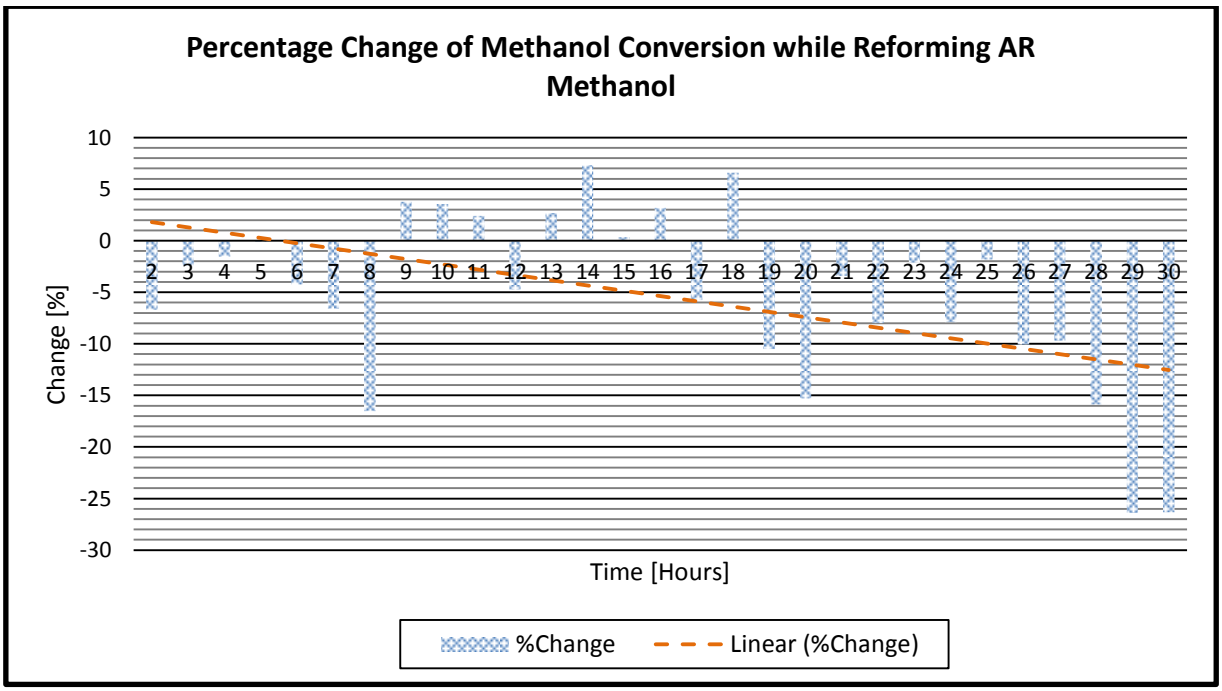

Figure 40 - Column graph of the Hourly Percentage Change in Methanol Conversion While Reforming AR Methanol

A negative percentage change value indicates a decrease in the hourly methanol conversion.

From Figure 40 it can be seen that the majority of percentage changes are negative, indicative of an overall methanol conversion decreasing trend. Between 2 and 10 hours the percentage changes are between 3.80 % and -16.52 %. From 9 hours to 19 hours the percentage changes vary between 7.34 % and -10.49 % indicating higher fluctuations and an overall increasing conversion trend.

When considering the time period between 25 hours and 30 hours the overall percentage change is exponentially negative from -1.81 % to -26.38 %. From Figure 40 it can be seen that the trend line has a larger negative gradient which eventually causes a methanol conversion of 16.43 %.

The pH values of the condensate were determined by using pH strips and by using the colour scale on the box as displayed in Figure 41, an accurate pH value can be determined. The hours from 1 to 26 displayed a constant neutral pH value of 7 and are not displayed below.

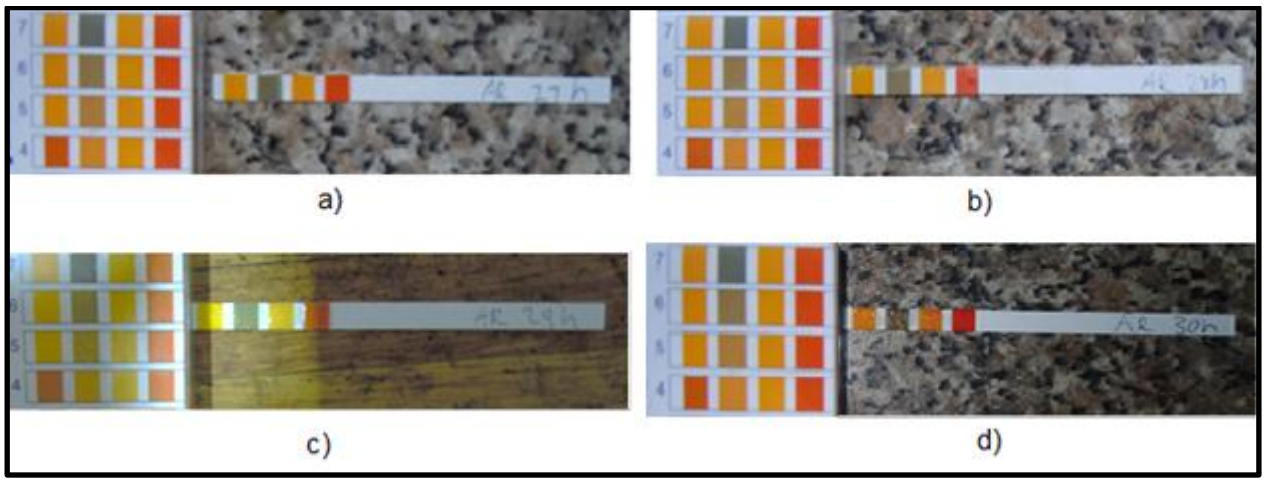

Figure 41 - pH Values of Methanol-Water Condensate after a) 27 hours, b) 28 hours, c) 29 hours, and d) 30 hours of Reforming AR Methanol

After 27 hours of reforming AR methanol the pH strips started to display a change in pH value and showed a slightly acidic value of between 6 and 7. Figure 41c) and Figure 41d) displayed a browner colour in the second block indicating acidity.

5.1.2 Results from Reformer Off-gas Condensate Analysis while Reforming CP Methanol

The same procedure is undertaken for the Chemically Pure methanol with fresh catalyst. Table 13 is produced from the volume and mass of each hourly sample taken from the reformer off-gas condensate.

Table 13 - Reformer Off-gas Condensate Analysis while Reforming CP Methanol

Time [hours]	Condensate Volume [ml]	Mass of 20ml Sample [g]	Density [gml^{-1}]	Methanol [%]	Methanol [g]	Methanol Conversion [%]
1	73.0	18.0136	0.9007	41.10	27.02	77.23
2	80.0	17.8612	0.8931	44.63	31.88	73.13
3	97.0	17.7456	0.8873	47.35	40.75	65.66
4	121.0	17.7561	0.8878	47.10	50.59	57.36
5	140.0	17.7148	0.8857	48.08	59.62	49.75
6	170.0	17.6940	0.8847	48.57	73.05	38.43
7	148.0	17.7046	0.8852	48.32	63.30	46.64
8	162.5	17.5800	0.8790	51.30	73.28	38.24
9	162.0	17.5960	0.8798	50.92	72.57	38.83
10	174.0	17.5580	0.8779	51.83	79.18	33.26
11	161.0	17.7490	0.8875	47.26	67.53	43.08
12	154.0	17.7372	0.8869	47.54	64.93	45.27
13	175.0	17.7280	0.8864	47.76	74.09	37.55
14	183.0	17.7079	0.8854	48.24	78.16	34.12
15	187.0	17.6955	0.8848	48.53	80.30	32.32
16	210.0	17.6617	0.8831	49.34	91.50	22.88
17	226.0	17.6379	0.8819	49.91	99.48	16.16
18	240.0	17.6100	0.8805	50.58	106.88	9.91

Figure 42 was drawn from the last column in Table 13 to display the methanol conversion over the 18 hour time period.

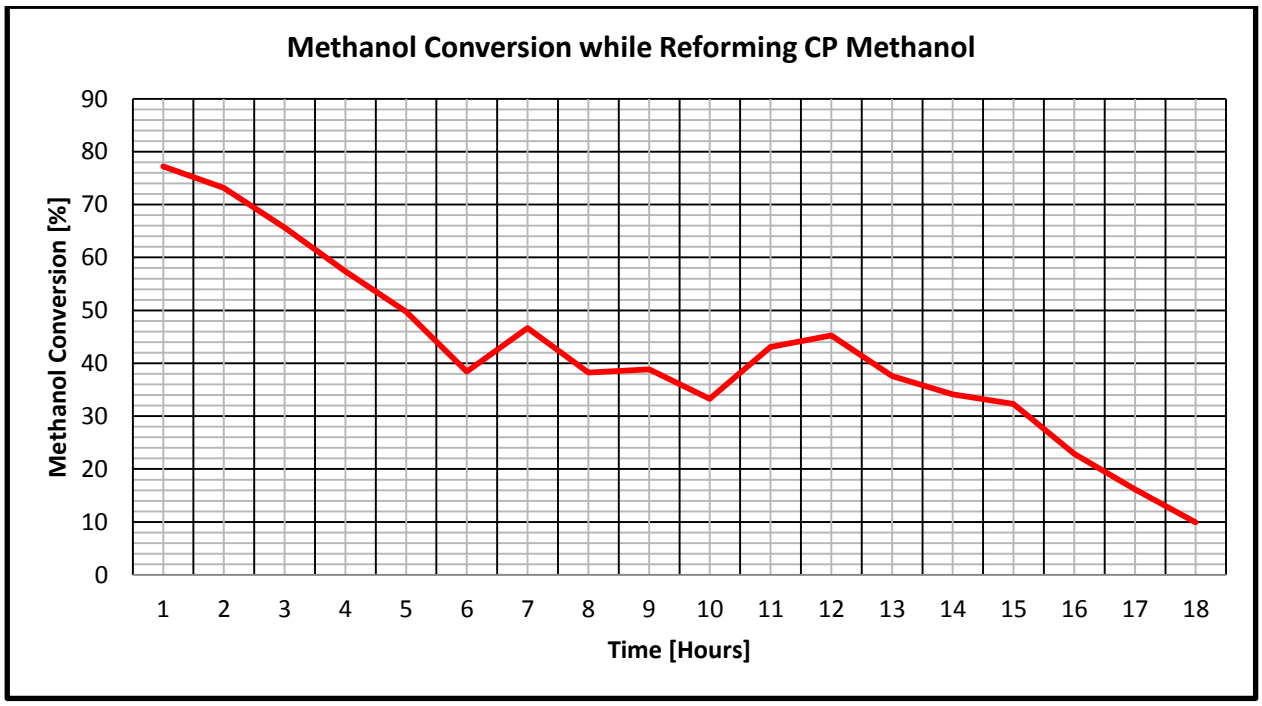

Figure 42 - Line Graph of Methanol Conversion Over Time while Reforming CP Methanol

Considering Figure 42, it can be seen that the methanol conversion starts at 77.23 % which is lower than the starting conversion of the catalyst while reforming the AR methanol at 91.96 %.

Between 1 hour and 6 hours the methanol conversion decreases linearly from 77.23 % to 38.43 %. Between 6 and 12 hours the methanol conversion varies between 46.64 % and 33.26 %. At 12 hours the conversion is higher at 45.27 % and after 12 hours the methanol conversion decreases to 9.91 % at 18 hours where the experiment ends.

From the above information in Table 13 and Figure 42 a change in hourly methanol conversion can be determined to see the change in methanol conversion. Figure 43 displays this percentage change and its overall trend.

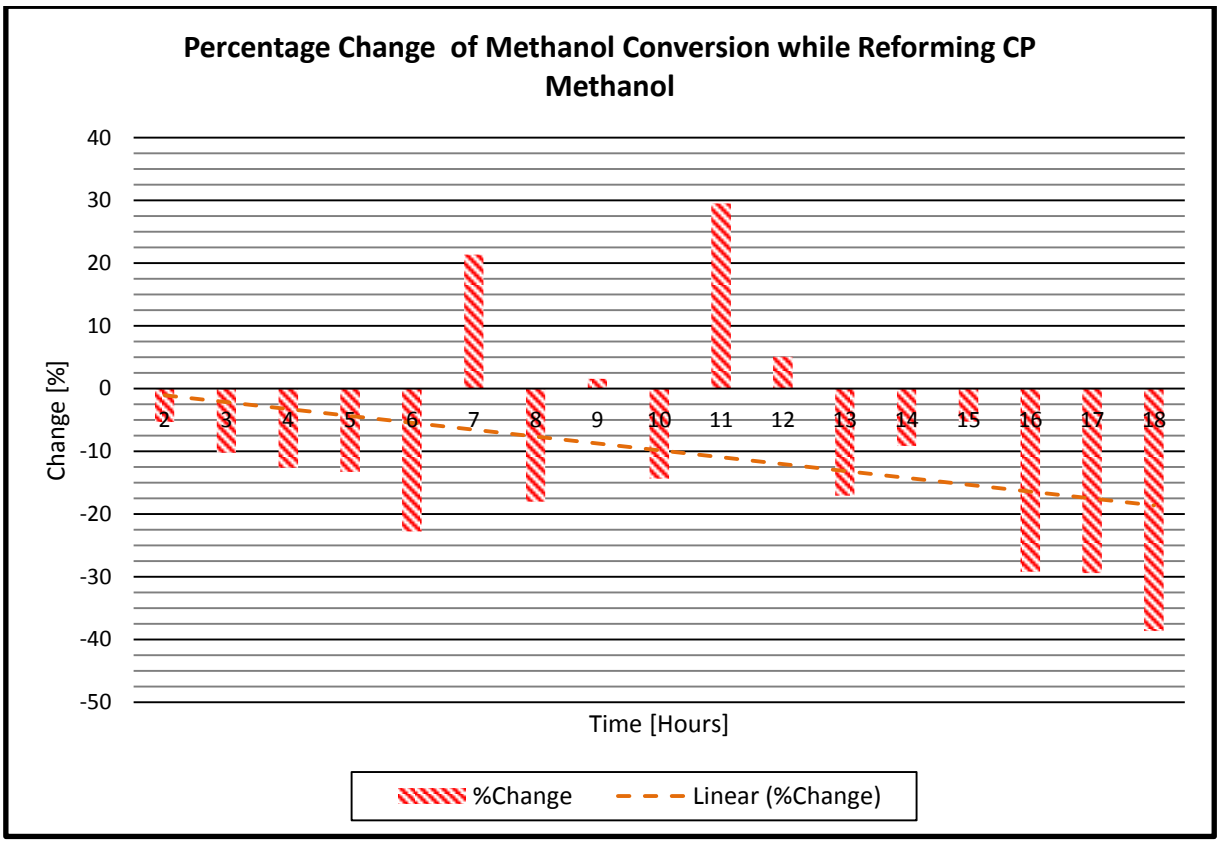

Figure 43 - Column graph of the Hourly Percentage Change in Methanol Conversion While Reforming CP Methanol

As displayed in Figure 43 from 2 hours to 6 hours the percentage change in methanol conversion has a negative gradient from -5.31 % to -22.76 %. Between 7 hours and 12 hours the methanol conversion fluctuates and produces a percentage change between -18.02 % and 29.51 %.

Between 13 hours and 18 hours the percentage change remains negative with values ranging between -5.29 % and -38.65 %. During this time the methanol conversion decreases to 9.9 % and the experiment was stopped at 18 hours due to the reaching of a methanol conversion value below 13 %.

The pH values of the condensate were determined by using pH strips, using the colour scale on the box as displayed in Figure 44, a reasonably accurate pH value can be determined. The hours from 1 to 14 displayed a constant neutral pH value of 7 and are not displayed below.

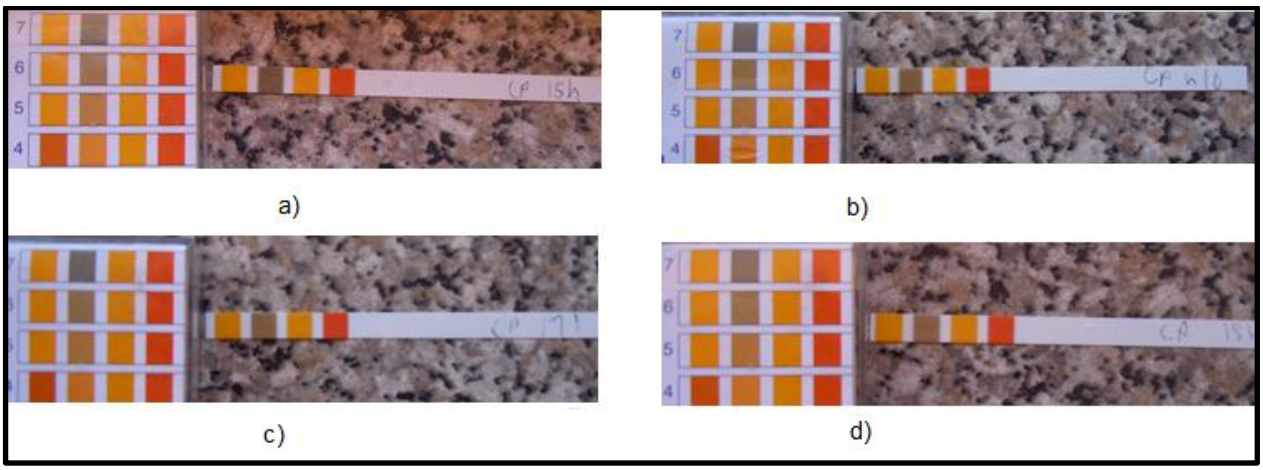

Figure 44 - pH Values of Methanol-Water Condensate After a) 15 hours, b) 16 hours, c) 17 hours, and d) 18 hours of Reforming CP Methanol

During the last 4 hours of the experiment the pH values started to change as displayed in Figure 44a), b), c), and d) where the light brown colour indicates a pH value between 6 and 7. Each hourly increment displays the pH strip turning lighter brown indicating a value closer to the pH of 6.

5.1.3 Results from Reformer Off-gas Condensate Analysis while Reforming Industrial grade Methanol

Similar to the previous two experiments, fresh catalyst was used along with Industrial grade methanol where the volume and mass of the reformer off-gas condensate was measured and recorded as displayed in Table 14.

Table 14 - Reformer Off-gas Condensate Analysis while Reforming Industrial grade Methanol

Time [hours]	Condensate Volume [ml]	Mass of 20ml Sample [g]	Density [gml^{-1}]	Methanol [%]	Methanol [g]	Methanol Conversion [%]
1	109.0	18.0136	0.9007	41.10	40.35	58.69
2	108.0	17.8612	0.8931	44.63	43.04	55.93
3	125.0	17.7456	0.8873	47.35	52.51	46.23
4	142.0	17.7561	0.8878	47.10	59.37	39.21
5	128.0	17.7148	0.8857	48.08	54.51	44.19
6	136.0	17.6940	0.8847	48.57	58.44	40.16
7	151.0	17.7046	0.8852	48.32	64.59	33.87
8	128.0	17.5800	0.8790	51.30	57.72	40.90
9	134.0	17.5960	0.8798	50.92	60.03	38.54
10	118.0	17.5580	0.8779	51.83	53.69	45.02
11	133.0	17.7527	0.8876	47.18	55.70	42.97
12	151.0	17.7432	0.8872	47.40	63.50	34.98
13	168.0	17.7306	0.8865	47.70	71.04	27.26
14	167.0	17.6768	0.8838	48.98	72.29	25.98
15	176.0	17.6719	0.8836	49.10	76.35	21.82
16	195.0	17.6345	0.8817	49.99	85.95	11.99

Table 14 above, is used to produce Figure 45, to display the methanol conversion of the catalyst in a line graph format.

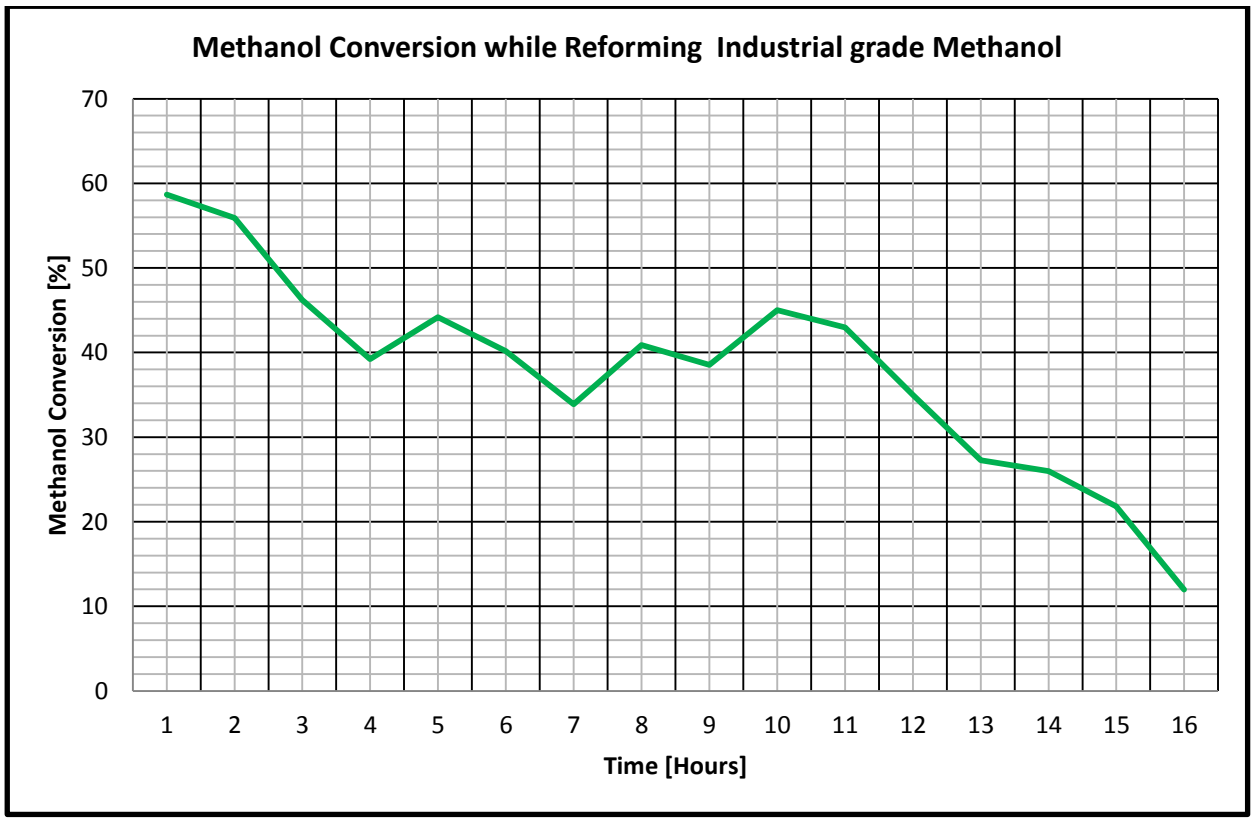

Figure 45 - Line Graph of Methanol Conversion over Time while Reforming Industrial grade Methanol

Figure 45 displays how the catalyst starts reforming the Industrial grade methanol at a maximum value of 58.69 %.

From 1 hour to 4 hours there is a negative gradient in methanol conversion from 58.69 % to 39.21 %. From the 4th hour to the 10th hour, the methanol conversion fluctuates between 33.87 % and 45.02 %, producing an overall increase in methanol conversion. Between 11 hours and 16 hours the conversion decreases linearly until it reaches 12 % where the experiment is stopped.

Table 14 and Figure 45 are used to determine the percentage change of the methanol conversion over the 16 hours as displayed in Figure 46.

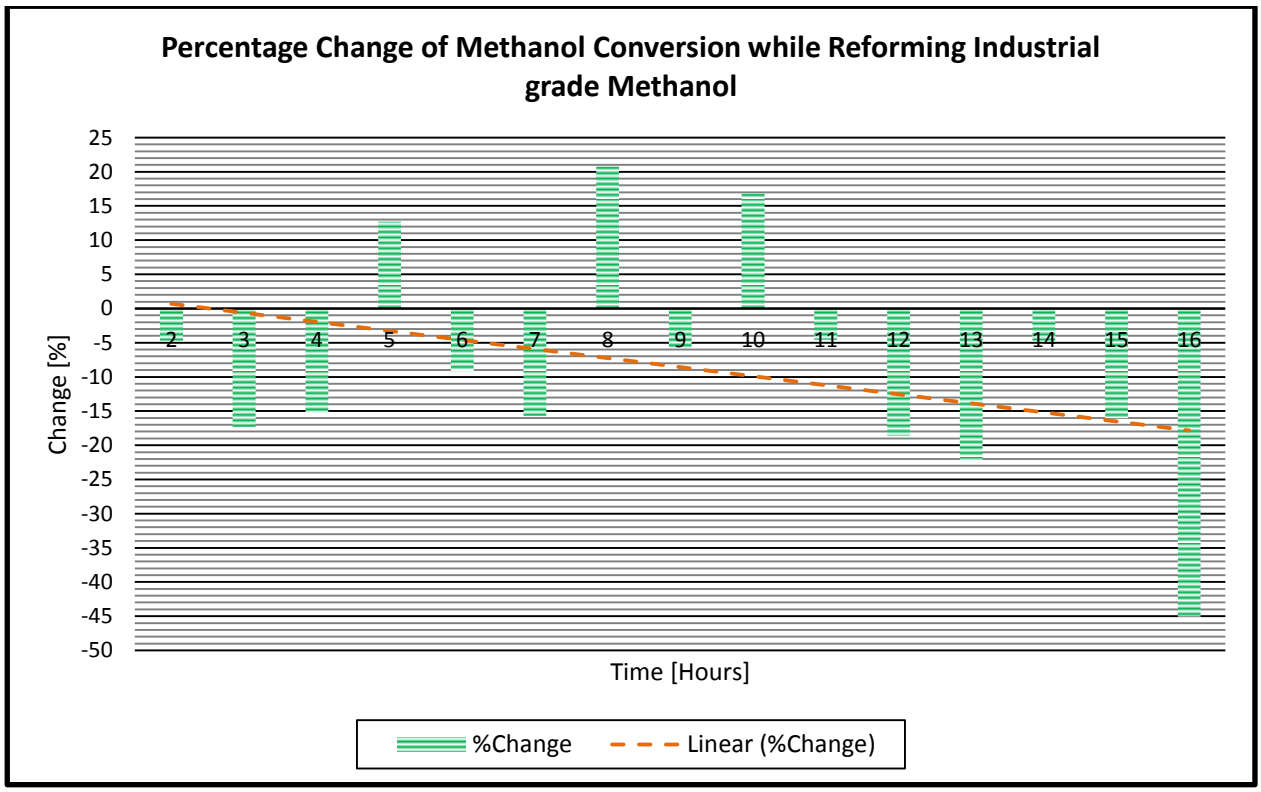

Figure 46 - Column graph of the Hourly Percentage Change in Methanol Conversion While Reforming Industrial grade Methanol

Between 2 hours and 4 hours there is a general negative percentage change in methanol conversion ranging from -4.71 % to -17.33 %. From 4 hours to 11 hours there are fluctuations, similarly seen in Figure 40 and Figure 43, ranging from -15.67 % to 20.76 % From 12 hours the gradient of the percentage change decreases until 16 hours. During this time the percentage decrease ranges from -4.70 % at 14 hours to -45.05 % at 16 hours.

The pH values of the condensate were determined by using pH strips, using the colour scale on the box displayed in Figure 47, a reasonably accurate pH value can be determined. The hours from 1 to 14 displayed a constant neutral pH value of 7 and are not displayed below.

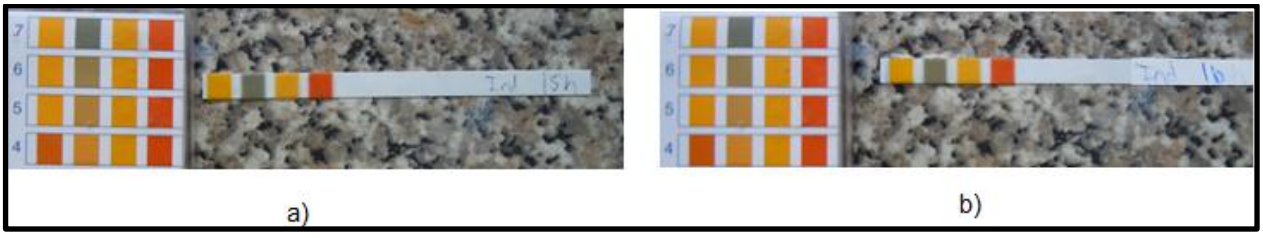

Figure 47 - pH Values of Methanol-Water Condensate After a) 15 hours and b) 16 hours of Reforming Industrial grade Methanol

Figure 47 displays the pH values of the methanol water condensate during the last two hours of the reforming of Industrial grade methanol during which the methanol conversion decreased to 13 % and the acidity of the condensate increased. Figure 47a) displays a value below 7 whereas the distinct browner colour of Figure 47b) indicates a pH value closer to 6.

5.1.4 Discussion of Results of Reformer Off-gas Condensate while Reforming AR, CP, and Industrial grade Methanol

After the methanol conversion of each methanol fuel quality, as well as their respective methanol conversion percentage changes has been presented in Section 5.1.1, 5.1.2, and 5.1.3, the results can be combined and compared more effectively by superimposing Figure 39, Figure 42, and Figure 45 onto one set of axes.

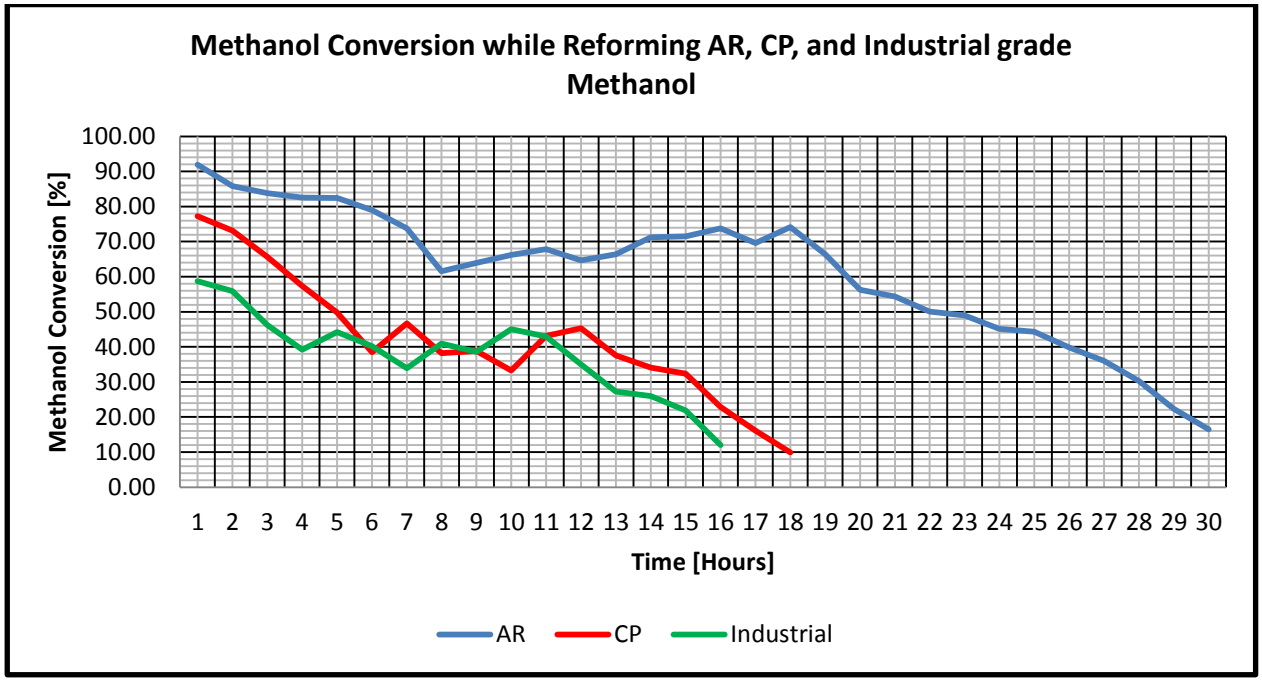

Figure 48 - Line graph for the Methanol Conversion over Time While Reforming AR, CP, and Industrial grade Methanol

Considering Figure 48 the following observations can be made:

- The time in which it takes the various quality methanol-water mixtures to deactivate the catalyst to a degree where the reforming ability of the reformer reaches 13% methanol conversion varies between methanol qualities.

- The maximum methanol conversion between 0 and 1 hours also varies depending on methanol qualities as well as the overall methanol conversion throughout the catalyst's lifetime.

- While reforming the 3 methanol qualities, a pattern was observed during which the methanol conversion decreases linearly, fluctuates between a certain range, and then finally decreases linearly towards the 13 % experimental end-point

The maximum methanol conversion appears to be related to the catalyst's ability to reform that specific methanol quality in the first hour while the catalyst is fresh. The lower the quality of the fuel the more difficult it is and the longer it takes to break the bonds between the carbon and hydrogen that make up the methanol molecule consequently decreasing methanol conversion rates during the first hour of reforming while the catalyst is fresh.

Table 15 - Observational Data for the Catalyst while reforming AR, CP, and Industrial grade Methanol

	AR	CP	Industrial
Maximum Methanol Conversion [%]	91.96	77.22	58.69
Average Methanol Conversion [%]	62.36	42.21	37.98
Time to reach 13% Conversion [hours]	30	18	16

From Table 15, it can be observed that in terms of the maximum methanol conversion there is a 16.03 % difference between AR and CP, and a 36.18 % difference between AR and the Industrial grade.

However, as sintering and poisoning takes place the overall methanol conversion decreases over time and the average methanol conversion over the life span of the catalyst can be taken into account as displayed in Table 15. There is a 32.12 % difference in average methanol conversion between the AR and CP methanol and a 39.10 % difference between the AR and Industrial grade methanol. This is a better indicator than the maximum methanol conversion as it considers the entire life span of the catalyst. The catalytic reforming of CP methanol is therefore, 32.12 % lower than that presented by reforming AR methanol; and 39.10 % lower catalytic reforming for the Industrial grade. Industrial grade methanol is therefore the least effective for hydrogen production throughout the catalyst life cycle.

By analysing Figure 39 through Figure 48 a pattern can be seen, where the catalyst undergoes a decrease in methanol conversion for a short time followed by a period where the trend in methanol conversion remains constant and finally reaches a point where the methanol conversion decreases rapidly once again. The duration of the first period is determined by the first instance where the percentage change turns from a negative to a positive. This period is displayed in Figure 49.

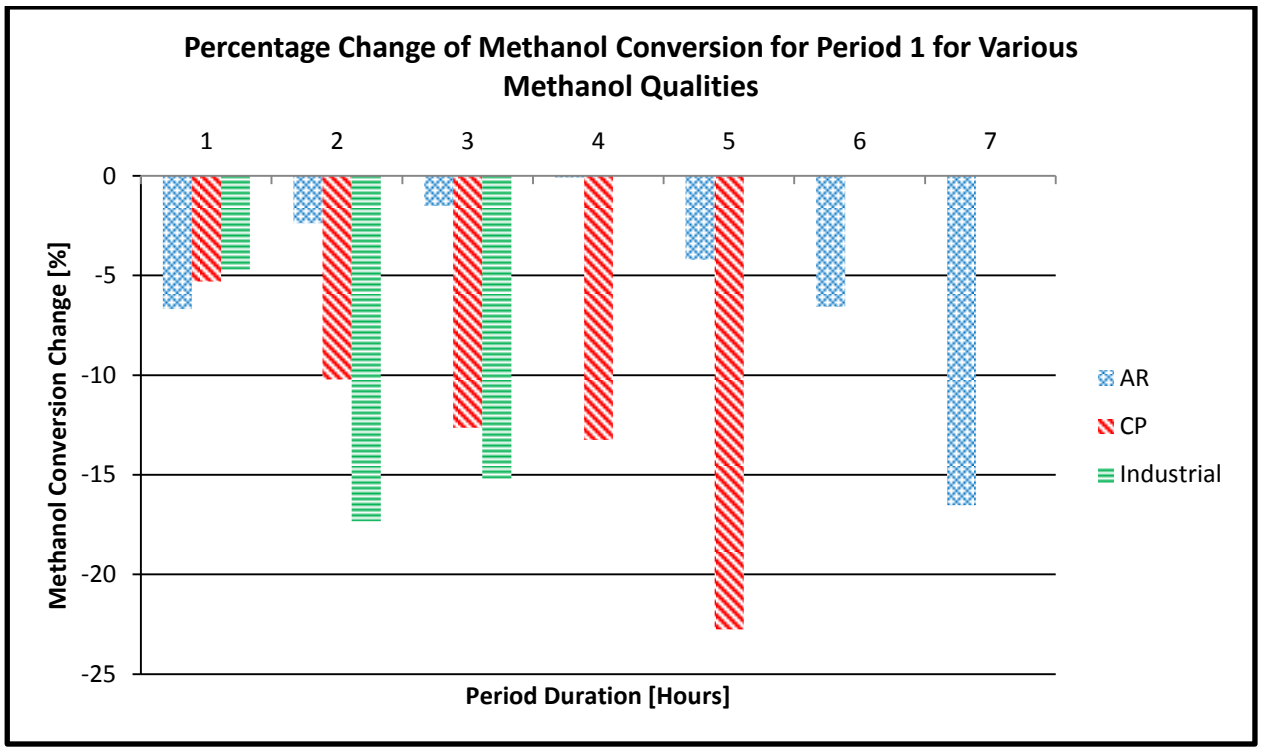

Figure 49 - Column Graph Representing Methanol Conversion Percentage Change for Period 1 while Reforming various Methanol Qualities

Table 16 - Period 1 for the AR, CP, and Industrial grade Methanol Conversion Percentage Change

Period 1	AR	CP	Industrial
Start	0	0	0
Duration	8	6	4
Average Percentage Change [%]	-5.40	-12.80	-12.41

By comparing methanol conversion percentage changes between reforming AR, CP, and Industrial grade methanol, the lowest decrease in methanol conversion was observed while reforming AR methanol. Reforming CP and Industrial grade methanol produced similar methanol conversion

decreases during the first period. This period provides a predictable linear decrease in methanol conversion while reforming all methanol qualities.

This methanol conversion decrease observed during the first period is attributed to a sintering process of the catalyst. This sintering process is further displayed and discussed later in the document when evaluating the catalyst's topology in Section 5.3. It will be noted that the catalyst porosity becomes less, with roughening and coarser surface texture observed, and cleavage detected, during the first 10 hours of operation.

Period 2 begins where the first positive methanol conversion percentage change value is displayed and ends before the methanol percentage change decreases sharply.

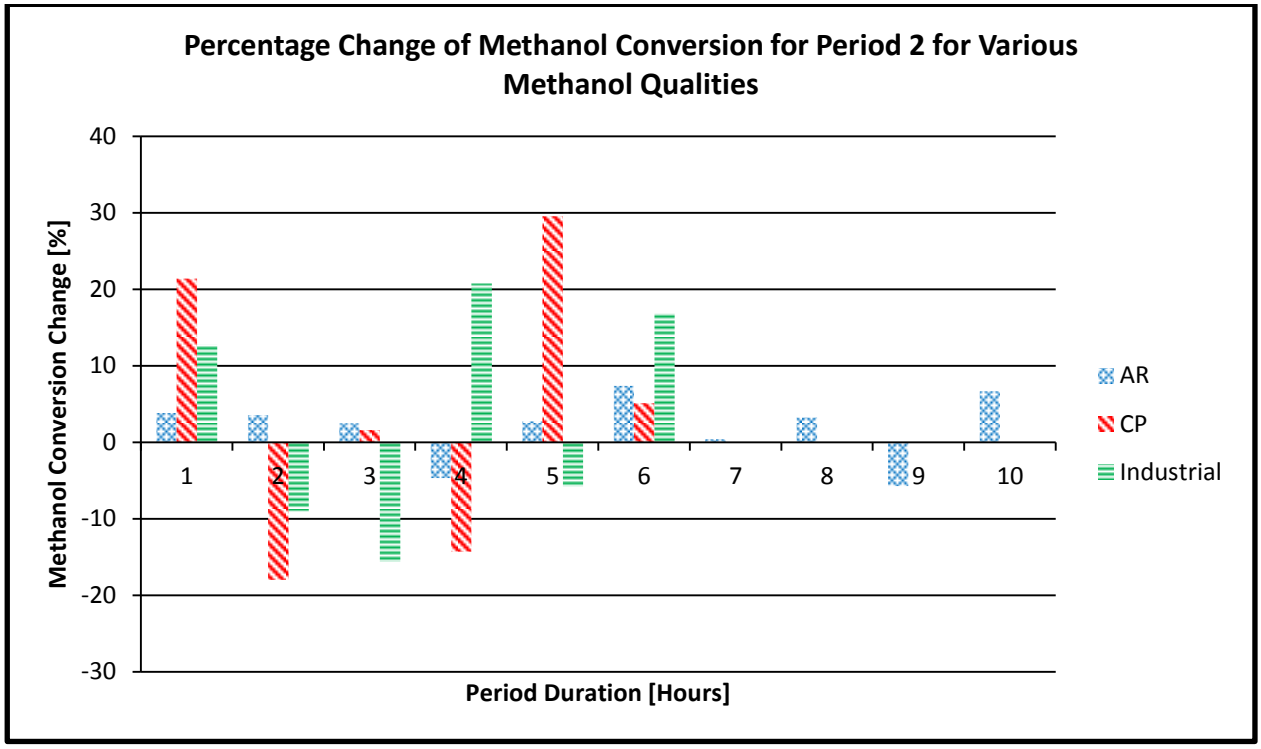

Figure 50 - Column Graph Representing Methanol Conversion Percentage Change for Period 2 while Reforming various Methanol Qualities

Table 17 - Period 2 for the AR, CP, and Industrial grade Methanol Conversion Percentage Change

Period 2	AR	CP	Industrial
Start	8	6	4
Duration	10	6	6
Average Percentage Change [%]	1.96	4.19	3.29

During period 2 it can be observed from Figure 50 and Table 17 that the percentage change has an overall increasing trend. Higher fluctuations are observed with less predictable methanol conversion over an hour to hour period. This does, however, produce a more constant methanol conversion trend. During Period 2, AR displays the lowest average percentage change values, which is indicative of a more predictable and stable methanol conversion. The strongest increasing trend is observed while reforming CP and Industrial grade.

For most of the methanol qualities, the longest duration is observed during Period 3 and shows the highest percentage decrease in methanol conversion.

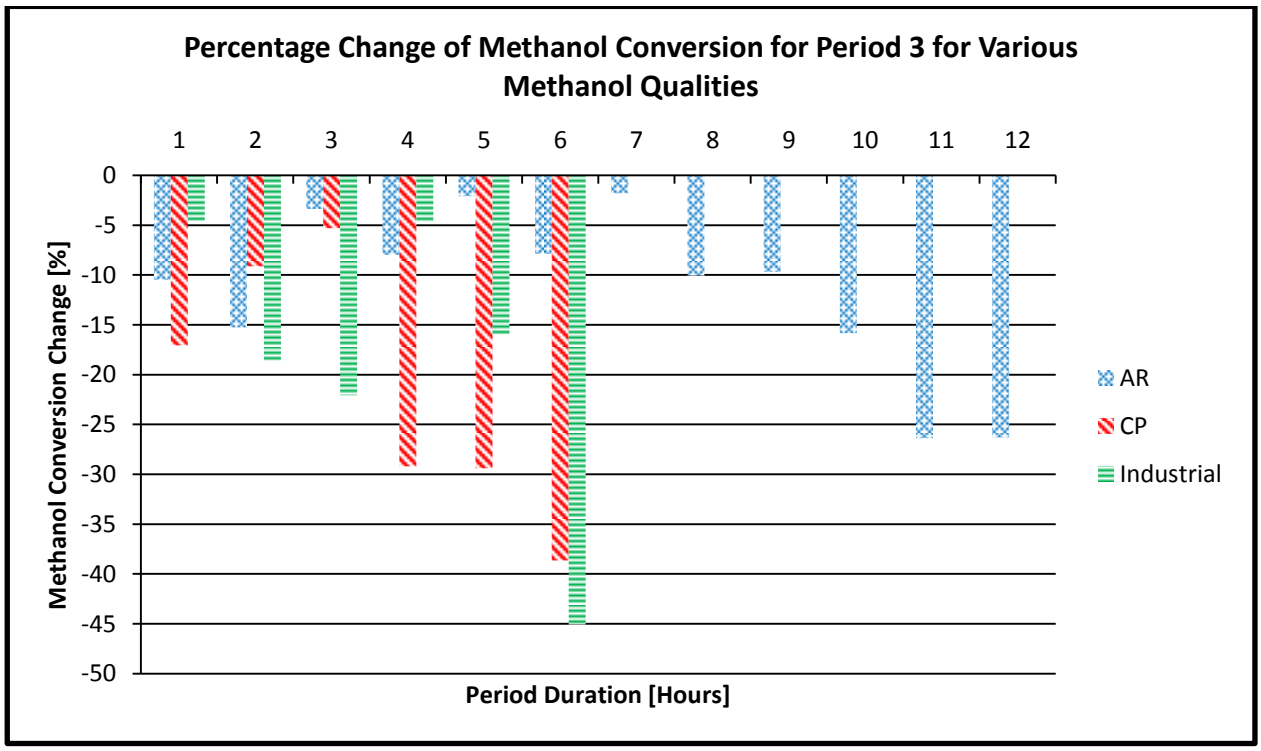

Figure 51 - Column Graph Representing Methanol Conversion Percentage Change for Period 3 while Reforming various Methanol Qualities

Table 18 - Period 3 for the AR, CP, and Industrial grade Methanol Conversion Percentage Change

Period 3	AR	CP	Industrial
Start	18	12	10
Duration	12	6	6
Average Percentage Change [%]	-11.4	-21.5	-18.5

In the final period CP methanol causes the highest average percentage decrease in methanol conversion. Both CP and Industrial grade methanol present percentage decreases larger than AR methanol and in a shorter reforming duration indicating an accelerated decrease in the catalyst lifespan.

It was observed that the duration of each period is proportional to the life span of the catalyst. While reforming AR methanol, the catalyst's life span was the highest and had the longest duration of each period; and inversely, the catalyst that reformed Industrial grade methanol had the shortest life span and the shortest period duration.

From the pH measurements of the reformer off-gas condensate presented during period 3, it can be concluded that although there is no significant difference between the acidity of the condensates, the duration with which the acidity increases varies between each methanol quality used. The timing of the change in pH coincides with the methanol conversion percentage decreasing and nearing 13 %. As discussed later, in Section 5.3, the chlorine concentration found in the catalyst increases during the last hours of the fuel qualifying experimentation for each methanol quality, and the chlorine ions that cannot be adsorbed by the catalyst were found in the methanol and water condensate increasing the acidity. By reforming a lower quality methanol, HCl will present itself in the condensate far quicker, degrading the membrane and substantially reducing its lifespan. When the membrane filter has been degraded its filtering ability will be compromised and the HCl would start affecting the fuel cell.

Due to the unreformed methanol and water condensate forming part of the reformer off-gas, its analysis and discussion along with the detection of HCl, contributes to the addressing of the problem statement of qualifying the effect that a variation in methanol quality would have on the reformer off-gas composition.

For the validation of the methanol conversion for the three different methanol fuel qualities, the methanol conversion values for literature used will be taken for temperatures at 250 °C and mass flow rates as near as possible for accurate comparison. For each methanol quality reformed, the

average methanol conversion of the stable duration period 2, after the sintering process, was used for validation. Relative error was used to measure the extent of the difference between the experimental results presented by this study to that of published literature.

Relative Error - $\text{RelErr} = \frac{x_{expected} - x_{practical}}{x_{expected}} * 100$ (5.6)

Table 19 - Validation of Methanol Conversion for Reforming of AR, CP, and Industrial grade Methanol Compared to Published Research Data

Study	Methanol Conversion of Study [%]	Experimental Methanol Conversion [%]			Relative Error [min%/ max%]
		AR	CP	Industrial	
(Gu *et al.,* 2003)	96.45	68.93	40.89	40.45	-28.53 / -58.06
(Purnama, 2003)	55.00	68.93	40.89	40.45	25.33 / -26.45
(Makertihartha & Gunawan, 2009)	78.00	68.93	40.89	40.45	-11.63 / -48.14
(Lee *et al.*, 2004)	97.00	68.93	40.89	40.45	-28.94 / -58.30
(Sá *et al.*, 2010)	39.00	68.93	40.89	40.45	3.72 / 79.74
(Sa´ *et al.,* 2011)	78.00	68.93	40.89	40.45	-11.63 / -48.14
(Kurr *et al.*, 2008)	84.40	68.93	40.89	40.45	-18.33 / -52.07
(Kim *et al.*, 2016)	36.00	68.93	40.89	40.45	12.36 / 91.47

From Table 19 it can be observed that throughout the range of published research results, the methanol conversions vary from one another despite reforming with similar commercial catalyst and having displayed methanol conversion at an operating temperature of 250 °C

The relative errors were lowest when compared to Lee *et al.* (2004) and Gu *et al.* (2003) with a methanol conversion of 97% and 96.45% respectively. The published research with WHSV nearest to that used by this study of $1.4h^{-1}$, was Makertihartha and Gunawan (2009) which presented relative errors between -11.63 % and -48.14 % for the methanol conversion of 78 %. Sa´ *et al.* (2010) and Kim *et al.* (2016) displayed the lowest methanol conversion of 39 % and 36 %

respectively, which presented relative errors between 3.72 % and 79.74% when compared to Sa´ *et al.* (2010), and between 12.36 % and 91.47 % compared to Kim *et al.* (2016).

The methanol conversions of the fuel qualifying experimental facility generally displayed lower than that presented by the published research results are attributed to the smaller pore sizes and reduced surface area of the manufactured catalyst.

It was observed that the methanol conversion by the reforming of the CP and Industrial grade methanol presented the largest relative errors when compared to that of the published research results. This is indicative of an unpredictable and lowered methanol conversion while reforming with these lower methanol qualities.

Variations between published research results are due to differences in reformer diameters, flow rates, and methanol-water molar ratios making accurate validation difficult. However, literature substantiates methanol conversion as the correct criteria to consider when evaluating catalyst and reformer performance. When considering the variation between the sources due to their flow rates as well as the positive and negative range of relative errors between the published research methanol conversion result values and experimental methanol conversion result values, the presented methanol conversion values from the experimentation can be considered an acceptable and an accurate depiction of the operation of a methanol steam reformer for all methanol qualities and is relevant to the field. Methanol condensate forms part of the reformer off-gas composition and is crucial to contributing to the addressing of the problem statement due to it determining fuel quality's effect on hydrogen production and the downstream subsystems.

5.2 Analysis of Reformer Product Off-gas

From Section 2.6 it was concluded that the reformer product off-gases are a mixture of hydrogen, carbon dioxide, and carbon monoxide. All of these gases are readily detected and quantified by a gas chromatograph. Methods to determine the presence and concentrations of hydrogen sulphide were implemented, as discussed in Section 2.6.1. The results and discussions of the reformer off-gases while reforming the various methanol fuel qualities analysed using the gas chromatograph and the wet lead acetate paper strips are presented in the sections below.

At 10 hour intervals and at the conclusion of the fuel qualifying experiments, the reformer off-gas samples taken from Sample Point 2 were analysed using a gas chromatograph, which displays the peaks and molar quantities of each gas it is calibrated to analyse. The figures produced by the gas chromatograph below display the peaks of Hydrogen, Nitrogen, Carbon Monoxide, and Carbon Dioxide respectively from left to right. The heights of the peaks and area under the curves

represent the mol% of the gases in relation to one another. Part b) of each Figure is an enlargement of Part a) for the purposes of focusing on the peak of carbon monoxide as well as the curve of carbon dioxide. The unusual presentation on the carbon dioxide curve is caused by a slight amount of moisture in the gas sample. The carbon dioxide graph sits above the moisture line causing the bottom left and right hand sections to have an offset from the origin line, therefore, the carbon dioxide curve was manually integrated.

5.2.1 Results from Reformer Product Off-gas Analysis while Reforming AR Methanol

The results provided from the analysis of the reformer product off-gases with fresh catalyst, while reforming AR methanol fuel mixture over three 10 hour time intervals are displayed below. The peaks and curves produced by the gas chromatograph are displayed in Figure 52, Figure 53, and Figure 54.

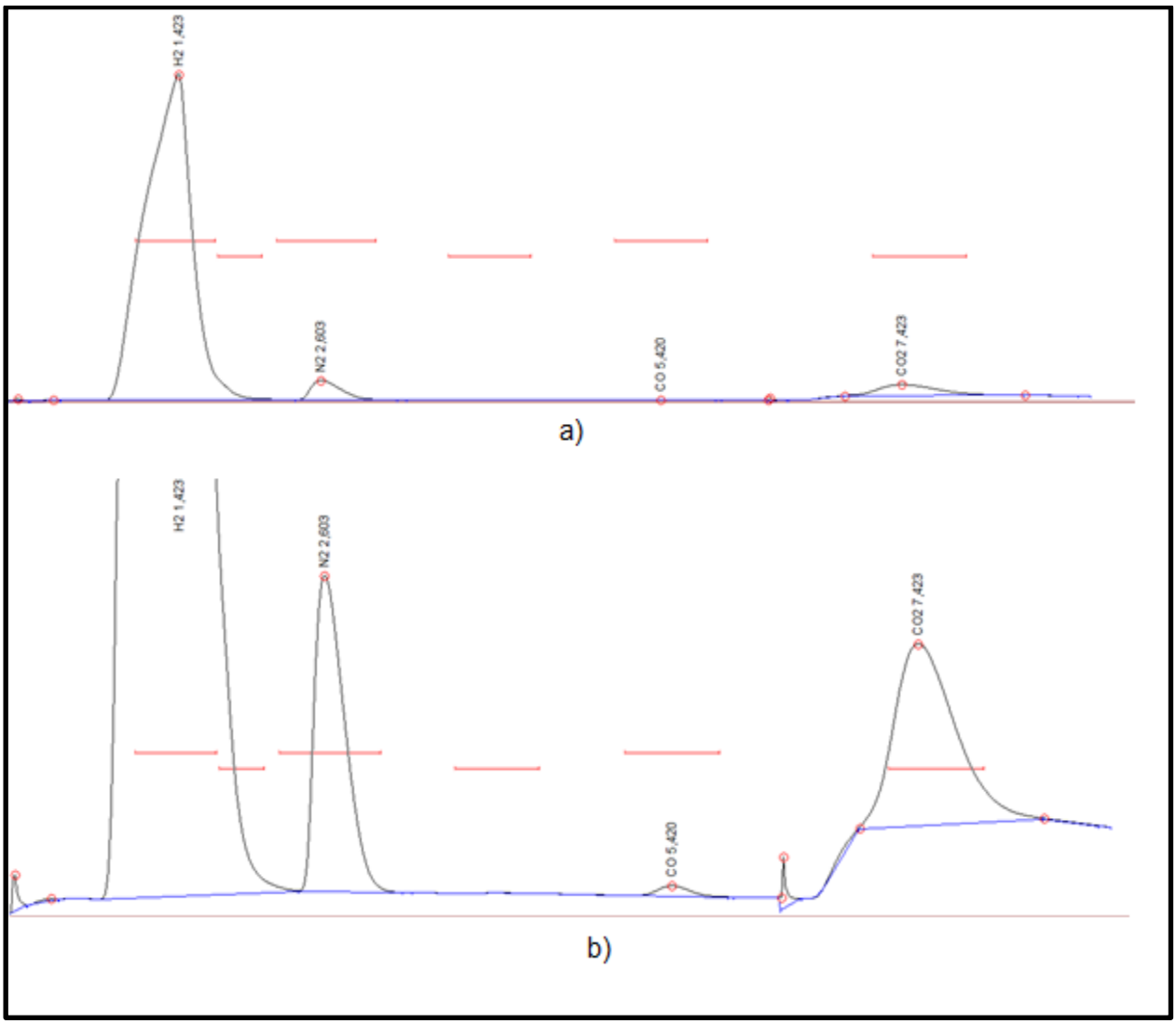

Figure 52 - Gas Chromatography Peaks of Reformer Off-Gas Sample while Reforming AR Methanol for 10 hours

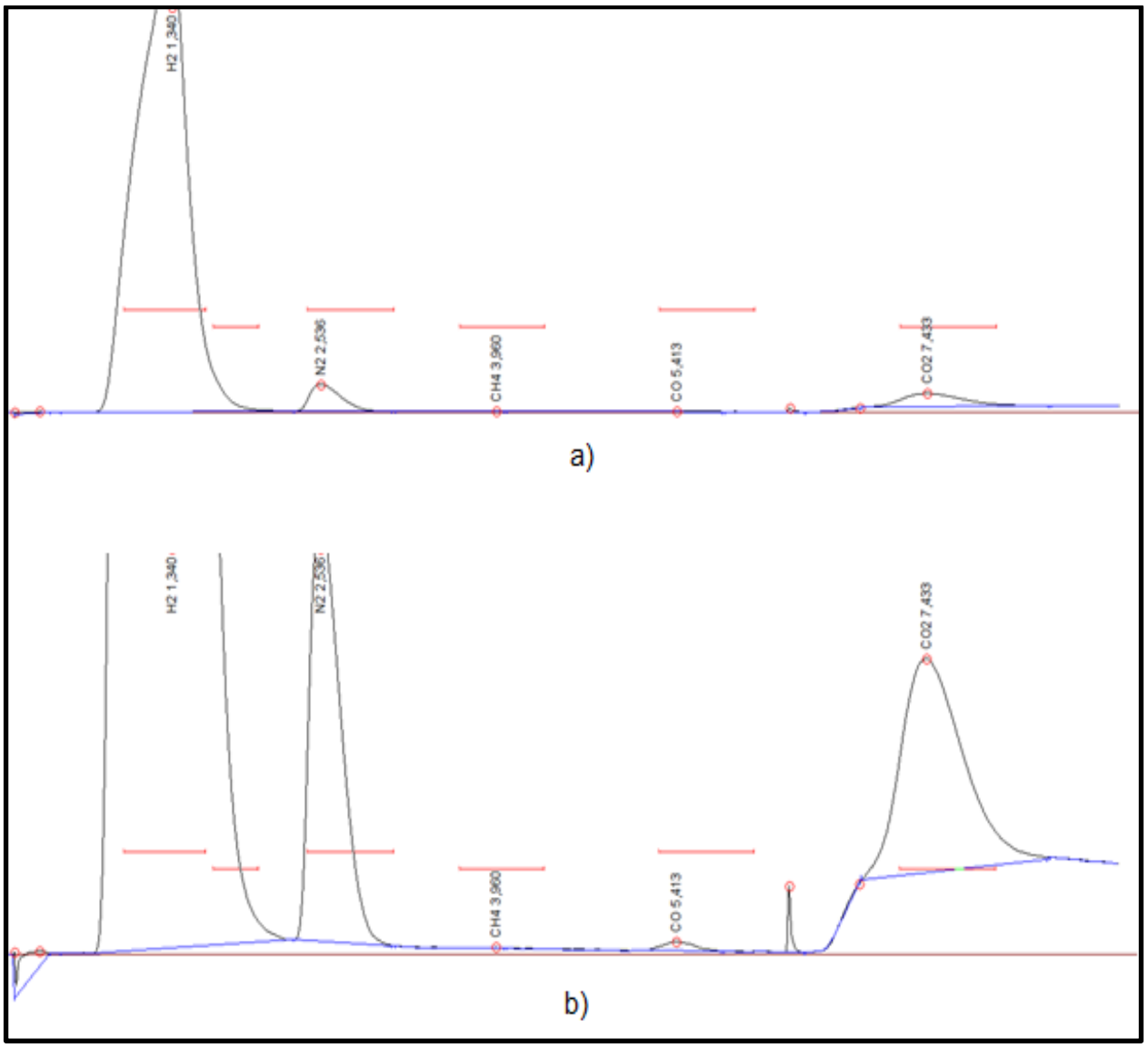

Figure 53 - Gas Chromatography Peaks of Reformer Off-Gas Sample while Reforming AR Methanol for 20 hours

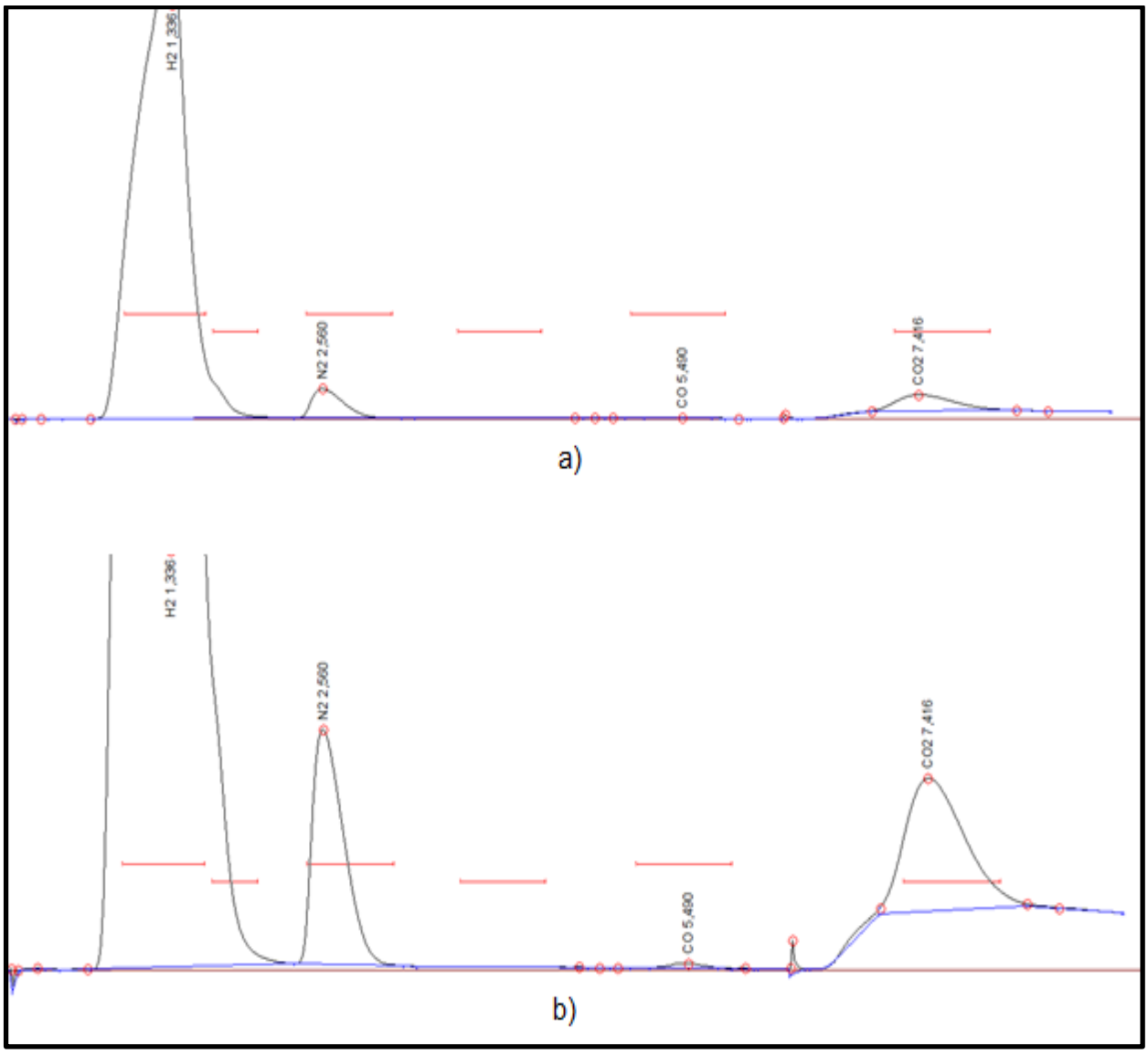

Figure 54 - Gas Chromatography Peaks of Reformer Off-Gas Sample while Reforming AR Methanol for 30 hours

Lead acetate strips were used to detect the presence of H_2S in the off-gas stream during the 30 hour experiment duration. The lead acetate strips are displayed in Figure 55.

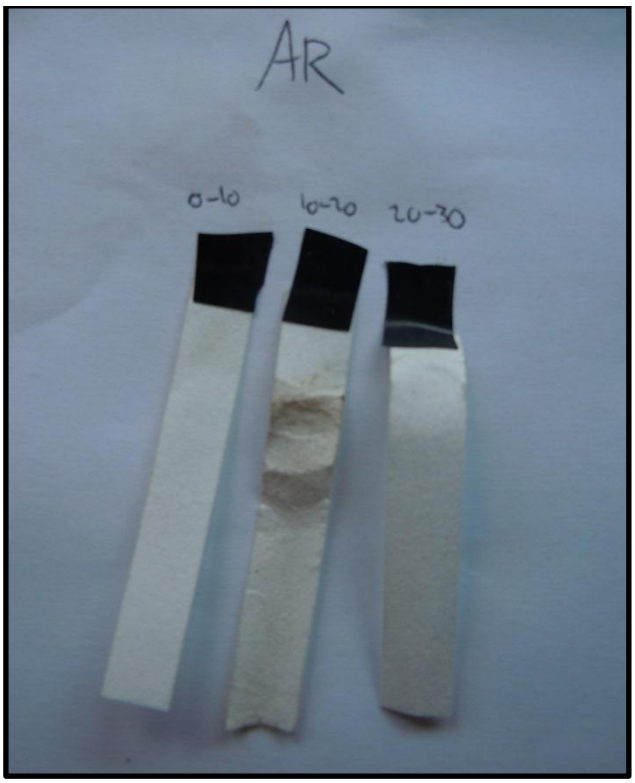

Figure 55 - Lead Acetate Paper for H_2S Detection and Measurement of Reformer Off-Gas while Reforming AR Methanol for 10, 20, and 30 hours

The lead acetate strips displayed in Figure 55 do not show any indication of hydrogen sulphide being present in the gas that has passed over it at any point during the three 10 hour intervals. If any H_2S were present a shade of black or brown precipitate would have formed depending on the concentration.

Table 20 is the combination of the mol% values from the three reformer off-gas samples taken during the 10 hour, 20 hour, and 30 hour intervals while reforming the AR methanol and water fuel mixture.

Table 20 - Gas Chromatography Results of Reformer Off-Gas Sample while Reforming AR Methanol for 10, 20, and 30 hours

Time [hours]	10	20	30
H_2 [mol%]	60.167	64.393	61.195
CO_2 [mol%]	21.015	17.590	19.560
CO [mol%]	0.460	0.276	0.273
Other [mol%]	N_2: 18.358	N_2: 17.742	N_2: 18.973
Total [mol%]	100.000	100.000	100.000
H_2S [ppm]	0	0	0

For the purposes of this study, the gas analysis results spectrum can be normalised for H_2, CO_2, and CO to present Figure 56 to further graphically display the gas composition.

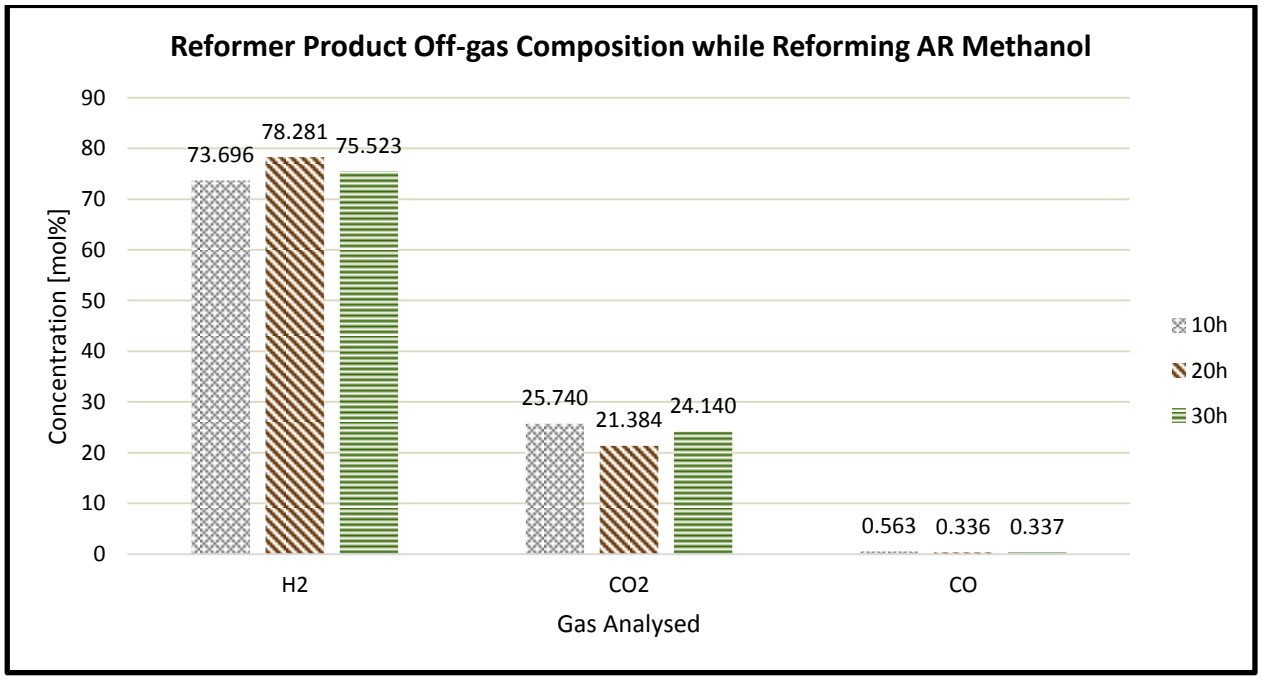

Figure 56 - Column Graph Representing Reformer Product Off-gas Composition while Reforming AR Methanol

Considering Figure 56, it was observed that hydrogen concentration increased by 6.21 % between the 10 hour and 20 hour interval along with a 16.94 % decrease in carbon dioxide concentration. Between the 20 hour and 30 hour intervals the hydrogen decreased by 3.50 % and the carbon dioxide increased by 12.91 %. The largest observable difference in gas composition is the carbon

monoxide decreasing by 40.32 % between the 10 hour and the 20 hour intervals. Thereafter the carbon monoxide mol% remains constant.

5.2.2 Results from Reformer Product Off-gas Analysis while Reforming CP Methanol

The results provided from the analysis of the reformer product off-gases with fresh catalyst while reforming CP methanol fuel mixture over a 10 hour time interval and after the end of the experiment at 18 hours are displayed below. The peaks and curves produced by the gas chromatograph are displayed in Figure 57, and Figure 58.

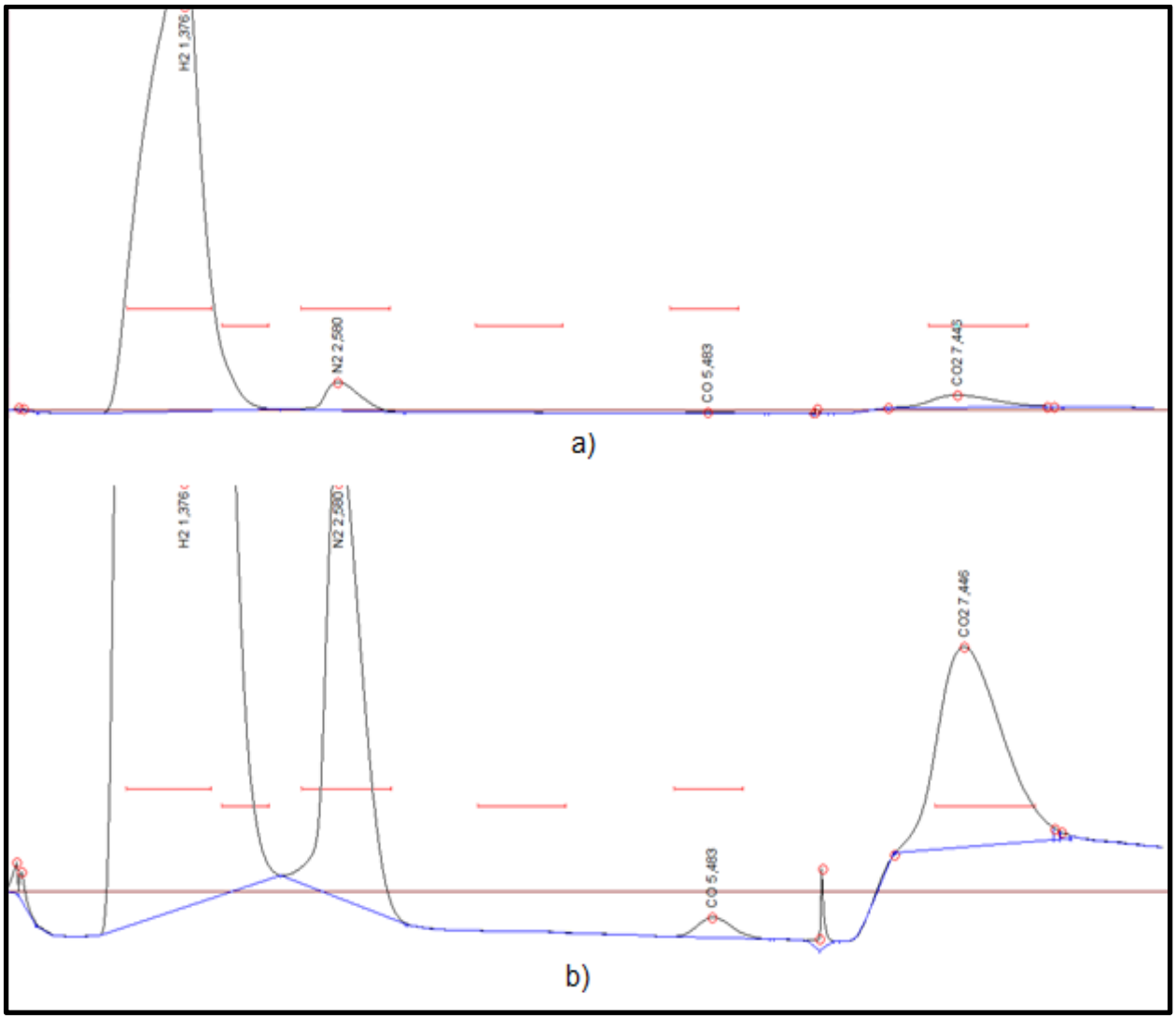

Figure 57 - Gas Chromatography Peaks of Reformer Off-Gas sample while Reforming CP Methanol for 10 hours

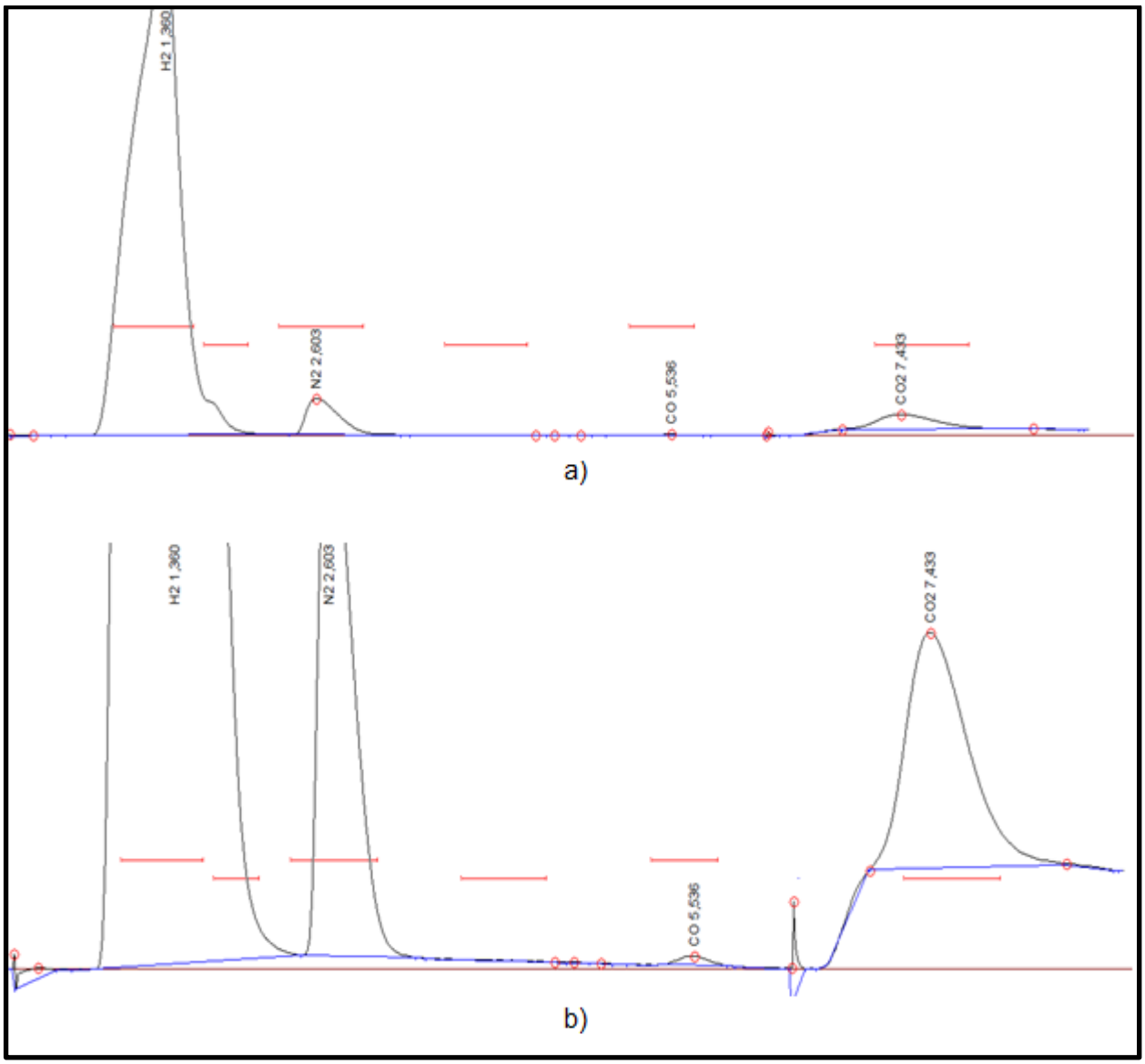

Figure 58 - Gas Chromatography Peaks of Reformer Off-Gas sample while Reforming CP Methanol for 18 hours

The gas chromatograph had undergone a calibration process the day before the analysis and some settings on the graphing were not yet correctly set in. This does not change the accuracy of the peaks or the results, it simply causes the aesthetics of the graph to differ slightly.

Figure 59 displays the lead acetate strips for the detection and measurement of hydrogen sulphide in the reformer off-gases over the 18 hours of reforming the CP methanol fuel mixture.

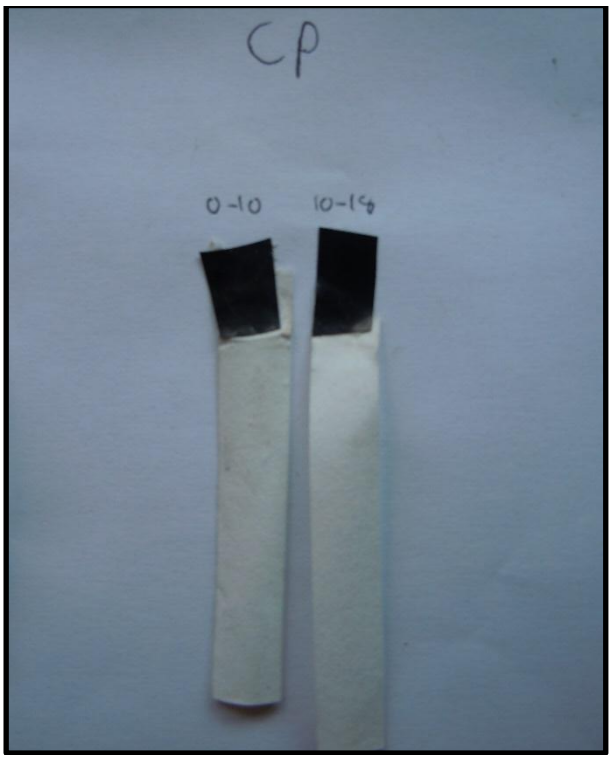

Figure 59 - Lead Acetate Paper for H2S Detection and Measurement of Off-Gas while Reforming CP Methanol for 10 and 18 hours

The lead acetate strips in Figure 59 do not have any distinct colour differences indicating that there was no hydrogen sulphide present in the gas that had passed over it at any point during the 18 hour experiment.

Table 21 is the combination of the mol% values from the two reformer off-gas samples taken during the 10 hour and 18 hour intervals while reforming the CP methanol and water fuel mixture.

Table 21 - Gas Chromatography Results of Reformer Off-Gas Sample while Reforming CP Methanol for 10 and 18 hours

Time [hours]	10	18
H_2 [mol%]	63.878	58.632
CO_2 [mol%]	15.038	17.157
CO [mol%]	0.595	0.227
Other [mol%]	N_2: 20.488	N_2: 23.983
Total [mol%]	100.000	100.000
H_2S [ppm]	0	0

As done in Section 5.2.1, the gas analysis results spectrum was normalised for H_2, CO_2, and CO to present Figure 60 to further graphically display the gas composition.

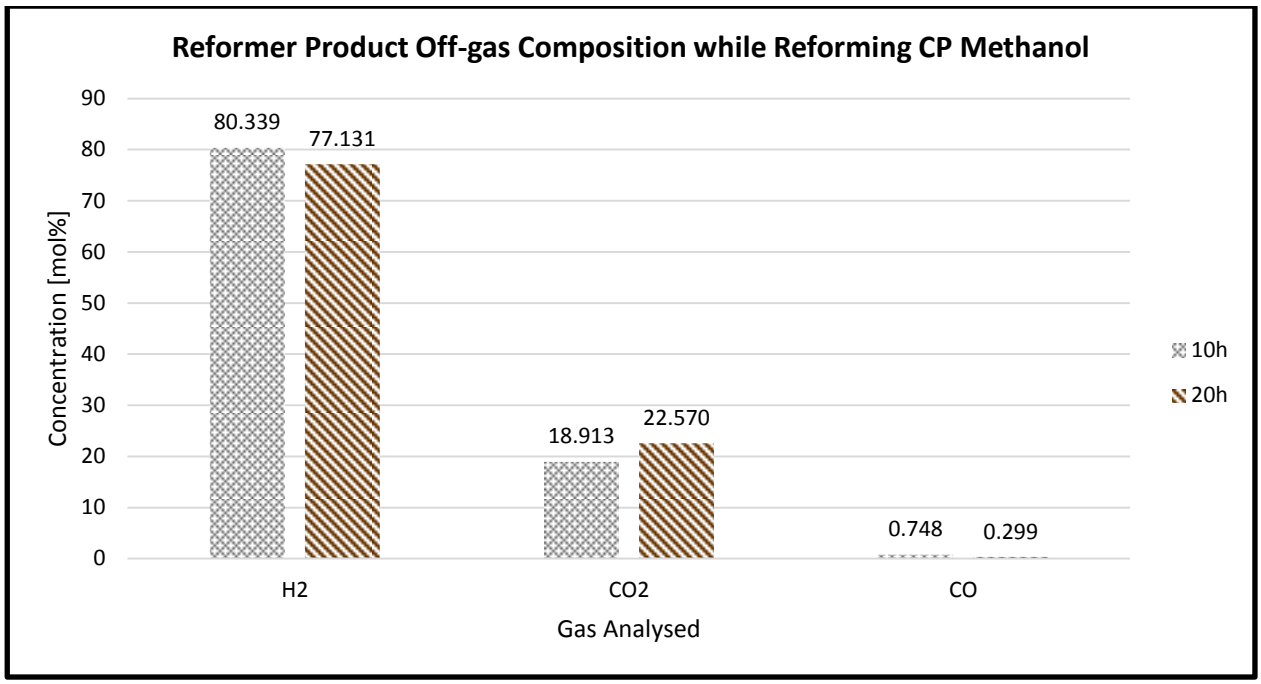

Figure 60 - Column Graph Representing Reformer Product Off-gas Composition while Reforming CP Methanol

Considering Figure 60, it is observed that the gas composition does not change significantly throughout the reforming of CP methanol. The hydrogen concentration decreased by 3.99 % between the 10 hour and 20 hour interval along with the carbon dioxide concentration increasing by 19.35 %. The largest observable difference in gas composition is the carbon monoxide decreasing by 60.03 % between the 10 hour interval and the 20 hour interval.

5.2.3 Results from Reformer Product Off-gas Analysis while Reforming Industrial grade Methanol

This section displays the results provided from the analysis of the reformer product off-gases with fresh catalyst while reforming Industrial grade methanol fuel mixture over a 10 hour time interval and after the end of the experiment at 16 hours. The peaks and curves produced by the gas chromatograph are displayed in Figure 61, and Figure 62.

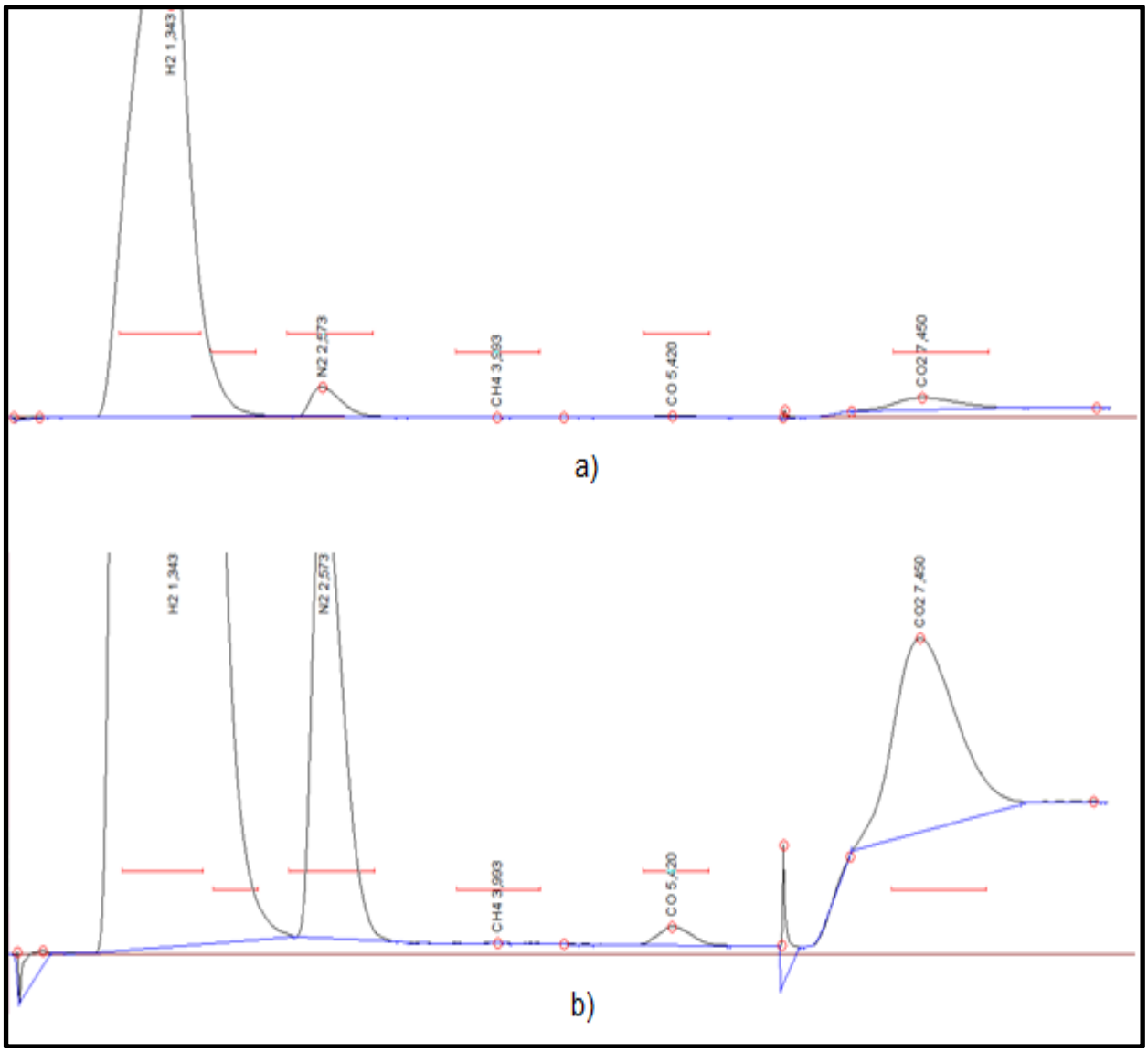

Figure 61 - Gas Chromatography Peaks of Reformer Off-Gas Sample while Reforming Industrial grade Methanol for 10 hours

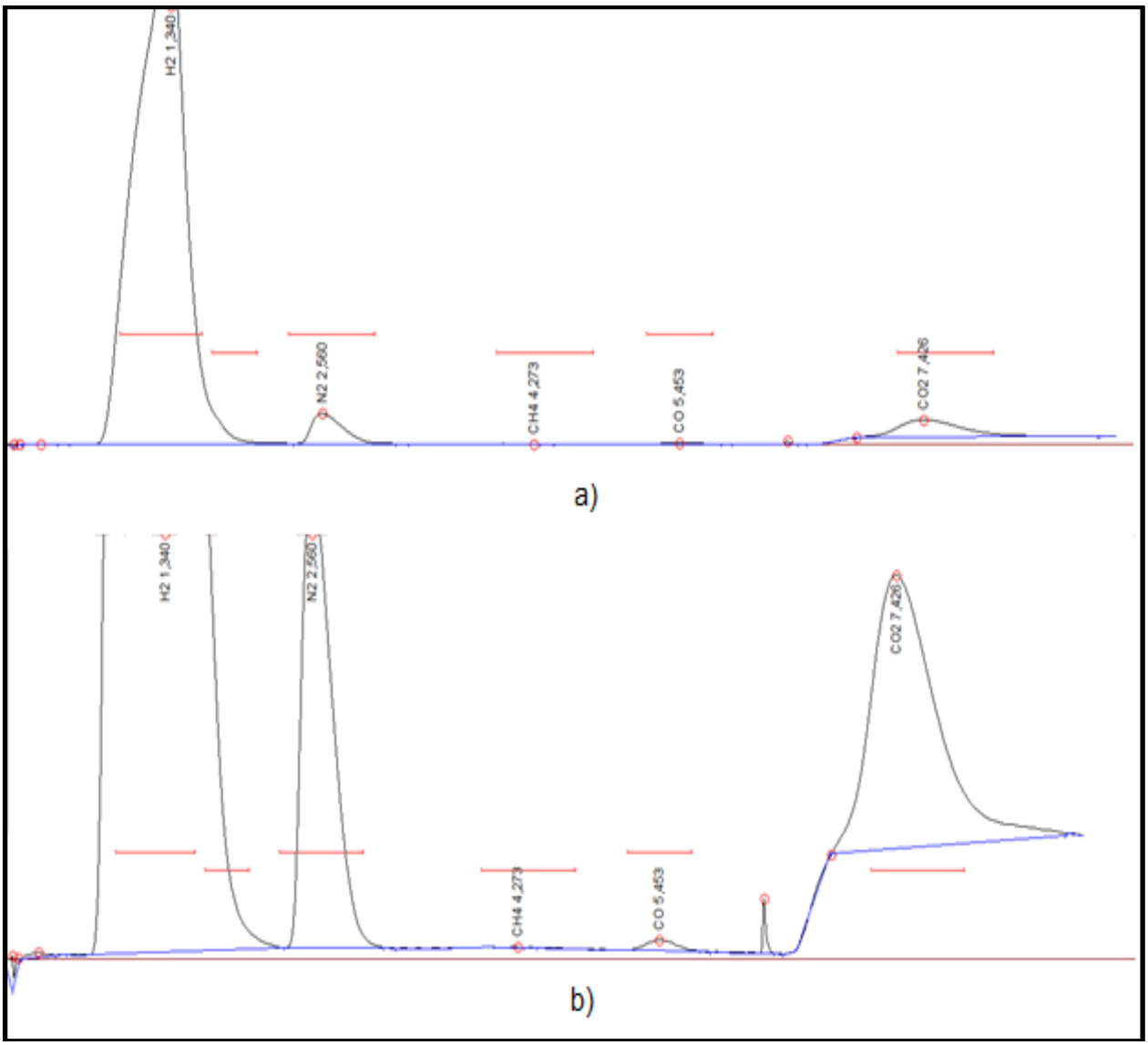

Figure 62 - Gas Chromatography Peaks of Reformer Off-Gas Sample while Reforming Industrial grade Methanol for 16 hours

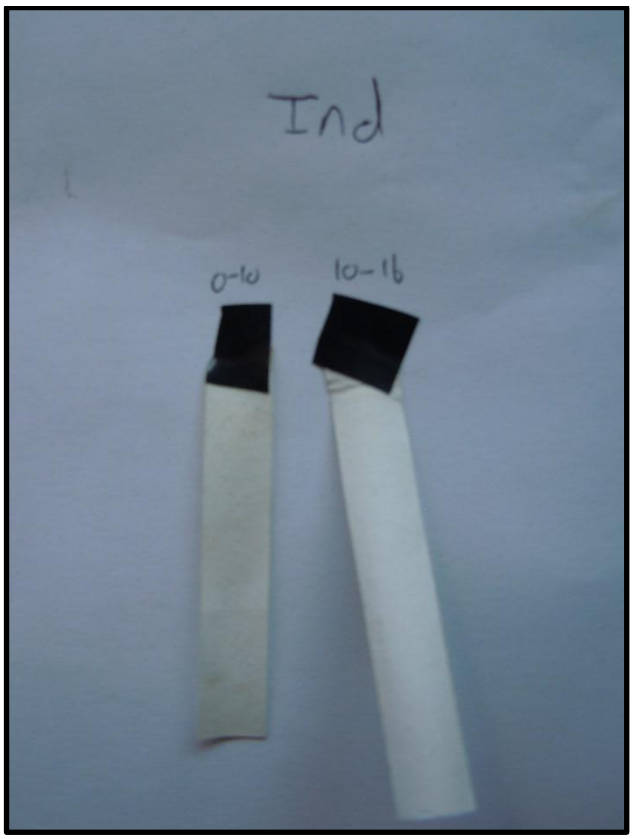

Figure 63 - Lead Acetate Paper for H2S Detection and Measurement of Off-Gas while Reforming Industrial grade Methanol for 10 and 16 hours

The lead acetate indicator strips displayed in Figure 63 do not show any distinct indication of hydrogen sulphide being passed over it during the 16 hours of reforming Industrial grade methanol.

Table 22 is the combination of the mol% values from the two reformer off-gas samples taken during the 10 hour and 16 hour intervals while reforming the Industrial grade methanol and water fuel mixture.

Table 22 - Gas Chromatography Results of Reformer Off- Gas Sample while Reforming Industrial grade Methanol for 10 and 16 hours

Time [hours]	10	16
H_2 [mol%]	67.580	58.894
CO_2 [mol%]	13.490	21.687
CO [mol%]	0.512	0.277
Other [mol%]	N_2: 18.418	N_2: 19.142
Total [mol%]	100.000	100.000
H_2S [ppm]	0	0

For the purposes of this study, the gas analysis results spectrum can be normalised for H_2, CO_2, and CO to present Figure 64 to further graphically display the gas composition.

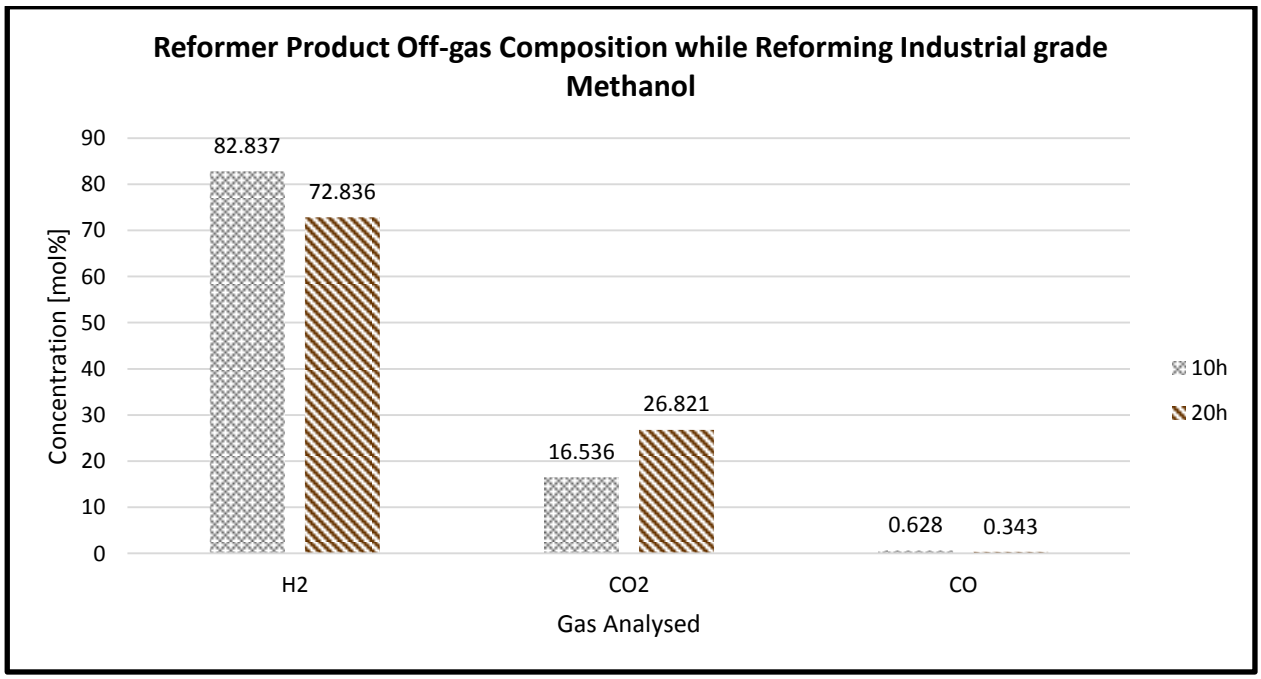

Figure 64 - Column Graph Representing Reformer Product Off-gas Composition while Reforming Industrial grade Methanol

Considering Figure 64, the hydrogen concentration decreased by 12.07 % between the 10 hour and 20 hour interval along with the carbon dioxide concentration increasing by 62.15 % which was the largest observable difference. The carbon monoxide concentration decreased by 45.38 % between the 10 hour interval and the 20 hour interval.

5.2.4 Discussion of Results from Reformer Product Off-gas while Reforming AR, CP, and Industrial grade Methanol

The analysis of each gas sample at the various intervals while reforming various methanol qualities, shows that the highest concentration by mol% of gas product formed is Hydrogen, followed by Carbon Dioxide, Nitrogen, and Carbon Monoxide respectively. It would have been ideal if there was no nitrogen in the gas sample due to it not being a product of the methanol steam reforming process, but the purging of the reformer and the gas sampler allows for the possibility of nitrogen being part of the gas sample.

When considering the curves and peaks produced by the gas chromatograph for the off-gas produced by each methanol quality, it was observed the peaks and curves do not vary significantly and no unidentifiable gases that did not form part of the expected gas composition were observed.

Figure 53, Figure 61, and Figure 62 display a label for methane (CH_4), which indicates the gas chromatograph was calibrated for measuring methane, however, due to the lack of a peak it can be concluded that there was none to be analysed or the concentration was below instrument detection limit. For the reforming of all methanol qualities, the gas chromatograph did not detect any foreign gases that were unexpected.

For the comparison of reformer product off-gas composition while reforming the three methanol qualities, Figure 65 and Figure 66 are displayed by superimposing Figure 56, Figure 60, and Figure 64 onto one set of axis.

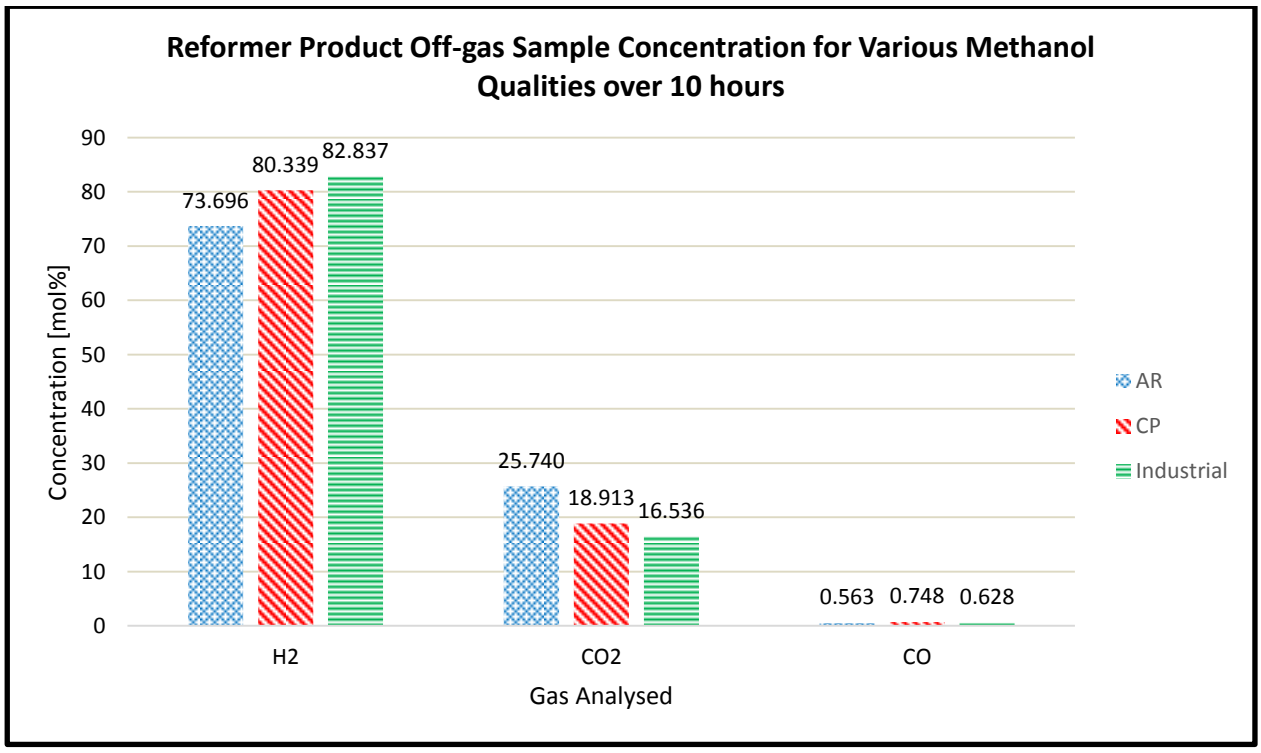

Figure 65 - Column Graph Representing Reformer Product Off-gas Composition while Reforming AR, CP, and Industrial grade Methanol during first 10 hour Interval

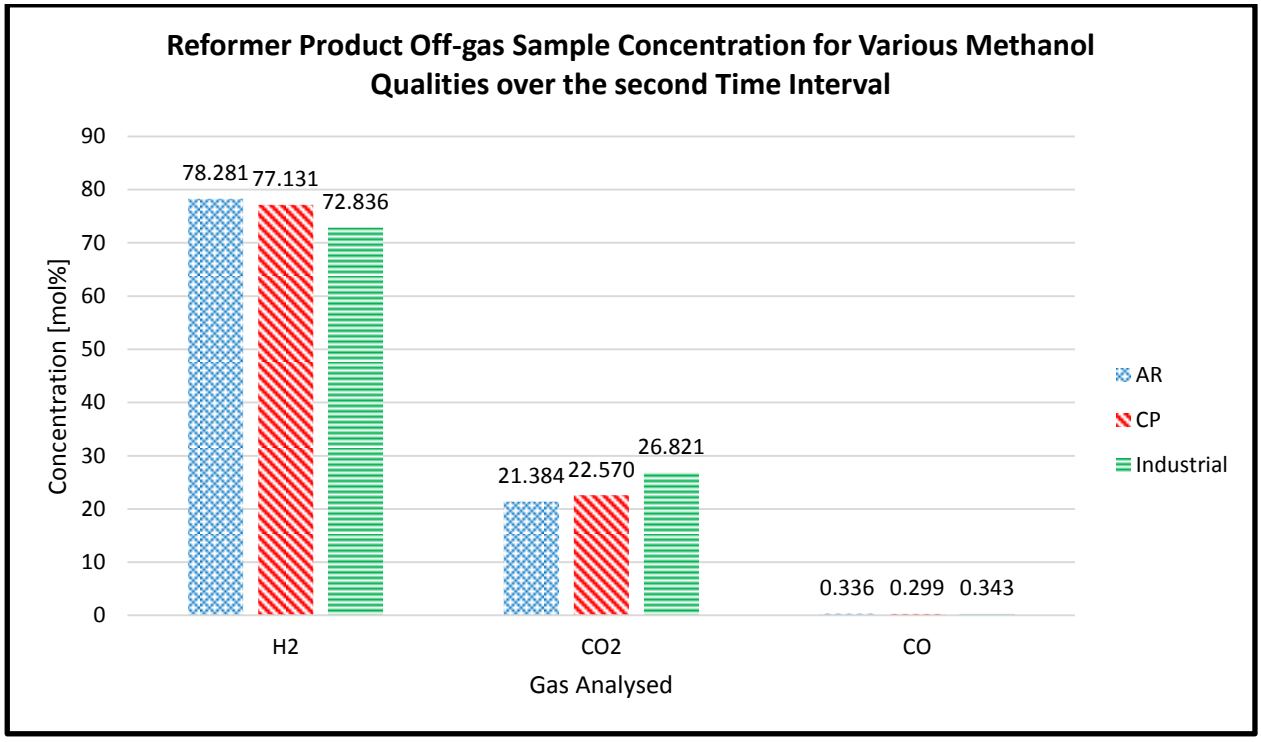

Figure 66 - Column Graph Representing Reformer Product Off-gas Composition while Reforming AR, CP, and Industrial grade Methanol during second time Interval

From Figure 65, it was observed that during the first 10 hour time interval the sample of reformer product off-gas composition produced by reforming Industrial grade contained the highest mol% of hydrogen followed by CP methanol and AR methanol. It was observed that the hydrogen and carbon dioxide mol% values are inversely proportional. From Figure 66 it was observed that during the second time interval the reforming of AR methanol produced the highest mol% of hydrogen followed by CP and Industrial grade methanol. Similar to Figure 65 the hydrogen and carbon dioxide mol% are inversely proportional.

Although during the first 10 hours the Industrial grade methanol produces a higher concentration of hydrogen, the overall methanol conversion remains below that of AR and CP methanol and coupled with a lower catalyst lifespan, reforming with Industrial grade methanol would, in total, produce lower hydrogen volumes.

The resulting gas composition values remain similar between each sample independent of the reforming time which is indicative of result repeatability. From Section 5.1, it can be observed how the methanol conversion decreases during experimentation to 13 %, however, the composition of the gas samples appear to remain independent of the methanol conversion. This observation was also made in Section 2.6 when discussing the gas analysis of the study presented by Kurr *et al.* (2008).

The only significant difference in gas composition was the change in carbon monoxide between the first 10 hour interval and the intervals subsequent to it. The carbon monoxide composition decreases by 39.13 %, 61.67 %, and 45.10 % while reforming AR, CP, and Industrial grade methanol respectively during the second time interval. Although these concentration decreases are a large difference, the changes in CO concentrations for all methanol qualities are small relative to the other gases in the spectrum. Thereafter, the carbon monoxide concentration remains constant while reforming AR methanol and it can be considered that the same will occur while reforming CP and Industrial grade if the catalyst lifespan had allowed further experiment duration.

As discussed in Section 2.6, the concentration of produced carbon monoxide is dependent on reformer temperature, however as displayed in Appendix H, the reformer average temperatures during the fuel qualifying experiments did not vary and remained constant at 250 °C for the reforming of all methanol qualities. CO concentrations measured in the product off-gases from the reforming of each methanol quality have been graphed below.

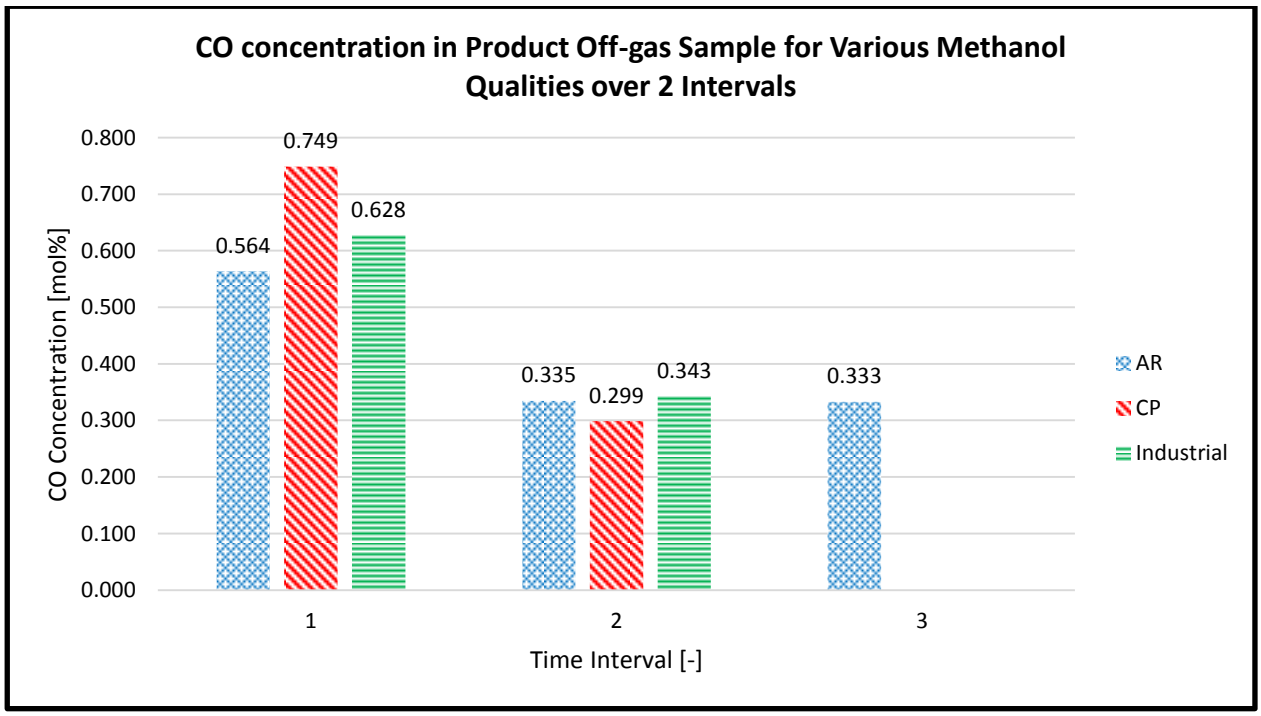

Figure 67 - Column Graph representing CO concentration in Product Off-gas for Each Methanol Quality Reformed

Figure 67 displays the comparison between the CO mol% produced by the reforming of each methanol quality. The initial 10 hour reforming period produces the most CO for all methanol qualities, however, the CP methanol produced the highest CO concentration of 0.749 %. This coincides with the duration with which the methanol conversion initially decreases in Section 5.1. The time following the first 10 hours, produced CO concentrations are very similar to one another.

The lead acetate strips displayed in Figure 55, Figure 59, and Figure 63 did not display any H_2S presence in the reformer product off-gas. They are specifically made for H_2S identification and other sulphur compounds may pass over undetected, however, an EDS analysis of the catalyst from Sample Point 3 and Sample Point 4 is discussed later in this study in Section 5.3 which would display sulphur poisoning if there was any to be observed.

The dense metallic membrane material and the fuel cell catalyst discussed in Section 2.4 are poisoned by CO and H_2S. It can be concluded that during the first 10 hours of the fuel qualifying experiment produced the highest and most varied CO mol% and would have the greatest effect on the membrane and fuel cell. Thereafter, the CO mol% converges to a similar value for all methanol qualities without any detectable H_2S.

The results of the reformer product off-gases were verified by comparing them to theoretical values expected by stoichiometry. The stoichiometry equations and the theoretical values were discussed in Section 2.6. This data is presented in Table 23.

Table 23 - Verification of Gas Composition while Reforming AR, CP, and Industrial grade Methanol by Comparing to Stoichiometry

	AR			CP		Industrial		Theoretical	Relative Error min/max [%]
	10h	20h	30h	10h	18h	10h	16h		
H_2 [mol%]	73.696	78.281	75.523	80.339	77.131	82.837	72.836	75.000	-2.885/ 10.449
CO_2 [mol %]	25.740	21.384	24.140	18.913	22.570	16.536	26.821	25.000	7.284/ -33.856
CO [mol %]	0.563	0.336	0.337	0.748	0.299	0.628	0.343	≈ 0.000	$299x10^6$/ $748x10^6$
H_2S [ppm]	0	0	0	0	0	0	0	N/A	N/A

While analysing Table 23 it can be observed that the hydrogen mol% is generally higher than the expected stoichiometric value with a maximum relative error of 10.449 % for the Industrial grade methanol conversion during the first 10 hours.

The CO_2 mol% values are close to stoichiometry and generally lower than the expected values. The minimum relative error is -33.856 % due to the Industrial grade during the first 10 hours.

Stoichiometry dictates a zero amount of carbon monoxide. Any amount of carbon monoxide, no matter how small, will be seen as a very large relative error. It can be observed that the first 10 hours of each experiment produces the maximum amount of carbon monoxide for that methanol quality. The hours following the first 10 hours produce a lower amount of carbon monoxide, near 0.3 mol%.

From Table 23 it can be observed that while reforming CP methanol and Industrial grade methanol, the highest relative errors are presented. It can be concluded that when reforming with these methanol qualities, more unpredictable gas compositions are observed.

The differences in gas composition between the intervals and methanol qualities are due to the gas chromatograph requiring a very small volume of gas for analysis. The sample taken is not necessarily a complete representation of the total gas sample and due to the gases each being different densities, slight separation can occur during delivery of the gas sample to the gas chromatograph. Despite this, all of the components in the gas sample are near expected stoichiometric values with low relative error values, except for the high error percentage of carbon

monoxide, which can be accounted for due to none being expected. The values can be considered acceptable and accurate and can be considered verified, and concludes that the fuel qualifying experimental setup functions as designed and expected. The validation process below will allow for further discussion and comparison to various published research results.

Validation of the product off-gas results are displayed in Table 24, Table 25, and Table 26. Minimum and maximum relative errors are displayed as a means of quantitively displaying the variation between the experimental results and the results provided by published literature to determine accuracy and relevance of the results to the current field.

Table 24 - Validation of Reformer Product Off-gas Composition while Reforming AR, CP, and Industrial grade Methanol Compared to (Kurr *et al.*, 2008)

	AR			**CP**		**Industrial**		**(Kurr *et al.*, 2008)**	**Relative Error min / max [%]**
	10h	20h	30h	10h	18h	10h	16h		
H_2[%]	73.696	78.281	75.523	80.339	77.131	82.837	72.836	75.230	-3.182/ 10.112
CO_2[%]	25.740	21.384	24.140	18.913	22.570	16.536	26.821	24.670	8.719/ -32.971
CO[%]	0.563	0.336	0.337	0.748	0.299	0.628	0.343	0.110	171.818 / 580.00
H_2S[ppm]	0	0	0	0	0	0	0	N/A	N/A

Table 24 compares the experimental gas compositions while reforming each methanol quality for each duration interval to the gas composition results from Kurr *et al.* (2008). All of the gas analysis experimental values are very similar to those displayed by Kurr *et al.* (2008) except for the CO_2 mol% while reforming Industrial grade methanol during the first 10 hour period resulting in a -32.971% relative error, and the CO mol% values which are much higher causing a maximum error of 580.00 % despite the results of Kurr *et al.* (2008) at 250 °C. The minimum and maximum relative errors for H_2 and CO_2 are cause by the reforming of the Industrial grade methanol indicating unpredictable gas composition results. The study presented by Kurr *et al.* (2008) does not investigate the precense of H_2S in the off-gas composition.

Table 25 - Validation of Reformer Product Off-gas Composition while Reforming AR, CP, and Industrial grade Methanol Compared to (Purnama, 2003)

	AR			CP		Industrial		(Purnama, 2003)	Relative Error min / max [%]
	10h	20h	30h	10h	18h	10h	16h		
H_2[%]	73.696	78.281	75.523	80.339	77.131	82.837	72.836	76.087	-4.267/ 8.875
CO_2[%]	25.740	21.384	24.140	18.913	22.570	16.536	26.821	21.739	23.373/ -23.916
CO[%]	0.563	0.336	0.337	0.748	0.299	0.628	0.343	2.174	-65.547/ -86.247
H_2S[ppm]	0	0	0	0	0	0	0	N/A	N/A

Table 25 indicates very similar hydrogen concentrations with low error percentages of -4.267 % to 8.875 %. The CO_2 concentration is varied with values above and below the 21.74 mol% presented by Purnama (2003). The minimum relative error of -23.916 % and maximum relative error of 23.373 % are both presented by the Industrial methanol during its first 10 hours and final 8 hours respectively.

The experimental facility produces up to 86.247 % less carbon monoxide than the reformer used by Purnama (2003) and the hydrogen and carbon dioxide content can be considered acceptable when compared to that presented by Purnama (2003). The study presented by Purnama (2003) also does not investigate the presence of H_2S in the off-gas composition.

Table 26 - Validation of Reformer Product Off-gas Composition while Reforming AR, CP, and Industrial grade Methanol Compared to (Kim *et al.*, 2016)

	AR			CP		Industrial		(Kim *et al.*, 2016)	Relative Error min/ max [%]
	10 h	20 h	30 h	10 h	18 h	10 h	16 h		
H_2[%]	73.696	78.281	75.523	80.339	77.131	82.837	72.836	N/A	N/A
CO_2 [%]	25.740	21.384	24.140	18.913	22.570	16.536	26.821	N/A	N/A
CO[%]	0.563	0.336	0.337	0.748	0.299	0.628	0.343	0.400	-25.250/ 87.250
H_2S [ppm]	0	0	0	0	0	0	0	N/A	N/A

The research presented by Kim *et al.* (2016) does not focus on the reformer off-gas compositions and emphasises the catalyst composition and catalyst physical properties and how it affects the methanol conversion. It does, however, display a temperature dependant CO concentration of about 0.4 % for a commercial catalyst at 250 °C. This presents error values between -25.250 % and 87.250 % both due to the reforming of CP methanol. According to the comparison to Kim *et al.* (2016), the hours after the initial 10 hour interval provides acceptable experimental data. The study presented by Kim *et al.* (2016) also does not discuss the possible presence of H_2S in the off-gases.

The research presented by Sá *et al.* (2011) also focuses more on the catalyst composition and catalyst physical properties and how it affects the methanol conversion. There is a temperature dependant graph for CO concentration for determining the reverse water shift reaction. At 250 °C there is about 0.75 % CO in the off-gas stream. This provides error values between -60.13 % and 0.133 % both due to the reforming of CP methanol indicative of unpredictable CO compositions. The experimental values for CO can be considered acceptable during the first 10 hours. Research presented by Sá *et al.* (2011) does not discuss the possible presence of H_2S in the off-gases.

From the validation of the experimental reformer product off-gas results, it can be concluded that the H_2 and CO_2 content can be considered acceptable and validated. The CO content is validated for the samples taken in the first 10 hours, or in the hours subsequent to the initial 10 hours, depending on the study. Published literature that does include gas composition uses similar GC equipment to that used by this study and the resulting gas spectrum is the same as literature providing successful validation.

The analysis and discussion of the results from the reformer product off-gas composition by the reforming of three methanol qualities contributes to the addressing of the problem statement.

5.3 Analysis of Catalyst by SEM and EDS

Due to the lack of H_2S being observed on the lead acetate strips and a pH value to indicate an increase in acidity of the condensate, it was deemed appropriate to analyse the catalyst samples collected from the reformer from the top of the reformer at Sample Point 3. These samples were analysed under a SEM to take note of the topology after reforming to observe any changes taking place. The elemental composition was analysed by EDS to identify possible poisons and provide an estimation to the concentration of poisons that have chemisorbed themselves to the catalyst. This was done for a catalyst pellet sample at 10 hour intervals and at the end of the experiment duration. This provides an identification method for poisons that may have been present in the off-gas composition due to the three methanol qualities that were reformed during the fuel qualifying experimental procedure.

The catalyst topology was compared to the properties previously discussed, in Section 2.3.4 and Section 4.4.3, as being a ceramic with a laminar porous structure. The catalyst composition will be compared to that discussed in Section 4.4 for the detection of foreign elements which may be poisons.

5.3.1 Results from Analysis of Catalyst having Reformed AR Methanol

The analysis of the reforming catalyst was done for a catalyst pellet after 10, 20, and 30 hours while reforming AR methanol.

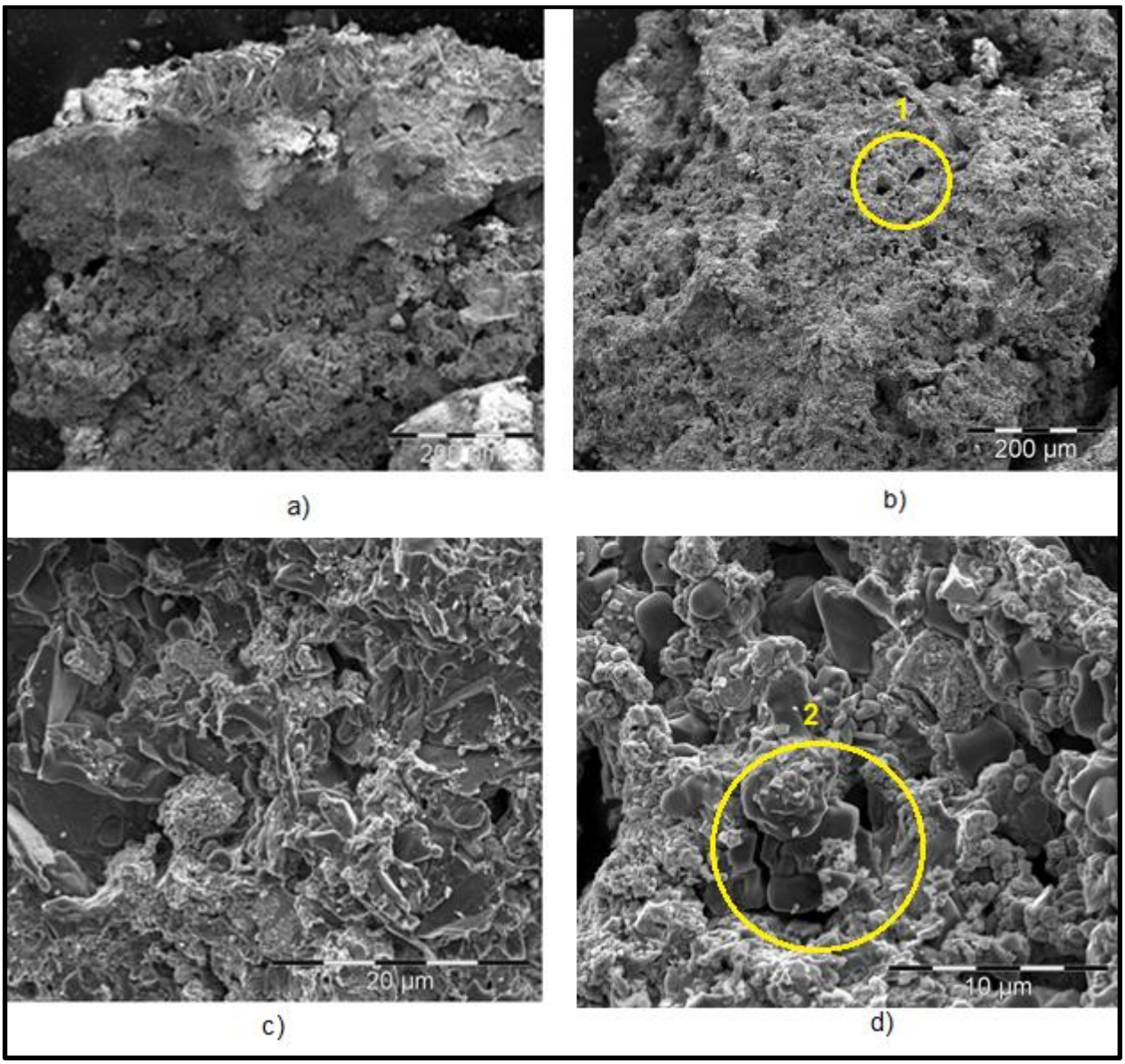

Figure 68 - SEM Micrographs of Catalyst Topography after 10 hours of Reforming AR Methanol

After 10 hours the catalyst in Figure 68 appears less porous than the micrographs displayed in Figure 36 in Section 4.4.3, just after activation, and before reforming had taken place. It remains a ceramic structure, however porosity has decreased due to a sintering process. Pores are displayed by Area 1 in Figure 68b).

Figure 68c) and d) displays a crystaline structure and shows how the various compounds form in a laminar structure as an agglomeration with pores formed inbetween emphasised by Figure 68d) Area 2.

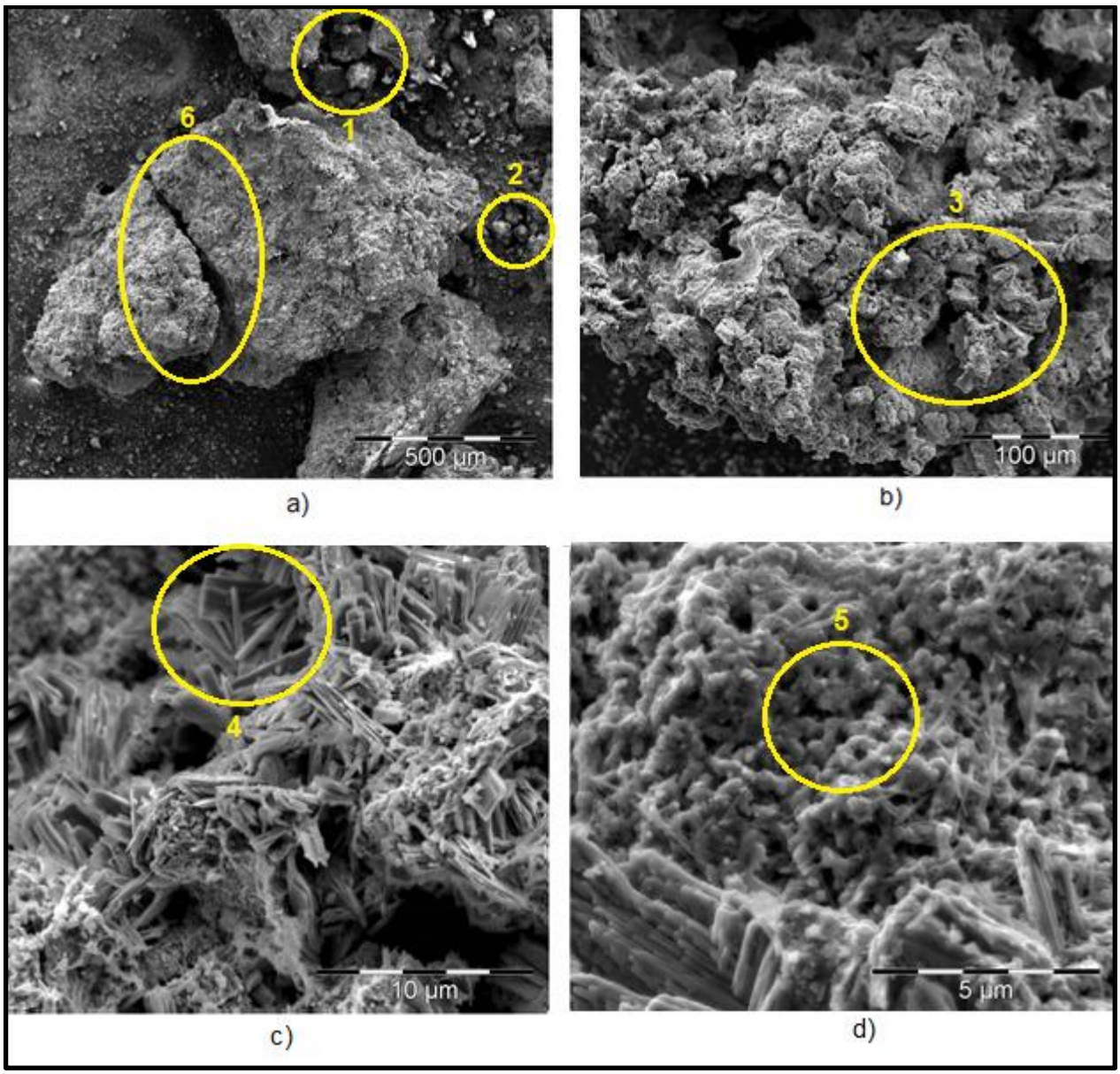

Figure 69 - SEM Micrographs of Catalyst Topography after 20 hours of Reforming AR Methanol

After 20 hours the surface of the catalyst in Figure 69a) and Figure 69b) displays a roughening of surface texture and coarser particles when compared to the fresh catalyst in Figure 36, however, porosity is displayed by Figure 69b) Area 3. Figure 69a) Area 1 and 2 display cleavage in the form of sintered particles that have fractured from the material. A fracture is displayed in Area 6.

Crystalline particles are displayed by Figure 69c) Area 4, with a delicate pore structure for reactions to take place displayed in Figure 69d) Area 5.

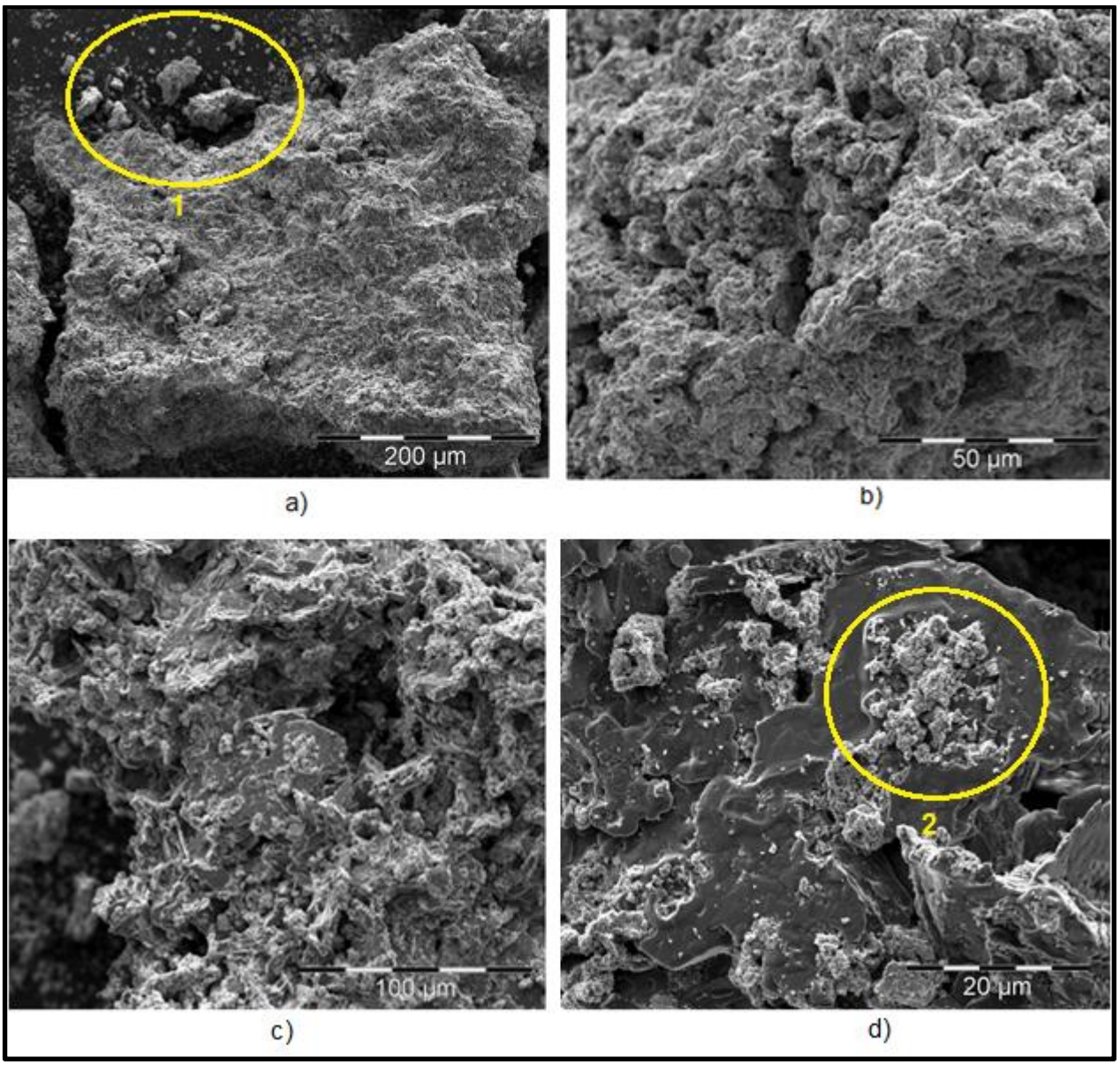

Figure 70 - SEM Micrographs of Catalyst Topography after 30 hours of Reforming AR Methanol

After 30 hours the laminar structure, displayed by Figure 70d) Area 2, remains unaffected by the reforming process and although the particles depicted by Figure 70a) and b) appear coarser with surface roughening due to sintering, there is still a reasonable porosity and good chemical binding. Figure 70a) Area 1 displays cleavage due to sintering. Sintering does not appear to propagate further.

From the SEM micrographs, there is no obvious carbon deposition that can be observed after 30 hours of reforming AR methanol, however, further analysis was done in Section 5.5 to determine total carbon content of each sample.

Table 27 - EDS Results for Composition of Catalyst after 10, 20, and 30 hours of Reforming AR Methanol

	O	Na	Al	Cl	S	Cu	Zn	Total
Sample	[wt%]							
10 Hours	39.71	35.49	4.30	0.00	0.00	12.45	8.05	100.00
20 Hours	31.31	26.3	4.63	0.00	0.00	23.24	14.51	100.00
30 Hours	28.69	28.43	2.47	0.29	0.00	23.45	16.66	100.00

Chlorine was detected and approximated at 0.29 weight% in the sample after 30 hours of reforming AR methanol. This chlorine was, therefore, adsorbed between the 20 and 30 hour intervals. After a total of 30 hours of reforming AR methanol, the catalyst did not show any indication of sulphur poisoning.

5.3.2 Results from Analysis of Catalyst having Reformed CP Methanol

The analysis of the reforming catalyst was done for catalyst after 10 and 18 hours while reforming CP methanol.

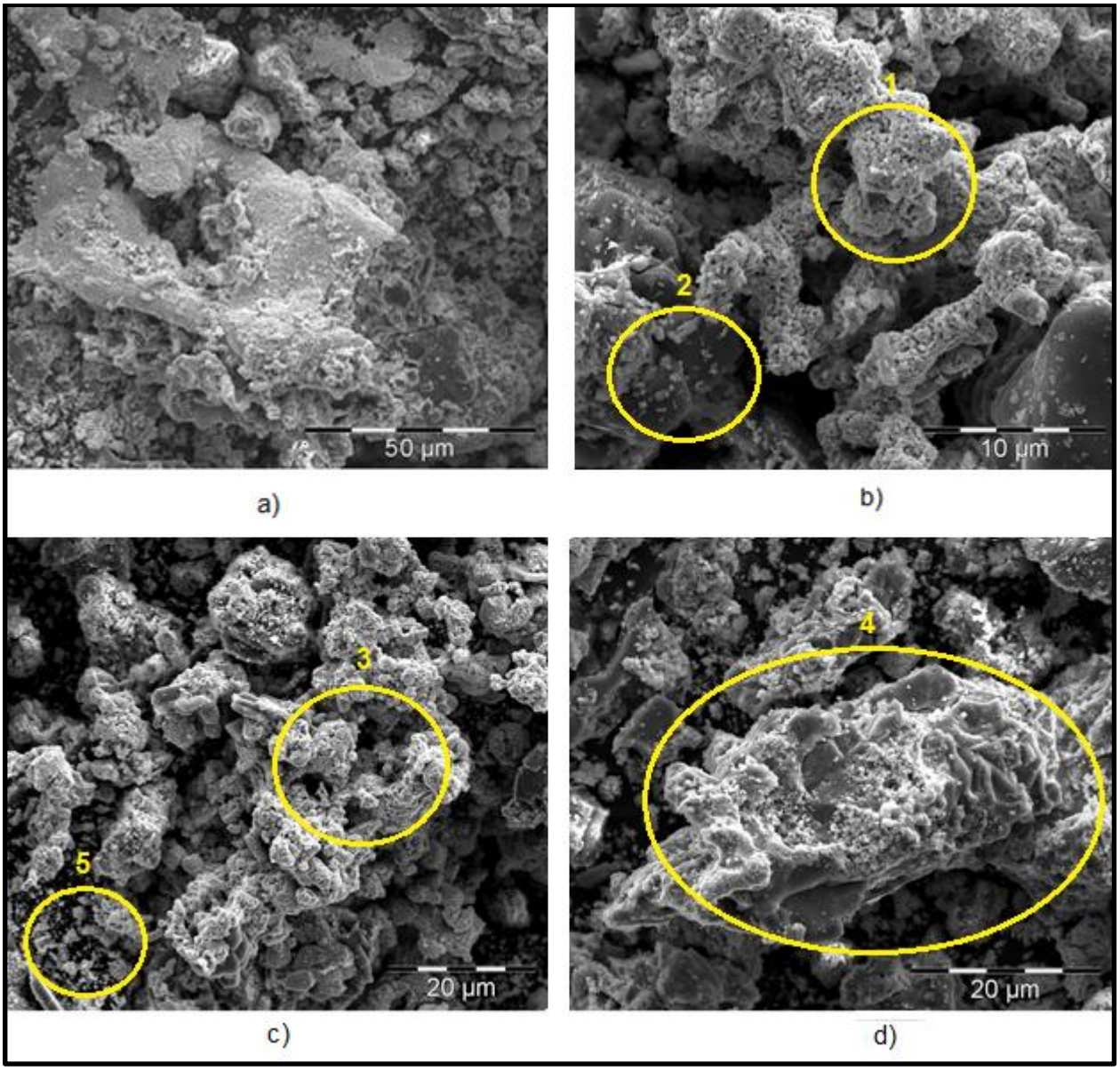

Figure 71 - SEM Micrographs of Catalyst Topography after 10 hours of Reforming CP Methanol

Figure 71a), Figure 71c), and Figure 71d) display the typical catalyst ceramic structure whereas Figure 71b) shows a more crystallite structure that has formed, indicated by Area 1. Good chemical bonding during co-precipitation is displayed by Figure 71b) Area 2.

Figure 71c) displays a courser catalytic surface due to the initial sintering of the catalyst during the first 10 hours of reforming. Figure 71d) Area 4 displays the layering of the laminar structure

achieved during co-precipitation. The pores are displayed by Figure 71c) Area 3 and Area 5 displays cleavage due to sintering.

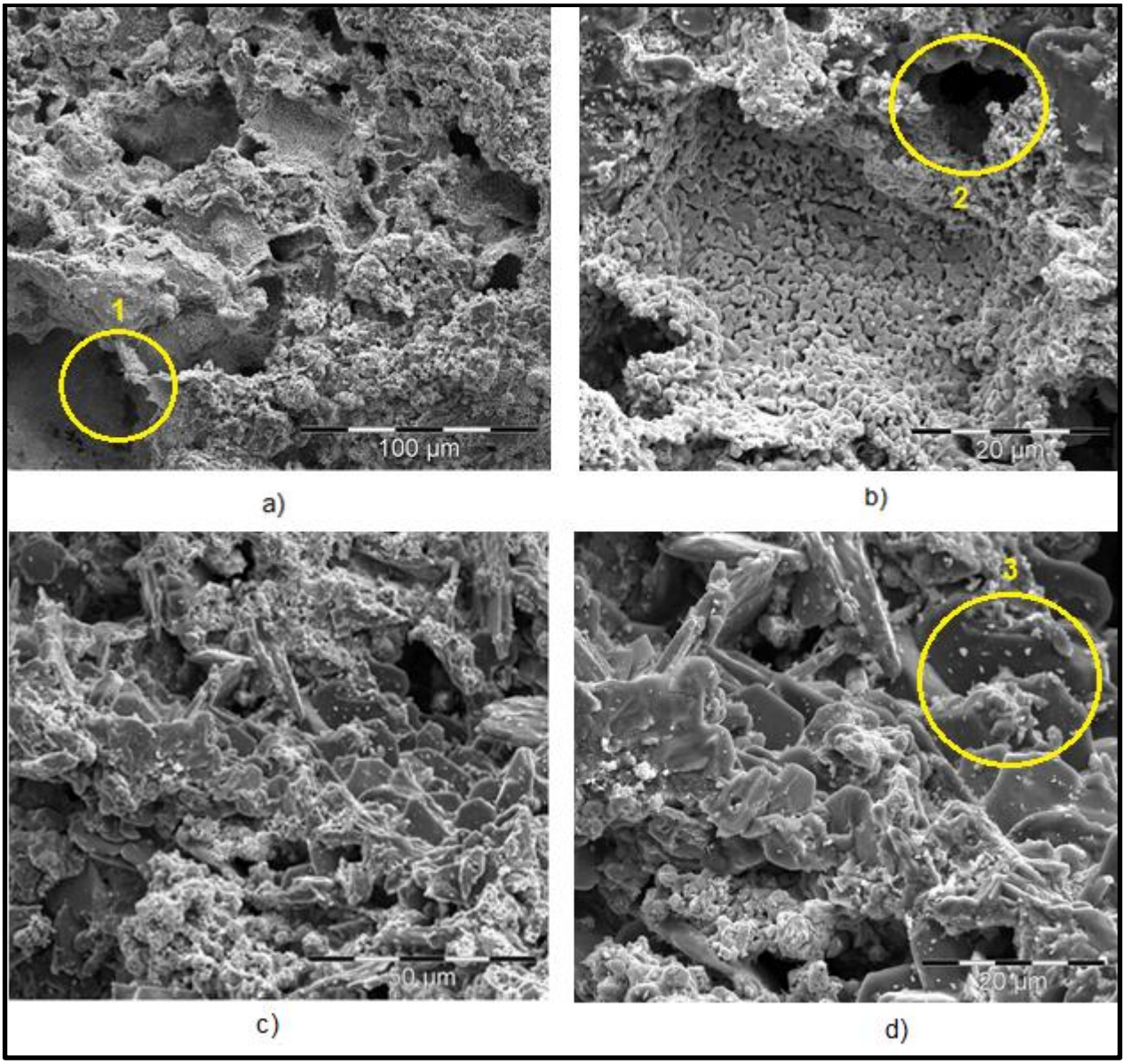

Figure 72 - SEM Micrographs of Catalyst Topography after 18 hours of Reforming CP Methanol

After 18 hours the surface and porosity appears similar to that which is depicted in Figure 71. The pores and voids are displayed by Figure 72a) Area 1 and Figure 72b) Area 2. Good adhesion of particles and agglomeration is displayed by Figure 72d) Area 3.

From the SEM micrographs, there is no observable carbon deposition after 18 hours of reforming CP methanol.

Table 28 - EDS Results for Composition of Catalyst after 10 and 18 hours of Reforming CP Methanol

	O	Na	Al	Cl	S	Cu	Zn	Total
Sample	[wt%]							
10 hours	27.73	27.55	2.15	0.00	0.00	26.34	16.23	100.00
18 hours	44.52	28.70	2.50	0.18	0.00	14.05	10.06	100.00

Considering Table 28, it can be observed that in the first time interval of 10 hours there is no chlorine detected, however, during the last 8 hours the weight percentage of chlorine is detected and approximated at 0.18 weight%. The catalyst does not display any presence of sulphur or sulphuric compounds in its composition.

5.3.3 Results from Analysis of Catalyst having Reformed Industrial grade Methanol

The analysis of the reforming catalyst was done for a catalyst after 10 and 16 hours while reforming Industrial grade methanol.

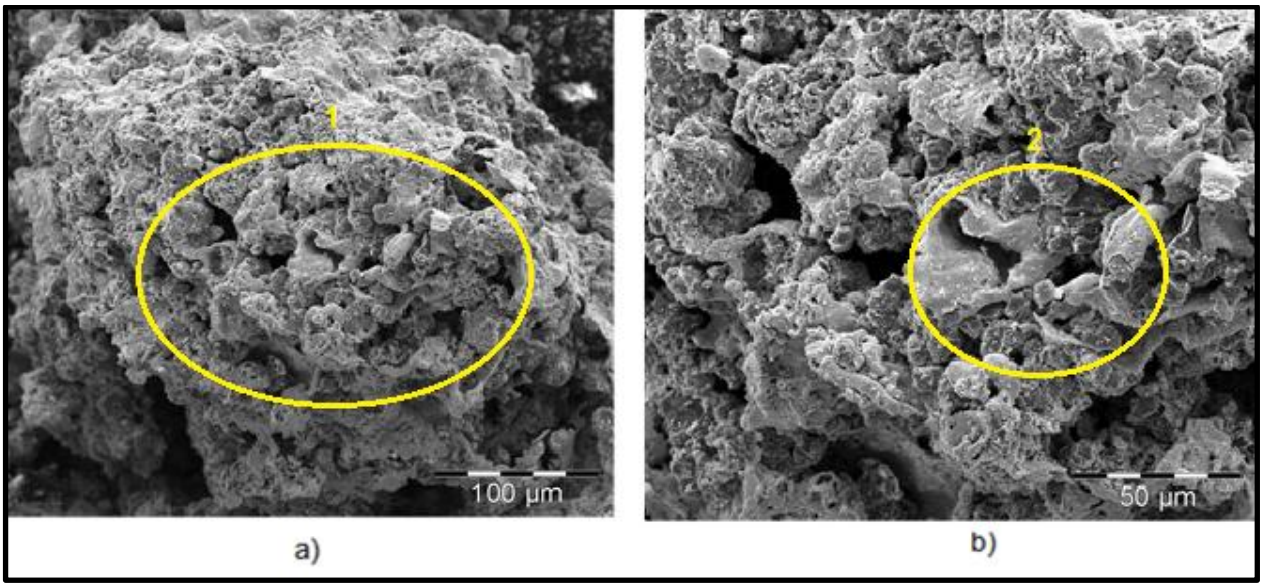

Figure 73 - SEM Micrographs of Catalyst Topography after 10 hours of Reforming Industrial grade Methanol

Figure 73 displays a coarse surface textured particle with reasonable porosity. The pores are displayed in Figure 73a) Area 1. The agglomeration of the particles seemed unaffected by the reforming of the Industrial grade methanol which is displayed by Figure 73b) in Area 2.

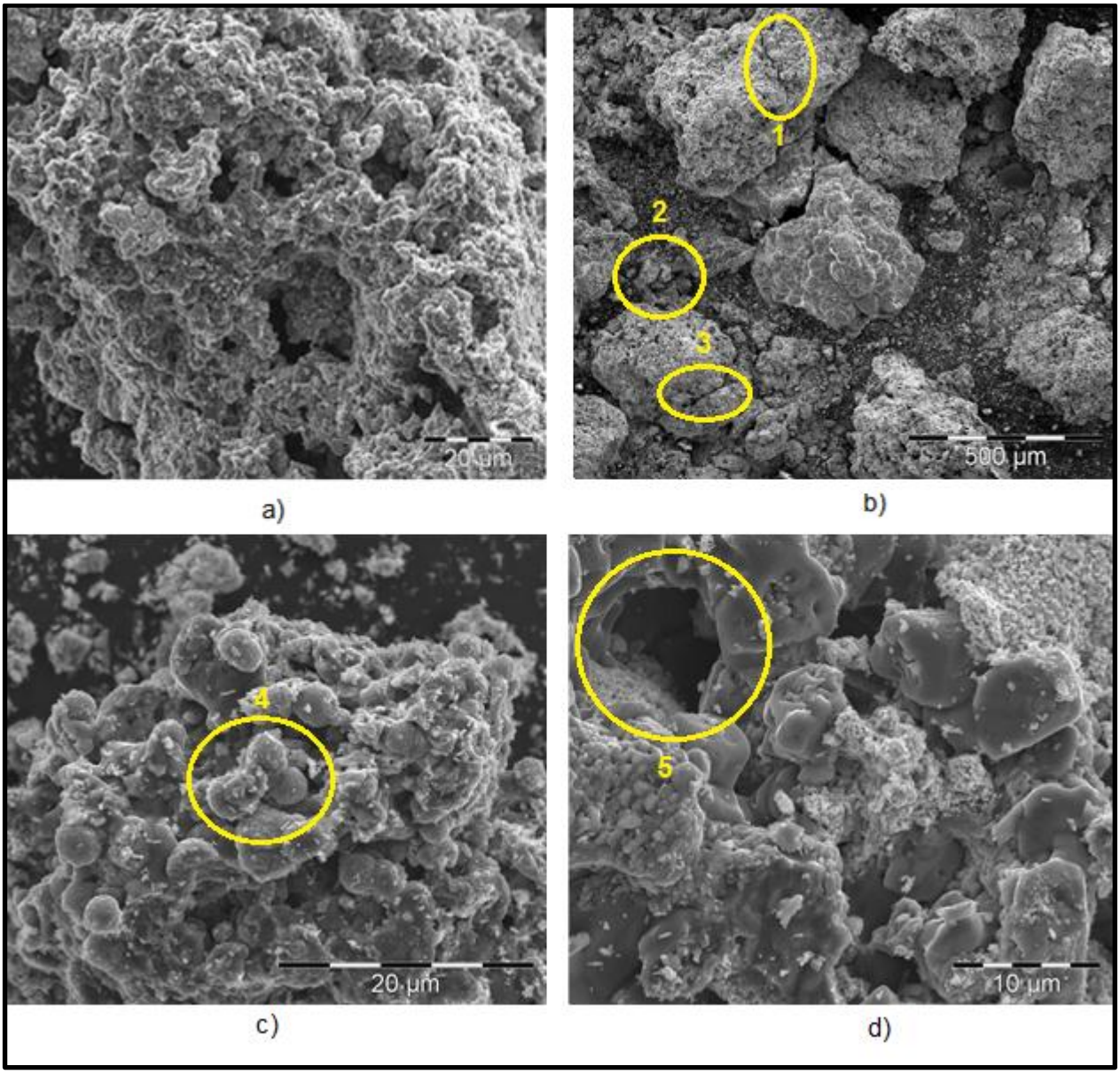

Figure 74 - SEM Micrographs of Catalyst Topography Ceramic Structure after 16 hours of Reforming Industrial grade Methanol

After 16 hours, the particle displayed by Figure 74a) shows similar pore sizes to those displayed by Figure 73. Figure 74b) displays the effect of sintering as observed due to the brittle fractures in Area 1 and Area 3, along with the appearance of cleavage in Area 2.

Figure 74 c) displays good particle bonding of small crystals having formed on the surface of the catalyst, as shown by Area 4. Figure 74d) magnifies Figure 74c) to display a pore void, as shown by Area 5.

Similar to the reforming of AR and CP methanol, there is no distinct presence of carbon deposition on the catalyst surface or in its pores observed by the SEM micrographs.

Table 29 - EDS Results for Composition of Catalyst after 10 and 16 hours of Reforming Industrial grade Methanol

	O	Na	Al	Cl	S	Cu	Zn	Total
Sample	wt [%]							
10 hours	27.95	26.22	2.73	0.00	0.00	28.04	15.06	100.00
16 hours	48.80	28.04	2.42	0.24	0.00	11.24	9.27	100.00

Table 29 displays the detection of chlorine and approximates its concentration as 0.24 weight%, however, even after reforming Industrial grade methanol for 16 hours and having reached 13 % methanol conversion, the catalyst does not show any indication of sulphur poisoning.

5.3.4 Discussion of Results from Catalyst SEM and EDS Analysis

From the results displayed in Sections 5.3.1, 5.3.2, and 5.3.3, it can be concluded that the reforming of AR, CP, and Industrial grade methanol does not significantly alter the crystalinity, laminar structure, and agglomeration of the catalyst. When considering Table 27, Table 28, and Table 29, the Cu, Zn, and Al elemental content differs by comparison due to the imperfect elemental distribution and does not affet the validity of the results.

From the observations displayed by the cleavage, decreasing of pore voids, and coarser catalytic surface it can be concluded that catalytic sintering took place and was the cause of the initial decrease in methanol conversion displayed in Section 5.1 during the first 10 hours of fuel qualifying experimentation for all methanol qualities. Furthermore, it appears as if the sintering of the catalyst is limited to the first 10 hours of the reforming process, with no further sintering taking place due to the lack of drastic change in appearance of the catalyst and no increase in the amount of cleavage and fractures being observed on the catalyst, indicative of the stable methanol conversion period in Section 5.1 for all methanol qualities. Only poisoning would negatively affect the methanol

conversion in the proceeding reforming duration and the decrease during the last few hours of the catalyst lifespan is not attributed to the catalyst topology but to the chlorine poisoning found.

For each methanol quality, chlorine was cumulatively chemisorbed to the catalyst active sites. During the last hours of the fuel qualifying experiment during which the methanol conversion decreased towards 13 % and the acidity of the reformer off-gas condensate increased as displayed in Section 5.1. This was due to chlorine ions no longer being able to be chemisorbed by the catalyst and being found in the reformer off-gas condensate.

When analysing the composition of the catalyst reforming CP methanol in Table 28, the chlorine weight% of 0.18 % was less than the weight percentage found in the catalyst having reformed AR methanol, displayed in Table 27 as 0.29 %. However, the total duration to chemisorb chlorine while reforming the CP methanol was significantly less than for the AR methanol. 0.18 % chlorine weight% was chemisorbed in the last 8 hours compared to the 0.29 % chlorine chemisorption presented between 20 and 30 hours. When considering the chlorine chemisorption presented by Industrial grade methanol in Table 29 as 0.24 % in the last 6 hours is nearly the same as when compared to AR methanol in a shorter period of time.

The other methanol impurities listed in Appendix E were not detected as having been chemisorbed to the catalyst and are not considered irreversibly harmful to the reformer catalyst, membrane, nor the fuel cell.

The results obtained from the catalyst topology and EDS elemental approximation composition contribute to the addressing of the problem statement by presenting poison detection and semi-quantitive analysis of the poisons that are found in the reformer off-gas by analysing that which has been chemisorbed to the catalyst and the time taken for the poisons to present themselves at the top of the reformer at Sample Point 3 for each methanol quality.

5.4 Analysis of Catalyst Cross Section

In Section 5.3.1, 5.3.2, and 5.3.3 the catalyst was crushed to analyse the inner structure and give an overall display of elemental content for that catalyst pellet. Although, it gives a fair indication of the time it takes for poisoning to occur and the amount of poisons to be found in the sample, it does not indicate the depth of penetration into the catalyst pellet, if any. A main concern when pelletizing catalyst is the decreasing of available surface area for reaction to take place even if the particles are very porous.

By taking catalyst out from near the centre of the reformer, Sample Point 4, where the concentration of poisons will be higher than the top of the reformer near Sample Point 3, the poison penetration depth can be displayed.

Figure 75 - Catalyst Pellets Cut through the Midsection to Analyse their Cross-section and Poison Penetration Depth

Electron Backscatter Diffraction (EBSD) was used during the cross-sectional analysis, which provides a high contrasted image. EBSD is a microstructural crystallographic characterisation technique used to study crystalline and polycrystalline materials providing information about the structure, crystal orientation, and strain in a material. The fluorescent screen detects diffracted electrons that form a pattern due to the interaction between the electron beam and a sample. The elements with higher atomic number provide more back scatter electrons and are displayed as being lighter on the greyscale, whereas the elements with lower atomic numbers are darker (Nano Science Instruments, 2019).

From the scale on Figure 76, it can be seen that Spectrum 1 is on the outside edge of the catalyst pellet 0.14 mm deep, the centre of Spectrum 2 is about 0.28 mm deep in the catalyst pellet, the centre of Spectrum 3 is 1.1 mm, and Spectrum 4 is 1.58 mm deep in the catalyst pellet.

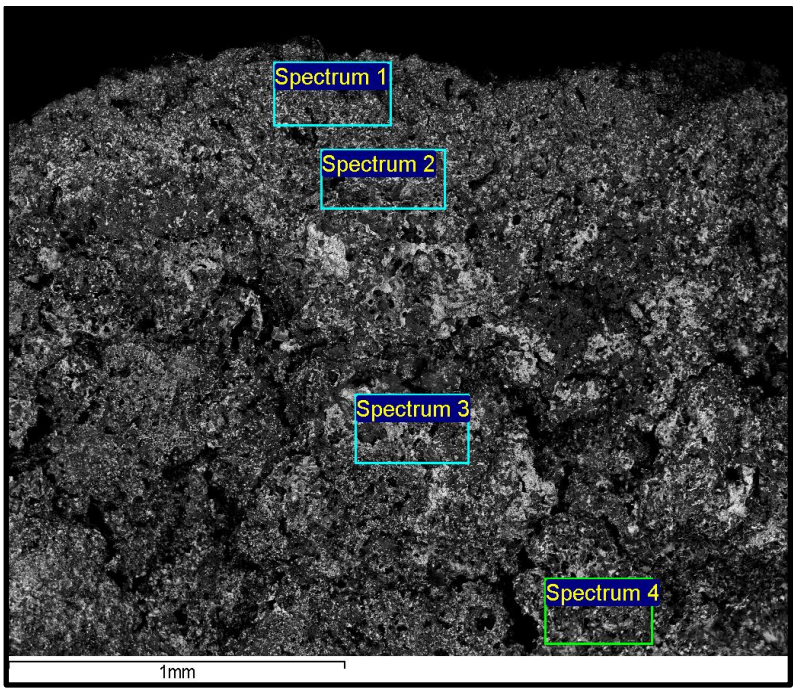

Figure 76 - Electron Backscatter Diffraction Image Indicating Analysis Spectrum Regions for EDS Analysis of Catalyst Cross Section after 30 hours of Reforming AR Methanol

Table 30 - Results of EDS Analysis of Catalyst Cross Section after 30 hours of Reforming AR grade Methanol

	O	Na	Al	Cl	S	Cu	Zn	Total
Spectrum	[wt %]							
1	36.99	40.10	1.53	1.20	0.00	2.54	17.64	100.00
2	34.96	36.13	4.50	0.00	0.00	9.54	14.86	100.00
3	31.35	30.27	5.73	0.00	0.00	15.79	16.86	100.00
4	31.55	32.55	4.63	0.00	0.00	17.58	13.70	100.00

Table 30 displays chlorine presence, of about 1.20 weight%, near the surface of the catalyst in the outermost spectrum. This indicates slight penetration of poisons after 30 hours of reforming AR grade methanol.

From the scale in Figure 77, Spectrum 1 is near the edge of the pellet at 0.14 mm depth, the centre of Spectrum 2 is 0.44 mm deep in the catalyst pellet, Spectrum 3 is 1.02 mm deep, and the centre of Spectrum 4 is 1.58 mm deep in the catalyst.

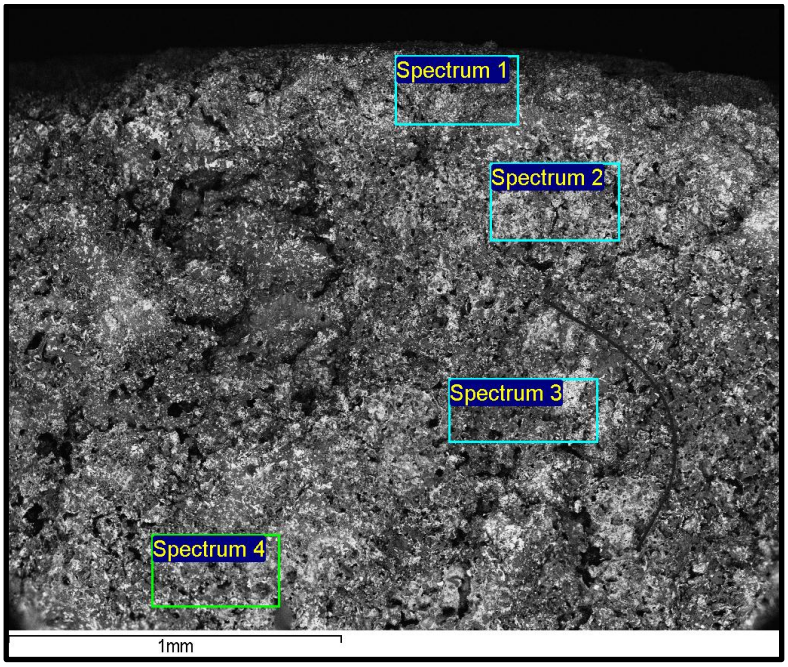

Figure 77 - Electron Backscatter Diffraction Image Indicating Analysis Spectrum Regions for EDS Analysis of Catalyst Cross Section after 18 hours of Reforming CP Methanol

Table 31 - Results of EDS Analysis of Catalyst Cross Section after 18 hours of Reforming CP Methanol

	O	Na	Al	Cl	S	Cu	Zn	Total
Spectrum	[wt%]							
1	35.22	35.86	3.33	0.00	0.00	3.87	21.72	100.00
2	30.10	30.05	4.66	0.15	0.00	16.00	19.03	100.00
3	33.27	34.75	5.43	0.00	0.00	22.36	4.19	100.00
4	31.50	30.34	6.62	0.12	0.00	13.65	17.77	100.00

The EDS results from Table 31 display lower chlorine concentrations than the EDS results from Table 30 from the AR methanol which was 1.20 weight% but it identifies chlorine penetrating much deeper, almost 1.58 mm and over a shorter duration.

From the scale in Figure 78, Spectrum 1 is near the edge of the pellet at 0.14 mm depth, the centre of Spectrum 2 is 0.42 mm deep in the catalyst pellet, Spectrum 3 is 1 mm deep, and the centre of Spectrum 4 is 1.66 mm deep in the catalyst.

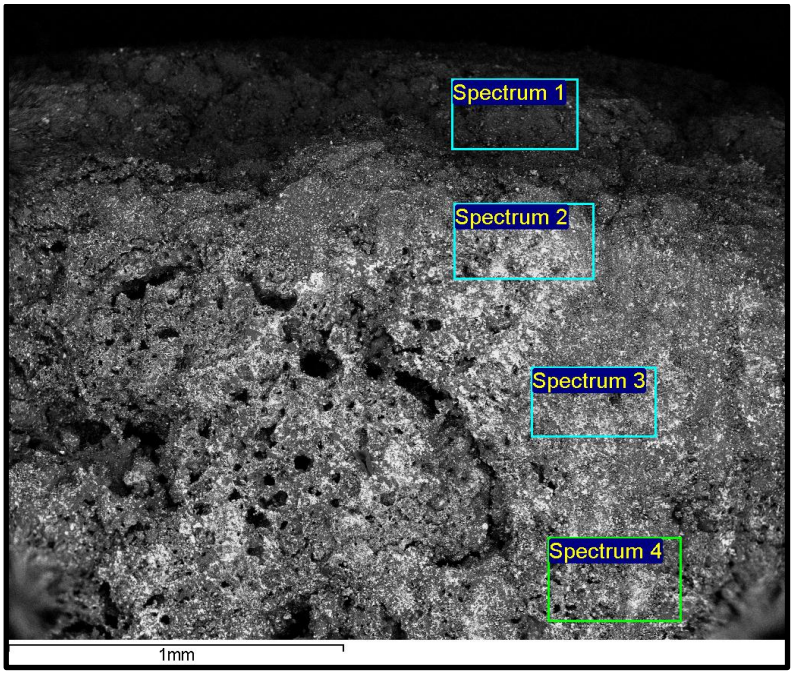

Figure 78 - Electron Backscatter Diffraction Image Indicating Analysis Spectrum Regions for EDS Analysis of Catalyst Cross Section after 16 hours of Reforming Industrial grade Methanol

Table 32 - Results of EDS Analysis of Catalyst Cross Section after 16 hours of Reforming Industrial grade Methanol

	O	Na	Al	Cl	S	Cu	Zn	Total
Spectrum	[wt%]							
1	42.81	44.24	1.68	0.89	0.00	2.63	7.75	100.00
2	31.32	35.51	2.19	0.41	0.00	11.70	18.86	100.00
3	31.67	37.04	2.82	0.23	0.00	13.68	14.55	100.00
4	31.71	33.82	4.76	0.00	0.00	10.45	19.26	100.00

The EDS of the cross section of catalyst reforming Industrial grade methanol has almost double the concentration of chlorine in the same spectrum depth and identified in more spectrums when compared to the catalyst reforming CP methanol, indicating far more chlorine being chemisorbed

to the catalyst with an increased penetration depth. The chlorine poisoning concentration and penetration depth when reforming each methanol quality can be displayed graphically in Figure 79.

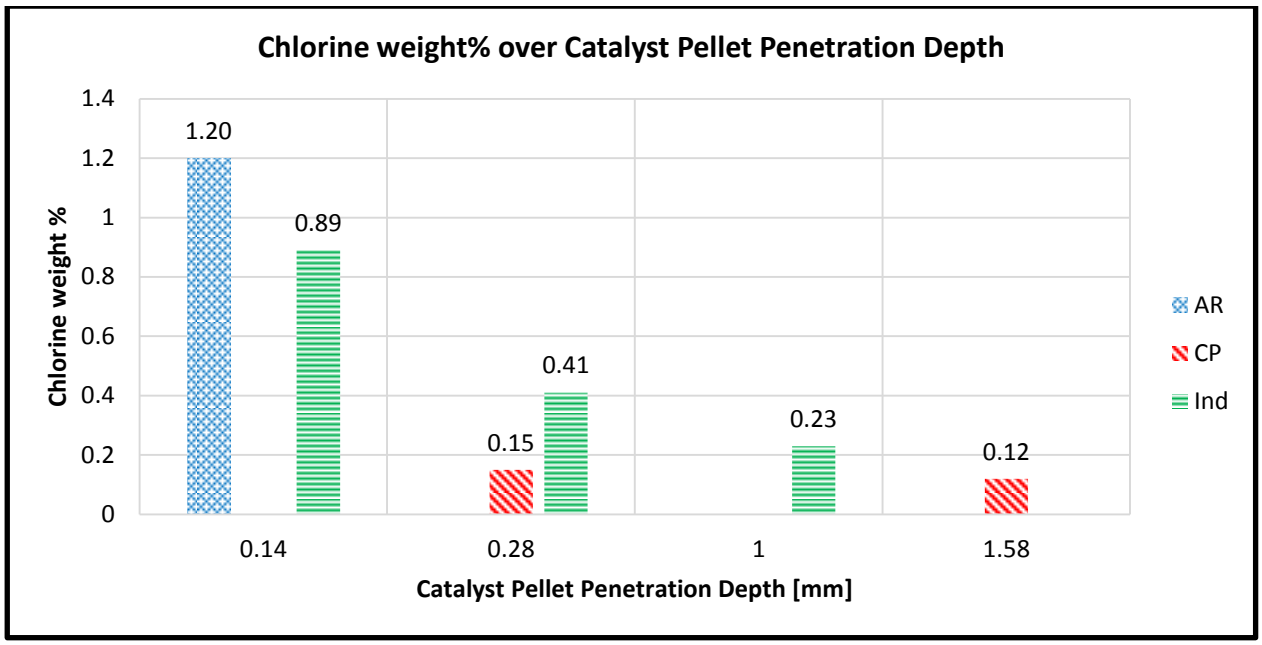

Figure 79 - Column Graph Displaying Chlorine weight% Poisoning over the Catalyst Pellet Penetration Depth for each Methanol Quality

The distilled water used with each methanol quality for each experiment remained constant, therefore the only variable was the methanol quality. This concludes that the poorer quality methanol accelerates the effect of the chlorine poisoning and increases the concentration and penetration depth of the chlorine by a mechanism that is not yet understood nor addressed in literature. The results from the cross-section analysis of the catalysts contribute to the addressing of the problem statement by estimating poison concentration and indicating poisoning rate at a fixed point in the reformer caused by each methanol quality as reforming fuel.

5.5 Analysis of Carbon Deposition on the Catalyst

From Section 5.3 it was noted that there was no carbon deposition observed on any of the SEM micrographs on the surface of the catalyst or inside the pores. The most effective way to determine the amount carbon deposition by the methanol on the catalyst during reforming is to use a loss on ignition process coupled with infrared mass spectrometry which is performed by the LECO TruSpecCN. The process described by the TruSpecCN user manual is by taking a 0.1 g sample and heating to 950 °C creating a loss-on-ignition of total carbon (organic and inorganic) in oxygen,

producing carbon dioxide as a gas. The gas passes through an afterburner at 850 °C for further oxidisation and finally analysed by an infrared mass spectrometer which is set to a specific wave length frequency that will only energise carbon dioxide. The energy absorbed by the carbon dioxide can be measured and the quantity of carbon originally on the sample can be deduced.

Table 33 displays the results of this procedure on the catalyst removed from Sample Point 3.

Table 33 - Results of Carbon Quantity Analysis by Infrared Mass Spectrometry of CO_2

Sample	Carbon [%]
AR 10 hours	4.26
AR 20 hours	3.74
AR 30 hours	3.26
CP 10 hours	2.99
CP 18 hours	3.48
Industrial 10 hours	3.66
Industrial 16 hours	2.74

The results from Table 33 remain constant with a range between 2.74 % and 4.26 %. There is no observable trend between the samples in terms of methanol quality reformed or the total reforming time. The values of carbon observed are from the carbonates that were not completely removed from the catalyst during the calcination procedure as discussed in Section 4.4. Therefore, it can be concluded that there is little to no observable carbon deposition by any of methanol qualities while reforming over the experimental durations.

The results displayed by the analysis of carbon deposition on the catalysts contribute to the addressing of the problem statement by providing the observation of no variation in carbon deposition when reforming each quality methanol.

5.6 Summary

In Chapter 5 it was concluded that by analysing the residue of evaporated methanol, the chlorine concentrations increase with a decrease in methanol quality.

It can be concluded from the processing of the reformer off-gas condensate data that the methanol conversion of the reformer and catalyst decreased significantly based on the quality of methanol reformed. The maximum methanol conversion, as well as the longevity of the catalyst, decreased with a decrease in methanol quality. The methanol conversion values were validated according to similar studies that use commercial catalyst or catalyst with similar chemical compositions. Furthermore, the off-gas condensate acidity increased from a pH value of 7 to a pH of between 6 and 7 indicating the presence of hydrochloric acid during the last hours of each experiment near the end of the catalyst lifespan. It was concluded that the active sites of the catalyst had been poisoned by chlorine molecules, and that the chlorine molecules from the methanol-water fuel were being carried over into the condensate.

The overall hydrogen and carbon dioxide values of the reformer product off-gas collected by the gas sampler remain constant for all methanol qualities and do not vary as the methanol conversion decreased over time. The carbon monoxide concentration, however, was observed to be higher during the first 10 hours of reforming despite the reformer maintaining a constant average temperature of 250 °C. However, it was concluded that the use of a lower quality methanol fuel during the subsequent time intervals would not negatively affect the membrane and fuel cell more than using a higher methanol quality due to the carbon monoxide concentration converging to about 0.3 mol% for all methanol qualities. The presence of hydrogen sulphide was not detected at any time during the experiments by the lead acetate strips regardless of the methanol quality, concluding that it was not a factor when reforming a lower quality methanol and would not negatively affect the H_2S poisoning of components downstream of the reformer. The gas compositions were verified according to expected stoichiometric values and validated according to similar studies that use commercial catalyst, or catalysts with similar chemical compositions which indicate the results' validity to the field.

At 10 hour intervals the catalyst topology was analysed by SEM and composition analysed by EDS. It was concluded that sintering does occur due to the observable roughing and coarser catalytic surface texture, decreased pore size, and presence of cleavage and brittle fractures. The amount of chlorine chemisorbed to the catalyst increased significantly in a shorter period of time with a decrease in methanol quality. However, no sulphur molecules were detected.

Furthermore, a catalyst cross-section was analysed and it was observed that the concentration estimation of chlorine molecules and poisoning penetration depth increased in a shorter period of time with a lower quality methanol indicating a more aggressive poisoning mechanism.

It was observed that there was no carbon deposition on the catalyst during methanol reforming and that a decrease in methanol quality did not influence carbon deposition in the duration of the fuel qualifying experimental procedure.

CHAPTER 6 - CONCLUSIONS

The problem statement of this study was presented as the qualification of the effect of methanol quality on the operation and off-gas composition of a methanol steam reformer. The objectives of this study were stipulated in terms of addressing the problem statement by research, design, evaluation and verification, as well as the experimental results and validation of the results.

Literature presented in Chapter 2 presented a maximum operating temperature of 300 °C with an optimal fuel flow rate of between 0.75 gh^{-1} and 2 gh^{-1} per gram of catalyst with a methanol:water molar ratio of 1:1.1. The poisons in the reformer off-gas affecting the membrane and fuel cell downstream were identified as H_2S and HCl.

The design was evaluated and verified in Chapter 4 according to the design requirements and its ability to produce valid results during fuel qualifying experimentation. The design outcomes of controlled delivery of methanol-water mixture to reformer, controlled reaction kinetics, off-gas liquid and gas separation, sampling ability, and automated control was achieved.

Chapter 5 concluded that the methanol conversion decreases significantly faster with a decreased maximum methanol conversion while reforming with a lower quality methanol fuel. The significantly decreased methanol conversion as a result of a decrease in methanol quality would reduce the hydrogen productivity and effectivity of a fuel cell system. Reforming with CP and Industrial grade methanol produces the most varied and unpredictable methanol conversions when compared to published literature. The condensate acidity increased due to HCl at an increased rate when reforming a lower quality methanol fuel. The composition of the reformer gas products did not vary significantly while reforming different quality fuels. The CO concentration increased in the gas composition by a lower methanol quality. After having reformed for 10 hours, the CO concentration converged to 0.3 mol% for each methanol quality. There was no H_2S in the off-gas stream and would not be a factor when reforming lower methanol qualities. The gas product compositions varied the most from theoretical stoichiometry and published literature when reforming with CP and Industrial grade methanol.

The catalyst topology displays sintering observed by the roughing and coarser catalytic surface texture, decreased porosity, and presence of cleavage and brittle fractures, which is limited to the first 10 hours for all methanol qualities. More chlorine molecules were detected with deeper penetration in a shorter amount when reforming with a lower quality methanol. The lower quality methanol increases chlorine chemisorption by a mechanism that is yet unknown and not addressed in literature.

Therefore, it is not advised to use CP or Industrial grade methanol qualities in a fuel cell system reformer as the off-gas composition is significantly impacted in terms of the decreased methanol conversion, increased presence of HCl in the off-gas condensate and catalyst, and increased CO concentration during the first 10 hours which would negatively impact the lifespan of the membrane and possibly the fuel cell.

6.1 Recommendations and Future Work

From Chapter 4 during the evaluation of the fuel qualifying experimental facility it was observed that:

- An adjustment to the fuel delivery method will be required to more accurately control and measure the flow rate during experimentation.
- A temperature recording method will have to be implemented that does not interfere with the heating element and the heat distribution, along with a higher quantity or higher quality insulation material, to maintain a well distributed reformer temperature. PID control can be considered to reduce temperature fluctuations of the evaporator and reformer.
- A compressed liquid with a thermal conductivity higher than water, at a lower than ambient temperature, can be implemented for the condenser to further cool and condense the off-gases to provide a drier off-gas to the gas chromatograph.
- A more efficient catalyst manufacturing method is suggested that can produce catalyst with better chemical composition and physical properties while producing large quantities.
- It can be considered placing a gas chromatograph in line with the reformer outlet to measure the total mass of hydrogen and other gas products during experimentation for the purpose of determining hydrogen production and the effect it would have on a fuel cell's effectivity.
- A detailed investigation is required into the effect of lower quality methanol fuels on the functioning of the evaporator components and the effect thereof on the rest of the reforming system.
- An investigation is required into the mechanism that enhances the chlorine chemisorption in the catalyst by the reforming of a lower quality methanol.

BIBLIOGRAPHY

Anon. (2017). *Hydrogen Sulphide*. Retrieved December 28, 2017, from Free Chemistry Online: http://freechemistryonline.com/hydrogen-sulphide.html

Bethea, R. M. (2012). Comparison of Hydrogen Sulfide Analysis. *Journal of the Air Pollution Control Association*, 711.

Borgnakke, C., & Sonntag, R. E. (2014). *Fundamentals of Thermodynamics.* Singapore: John Wiley & Sons, Inc.

BST. (2009, November 26). *BSTFlex*. Retrieved from Ningguo BST Thermal Products Co.,Ltd: http://www.directindustry.com/prod/ningguo-bst-thermal-products-co-ltd/product-113675-1388153.html

Carey, F. A. (2019). *Hydrocarbon Chemical Compound*. Retrieved September 24, 2017, from Britannica: https://www.britannica.com/science/hydrocarbon

Danila, E., Morarua, L., Dey, N., Ashour, A. S., Shi, F., Fong, S. J., et al. (2018). Multifractal analysis of ceramic pottery SEM images in Cucuteni-Tripolye culture. *Optik*, 540, 541.

Duffy, G. (2018, November 26). *Underlying Principles of Distillation Boiling a Binary Mixture.* Retrieved from ElecEng: http://eleceng.dit.ie/gavin/Distillation/Boiling%20a%20mixture.pdf

Fogler, S. H. (2005). *Elements of Chemical Reactions Engineering* (4th Edition ed.). New Jersey: Pearson Education, Inc.

Forzatti, P., & Lietti, L. (1999). Catalyst Deactivation. *Catalysis Today*, 167.

Gu, W., Shen, J.-P., & Song, C. (2003). HYDROGEN PRODUCTION FROM INTEGRATED METHANOL REFORMING OVER Cu-ZnO/Al2O3 ANDPt/Al2O3 CATALYSTS FOR PEM FUEL CELLS. *Clean Fuel and Catalysis Program*, 1.

Hachoose, R. C. (2006, April 1). *How to Handle Hydrogen In Process Plants*. Retrieved March 12, 2018, from Chemical Engineering: http://www.chemengonline.com/how-to-handle-hydrogen-in-process-plants/

Hammoud, D., Gennequin, C., Aboukais, A., & Abi Aad, E. (2014). Steam reforming of methanol over x% Cu/ZneAl 400 500 based catalysts for production of hydrogen:Preparation by adopting memory effect ofhydrotalcite and behavior evaluation. *International Journal of Hydrogen Energy*, 1285.

Hydrogenics. (2019). *Fuel Cells*. Retrieved July 5, 2017, from Hydrogenics: https://www.hydrogenics.com/technology-resources/hydrogen-technology/fuel-cells/

IMPCA. (2015, December 8). *IMPCA Methanol Reference Specifications.* Retrieved from Methanol: http://www.methanol.org/wp-content/uploads/2016/07/IMPCA-Ref-Spec-08-December-2015.pdf

Incpropera, F. P., Dewitt, D. P., Bergman, T. L., & Lavine, A. S. (2013). *Principles of Heat and Mass Transfer.* Singapore: John Wiley & Sons, Inc.

Iulianelli, A., Ribeirinha, P., Mendes, A., & Basile, A. (2013, August 11). Methanol steam reforming for hydrogen generation via conventional and membrane reactors: A review. *Elsevier*, 2-4.

Kim, W. K., Mohaideen, K., Seo, D. J., & Yoon, W. L. (2016). Methanol-steam reforming reaction over. *International Journal of Hydrogen Energy, 1*(42), 2082,2085,2086.

Kurr, P., Kasatkin, I., Girgsdies, F., Trunschke, A., Schlögl, R., & Ressler, T. (2008). Microstructural characterization of Cu/ZnO/Al2O3 catalysts for methanol steam reforming - A comparative study. *Applied Catalysis A: General, 1*(348), 153-157,160.

Lee, J. K., Ko, J. B., & Kim, D. H. (2004). Methanol steam reforming over Cu/ZnO/Al2O3 catalyst:. *Applied Catalysis A: General, 1*(278), 1-4.

Luan, C., Zhang, A., Wang, X., Huang, W., & Yin, L. (2012). Catalytic Activity of Liquid Phase Prepared Cu-Zn-Al Catalyst for CO Hydrogenation in a Fixed Bed Reactor. *Indian Journal of Chemistry*, 1,2.

Makertihartha, S., & Gunawan, M. (2009). Synthesis and Activity Test of Cu/ZnO/Al2O3. *ITB J. Eng. Sci.*, 37-49.

Marine Methanol. (2018, November 29). *Methanol Production*. Retrieved from Marine Methanol: http://www.marinemethanol.com/about-methanol/methanol-in-fuel

Materials Evaluation and Engineering, inc. (2019). *Energy Dispersive X-Ray Spectroscopy (EDS)*. Retrieved from MEE-Inc: https://www.mee-inc.com/hamm/energy-dispersive-x-ray-spectroscopyeds/

Matthey, J. (2017). *PEMFC*. Retrieved April 3, 2017, from Fuel Cell Today: http://www.fuelcelltoday.com/technologies/pemfc

Moore, P. J., & Spitler, R. W. (2003). *HYDROGEN SULFIDE MEASUREMENT AND DETECTION.* Texas: AMERICAN SCHOOL OF GAS MEASUREMENT TECHNOLOGY.

MyScope. (2014, April 16). *Accuracy, Precision and Detection Limits*. Retrieved August 21, 2019, from MyScope: https://myscope.training/legacy/analysis/eds/accuracy/

Nano Science Instruments. (2019). *Components in a SEM*. Retrieved from Nano Science: https://www.nanoscience.com/techniques/scanning-electron-microscopy/components/#bsd

Nauman, B. E. (2002). *Chemical Reactor Design, Optimization, and Scaleup* (1st Edition ed.). New York: McGraw-Hill.

NCHT. (2010). *Hydrogen Separation Membranes.* North Dakota: EERC.

Prasetyaningsih, Y., Hendriyana, & Susanto, H. (2016). Influence of Impregnation and Coprecipitation Method in. *J. Eng. Technol. Sci., 48*(4), 444-448.

Purnama, H. (2003). Catalytic Study of Copper based Catalysts for Steam Reforming of Methanol. *Mathematik und NaturwissenschaftenderTechnischen Universität Berlin*, 60-65.

Rojas, S. (2013). *Preparation of Catalysts.* ICP-CSIC.

Sá, S., Silva, H., Brandão, L., Sousa, J. M., & Mendes, A. (2010). Catalysts for methanol steam reforming—A review. *Applied Catalysis B: Environmental, 1*(99), 45.

Sa´, S., Sousa, J. M., & Mendes, A. l. (2011). Steam reformingofmethanoloveraCuO/ZnO/Al2O3 catalyst,. *Chemical Engineering Science, 1*(66), 4914, 4915.

Shekhawat, D., Spivey, J., & Berry, D. A. (2011). *Fuel Cells: Technologies for Fuel Processing.* Netherlands: Elsevier.

UNSW Sydney School of Materials Science and Engineering. (2013, December 11). *Brittle Fracture Surface*. Retrieved from UNSW Sydney: http://www.materials.unsw.edu.au/tutorials/online-tutorials/1-brittle-fracture-surface

US Department of Energy. (2012). *Hydrogen Production: Natural Gas Reforming*. Retrieved March 20, 2017, from Energy.gov: https://energy.gov/eere/fuelcells/hydrogen-production-natural-gas-reforming

APPENDIX A - STUDY FLOW DIAGRAM AND WBS

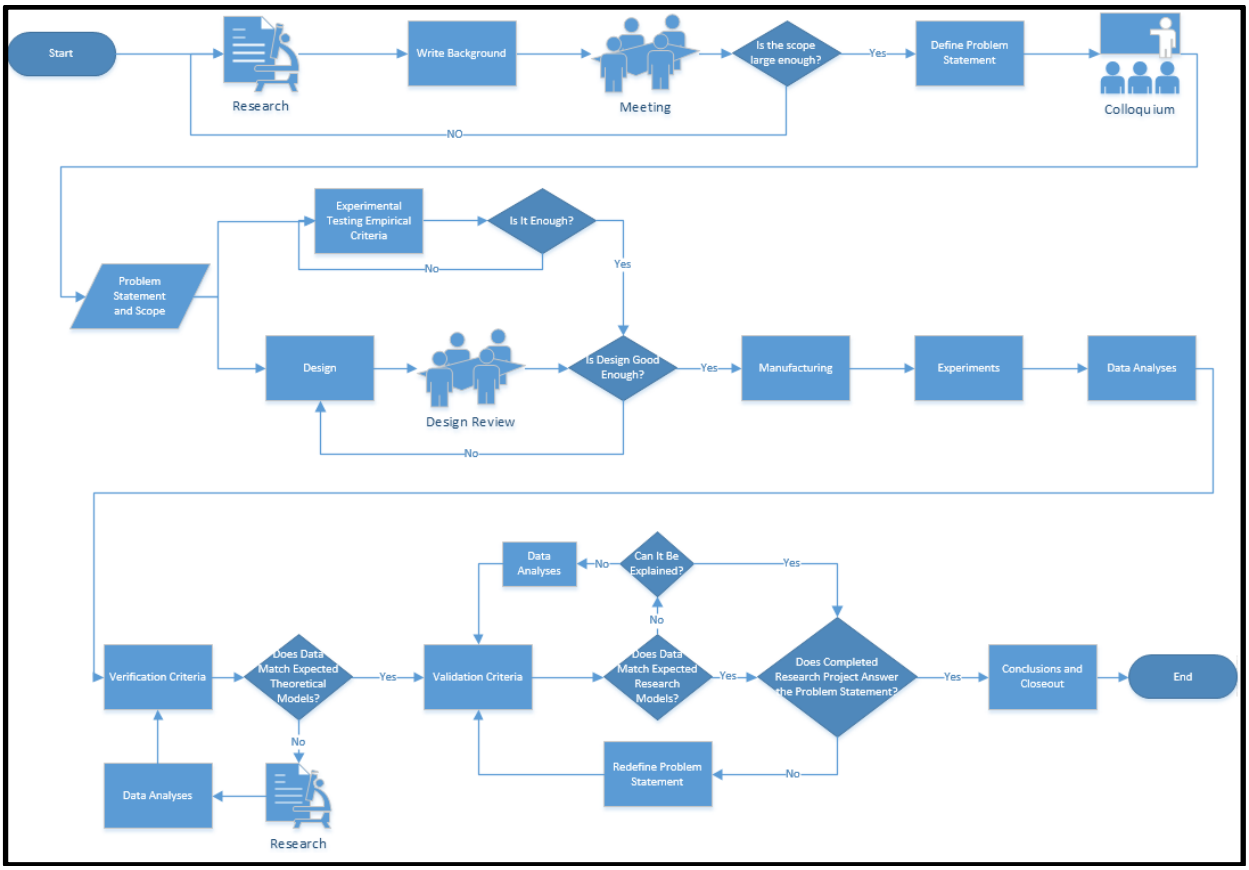

Figure 80 - Study Flow Diagram

Table 34 - Work Breakdown Structure

Phase 1 - Outfitting					
Outcomes	**Outputs**	**Supplier**	**Details/Comments**	**Requirements to be met to facilitate outputs**	Arrived
Installation of Draw cupboard	Structural Support of cupboard	Charlie		Quotes and orders	Ordered
	Removal of window and installation of ducting interface	PG Glass			Quoted
	Structural Support of ducting/piping	Charlie, Vescotech	3m 225mm Flexi-duct		Progress

	Purchase and installation of blower	Charlie, TCN	APT20-4C 200mm (8")		No Progress
	Electrical work to switch blower				
Basin	Purchase of Basin	Plumber		Quotes and orders	
	Purchase of Tap	Plumber			
	Purchase and installation of supply	Plumber			
	Purchase and installation of drainage	Plumber			
Network Points	Network points	PUK			
Electrical Outlets	Purchase and installation of electrical outlets	Electrician	Speak to Electrician Monday		
Compressed air	Purchase and installation of air outlet	Plumber	Speak to Plumber Wednesday		
Nitrogen	Deposit of bottle and purchase gas	Afrox	Create Online Account & order		
Phase 2 - Fuel Delivery					
Fuel Delivery Chamber	Pressure Gauge	TCN	600kpa, 63mm dia, Liq	Quotes and orders	
	Fitting for gauge	TCN	1/2" T-Piece		
	Fitting for purge	TCN	1/2" T-Piece		
	Pressure Regulator(Relief valve)	TCN	300kpa		
	Pressure controller	TCN	700kpa - 300kpa, 3/4" air inlet		
Phase 3 - Fuel Evaporation					
Fuel evaporation and heating chamber	Flow controller	FlowJetWest	1/2", bi directional, KEN-259-6420K	Quotes and orders	
	Balls	TCN	3mm		

	Pressure Pipe (Chamber wall)	Steel&Alloy	Dia: 33.4mm, L:150mm, sch:10	
	Slip-on flange	TCN		
	Blank Flange - Bottom	TCN		
	Slip-on interface flange	TCN		
	Induction heater, etc.	HySa, Amazon, Markgraaff	48V, 20A	
	Pump & piping	TCN	450L/h, FONT 08C5-2	
	Power supply	Mantech	30V, 30A	
	Power supplies	Vepac	TDK Lambda:Genesys 1500W Model 50-30 Elektro Automatik:PS 8032-20 T, PS3032-20B	
	Silicon Gaskets	Builders warehouse	Silicon rubber 300°C	
	Temperature Probes	DIY		
	Controller/switch/SSR	TCN		
	Aluminium Oxide Insulation		Not Electrically conductive while solid	
	Polyester (think green insulation)			
	Silica insulation			
	Mineral wool, stone or ceramic fibre			
Phase 4 - Fuel Reforming				
Fuel reforming chamber and heating	Pressure Pipe (Chamber wall)	Alloy&steel	Dia: 33.4mm, L:200mm, sch:10	Quotes and orders
	Slip-on flange	TCN		
	Pipe end-cap	TCN	Dia:48.26mm (1 1/2")	

	Purchase sparger plate/mesh	Fitow Metal	316L SS Dia:40mm t:2	
	Temperature Probes	DIY		
	Pressure Gauges	TCN	400kpa, 63mm dia, gas	
	Fitting for gauge	TCN	1/4" T-Piece	
	Pressure Regulator(Relief valve)	TCN	200kpa	
	Heating wire	Industrial Alloys	2mm spool	
	Power supply	Mantech	30V, 30A	
	Controller/switch/SSR	TCN		
	Arduino Controller	DIY		
	Pressure Pipe Gas Sampler	Steel&Alloy	Dia:42.2mm, L :150, Sch 10	
	Pipe end-capx2	TCN	2x Dia:42.2mm (1 1/4")	
Phase 5 - Catalyst preparation				
	Copper, zinc, aluminium nitrate	ACE chemicals		Quotes and orders
	Sodium carbonate	ACE chemicals		
	Sodium hydroxide	ACE chemicals		
	Filter paper	ACE chemicals		
	Gloves	Rochelle Chemicals and lab equipment		
	Glassware	Rochelle Chemicals and lab equipment		
	Merk Chemicals	Merk Chemicals		
	pH Paper	Chemical department		
	Catalyst Activation	Build and commission Activation Oven		
	Catalyst Pelletization	ChemEng/pharmacy		
Phase 6 - Cold Commissioning				

	Pressure Test	Passed		
	Temperature Test	Passed		
	Pressure+Temperature	Passed		
Phase 7 -Hot Commissioning				
	Catalytic test	Passed	CaCO3 - Chemical department	
	Condenser	Passed		
Phase 8 - Experimental, Sampling, Analysis				
	Evaporator	Record temperatures & determine heat energy transfer		
	Reformer	Record temperatures & determine heat energy transfer		
	Condenser	Record outlet temperature		
	Lead Acetate Strips		Chemical department	
	BET		Greg Okolo	
	SEM		Dr. Anin Jordaan	
	Gas Chromatograph		Nikolaas (HySA)	

Work Package 1.1	
Plugs	
Deliverables:	**Due Date**
Plugs installed in lab	11-Apr
Activities	
Mark Plug locations	13-Mar
Send P&O	04-Apr
Have Plugs installed	11-Apr

Work Package 1.2	
Extraction Fan	
Deliverables:	**Due Date**
Operational Extraction Fan	11-Apr
Activities	
Send P&O	
Remove window	10-Apr
Have installed	11-Apr
Install Ducting&fan	

Work Package 1.3	
Sink	
Deliverables:	**Due Date**
Flowing water	
Operational Sink	

Work Package 1.4	
Air Pressure	
Deliverables:	**Due Date**
Working adjustable air pressure	

Work Package 1.5	
Shelf Backing	
Deliverables:	**Due Date**
Wood behind	

Work Package 2.1	
Assemble	
Deliverables:	
Tested Tank	
Assembled Evaporator	
Assembled Reactor	
Assembled Condensor & fluid trap	
Assembled Gas sampler	
Activities:	**Due Date:**
Tank Pressure test 2.5bar	
Assemble pipe &flanges	
Install ports for temp sensors	
Install induction heater&kanthal	
Install piping between sub-systems	
Assemble sparger plate	

Work Package 3.1	
Assemble	
Deliverables:	
Assembled Induction heater	
Assembled Kanthal	
Activities:	**Due Date:**
Connect power supplies	
Shape insulation	
Build cooling boxes	
Build water fountain	

Work Package 4.1	
Code	
Deliverables:	**Due Date**
Working code	
Activities	
Install Software	
Download code	
Alter code	
Test run	

Work Package 4.2	
Install	
Deliverables:	**Due Date**
Sensors installed in system	

Work Package 4.1	
Code	
Deliverables:	**Due Date**
Working code	
Activities	
Install Software	
Download code	
Alter code	
Test run	

Work Package 4.2	
Install	
Deliverables:	**Due Date**
Sensors installed in system	

Work Package 5.1	
Cold Commisioning	
Deliverables:	**Due Date**
Results for water system	
Activities	
Check for leaks	

Work Package 5.2	
Warm Commisioning	
Deliverables:	**Due Date**
Results for steam system	
Activities	
Check for leaks	
Ensure proper function	

Work Package 5.3	
Hot Commisioning	
Deliverables:	**Due Date**
Results for meth-steam & catalyst	
Activities	
Ensure proper function	

Work Package 6.1	
Pipe Oven	
Deliverables:	**Due Date**
Table of Settings vs Temps	13-Apr

Work Package 6.2	
Mixers	
Deliverables:	**Due Date**
A working mixer	13-Apr
Fail? To Work Package 6.3	
Activities	
Test each mixer	
Install better mixing heads	
Dispose of old mixers	

Work Package 6.3	
Manufacture	
Deliverables:	**Due Date**
Catalyst	
Activities	
Manufctr Catalyst to Exp Proc	dr

APPENDIX B - HAZARD IDENTIFICATION AND RISK ASSESSMENT FOR EXPERIMENTAL FACILITY

Table 35 - HIRA for Fuel Qualifying Experimental Facility

Hazard Identification	Hazard Effect	Risk Assessment				Risk Control	
		P [/10]	E [/10]	S [/100]	Risk [/400]	Method	Description
High Temperatures	Burn wounds	9	10	3	270 High	Safeguards	Insulation, Warning signs, PPE
Pressure	Component Failure	1	10	3	30 Low	Elimination	Pressure design.
	Gas Bottle damage	6	10	15	900 Very High	Safeguards	Chain bottle horizontally on the floor, Pressure reducer, Pressure design
Electricity	Electrocution from power supply	6	10	15	900 Very High	Safeguards	Insulate all exposed areas of wires, Replace old wires, Keep dry, PPE
	Shock from sensors	0.1	10	0.4	0.4 Acceptable	Safeguards	Insulation, PPE
Hydrogen	Gas ignition and possible explosion	3	10	3	90 Substantial	Elimination	Extraction fan, No open flames,
						Safeguards	Fire extinguisher Warning signs
CO_2 & N_2 Gases	Asphyxiation	3	10	15	450 Very High	Elimination	Extraction fan, Open windows,
Chemicals	Chemical Exposure (hands, eyes, mouth)	9	9	1	86 Substantial	Safeguards	PPE, MSDS
						Elimination	Extraction fan

APPENDIX C - CATALYST MANUFACTURE

ScienceLab.com
Chemicals & Laboratory Equipment

Health	2
Fire	0
Reactivity	0
Personal Protection	E

Material Safety Data Sheet
Cupric nitrate trihydrate MSDS

Section 1: Chemical Product and Company Identification

Product Name: Cupric nitrate trihydrate

Catalog Codes: SLC3202, SLC4990

CAS#: 10031-43-3

RTECS: GL7875000

TSCA: TSCA 8(b) inventory: No products were found.

CI#: Not available.

Synonym: Copper (II) Nitrate trihydrate; Nitric acid, copper (2+) salt, trihydrate; Copper nitrate trihydrate; Copper Dinitrate Trihydrate; Copper (II) Nitrate trihydrate (1:2:3)

Chemical Name: Copper (II) nitrate, trihydrate

Chemical Formula: Cu(NO3)2.3H2O

Contact Information:

Sciencelab.com, Inc.
14025 Smith Rd.
Houston, Texas 77396

US Sales: 1-800-901-7247
International Sales: 1-281-441-4400

Order Online: ScienceLab.com

CHEMTREC (24HR Emergency Telephone), call: 1-800-424-9300

International CHEMTREC, call: 1-703-527-3887

For non-emergency assistance, call: 1-281-441-4400

Section 2: Composition and Information on Ingredients

Composition:

Name	CAS #	% by Weight
Cupric nitrate trihydrate	10031-43-3	100

Toxicological Data on Ingredients: Cupric nitrate trihydrate: ORAL (LD50): Acute: 940 mg/kg [Rat].

Section 3: Hazards Identification

Potential Acute Health Effects:
Hazardous in case of skin contact (irritant), of eye contact (irritant), of ingestion, of inhalation. Prolonged exposure may result in skin burns and ulcerations. Over-exposure by inhalation may cause respiratory irritation.

Potential Chronic Health Effects:
Slightly hazardous in case of skin contact (sensitizer). CARCINOGENIC EFFECTS: Not available. MUTAGENIC EFFECTS: Not available. TERATOGENIC EFFECTS: Not available. DEVELOPMENTAL TOXICITY: Not available. The substance may be toxic to blood, kidneys, liver, cardiovascular system, central nervous system (CNS). Repeated or prolonged exposure to the substance can produce target organs damage.

Section 4: First Aid Measures

Eye Contact:
Check for and remove any contact lenses. In case of contact, immediately flush eyes with plenty of water for at least 15 minutes. Cold water may be used. Get medical attention.

Skin Contact:
In case of contact, immediately flush skin with plenty of water. Cover the irritated skin with an emollient. Remove contaminated clothing and shoes. Cold water may be used.Wash clothing before reuse. Thoroughly clean shoes before reuse. Get medical attention.

Serious Skin Contact:
Wash with a disinfectant soap and cover the contaminated skin with an anti-bacterial cream. Seek immediate medical attention.

Inhalation:
If inhaled, remove to fresh air. If not breathing, give artificial respiration. If breathing is difficult, give oxygen. Get medical attention.

Serious Inhalation:
Evacuate the victim to a safe area as soon as possible. Loosen tight clothing such as a collar, tie, belt or waistband. Seek medical attention.

Ingestion:
Do NOT induce vomiting unless directed to do so by medical personnel. Never give anything by mouth to an unconscious person. If large quantities of this material are swallowed, call a physician immediately. Loosen tight clothing such as a collar, tie, belt or waistband.

Serious Ingestion: Not available.

Section 5: Fire and Explosion Data

Flammability of the Product: Non-flammable.

Auto-Ignition Temperature: Not applicable.

Flash Points: Not applicable.

Flammable Limits: Not applicable.

Products of Combustion: Not available.

Fire Hazards in Presence of Various Substances: combustible materials

Explosion Hazards in Presence of Various Substances:
Risks of explosion of the product in presence of mechanical impact: Not available. Risks of explosion of the product in presence of static discharge: Not available.

Fire Fighting Media and Instructions: Not applicable.

Special Remarks on Fire Hazards: Ignites paper spontaneously in the presence of moisture.

Special Remarks on Explosion Hazards: Not available.

Section 6: Accidental Release Measures

Small Spill: Use appropriate tools to put the spilled solid in a convenient waste disposal container.

Large Spill:
Oxidizing material. Stop leak if without risk. Avoid contact with a combustible material (wood, paper, oil, clothing...). Keep substance damp using water spray. Do not touch spilled material. Prevent entry into sewers, basements or confined areas; dike if needed. Call for assistance on disposal. Be careful that the product is not present at a concentration level above TLV. Check TLV on the MSDS and with local authorities.

Section 7: Handling and Storage

Precautions:
Oxidizer. Keep away from heat. Keep away from sources of ignition. Keep away from combustible material. Do not ingest. Do not breathe dust. Wear suitable protective clothing. In case of insufficient ventilation, wear suitable respiratory equipment. If ingested, seek medical advice immediately and show the container or the label. Avoid contact with skin and eyes. Keep away from incompatibles such as oxidizing agents, reducing agents, combustible materials, organic materials.

Storage:
Deliquescent. Keep container tightly closed. Keep container in a cool, well-ventilated area. Separate from acids, alkalies, reducing agents and combustibles. See NFPA 43A, Code for the Storage of Liquid and Solid Oxidizers.

Section 8: Exposure Controls/Personal Protection

Engineering Controls:
Use process enclosures, local exhaust ventilation, or other engineering controls to keep airborne levels below recommended exposure limits. If user operations generate dust, fume or mist, use ventilation to keep exposure to airborne contaminants below the exposure limit.

Personal Protection:
Splash goggles. Lab coat. Dust respirator. Be sure to use an approved/certified respirator or equivalent. Gloves.

Personal Protection in Case of a Large Spill:
Splash goggles. Full suit. Dust respirator. Boots. Gloves. A self contained breathing apparatus should be used to avoid inhalation of the product. Suggested protective clothing might not be sufficient; consult a specialist BEFORE handling this product.

Exposure Limits:
TWA: 1 CEIL: 2 from OSHA (PEL) [United States] Consult local authorities for acceptable exposure limits.

Section 9: Physical and Chemical Properties

Physical state and appearance: Solid. (Deliquescent crystals solid.)

Odor: Not available.

Taste: Not available.

Molecular Weight: 241.6 g/mole

Color: Blue.

pH (1% soln/water): Not available.

Boiling Point: Decomposition temperature: 170°C (338°F)

Melting Point: 114.5°C (238.1°F)

Critical Temperature: Not available.

Specific Gravity: 2.05 (Water = 1)

Vapor Pressure: Not applicable.

Vapor Density: 8.33 (Air = 1)

Volatility: Not available.

Odor Threshold: Not available.

Water/Oil Dist. Coeff.: Not available.

Ionicity (in Water): Not available.

Dispersion Properties: See solubility in water.

Solubility:
Soluble in cold water. Solubility in Water: 137.8 g/100 cc water @ 0 deg. C.; 1270 g/100 cc @ 100 deg. C. Solubility in alcohol: 100 g/100 cc alcohol @ 12.5 deg. C. Very slightly soluble in liquid ammonia. Practically insoluble in Ethyl acetate.

Section 10: Stability and Reactivity Data

Stability: The product is stable.

Instability Temperature: Not available.

Conditions of Instability: Incompatible materials, moisture

Incompatibility with various substances: Reactive with reducing agents, combustible materials, organic materials, metals.

Corrosivity: Non-corrosive in presence of glass.

Special Remarks on Reactivity:
Incompatible with easily oxidizable materials, paper, wood, organic substances, acetylene, hydrazine, nitromethane, ammonia + potassium amide, acetic anhydride, sodium hypobromide, nitromethanes, potassium ferrocyanide, ether, tin. Reacts vigorously with ether.

Special Remarks on Corrosivity: Not available.

Polymerization: Will not occur.

Section 11: Toxicological Information

Routes of Entry: Inhalation. Ingestion.

Toxicity to Animals: Acute oral toxicity (LD50): 940 mg/kg [Rat].

Chronic Effects on Humans:
May cause damage to the following organs: blood, kidneys, liver, cardiovascular system, central nervous system (CNS).

Other Toxic Effects on Humans: Hazardous in case of skin contact (irritant), of ingestion, of inhalation.

Special Remarks on Toxicity to Animals: Not available.

Special Remarks on Chronic Effects on Humans: Not available.

Special Remarks on other Toxic Effects on Humans:
Acute Potential Health Effects: Skin: May cause severe irritation with possible burns. May cause dermatitis, and skin discoloration. Eyes: May cause severe irritation and possible eye burns. May cause ulceration of the conjunctiva and cornea. Inhalation: May cause severe irritation of the respiratory tract (nose, throat, lungs) with coughing, wheezing, headache, pain, shortness of breath, inflammation, and possible burns. May cause ulceration and perforation of the nasal septum is inhaled in excessive amounts. Other symptoms may include spasm, inflammation and edema of the larynx and bronchi, chemical pneumonitis and pulmonary edema. Ingestion: May be harmful if swallowe. May cause severe gastrointestinal tract irritation with salivation, headache coldsweats, nausea, vomiting and abdominal pain, diarrhea, burning of the mouth, esophagus, or stomach, metallic taste, possible burns resulting in gastric bleeding, hemorrhaging of the digestive tract. Other symptoms of over exposure may include cramps in the calves, muscle rigor, prostration, convulsions, paralysis. May affect behavior/ central nervous system (convulsions, somnolence, excitation followed by central nervous system depression). May cause liver (jaundice) and kidney damage/failure. This product is a nitrate. The toxicity of nitrates is due to in vivo conversion into nitrites. Nitrites can affect the blood and produce methemoglobinemia which results in deficient oxygenation of the blood, causing difficulty breathing, and cyanosis(a bluish discoloration of the skin). Nitrites may also affect the cardiovascular system (hypotension, cardiac arrhythmias, vasodilation, decreased peripheral vascular resistance, hypotension, bradycardia, shock, cardiovascular collapse) which may result in death. Chronic Potential health effects: Repeated exposure by inhalation may cause shrinking of the inner lining of the nose and may cause ulcers and a hole(perforation) in the bone (septum) dividing the inner nose. Repeated ingestion may cause similar effects to those of acute ingestion. It may cause kidney and liver damage. Repeated exposure by skin contact may cause thickening of the skin, and may cause a greenish color (discoloration) to

the skin and hair. May also cause dermatitis, a skin allergy. Medical Conditions Aggravated by Exposure: Persons with pre-existing skin disorders, impaired liver, kidney or pulmonary function, glucose-6-phosphate dehydrogenase deficiency, or pre-existing Wilson's disease. Individual's with Wilson's disease are unable to metabolize copper. Therefore, copper accumulates in various tissues and may result in liver, kidney, and brain damage.

Section 12: Ecological Information

Ecotoxicity: Not available.

BOD5 and COD: Not available.

Products of Biodegradation:
Possibly hazardous short term degradation products are not likely. However, long term degradation products may arise.

Toxicity of the Products of Biodegradation: The products of degradation are less toxic than the product itself.

Special Remarks on the Products of Biodegradation: Not available.

Section 13: Disposal Considerations

Waste Disposal:
Waste must be disposed of in accordance with federal, state and local environmental control regulations.

Section 14: Transport Information

DOT Classification: CLASS 5.1: Oxidizing material.

Identification: : Nitrate, inorganic, n.o.s. (Cupric Nitrate) UNNA: 1477 PG: III

Special Provisions for Transport: Marine Pollutant

Section 15: Other Regulatory Information

Federal and State Regulations:
Connecticut hazardous material survey.: Cupric nitrate (CAS no. 3251-23-8) Illinois chemical safety act: Cupric nitrate (CAS no. 3251-23-8) New York release reporting list: Cupric nitrate (CAS no. 3251-23-8) Rhode Island RTK hazardous substances: Cupric nitrate CAS no. 3251-23-8) Pennsylvania RTK: Cupric nitrate or Nitric Acid, Copper (2+) salt (CAS no. 3251-23-8) Massachusetts RTK: Cupric nitrate (CAS no. 3251-23-8) Massachusetts spill list: Cupric nitrate (CAS no. 3251-23-8) New Jersey: Cupric nitrate (CAS no. 3251-23-8) New Jersey spill list: Cupric nitrate CAS no. 3251-23-8) Louisiana spill reporting: Cupric nitrate (CAS no. 3251-23-8) SARA 313 toxic chemical notification and release reporting: Listed as Copper compounds CERCLA: Hazardous substances.: Cupric Nitrate (CAS no. 3251-23-8): 100 lbs. (45.36 kg) TSCA: Cupric Nitrate or Nitric Acid, Copper (II) salt (CAS no. 3251-23-8) is TSCA listed, but Cupric Nitrate trihydrate (CAS no. 10031-43-3) is exempt from TSCA listing (not TSCA listed) since it is a hydrate.

Other Regulations: OSHA: Hazardous by definition of Hazard Communication Standard (29 CFR 1910.1200).

Other Classifications:

WHMIS (Canada):
CLASS C: Oxidizing material. CLASS D-2B: Material causing other toxic effects (TOXIC).

DSCL (EEC):

HMIS (U.S.A.):

Health Hazard: 2

Fire Hazard: 0

Reactivity: 0

Personal Protection: E

National Fire Protection Association (U.S.A.):

Health: 2

Flammability: 0

Reactivity: 0

Specific hazard:

Protective Equipment:
Gloves. Lab coat. Dust respirator. Be sure to use an approved/certified respirator or equivalent. Splash goggles.

Section 16: Other Information

References: Not available.

Other Special Considerations: Not available.

Created: 10/10/2005 08:17 PM

Last Updated: 05/21/2013 12:00 PM

The information above is believed to be accurate and represents the best information currently available to us. However, we make no warranty of merchantability or any other warranty, express or implied, with respect to such information, and we assume no liability resulting from its use. Users should make their own investigations to determine the suitability of the information for their particular purposes. In no event shall ScienceLab.com be liable for any claims, losses, or damages of any third party or for lost profits or any special, indirect, incidental, consequential or exemplary damages, howsoever arising, even if ScienceLab.com has been advised of the possibility of such damages.

Figure 81 - MSDS for CuNO3

ScienceLab.com
Chemicals & Laboratory Equipment

Health	2
Fire	1
Reactivity	0
Personal Protection	E

Material Safety Data Sheet
Zinc nitrate hexahydrate MSDS

Section 1: Chemical Product and Company Identification

Product Name: Zinc nitrate hexahydrate

Catalog Codes: SLZ1234

CAS#: 10196-18-6

RTECS: ZH4775000

TSCA: TSCA 8(b) inventory: Zinc nitrate hexahydrate

CI#: Not available.

Synonym:

Chemical Formula: H12N2O12Zn

Contact Information:

Sciencelab.com, Inc.
14025 Smith Rd.
Houston, Texas 77396

US Sales: **1-800-901-7247**
International Sales: **1-281-441-4400**

Order Online: ScienceLab.com

CHEMTREC (24HR Emergency Telephone), call:
1-800-424-9300

International CHEMTREC, call: 1-703-527-3887

For non-emergency assistance, call: 1-281-441-4400

Section 2: Composition and Information on Ingredients

Composition:

Name	CAS #	% by Weight
Zinc nitrate hexahydrate	10196-18-6	100

Toxicological Data on Ingredients: Zinc nitrate hexahydrate: ORAL (LD50): Acute: 1190 mg/kg [Rat]. 926 mg/kg [Mouse].

Section 3: Hazards Identification

Potential Acute Health Effects:
Hazardous in case of skin contact (irritant), of eye contact (irritant), of ingestion, of inhalation. Prolonged exposure may result in skin burns and ulcerations. Over-exposure by inhalation may cause respiratory irritation.

Potential Chronic Health Effects:
Hazardous in case of skin contact (irritant), of eye contact (irritant), of ingestion, of inhalation. CARCINOGENIC EFFECTS: Not available. MUTAGENIC EFFECTS: Not available. TERATOGENIC EFFECTS: Not available. DEVELOPMENTAL TOXICITY: Not available. The substance is toxic to mucous membranes. Repeated or prolonged exposure to the substance can produce target organs damage.

Section 4: First Aid Measures

Eye Contact:

Check for and remove any contact lenses. Immediately flush eyes with running water for at least 15 minutes, keeping eyelids open. Cold water may be used. Do not use an eye ointment. Seek medical attention.

Skin Contact:
After contact with skin, wash immediately with plenty of water. Gently and thoroughly wash the contaminated skin with running water and non-abrasive soap. Be particularly careful to clean folds, crevices, creases and groin. Cold water may be used. Cover the irritated skin with an emollient. If irritation persists, seek medical attention. Wash contaminated clothing before reusing.

Serious Skin Contact:
Wash with a disinfectant soap and cover the contaminated skin with an anti-bacterial cream. Seek immediate medical attention.

Inhalation: Allow the victim to rest in a well ventilated area. Seek immediate medical attention.

Serious Inhalation:
Evacuate the victim to a safe area as soon as possible. Loosen tight clothing such as a collar, tie, belt or waistband. If breathing is difficult, administer oxygen. If the victim is not breathing, perform mouth-to-mouth resuscitation. Seek medical attention.

Ingestion:
Do not induce vomiting. Examine the lips and mouth to ascertain whether the tissues are damaged, a possible indication that the toxic material was ingested; the absence of such signs, however, is not conclusive. Loosen tight clothing such as a collar, tie, belt or waistband. If the victim is not breathing, perform mouth-to-mouth resuscitation. Seek immediate medical attention.

Serious Ingestion: Not available.

Section 5: Fire and Explosion Data

Flammability of the Product: May be combustible at high temperature.

Auto-Ignition Temperature: Not available.

Flash Points: Not available.

Flammable Limits: Not available.

Products of Combustion: Not available.

Fire Hazards in Presence of Various Substances: Flammable in presence of reducing materials.

Explosion Hazards in Presence of Various Substances:
Risks of explosion of the product in presence of mechanical impact: Not available. Risks of explosion of the product in presence of static discharge: Not available.

Fire Fighting Media and Instructions:
Oxidizing material. Do not use water jet. Use flooding quantities of water. Avoid contact with organic materials.

Special Remarks on Fire Hazards: Not available.

Special Remarks on Explosion Hazards: Not available.

Section 6: Accidental Release Measures

Small Spill: Use appropriate tools to put the spilled solid in a convenient waste disposal container.

Large Spill:
Oxidizing material. Stop leak if without risk. Avoid contact with a combustible material (wood, paper, oil, clothing...). Keep substance damp using water spray. Do not touch spilled material. Prevent entry into sewers, basements or confined areas; dike if needed. Eliminate all ignition sources. Call for assistance on disposal.

Section 7: Handling and Storage

Precautions:
Keep away from heat. Keep away from sources of ignition. Keep away from combustible material Empty containers pose a fire risk, evaporate the residue under a fume hood. Ground all equipment containing material. Do not ingest. Do not breathe dust. Wear suitable protective clothing in case of insufficient ventilation, wear suitable respiratory equipment If ingested, seek medical advice immediately and show the container or the label. Avoid contact with skin and eyes

Storage:
Keep container dry. Keep in a cool place. Ground all equipment containing material. Oxidizing materials should be stored in a separate safety storage cabinet or room.

Section 8: Exposure Controls/Personal Protection

Engineering Controls:
Use process enclosures, local exhaust ventilation, or other engineering controls to keep airborne levels below recommended exposure limits. If user operations generate dust, fume or mist, use ventilation to keep exposure to airborne contaminants below the exposure limit.

Personal Protection:
Splash goggles. Lab coat. Dust respirator. Be sure to use an approved/certified respirator or equivalent. Gloves.

Personal Protection in Case of a Large Spill:
Splash goggles. Full suit. Dust respirator. Boots. Gloves. A self contained breathing apparatus should be used to avoid inhalation of the product. Suggested protective clothing might not be sufficient; consult a specialist BEFORE handling this product.

Exposure Limits: Not available.

Section 9: Physical and Chemical Properties

Physical state and appearance: Solid. (Crystalline solid.)

Odor: Not available.

Taste: Not available.

Molecular Weight: 297.47 g/mole

Color: White.

pH (1% soln/water): 6 [Acidic.]

Boiling Point: Decomposes.

Melting Point: 36.4°C (97.5°F)

Critical Temperature: Not available.

Specific Gravity: 2.065 (Water = 1)

Vapor Pressure: Not applicable.

Vapor Density: Not available.

Volatility: Not available.

Odor Threshold: Not available.

Water/Oil Dist. Coeff.: Not available.

Ionicity (in Water): Not available.

Dispersion Properties: See solubility in water.

Solubility: Easily soluble in cold water.

Section 10: Stability and Reactivity Data

Stability: The product is stable.

Instability Temperature: Not available.

Conditions of Instability: Not available.

Incompatibility with various substances: Not available.

Corrosivity: Non-corrosive in presence of glass.

Special Remarks on Reactivity: Not available.

Special Remarks on Corrosivity: Not available.

Polymerization: No.

Section 11: Toxicological Information

Routes of Entry: Eye contact. Inhalation. Ingestion.

Toxicity to Animals: Acute oral toxicity (LD50): 926 mg/kg [Mouse].

Chronic Effects on Humans: The substance is toxic to mucous membranes.

Other Toxic Effects on Humans: Hazardous in case of skin contact (irritant), of ingestion, of inhalation.

Special Remarks on Toxicity to Animals: Not available.

Special Remarks on Chronic Effects on Humans: Not available.

Special Remarks on other Toxic Effects on Humans: Not available.

Section 12: Ecological Information

Ecotoxicity: Not available.

BOD5 and COD: Not available.

Products of Biodegradation:
Possibly hazardous short term degradation products are not likely. However, long term degradation products may arise.

Toxicity of the Products of Biodegradation: The products of degradation are more toxic.

Special Remarks on the Products of Biodegradation: Not available.

Section 13: Disposal Considerations

Waste Disposal:

Section 14: Transport Information

DOT Classification: CLASS 5.1: Oxidizing material.

Identification: : Zinc nitrate : UN1514 PG: II

Special Provisions for Transport: Marine Pollutant

Section 15: Other Regulatory Information

Federal and State Regulations: TSCA 8(b) inventory: Zinc nitrate hexahydrate

Other Regulations: OSHA: Hazardous by definition of Hazard Communication Standard (29 CFR 1910.1200).

Other Classifications:

WHMIS (Canada):
CLASS C: Oxidizing material. CLASS D-2B: Material causing other toxic effects (TOXIC).

DSCL (EEC):
R22- Harmful if swallowed. R36/38- Irritating to eyes and skin.

HMIS (U.S.A.):

Health Hazard: 2

Fire Hazard: 1

Reactivity: 0

Personal Protection: E

National Fire Protection Association (U.S.A.):

Health: 2

Flammability: 1

Reactivity: 0

Specific hazard:

Protective Equipment:
Gloves. Lab coat. Dust respirator. Be sure to use an approved/certified respirator or equivalent. Wear appropriate respirator when ventilation is inadequate. Splash goggles.

Section 16: Other Information

References: Not available.

Other Special Considerations: Not available.

Created: 10/11/2005 12:56 PM

Last Updated: 05/21/2013 12:00 PM

The information above is believed to be accurate and represents the best information currently available to us. However, we make no warranty of merchantability or any other warranty, express or implied, with respect to such information, and we assume no liability resulting from its use. Users should make their own investigations to determine the suitability of the information for their particular purposes. In no event shall ScienceLab.com be liable for any claims, losses, or damages of any third party or for lost profits or any special, indirect, incidental, consequential or exemplary damages, howsoever arising, even if ScienceLab.com has been advised of the possibility of such damages.

Figure 82 - MSDS for $ZnNO_3$

ScienceLab.com
Chemicals & Laboratory Equipment

Health	2
Fire	0
Reactivity	0
Personal Protection	E

Material Safety Data Sheet
Aluminum nitrate nonahydrate MSDS

Section 1: Chemical Product and Company Identification

Product Name: Aluminum nitrate nonahydrate

Catalog Codes: SLA1981

CAS#: 7784-27-2

RTECS: BD1050000

TSCA: TSCA 8(b) inventory: Aluminum nitrate nonahydrate

CI#: Not available.

Synonym:

Chemical Name: aluminum nitrate nonahydrate

Chemical Formula: Al(NO3)3.9H2O

Contact Information:

Sciencelab.com, Inc.
14025 Smith Rd.
Houston, Texas 77396

US Sales: 1-800-901-7247
International Sales: 1-281-441-4400

Order Online: ScienceLab.com

CHEMTREC (24HR Emergency Telephone), call: 1-800-424-9300

International CHEMTREC, call: 1-703-527-3887

For non-emergency assistance, call: 1-281-441-4400

Section 2: Composition and Information on Ingredients

Composition:

Name	CAS #	% by Weight
Aluminum nitrate nonahydrate	7784-27-2	100

Toxicological Data on Ingredients: Aluminum nitrate nonahydrate: ORAL (LD50): Acute: 3632 mg/kg [Rat]. 3980 mg/kg [Mouse]. 4280 mg/kg [Rat].

Section 3: Hazards Identification

Potential Acute Health Effects:
Hazardous in case of skin contact (irritant), of eye contact (irritant), of ingestion, of inhalation. Slightly hazardous in case of skin contact (permeator). Prolonged exposure may result in skin burns and ulcerations. Over-exposure by inhalation may cause respiratory irritation.

Potential Chronic Health Effects:
CARCINOGENIC EFFECTS: Not available. MUTAGENIC EFFECTS: Not available. TERATOGENIC EFFECTS: Not available. DEVELOPMENTAL TOXICITY: Not available. The substance is toxic to lungs, mucous membranes. Repeated or prolonged exposure to the substance can produce target organs damage.

Section 4: First Aid Measures

Eye Contact:

Check for and remove any contact lenses. In case of contact, immediately flush eyes with plenty of water for at least 15 minutes. Cold water may be used. Get medical attention.

Skin Contact:
In case of contact, immediately flush skin with plenty of water. Cover the irritated skin with an emollient. Remove contaminated clothing and shoes. Cold water may be used.Wash clothing before reuse. Thoroughly clean shoes before reuse. Get medical attention.

Serious Skin Contact:
Wash with a disinfectant soap and cover the contaminated skin with an anti-bacterial cream. Seek medical attention.

Inhalation:
If inhaled, remove to fresh air. If not breathing, give artificial respiration. If breathing is difficult, give oxygen. Get medical attention.

Serious Inhalation:
Evacuate the victim to a safe area as soon as possible. Loosen tight clothing such as a collar, tie, belt or waistband. If breathing is difficult, administer oxygen. If the victim is not breathing, perform mouth-to-mouth resuscitation. Seek medical attention.

Ingestion:
Do NOT induce vomiting unless directed to do so by medical personnel. Never give anything by mouth to an unconscious person. Loosen tight clothing such as a collar, tie, belt or waistband. Get medical attention if symptoms appear.

Serious Ingestion: Not available.

Section 5: Fire and Explosion Data

Flammability of the Product: Non-flammable.

Auto-Ignition Temperature: Not applicable.

Flash Points: Not applicable.

Flammable Limits: Not applicable.

Products of Combustion: Not available.

Fire Hazards in Presence of Various Substances: Not applicable.

Explosion Hazards in Presence of Various Substances:
Risks of explosion of the product in presence of mechanical impact: Not available. Risks of explosion of the product in presence of static discharge: Not available.

Fire Fighting Media and Instructions: Not applicable.

Special Remarks on Fire Hazards: Not available.

Special Remarks on Explosion Hazards: Not available.

Section 6: Accidental Release Measures

Small Spill: Use appropriate tools to put the spilled solid in a convenient waste disposal container.

Large Spill:
Oxidizing material. Stop leak if without risk. Avoid contact with a combustible material (wood, paper, oil, clothing...). Keep substance damp using water spray. Do not touch spilled material. Prevent entry into sewers, basements or confined areas; dike if needed. Call for assistance on disposal. Be careful that the product is not present at a concentration level above TLV. Check TLV on the MSDS and with local authorities.

Section 7: Handling and Storage

Precautions:
Keep away from heat. Keep away from sources of ignition. Keep away from combustible material.. Do not ingest. Do not breathe dust. Wear suitable protective clothing. In case of insufficient ventilation, wear suitable respiratory equipment. If ingested, seek medical advice immediately and show the container or the label. Avoid contact with skin and eyes.

Storage:
Keep container tightly closed. Keep container in a cool, well-ventilated area. Separate from acids, alkalies, reducing agents and combustibles. See NFPA 43A, Code for the Storage of Liquid and Solid Oxidizers.

Section 8: Exposure Controls/Personal Protection

Engineering Controls:
Use process enclosures, local exhaust ventilation, or other engineering controls to keep airborne levels below recommended exposure limits. If user operations generate dust, fume or mist, use ventilation to keep exposure to airborne contaminants below the exposure limit.

Personal Protection:
Splash goggles. Lab coat. Dust respirator. Be sure to use an approved/certified respirator or equivalent. Gloves.

Personal Protection in Case of a Large Spill:
Splash goggles. Full suit. Dust respirator. Boots. Gloves. A self contained breathing apparatus should be used to avoid inhalation of the product. Suggested protective clothing might not be sufficient; consult a specialist BEFORE handling this product.

Exposure Limits:
TWA: 2 Consult local authorities for acceptable exposure limits.

Section 9: Physical and Chemical Properties

Physical state and appearance: Solid.

Odor: Not available.

Taste: Not available.

Molecular Weight: 375.13 g/mole

Color: Not available.

pH (1% soln/water): Not available.

Boiling Point: Decomposition temperature: 135°C (275°F)

Melting Point: 73°C (163.4°F)

Critical Temperature: Not available.

Specific Gravity: 1.058 (Water = 1)

Vapor Pressure: Not applicable.

Vapor Density: Not available.

Volatility: Not available.

Odor Threshold: Not available.

Water/Oil Dist. Coeff.: Not available.

Ionicity (in Water): Not available.

Dispersion Properties: See solubility in water.

Solubility:

Easily soluble in cold water. Soluble in hot water.

Section 10: Stability and Reactivity Data

Stability: The product is stable.

Instability Temperature: Not available.

Conditions of Instability: Not available.

Incompatibility with various substances: Not available.

Corrosivity: Non-corrosive in presence of glass.

Special Remarks on Reactivity: Not available.

Special Remarks on Corrosivity: Not available.

Polymerization: Will not occur.

Section 11: Toxicological Information

Routes of Entry: Eye contact. Inhalation. Ingestion.

Toxicity to Animals: Acute oral toxicity (LD50): 3632 mg/kg [Rat].

Chronic Effects on Humans: Causes damage to the following organs: lungs, mucous membranes.

Other Toxic Effects on Humans:
Hazardous in case of skin contact (irritant), of ingestion, of inhalation. Slightly hazardous in case of skin contact (permeator).

Special Remarks on Toxicity to Animals: Not available.

Special Remarks on Chronic Effects on Humans: Not available.

Special Remarks on other Toxic Effects on Humans: Not available.

Section 12: Ecological Information

Ecotoxicity: Not available.

BOD5 and COD: Not available.

Products of Biodegradation:
Possibly hazardous short term degradation products are not likely. However, long term degradation products may arise.

Toxicity of the Products of Biodegradation: The products of degradation are more toxic.

Special Remarks on the Products of Biodegradation: Not available.

Section 13: Disposal Considerations

Waste Disposal:

Section 14: Transport Information

DOT Classification: CLASS 5.1: Oxidizing material.

Identification: : Aluminum Nitrate UNNA: UN1438 PG: III

Special Provisions for Transport: Marine Pollutant

Section 15: Other Regulatory Information

Federal and State Regulations: TSCA 8(b) inventory: Aluminum nitrate nonahydrate

Other Regulations: OSHA: Hazardous by definition of Hazard Communication Standard (29 CFR 1910.1200).

Other Classifications:

WHMIS (Canada):
CLASS C: Oxidizing material. CLASS D-2B: Material causing other toxic effects (TOXIC).

DSCL (EEC):
R8- Contact with combustible material may cause fire. R36/38- Irritating to eyes and skin.

HMIS (U.S.A.):

Health Hazard: 2

Fire Hazard: 0

Reactivity: 0

Personal Protection: E

National Fire Protection Association (U.S.A.):

Health: 2

Flammability: 0

Reactivity: 0

Specific hazard:

Protective Equipment:
Gloves. Lab coat. Dust respirator. Be sure to use an approved/certified respirator or equivalent. Wear appropriate respirator when ventilation is inadequate. Splash goggles.

Section 16: Other Information

References: Not available.

Other Special Considerations: Not available.

Created: 10/11/2005 11:15 AM

Last Updated: 05/21/2013 12:00 PM

The information above is believed to be accurate and represents the best information currently available to us. However, we make no warranty of merchantability or any other warranty, express or implied, with respect to such information, and we assume no liability resulting from its use. Users should make their own investigations to determine the suitability of the information for their particular purposes. In no event shall ScienceLab.com be liable for any claims, losses, or damages of any third party or for lost profits or any special, indirect, incidental, consequential or exemplary damages, howsoever arising, even if ScienceLab.com has been advised of the possibility of such damages.

Figure 83 - MSDS for $AlNO_3$

Precipitation

The specific measurements used are displayed in Table 36.

Table 36 - Chemical Weights and Water Volumes

Chemical	Weight [g]	Beaker Size [L]	Volume [mL]
$Cu(NO_3)_2$	283.0	0.6	100.0
$Zn(NO_3)_3$	139.6	0.6	100.0
$Al(NO_3)_3$	83.6	1.0	150.0
Na_2CO_3	300.4	2.0	1300.0

To make 200 g of catalyst the procedure below was followed:

- The oven was pre-heated to 60 °C.
- The beakers were filled with the required amounts of distilled water and were placed into the oven to heat.
- While the beakers of water were heating, the required weights of each chemical were measured out.

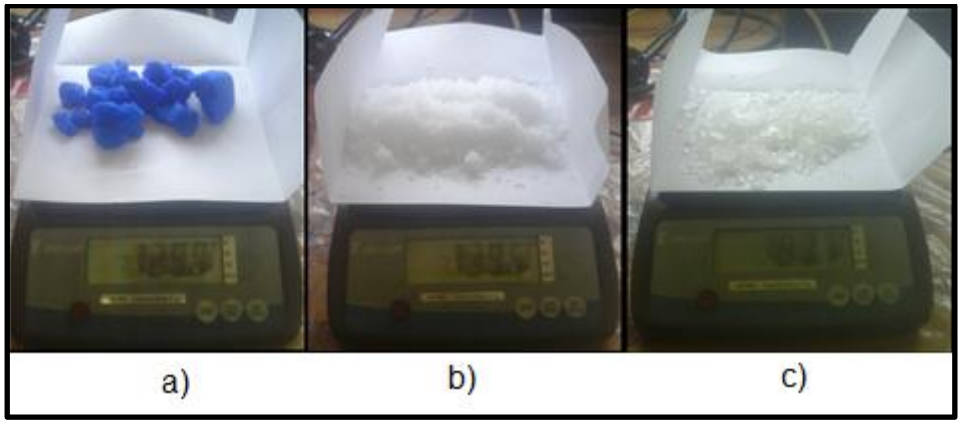

Figure 84 - Weighing a) Copper Nitrate, b) Zinc Nitrate c) Aluminium Nitrate

- The chemicals were dissolved into their corresponding beakers of water using a magnetic mixer with a heated plate.

- The various nitrates were poured into one beaker while mixing vigorously with the magnetic mixer. Very slowly, the mixture of nitrates was poured into the beaker containing the Na_2CO_3.

Figure 85 - Heating and Magnetic Mixing Precipitate

- While mixing, the pH of the solution was noted. A mixture of NaOH and Na_2CO_3 was added to keep the pH above 7 and as close to 10 as possible.

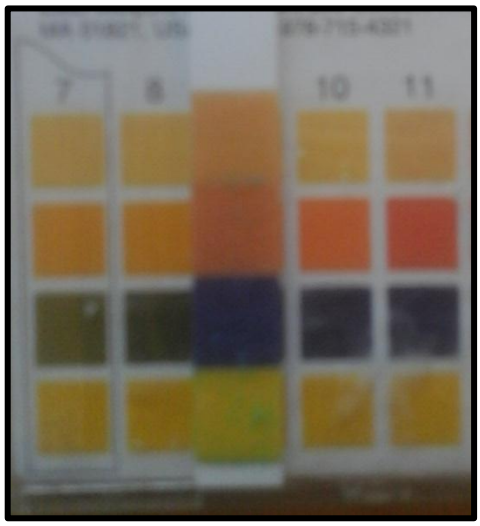

Figure 86 - pH Measurement of Precipitate

- Mixing was then continued for 15 minutes ensuring complete precipitation

- The precipitate was placed into the oven and allowed to age in the mother liquid at 60 °C for 3 to 4 hours.

Figure 87 - Aging Precipitate

Figure 88 - Aging Temperature of 60°C

- The precipitate was filtered with filter paper and rinsed with distilled water to remove remaining sodium ions.

Figure 89 - Filtering Precipitate a) Top View, b) Side view

- The precipitate was returned to the oven at 60 °C to dry for 6 hours.

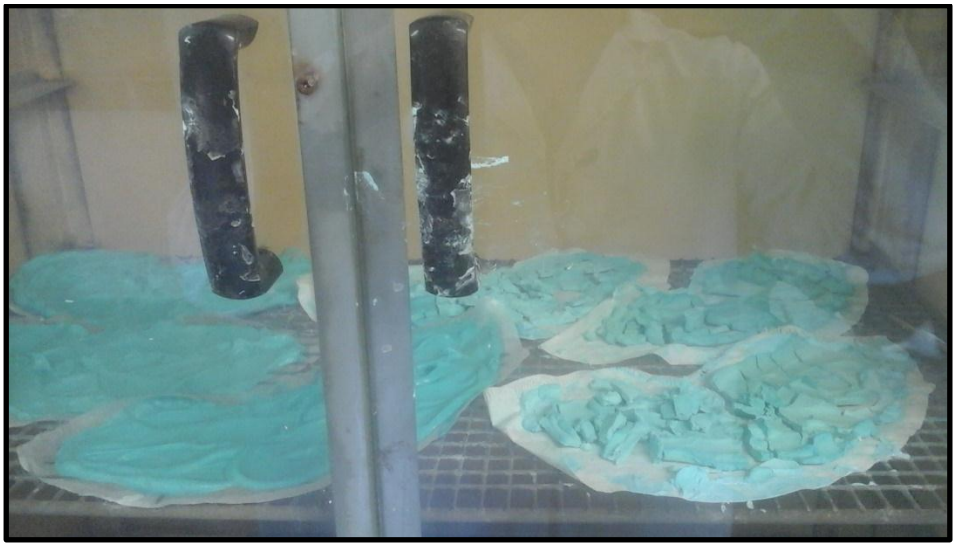

Figure 90 - Drying Filtered Precipitate at 60°C

- The dry carbonates were crushed in a ball-mixer.

Figure 91 - Ball Crushing of Precipitate

Calcination

The crushed carbonates were placed in an oven with a temperature increase of 5 °C/min until 400 °C was reached and then left to calcinate for 2 to 3 hours with agitation every half hour.

a) b)

Figure 92 - a) Calcination Oven b) Oven Temperature Measurement

Activation

In order to remove the oxygen molecule from the CuO and have a final product of $Cu/ZnO/Al_2O_3$, the oxides needed to be heated in a hydrogen atmosphere at a temperature between 200 °C and 300 °C. Hydrogen is, however, explosively flammable, and a Hazard and Operability Study was presented to control and mitigate the potential hazards. This HAZOP can be found in Appendix D.

In order to activate 100 g in 3 hours, the amount of Hydrogen required, and the flow rate to provide that amount of hydrogen in the required amount of time, needed to be determined.

The stoichiometry equation was as follows:

$CuO + H_2 + Heat \longrightarrow Cu + H_2O$

For 100 g of catalyst there is 60 g of CuO.

$$m_{H_2} = 0.06 \times (\frac{2}{79.545})$$

Therefore, 0.0015g of Hydrogen was required.

$$\dot{m}_{H_2} = \frac{0.0015\ kg}{3hours \times 60}$$

$$\dot{m}_{H_2} = 8.38 \times 10^{-6}\ \text{kgs}^{-1}$$

However, the gas mixture is 95 % argon and 5 % hydrogen which is called H_5. If the flow rate of hydrogen required is $8.38x10^{-6}$ kgs^{-1} then the gas flowrate was:

$$\dot{m}_{H_2} = \dot{m}_{gas} \times 0.05$$

$$\dot{m}_{gas} = 0.16762 \times 10^{-3}\ \text{kgs}^{-1}$$

$$\dot{Q}_{gas} = \frac{\dot{m}_{gas}}{\rho_{gas}}$$

$$\rho_{gas} = \frac{1}{\frac{x_{H_2}}{\rho_{H_2}} + \frac{1-x_{H_2}}{\rho_{Ar}}}$$

$$\rho_{gas} = \frac{1}{\frac{0.05}{0.08988} + \frac{1-0.05}{1.784}}$$

$$\rho_{\text{gas}} = 0.9184\ \text{kgm}^{-3}$$

$$\therefore \dot{\text{Q}}_{\text{gas}} = \frac{0.16762 \times 10^{-3}}{0.9184}$$

$$\dot{\text{Q}}_{\text{gas}} = 0.1825 \times 10^{-3}\ \text{m}^3\text{s}^{-1}$$

Due to the use of a flow meter that is calibrated for air, correction equations were required to determine the volume flow rate that will be displayed when $0.1825\text{x}10^{-3}\text{m}^3/\text{s}$ of the H_5 gas was flowing through it.

$$SG_{scale} = SG_{air} = 1$$

$$SG_{gas} = \frac{Molecular\ Weight_{Gas}}{molecular\ Weight_{Air}} = \frac{0.05 \times 2 + 0.95 \times 39.948}{28.97}$$

$$SG_{gas} = 1.3134$$

$$\text{Factor } = \sqrt{\frac{SG_{scale}}{SG_{gas}}}$$

$$\text{Factor } = \sqrt{\frac{1}{1.3134}}$$

$$\text{Factor } = 0.87257$$

$$\dot{Q}_{scale} = \dot{Q}_{gas} \times Factor$$

$$\dot{Q}_{scale} = 0.1825\text{x}10^{-3} \times 0.87257$$

$$\dot{Q}_{scale} = 0.2092 \times 10^{-3} \ \text{m}^3\text{s}^{-1}$$

$$\dot{Q}_{scale} = 0.2092 \ \text{ls}^{-1}$$

A flow meter reads Normal Litres per second.

$$\therefore \dot{Q}_{normal} = \dot{Q}_{scale} \times \frac{235}{101.325} \times \frac{273.15}{273.15 + 25}$$

$$\dot{Q}_{normal} = 0.4445 \ \text{Nls}^{-1}$$

This volumetric flow rate would have been adequate if every hydrogen particle reacted with the catalyst, however, due to possible sintering and preferential flow, not every hydrogen particle will have the chance to react with the catalyst, and therefore manual agitation was induced by shaking the activation oven as well as an increased volumetric flow rate of 0.34494 l/s (0.8Nl/s) which can be easily controlled based on the readings from the flow meter. This allowed a larger amount of hydrogen to come into contact with the catalyst while maintaining the required 3 hours of activation time.

Figure 93 - Activation Oven Setup

This final product was then pelletized into cylinders of 6 mm diameter and 6 mm long.

Figure 94 - Catalyst Pelletizer

This process was repeated 4 times to produce 800 g of catalyst.

APPENDIX D - ACTIVATION OVEN

Design

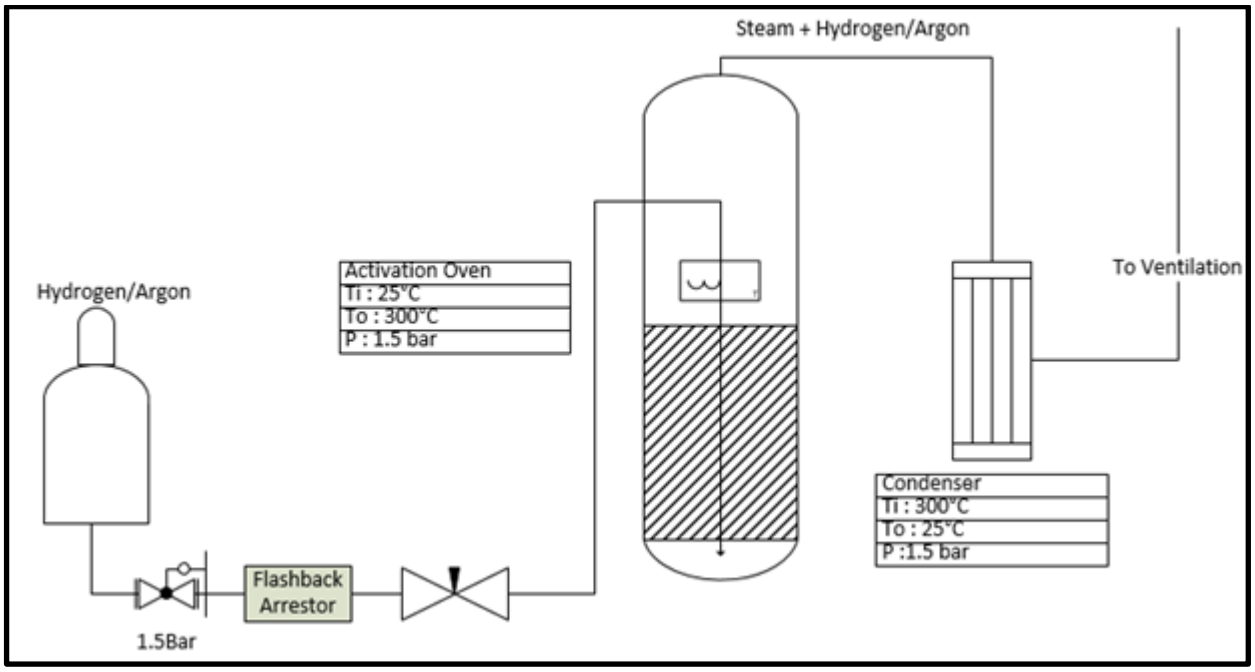

Figure 95 - P&ID of Activation Oven

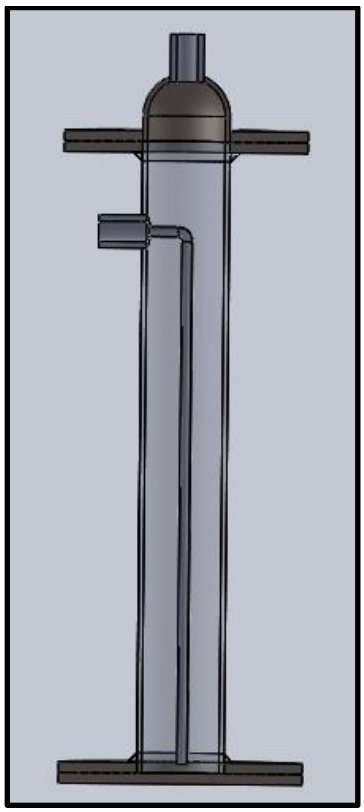

Figure 96 - Cross-Section View of Activation Oven

Hazard and Operability Study

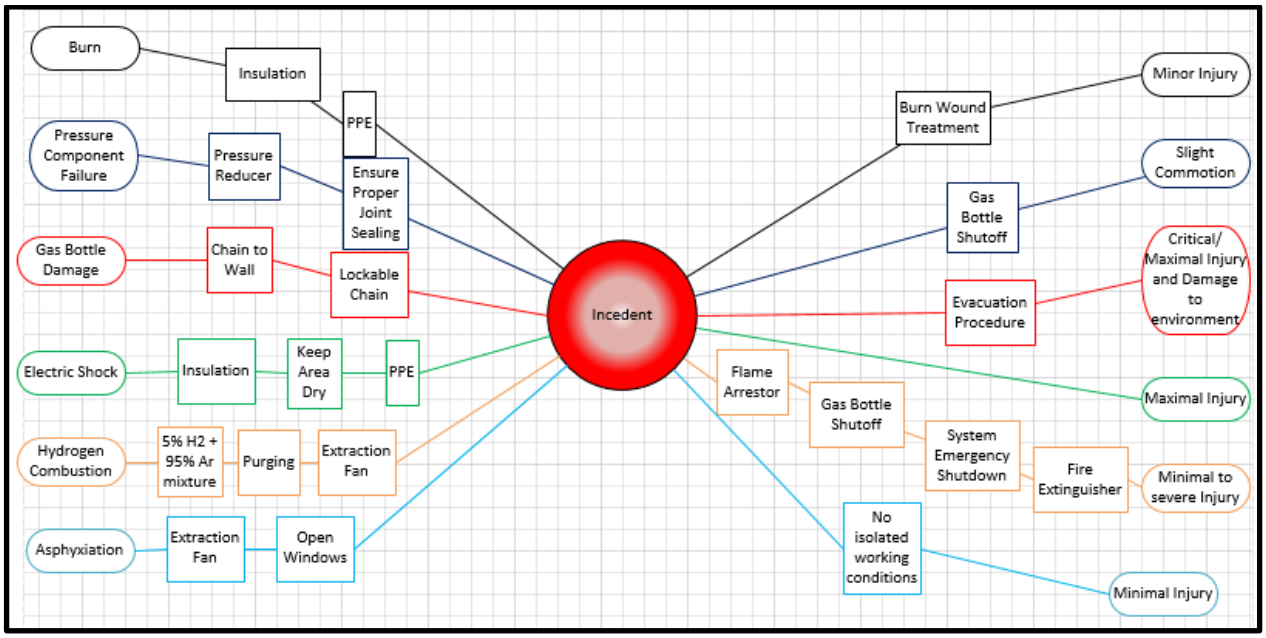

Figure 97 - HAZOP Bowtie Diagram

Key:

Table 37 - HAZOP HIRA Table for Activation Oven

	Rank				
Probability	0.1 – Impossible			10 – Very Likely	
Exposure	0.1 – None			10 - Continuous	
Consequences	0.4 – Negligible (paper cut)			100 - Catastrophic (many deaths)	
Risk	<20 - Acceptable	20-70 - Low (needs attention)	70-200 Substantial (Correction needed)	200-400 High (Immediate correction needed)	>400 Very High (Discontinue operation)

Hazard Identification	**Hazard Effect**	**Risk Assessment**				**Risk Control**	
		P [/10]	E [/10]	C [/100]	Risk [/400]	Method	Description
High Temperatures	Burn wounds	9	10	3	270 High	Safeguards	Insulation, Warning signs, PPE
Pressure	Component Failure	3	10	15	450 Very High	Elimination	Pressure regulator, Proper Joint sealing
	Gas Bottle damage	6	10	20	1200 Very High	Safeguards	Chain bottle Vertically to the wall, lockable chain
Electricity	Electrocution from power supply	6	10	15	900 Very High	Safeguards	Insulate all exposed wires, Keep area dry, PPE
	Shock from sensors	0.1	10	0.4	0.4 Acceptable	Safeguards	Insulation, PPE
Hydrogen	Gas ignition and possible	0.2	10	30	60	Elimination	Extraction fan,

	explosion				Low		No open flames, Purging process, Hydrogen Argon mixture, Flame arrestor before tank
						Safeguards	Fire extinguisher
Ar & N_2 Gases	Asphyxiation	3	10	15	450 Very High	Elimination	Extraction fan, Open windows,
Chemical Exposure	Skin and eye irritation	10	10	5	500 Very High	Safeguards	PPE

Hazard Identification	Hazard Effect	Renewed Risk Assessment			
		P [/10]	E [/10]	C [/100]	Risk [/400]
High Temperatures	Burn wounds	0.2	10	1	2 Acceptable
Pressure	Component Failure	0.2	10	1	30 Low
	Gas Bottle damage	0.1	10	20	20 Low
Electricity	Electrocution from power supply	0.2	10	15	30 Low
	Shock from sensors	0.1	10	0.4	0.4 Acceptable
Hydrogen	Gas ignition and possible explosion	0.1	10	30	30 Low
Ar & N_2 Gases	Asphyxiation	0.1	10	15	15 Acceptable
Chemical Exposure	Skin and eye irritation	0.1	10	5	5 Acceptable

It must be noted that the use of this facility will be limited to a maximum period of one month. This facility is not a permanent inclusion to the laboratory and will be disassembled when it is no longer needed. Therefore, the gas bottles will not have an enclosed cage outside the building as this will require time and finances to install, which will not be feasible for a temporary facility of such a short duration.

This hazard and operability study was attended by:

Safety Officer: Mr. Sarel Naude.

Study leader: Mr. Johan Markgraaff.

Consultant: Dr. Gerhard Human.

Engineer: Mr. Herculaas Botha

Engineer: Mr. Coetsee Stander

APPENDIX E - METHANOL QUALITY SPECIFICATION SHEETS

Table 38 - Adaptation of Supplier Product Specifications for each Methanol Quality

Supplier	**Minema Chemicals**		**Ethanol SA**
Quality	Analytical Reagent	Chemically Pure	Industrial grade
Purity [%]	99.5	99.5	100
Impurities Listed [%]	0.11205	0.255	0.0803
Total Accounted for [%]	99.61205	99.755	100.0803
Unaccounted for [%]	0.38795	0.245	-0.0803
Acetone ($(CH_3)_2CO$) [%]	<0.005	<0.04	Not Disclosed
Acidity (HCOOH) [%]	<0.005	<0.004	0.0003
Alkalinity (NH_3) [%]	<0.0005	Not Disclosed	Not Disclosed
Heavy Metals (Pb) [%]	<0.00005	Not Disclosed	Not Disclosed
Residue on Evaporation [%]	<0.001	<0.01	Not Disclosed
Substances reducing $KMnO_4$ [%]	<0.0005	Not Disclosed	Not Disclosed
Water (H_2O) [%]	<0.1	<0.2	0.08
Sulphur Compounds[ppm]	Not Disclosed	10	Not Disclosed

Considering Table 38, it can be observed that the higher quality methanol impurities are discussed in more detail than the two lower methanol qualities. There are an increased number of “Not Disclosed” comments for the CP and Industrial grade methanol, however, the impurities unaccounted for in the percentage composition becomes less as the methanol quality decreases.

According to the IMPCA standards there is a possibility 0.5ppm of sulphur and chlorine compounds but only the Chemically Pure quality presents a sulphur compound value. This is possibly an oversight of the suppliers and it is the consumer’s responsibility to purchase and use the correct methanol quality depending on the application, but the lack of definitive information on the subject is the reason for the proposed problem statement.

APPENDIX F - EVAPORATION METHODS

Due to the fact that methanol has a lower evaporation point than water, when attempting to vaporize a water-methanol mixture with a boiling process the methanol will evaporate first, leaving the water behind. Even at higher temperatures and pressures methanol will evaporate at a higher rate than water, which will result in a gas with a water-methanol ratio that is not ideal for reforming. The various temperatures and gas compositions can be seen by Figure 98.

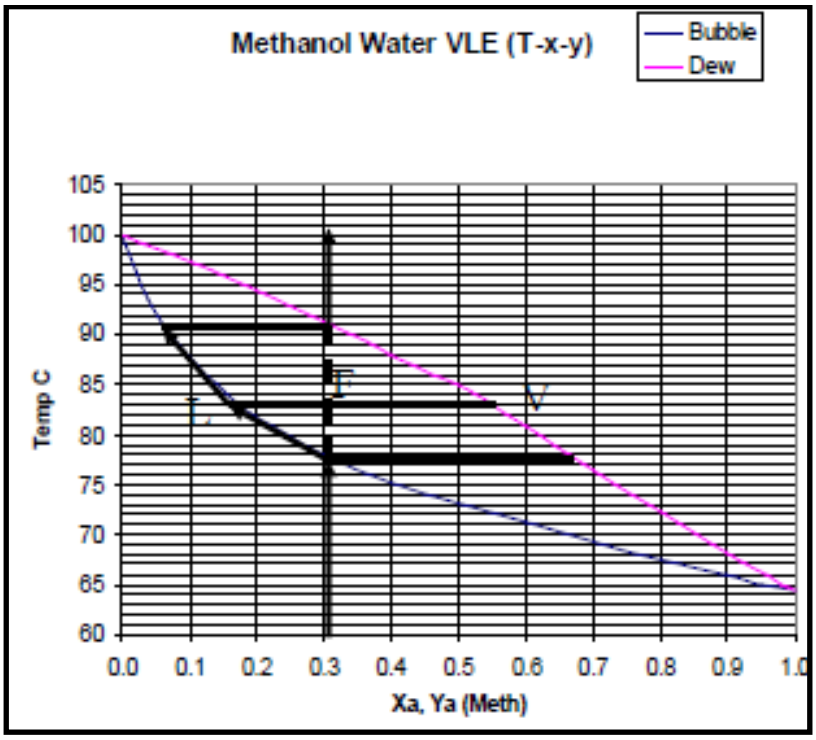

Figure 98 - Methanol Water Vapour Liquid Equilibrium (Duffy, 2018)

Due to this boiling mechanism, a method must be determined that can deliver the correct water-methanol ratio.

A possible option would be to mix the fuel with 60 % methanol and heat it to 81 °C. This would create a vapour that consists of 60 % methanol and continue in this manner until the density indicates 20 % methanol. At 81 °C the vapour should remain 60 % methanol throughout the boiling procedure. Although, theoretically this method will work, the temperature will not constantly remain at 81 °C. There will be temperature fluctuations and the vapour consistency will fluctuate as a result. This is not a viable solution for long periods of operation.

The water-methanol mixture can undergo a flash evaporation procedure. By spraying the fuel under high pressure into a low pressure environment with a misting nozzle, small particles of the correct water-methanol ratio will be created that can be evaporated with a small amount of energy very quickly, allowing the vapour to remain constant and essentially no boiling taking place.

However, flash evaporation is generally used to separate certain liquids with different densities and different evaporating points to purify them. Methanol and water have different densities and boiling points and by using a flash evaporation procedure the water and methanol could partially separate. There would be a number of particles with different water-methanol ratios. Furthermore, the use of a misting nozzle requires incredibly high operating pressures to supply small flow rates. In order to create the continuous flow rate required by the system a very small nozzle orifice would be used which would require a large minimum operating pressure of nearly 70bar.

Using the principles of flash evaporation, a different method can be considered. Introducing a very small amount of fuel into a heated system with a large surface area would evaporate the fuel very quickly at the correct ratio. Even though boiling took place it would happen so quickly it would not change the gas composition.

Induction heating has become very popular to melt metals very quickly with less electrical energy required. By using a metal surface that is magnetically inductive but not electrically conductive, the fuel would be able to evaporate on the heated surface and the induction heating would be able to maintain the temperature of the metal surface at the required temperature very quickly and efficiently.

Selection Matrix for Evaporation

The various options must be compared with one another according to the most important criteria. By simply giving a “-“, “0”, or “+” states that the concept is bad, average, or good respectively, in each specific criteria.

Furthermore, the worst scoring concept is removed and the remaining concepts are compared by giving the criteria a weight depending on how important it is, and then each concept is scored with a value from 0 to 5 for each criterion.

Table 39 - Evaporation Selection and Scoring Matrix

	Concepts		
	1 Boiler	2 Spray Nozzle	3 Induction heater
Ease of use	-	0	0
Length of experiment	-	+	+
Manufacturability	+	+	+
Cost	0	-	-
Viability	0	-	+
Energy Consumption	-	+	-
Safety	0	-	0
Sum "+"	1	3	3
Sum "0"	3	1	2
Sum "-"	3	3	2
Total	-2	0	1

		1 Spray Nozzle		2 Induction heater	
	Weight	Rating	Weighted Score	Rating	Weighted Score
Ease of use	10	3	0.3	4	0.4
Length of experiment	20	5	1	5	1
Manufacturability	10	3	0.3	4	0.4
Cost	15	3	0.45	1	0.15
Viability	20	2	0.4	4	0.8
Energy Consumption	10	3	0.3	1	0.1
Safety	40	2	0.8	4	1.6
Total Score Rank	100%	3.55		4.45	
Continue?		**No**		**Yes**	

Table 39 displays how the concept of boiling was the worst scoring concept during the selection process. The induction heater proved to be the best concept when compared to the spray nozzle in the scoring matrix. Therefore, the further design considerations will take induction heating into account as the method for evaporation.

APPENDIX G - EVAPORATOR RESULTS AND CONCLUSIONS

For the induction heater, the following tables show the temperature values read from the induction heater evaporator under various pipe diameters.

33.4mm Diameter – Graphite Air heating

Table 40 - Temperature and Time for 33.4mml Diameter Pipe Evaporator filled with Graphite

Timer [Sec]	Temperature [ºC]
0	10.25
10	10.75
20	11.5
30	14.25
40	17.75
50	21.25
60	25.25
70	3.50
80	34.75
90	41.00
100	46.50
110	52.00
120	56.75
130	64.50
140	71.75
150	79.25
160	88.00
170	95.50
180	104.00
190	112.50
200	120.25
210	129.00
220	138.50
230	146.50
240	155.25
250	163.75
260	171.00
270	179.75
280	187.25
290	194.75
300	192.25

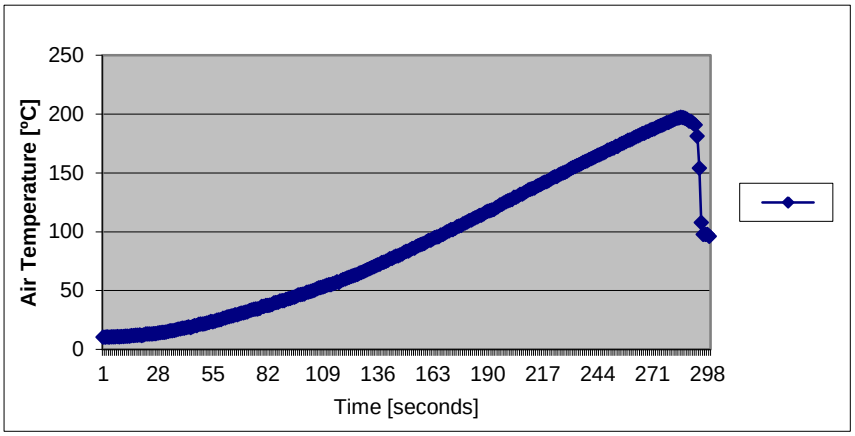

Figure 99 - Line Graph for Temperature over Time for 33.4mml Diameter Pipe filled with Graphite

42.2mm Diameter - Graphite Air Heating

Table 41 - Air Temperature and Time for 42.2mm Diameter Pipe Evaporator filled with Graphite

Timer [sec]	Temperature [°C]
0	14.00
10	14.00
20	16.30
30	20.80
40	28.00
50	36.50
60	44.80
70	52.30
80	57.00
90	61.50
100	64.80
110	67.50
120	71.00
130	74.30
140	78.50
150	86.50
160	97.30
170	107.00
180	118.00
190	130.50
200	141.80
210	154.50
220	167.30
230	179.30
240	193.00
250	205.50

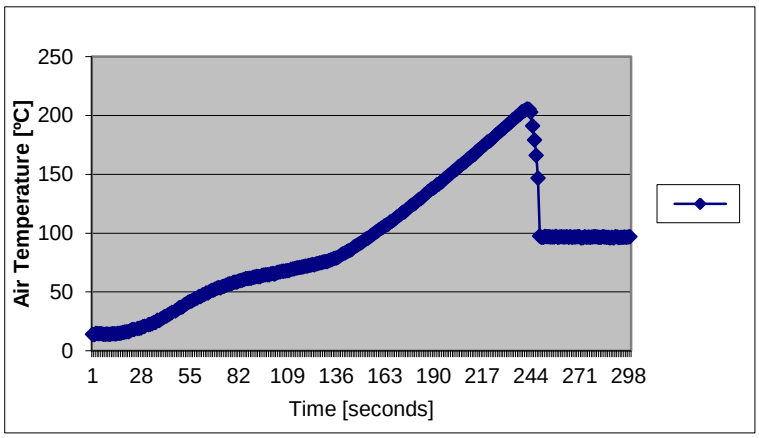

Figure 100 - Line Graph for Temperature over Time for 42.2mm Diameter Pipe filled with Graphite

33.4mm Diameter – Empty Air heating

Table 42 - Air Temperature and Inner Wall Surface Temperature for Empty 33.4mm Diameter Pipe Evaporator

Timer [sec]	Temperature [ºC]	Surface Temperature [ºC]
0	23.75	17.75
10	23.5	18.00
20	23.75	20.50
30	24.75	25.50
40	28.00	29.25
50	30.75	33.00
60	33.00	36.50
70	35.75	40.00
80	38.25	42.00
90	44.50	45.25
100	52.75	49.50
110	56.50	54.25
120	61.00	60.00
130	66.75	65.00
140	71.50	71.00
150	78.00	78.25
160	87.75	85.25
170	93.25	92.25
180	99.25	100.25
190	105.25	105.00
200	111.75	
210	118.75	
220	124.75	
230	130.75	
240	139.00	
250	146.00	
260	148.75	

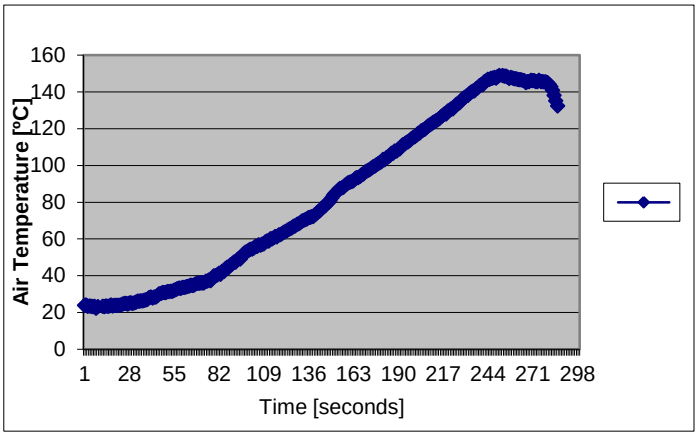

Figure 101 - Line Graph for Air Temperature over Time for Empty 33.4mm Diameter Pipe

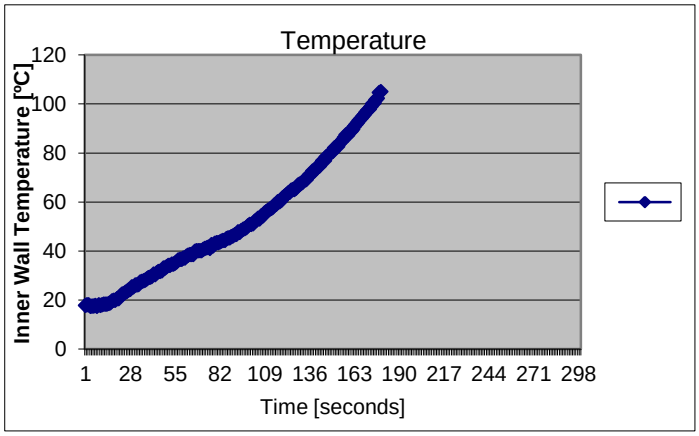

Figure 102 - Line Graph for Inner Wall Temperature over Time for Empty 33.4mm Diameter Pipe

42.2mm Diameter – Empty Air heating

Table 43 - Air Temperature and Inner Wall Surface Temperature for Empty 42.2mm Diameter Pipe Evaporator

Timer [sec]	Temperature [ºC]	Wall Temperature [ºC]
0	21.70	19.25
10	23.50	21.00
20	24.50	23.50
30	26.50	27.50
40	28.00	35.25
50	31.75	43.75
60	37.50	54.00
70	43.25	65.25
80	48.00	76.25
90	53.75	87.50
100	60.50	95.50
110	72.75	104.75
120	85.00	125.50
130	95.50	
140	104.25	
150	113.25	
160	125.00	
170	136.50	
180	147.75	
190	157.25	
200	175.50	
210	195.75	
220	213.75	
230	223.75	
240	234.50	
250	256.00	

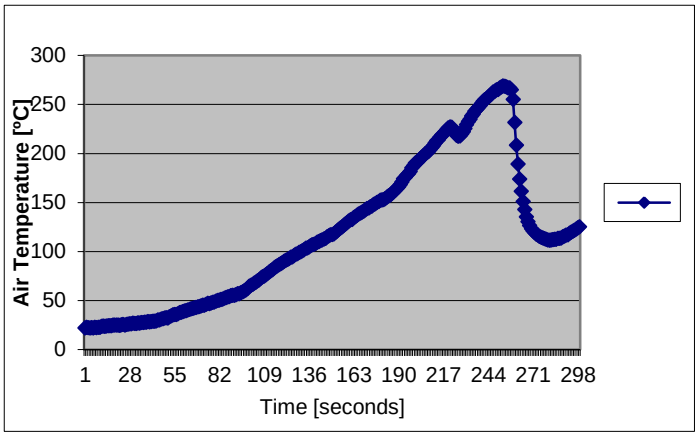

Figure 103 - Line Graph for Inner Wall Temperature over Time for Empty 42.2mm Diameter Pipe

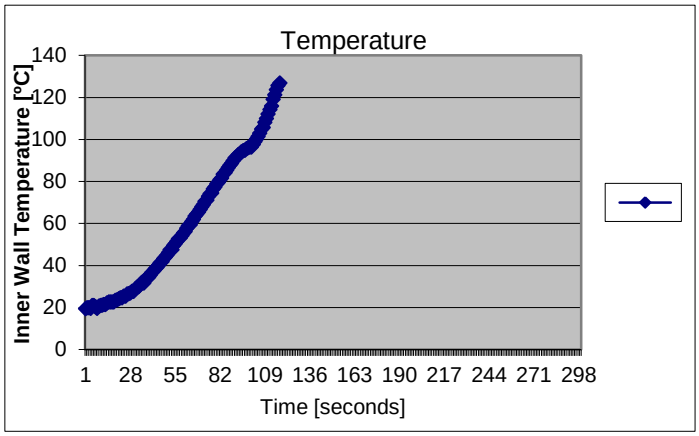

Figure 104 - Line Graph for Inner Wall Temperature over Time for Empty 42.2mm Diameter Pipe

By comparing the larger and smaller diameter pipes inside the induction heater coil, the closer the wall of the pipe is to the induction coil the better the heating is. This is also indicated by the current used when each pipe was inserted. What can also be deduced from the tables above is that all of the induction created is applied to the surface of the outer diameter of the pipe and cannot penetrate into the pipe. This is observed by the heating ability and the required current being the same for when the evaporator is filled with graphite and when it is empty. The heat generated inside the pipe is through conduction from the outer diameter to the inner. Therefore, a thin walled pipe will be required to increase the effectivity of conduction from the outer diameter to the inner diameter of the pipe.

APPENDIX H - TEMPERATURE VALUES OF EACH COMPONENT DURING FUEL QUALIFYING EXPERIMENTATION

Monitoring the temperatures in the fuel qualifying experimental facility was required to determine the effect the fuel quality had on the functioning of the various components.

AR Methanol as Working Fluid

Timer	Temp Evap	Temp Reac_ Bot	Temp Reac_ 1-1	Temp Reac_ 1-2	Temp Reac_ 1-3	Temp Reac_ Mid	Temp Reac_ 2-1	Temp Reac_ 2-2	Temp Reac _ 2-3	Temp Reac_ Top	Temp_ Ave	Temp_ Cond	Reac Min	Reac Max
1	188.1	257.86	235.8	268.1	252.5	296.42	247.9	252.8	229.11	224.5	251.65	36.893	224.5	296.4
2	192.4	256.74	234.2	266.9	258.78	295.54	241.7	255.1	232.59	230.1	252.4	35.344	230.1	295.5
3	191.84	258.49	233.6	266.2	256.62	296.18	253.5	256.3	233.02	240.1	254.9	36.637	233	296.2
4	192.12	256.44	232.7	264.2	259.46	296.3	249.1	255	231.86	238.2	253.7	36.777	231.9	296.3
5	186.42	257.43	233.2	265.6	260.07	294.76	249.4	255.4	234.07	236.3	254.02	38.265	233.2	294.8
6	185.97	253.49	232	264.3	256.89	294.95	249	255.5	234.46	235.8	252.92	38.534	232	294.9
7	174.79	259.52	236.2	272.5	262.91	295.2	251.4	257.1	235.52	236.5	256.3	39.892	235.5	295.2
8	181.46	256.66	234.8	270.7	266.95	293.91	247.1	255.5	234.83	237	255.27	39.727	234.8	293.9
9	171.34	247.43	229.1	263.9	265.33	293.89	248.2	257	237.8	243.6	254.04	39.284	229.1	293.9
10	185.34	252.07	251.5	249.1	269.66	295.97	245.2	252.3	237.94	239.9	254.83	37.668	237.9	296
Min	171.34	247.43	229.1	249.1	252.5	293.89	241.7	252.3	229.11	224.5	251.65	35.344		
Max	192.4	259.52	251.5	272.5	269.66	296.42	253.5	257.1	237.94	243.6	256.3	39.892		

a)

Timer	Temp Evap	Temp Reac_ Bot	Temp Reac_ 1-1	Temp Reac_ 1-2	Temp Reac_ 1-3	Temp Reac_ Mid	Temp Reac_ 2-1	Temp Reac_ 2-2	Temp Reac _ 2-3	Temp Reac_ Top	Temp_ Ave	Temp_ Cond	Reac Min	Reac Max
1	195.85	251.43	271.2	210.9	254.6	291	233.8	247.1	228	238.6	247.39	33.068	210.88	291
2	194.56	251.11	272.2	218.3	264.7	294.6	247	249.7	242.68	251.5	254.65	34.389	218.3	294.6
3	194.66	250.66	270.6	226.4	261.6	294.7	246.3	250.4	240.87	260.2	255.75	35.361	226.43	294.7
4	194.61	259.00	278.46	231.17	262.68	292.72	248.46	257.71	241.49	270.55	260.25	37.59	231.17	292.7
5	195	239.41	256.6	213.8	249.1	272.4	230.5	237.6	224.27	277.7	244.61	38.946	213.78	277.7
6	193.31	253.83	271.8	229.2	266.3	291.4	241.8	249.6	235.58	245.6	253.92	38.823	229.23	291.4
7	194.54	252.64	271.2	230.3	262.4	293.5	246.3	251.8	240.76	245	254.88	38.543	230.26	293.5
8	195.61	249.62	268	229.9	260.4	291.5	242.2	247.8	235.55	238.8	251.51	38.19	229.9	291.5
9	192.33	250.23	269.5	229.4	268	292.7	242.7	249.7	237.46	237.9	253.07	37.12	229.35	292.7
10	189.71	245.5	266.9	223.6	261.8	291.3	244.9	246.9	239.39	244	251.57	37.937	223.57	291.3
Min	189.71	239.41	256.6	210.9	249.1	272.4	230.5	237.6	224.27	237.9	244.61	33.068		
Max	195.85	259	278.5	231.2	268	294.7	248.5	257.7	242.68	277.7	260.25	38.946		

b)

Timer	Temp Evap	Temp Reac_ Bot	Temp Reac_ 1-1	Temp Reac_ 1-2	Temp Reac_ 1-3	Temp Reac_ Mid	Temp Reac_ 2-1	Temp Reac_ 2-2	Temp Reac _ 2-3	Temp Reac_ Top	Temp_ Ave	Temp_ Cond	Reac Min	Reac Max
1	190.97	250.44	274.36	227	254.5	293	244.5	252.92	237.37	240.21	252.69	33.969	227	292.96
2	190.68	245.08	267.74	222.75	204.8	293.6	245.6	253.05	239.99	245.43	246.45	33.6	204.78	293.61
3	191.15	247.96	269.81	225.78	228.6	294.9	247.8	249.64	242.65	249.67	250.75	35.799	225.78	294.88
4	189.23	247.57	269.26	227.24	266.81	294.14	249.19	250.15	244.91	254.62	255.99	39.35	227.24	294.14
5	186.62	246.01	269.87	229.05	267.6	295.5	250.2	249.17	246.23	253.64	256.36	39.499	229.05	295.5
6	189.06	247.8	271.31	229.92	268.8	295.7	251.6	252.68	246.55	256.35	257.86	39.469	229.92	295.72
7	186.24	245.43	268.75	228.01	266.5	295.1	249.9	251.56	245.76	252.01	255.89	40.489	228.01	295.07
8	184.43	245.28	269.52	228.36	267.6	296.1	252.3	252	248.92	254.94	257.22	42.323	228.36	296.15
9	182.2	243.5	268.64	226.09	267.8	295.7	254.3	256.2	251.47	257.83	257.93	45.446	226.09	295.74
10	182.34	243.54	268.48	223.71	267.9	295.9	253.2	257.51	250.28	256.7	257.43	44.694	223.71	295.91
Min	182.2	243.5	267.74	222.75	204.8	293	244.5	249.17	237.37	240.21	246.45	33.6		
Max	191.15	250.44	274.36	229.92	268.8	296.1	254.3	257.51	251.47	257.83	257.93	45.446		

c)

Figure 105 - Temperature Data of Fuel Qualifying Experimental Facility while Operating with AR Methanol

Table 44 - Duty Cycle Data for Reformer while Reforming AR Methanol

Experiment	Experiment Time [HH:MM:SS]	Duty Time [HH:MM:SS]	Duty Cycle [%]
1	10:00:00	05:45:22	57.56
2	10:00:00	06:21:50	63.64

Table 45 - Duty Cycle Data for Evaporator while Evaporating AR Methanol

Experiment	Experiment Time [HH:MM:SS]	Duty Time [HH:MM:SS]	Duty Cycle [%]
1	10:00:00	05:21:43	53.62
2	10:00:00	05:46:59	57.83
3	10:00:00	07:34:19	75.72

CP Methanol as Working Fluid

Timer	Temp Evap	Temp Reac_ Bot	Temp Reac_ 1-1	Temp Reac_ 1-2	Temp Reac_ 1-3	Temp Reac_ Mid	Temp Reac_ 2-1	Temp Reac_ 2-2	Temp Reac _ 2-3	Temp Reac_ Top	Temp_ Ave	Temp_ Cond	Reac Min	Reac Max
1	183.5	243.96	230.3	271.61	263.2	295.6	243.4	244.71	235.45	239.12	251.92	34.639	230.3	295.6
2	191.5	238.63	234.23	270.1	262	293.5	236.6	247.53	236.31	247.86	251.88	34.237	234.23	293.52
3	190.4	251.8	232.6	270.21	266.2	295.2	230.9	258.47	238.36	240.31	253.79	26.336	230.91	295.24
4	190.74	251.48	232.23	270.29	266.44	295.16	232.86	257.46	237.87	240.15	253.77	29.46	232.23	295.16
5	189.56	247.20	228.70	267.94	265.22	295.25	234.94	259.95	241.42	247.15	254.20	31.01	228.7	295.25
6	188.36	246.03	227.64	267.03	261.41	294.96	233.40	261.67	243.47	248.82	253.83	33.91	227.64	294.96
7	188.7	250.28	231.5	269.97	263.8	294.9	233	257.34	237.85	240.5	253.23	39.043	231.5	294.86
8	180.3	248.27	229.76	267.48	264.4	295.1	235.2	260.72	242.57	245.99	254.39	39.683	229.76	295.11
9	184.1	251.37	230.91	267.48	266.2	295.3	235.1	257.98	240.14	243	254.17	38.309	230.91	295.3
10	182.7	256.26	233.8	270.19	267.7	295.5	232.5	256.32	237.57	238.57	254.27	36.452	232.51	295.47
Min	180.3	238.63	227.64	267.03	261.4	293.5	230.9	244.71	235.45	238.57	251.88	26.336		
Max	191.5	256.26	234.23	271.61	267.7	295.6	243.4	261.67	243.47	248.82	254.39	39.683		

a)

Timer	Temp Evap	Temp Reac_ Bot	Temp Reac_ 1-1	Temp Reac_ 1-2	Temp Reac_ 1-3	Temp Reac_ Mid	Temp Reac_ 2-1	Temp Reac_ 2-2	Temp Reac _ 2-3	Temp Reac_ Top	Temp_ Ave	Temp_ Cond	Reac Min	Reac Max
1	185.4	254.63	233.1	272.2	270.3	296.1	228.7	252.46	229.14	226.8	251.49	31.687	226.8	296.09
2	168.4	249.49	228.9	267.9	270.7	295.3	232.1	259.65	239.33	239.6	253.68	32.61	228.93	295.31
3	172.6	246.57	226.2	265	272.5	295	233.3	263.19	244.07	244.09	254.43	33.942	226.21	294.95
4	168.87	246.99	225.99	259.60	268.11	294.60	235.46	262.64	244.31	245.35	253.67	32.94	225.99	294.6
5	160.27	245.18	224.34	262.71	267.57	294.61	234.37	263.62	245.95	244.82	253.69	35.46	224.34	294.61
6	154.09	245.12	225.14	266.88	267.17	294.81	234.79	264.95	247.29	250.52	255.19	38.00	225.14	294.81
7	144.4	244.09	223.7	265.9	266.7	294.3	237.6	265.14	247.92	250.65	255.11	38.911	223.73	294.28
8	133.6	243.52	223.6	266.2	267.7	294.4	239	267.86	250.78	248.55	255.73	40.842	223.57	294.39
9													0	0
10													0	0
Min	133.6	243.52	223.6	259.6	266.7	294.3	228.7	252.46	229.14	226.8	251.49	31.687		
Max	185.4	254.63	233.1	272.2	272.5	296.1	239	267.86	250.78	250.65	255.73	40.842		

b)

Figure 106 - Temperature Data of Fuel Qualifying Experimental Facility while Operating with CP Methanol

Table 46 - Duty Cycle Data for Reformer while Reforming CP Methanol

Experiment	Experiment Time [HH:MM:SS]	Duty Time [HH:MM:SS]	Duty Cycle [%]
1	10:00:00	05:54:32	59.09
2	08:00:00	04:47:31	59.9

Table 47 - Duty Cycle Data for Evaporator while Evaporating CP Methanol

Experiment	Experiment Time [HH:MM:SS]	Duty Time [HH:MM:SS]	Duty Cycle [%]
1	10:00:00	06:32:06	65.35
2	08:00:00	06:25:29	80.31

Industrial grade Methanol as Working Fluid

Timer	Temp Evap	Temp Reac_ Bot	Temp Reac_ 1-1	Temp Reac_ 1-2	Temp Reac_ 1-3	Temp Reac_ Mid	Temp Reac_ 2-1	Temp Reac_ 2-2	Temp Reac _ 2-3	Temp Reac_ Top	Temp_ Ave	Temp_ Cond	Reac Min	Reac Max
1	164.9	245.1	224.02	267.9	263.84	293.79	225.6	249.19	229.35	224.88	247.08	33.451	224.02	293.8
2	171	250.1	227.82	270.3	266.99	294.35	229.3	258.45	241.01	238.89	253.03	34.979	227.82	294.4
3	170.8	248.4	227.6	269.2	265.83	293.92	229.1	258.08	240.52	238.9	252.4	36.749	227.6	293.9
4	170.27	247.07	226.41	268.79	265.97	293.75	230.78	259.16	242.44	240.67	252.78	38.60	226.41	293.7
5	167.96	247.95	226.43	269.12	266.43	293.50	231.05	258.16	241.49	240.83	252.77	38.45	226.43	293.5
6	170.22	247.51	225.29	268.58	265.06	293.37	233.44	259.55	241.63	240.73	252.79	40.20	225.29	293.4
7	161.9	247.7	224.48	269	265.22	294.06	235	260.25	242.25	242.34	253.35	40.845	224.48	294.1
8	166	250.4	226.37	269	265.81	294.09	235.6	259.99	241.51	241.19	253.77	40.878	226.37	294.1
9	165.5	252.7	226.63	268.6	265.89	293.98	232.8	259.53	241.22	241.16	253.6	40.768	226.63	294
10	170.6	252.5	230.41	270.1	267.11	294.81	230.8	259.94	241.26	240.1	254.11	40.198	230.41	294.8
Min	161.9	245.1	224.02	267.9	263.84	293.37	225.6	249.19	229.35	224.88	247.08	33.451		
Max	171	252.7	230.41	270.3	267.11	294.81	235.6	260.25	242.44	242.34	254.11	40.878		

a)

Timer	Temp Evap	Temp Reac_ Bot	Temp Reac_ 1-1	Temp Reac_ 1-2	Temp Reac_ 1-3	Temp Reac_ Mid	Temp Reac_ 2-1	Temp Reac_ 2-2	Temp Reac _ 2-3	Temp Reac_ Top	Temp_ Ave	Temp_ Cond	Reac Min	Reac Max
1	164.6	245.1	222.43	267.18	265.59	293.71	231.1	254.55	235.32	230.7	249.52	33.35	222.43	293.71
2	160.7	245.94	215.94	265.27	257.18	293.32	236.2	255.76	236.82	234.8	249.03	34.995	215.94	293.32
3	163.7	242.49	214.35	263.61	260.93	293.06	237.1	258.85	240.62	239.54	250.04	36.985	214.35	293.06
4	155.88	241.99	218.18	262.22	260.77	291.89	236.80	257.24	240.65	237.84	249.73	39.06	218.18	291.89
5	166.80	246.55	220.06	265.26	262.57	293.67	236.62	258.71	241.82	241.01	251.81	40.03	220.06	293.67
6	152.76	245.26	224.36	266.64	265.27	294.27	236.05	259.13	242.20	239.89	252.56	39.18	224.36	294.27
7													0	0
8													0	0
9													0	0
10													0	0
Min	152.8	241.99	214.35	262.22	257.18	291.89	231.1	254.55	235.32	230.7	249.03	33.35		
Max	166.8	246.55	224.36	267.18	265.59	294.27	237.1	259.13	242.2	241.01	252.56	40.034		

b)

Figure 107 - Temperature Data of Fuel Qualifying Experimental Facility while Operating with Industrial grade Methanol

Table 48 - Duty Cycle Data for Reformer while Reforming Industrial grade Methanol

Experiment	Experiment Time	Duty Time [HH:MM:SS]	Duty Cycle [%]
Industrial 1	10:00:00	06:12:36	62.1
Industrial 2	06:00:00	03:53:41	64.91

Table 49 - Duty Cycle Data for Evaporator while Evaporating Industrial grade Methanol

Experiment	Experiment Time [HH:MM:SS]	Duty Time [HH:MM:SS]	Duty Cycle
Industrial 1	10:00:00	06:46:52	67.81
Industrial 2	06:00:00	04:48:30	80.14

The reformer's duty cycles remain reasonably constant during the experimentation time periods. The slight differences would be due to how the catalyst is packed or variations in gas flow patterns which are not in the scope of this study. However, the duty cycles are reasonably high between 57.56% and 64.91% which are more than half the experimental time period. This can be due to the inefficient way in which the resistance wire is wrapped around the reformer, as mentioned previously, as well as a need for a higher quantity or better quality insulation.

Each time a different methanol quality was used, the surfaces of the evaporator were first cleaned and the induction heater was replaced. It can be observed from Figure 105, Figure 106, and Figure 107 that the average evaporation temperatures vary depending on the methanol quality used and the total duration of operation.

It can be observed that the average temperature of the evaporator was the greatest and for the longest period of time while evaporating AR methanol and the average temperature was the lowest while evaporating CP methanol. However, the shortest duration of operation before a decrease in average temperature was observed by the Industrial grade.

The duty cycle of the evaporator is also very dependent on the methanol quality. While evaporating AR methanol the evaporator had the smallest duty cycle for the longest duration. The evaporator's duty cycle was the highest while evaporating CP and Industrial grade methanol. The duty cycle observed while evaporating Industrial grade reached the same value as with the CP methanol in a shorter duration.

It can be concluded that the methanol quality has a significant impact on the operating temperatures and duty cycles of the evaporator. Lower methanol quality decreased the average operating temperatures and increased the duty cycle times of the evaporator. This became more pronounced over time and was most noticeable with the Industrial grade methanol. The effect that the methanol quality has on the evaporating components was not part of the scope of this study but is recommended for future work

For all the experiments done, the temperatures of the gases exiting the condenser remained reasonably constant. The variations were dependent on the time of day, weather, and the higher than average ambient temperatures caused by the radiation energy of the reformer which heated the airflow and the water inlet temperature flowing into the heat exchanger.

APPENDIX I - ARDUINO CODING

Final System Automation:

```
#include "max6675.h"

int evapcount = 0;

int EvapCLK1 = 4;

int EvapCS1 = 5;

int EvapDO1 = 6;


int ReacCLK1 = 7;

int ReacCS1 = 8;

int ReacDO1 = 9;


int ReacCLK2 = 10;

int ReacCS2 = 11;

int ReacDO2 = 12;


int ReacCLK3 = 40;

int ReacCS3 = 39;

int ReacDO3 = 38;


int ReacCLK4 = 37;

int ReacCS4 = 36;

int ReacDO4 = 35;


int ReacCLK5 = 34;

int ReacCS5 = 33;

int ReacDO5 = 32;
```

```
int ReacCLK6 = 31;
int ReacCS6 = 30;
int ReacDO6 = 29;

int ReacCLK7 = 28;
int ReacCS7 = 27;
int ReacDO7 = 26;

int ReacCLK8 = 25;
int ReacCS8 = 24;
int ReacDO8 = 23;

int ReacCLK9 = 49;
int ReacCS9 = 48;
int ReacDO9 = 47;

float TempEvap;
float Temp1;
float Temp2;
float Temp3;
float Temp4;
float Temp5;
float Temp6;
float Temp7;
float Temp8;
float Temp9;
unsigned long int seconds;

MAX6675 thermocouple1(EvapCLK1, EvapCS1, EvapDO1);
```

```
MAX6675 thermocouple2(ReacCLK1, ReacCS1, ReacDO1);

MAX6675 thermocouple3(ReacCLK2, ReacCS2, ReacDO2);

MAX6675 thermocouple4(ReacCLK3, ReacCS3, ReacDO3);

MAX6675 thermocouple5(ReacCLK4, ReacCS4, ReacDO4);

MAX6675 thermocouple6(ReacCLK5, ReacCS5, ReacDO5);

MAX6675 thermocouple7(ReacCLK6, ReacCS6, ReacDO6);

MAX6675 thermocouple8(ReacCLK7, ReacCS7, ReacDO7);

MAX6675 thermocouple9(ReacCLK8, ReacCS8, ReacDO8);

MAX6675 thermocouple10(ReacCLK9, ReacCS9, ReacDO9);


void setup() {

  Serial.begin(9600);

  pinMode(41,OUTPUT);

  pinMode(42,OUTPUT);

  pinMode(43,OUTPUT);

  pinMode(44,OUTPUT);

  pinMode(45,OUTPUT);

  digitalWrite(41,LOW);

  digitalWrite(42,LOW);

  digitalWrite(43,LOW);

  digitalWrite(44,LOW);

  digitalWrite(45,LOW);

 Serial.println("LABEL, Computer Time, Timer, TemperatureEvap, TemperatureReac_Bot, TemperatureReac_1-1, TemperatureReac_1-2, TemperatureReac_1-3, TemperatureReac_Mid, TemperatureReac_2-1, TemperatureReac_2-2, TemperatureReac_2-3, TemperatureReac_Top");

  delay(500);

}


void loop() {

   seconds = millis()/1000;
```

```
TempEvap = thermocouple1.readCelsius();
Temp1 = thermocouple2.readCelsius();
Temp2 = thermocouple3.readCelsius();
Temp3 = thermocouple4.readCelsius();
Temp4 = thermocouple5.readCelsius();
Temp5 = thermocouple6.readCelsius();
Temp6 = thermocouple7.readCelsius();
Temp7 = thermocouple8.readCelsius();
Temp8 = thermocouple9.readCelsius();
Temp9 = thermocouple10.readCelsius();

Serial.print("DATA,TIME,");
Serial.print(seconds);
Serial.print(",");
Serial.print(TempEvap);
Serial.print(",");
Serial.print(Temp1);
Serial.print(",");
Serial.print(Temp2);
Serial.print(",");
Serial.print(Temp3);
Serial.print(",");
Serial.print(Temp4);
Serial.print(",");
Serial.print(Temp5);
Serial.print(",");
Serial.print(Temp6);
Serial.print(",");
Serial.print(Temp7);
```

```
  Serial.print(",");

  Serial.print(Temp8);

  Serial.print(",");

  Serial.println(Temp9);


if ((Temp1>= 300) ||(Temp2>= 300) || (Temp3>= 300) || (Temp4>= 300) || (Temp5>= 300) ||(Temp6>= 300)||(Temp7>= 300)||(Temp8>= 300)||(Temp9>= 300))

  {digitalWrite(45,LOW);

   evapcount = 1;

  }

  if ((Temp1<= 297) && (Temp2<= 297) && (Temp3<= 297) && (Temp4<= 297) && (Temp5<= 295) && (Temp6<= 297)&&(Temp7<= 297)&&(Temp8<= 297) && (Temp9<= 297))

  digitalWrite(45,HIGH);


if ((TempEvap>=200)&&(evapcount == 1))

  digitalWrite(44,LOW);


if ((TempEvap<=195)&&(evapcount == 1))

  digitalWrite(44,HIGH);


  delay(1000);

}
```